DELFT UNIVERSITY OF TECHNOLOGY
Department of civil engineering
Division of sanitary engineering

AERATION AND GAS TRANSFER

Prof.Dr.-Ing. H.J. Pöpel

herdruk
maart 1976

DELFT UNIVERSITY OF TECHNOLOGY
Department of civil engineering
Division of sanitary engineering

AERATION AND GAS TRANSFER

Prof. Dr.-Ing. H.J. Pöpel

Uitgave 1974	2e herdruk jan. 1979			753070					f 4,--

L.S.

Bij de samenstelling van elk diktaat wordt er uiteraard naar gestreefd om fouten te voorkomen en de inhoud zo overzichtelijk mogelijk aan te bieden.
Niettegenstaande dat kunnen toch onduidelijkheden voorkomen en kunnen fouten zijn ingeslopen.
Indien U dan ook bij de bestudering van dit diktaat:

- onjuistheden ontdekt
- op onduidelijkheden stuit
- of gedeelten ontmoet, die naar Uw mening nadere uitwerking behoeven, verzoeken de samenstellers U dringend hen daarvan mededeling te doen.

Bij de volgende drukken kunnen dan op- en aanmerkingen worden verwerkt ten gerieve van toekomstige gebruikers.
Zonodig kan ook nog in de lopende cursus voor verduidelijking worden gezorgd.

Table of Contents

Abbreviations and Symbols

The dimensions of the following abbreviations and symbols are chosen in accordance with the International System and are hence based on the following basic dimensions:
length (m), mass (kg), time (s), temperature (K, ^{o}C is also being used here).
Deducted units are

force (Newton) : 1 N = 0,101972 kgf
1 kgf = 9,80665 N
work, energy (Joule) : 1 J = 1 N.m
power (Watt) : 1 W = 1 J/s
pressure (Pascal) : 1 Pa = 1 N/m^2
(bar) : 1 bar = 10^5 Pa

The various units used in the literature for pressure require some further explanation, whereas the conversion of other applied units is straight forward.
Basically, pressure has been defined in terms of "atmosphere" by the following ways:
a) 1 technical atmosphere = 1 kgf/cm^2
b) 1 physical atmosphere = 760 mm Hg (Torr)
c) 1 absolute atmosphere = 1 bar

From the above definitions and the density of mercury of 13595,1 kg/m^3 the following conversion table is obtained.

Convenient units for the pressure of gases within the International System would be
- mbar, the normal atmospheric pressure being 1013 mbar
- kPa , the normal atmospheric pressure being 101,3 kPa

In the following "kPa" is used as the standard unit for pressure.
Roughly is 1 kPa = 30/4 mm Hg
1 mm Hg = 4/30 kPa
Further it is seen from the conversion table that there is not too great a difference between the "atmospheres", the smallest (technical atmosphere) being but 3,2 % less than the greatest (physical atmosphere).

Conversion table for pressure units					
	techn. atm.	phys. atm.	abs. atm.=bar	Pa	mm Hg
1 techn. atm. =	1	0,967841	0,980665	98066,5	735,559
1 phys. atm. =	1,03323	1	1,01325	101325	760
1 abs. atm. = 1 bar =	1,01972	0,986923	1	100000	750,062
1 Pa =	$1{,}01972.10^{-5}$	$0{,}986923.10^{-5}$	10^{-5}	1	$7{,}50062.10^{-3}$
1 mm Hg =	$1{,}35951.10^{-3}$	$1{,}31579.10^{-3}$	$1{,}33322.10^{-3}$	133,322	1

Greek Symbols

α	-	factor to account for the influence of surface active agents on the rate of gas transfer
ε_G	W/m^3	gross power input per unit volume
η	-, %	efficiency
γ	-	activity coefficient
μ	Pa.s	absolute viscosity
σ	N/m	surface tension
τ	s	theoretical detention time (V/Q)
Θ	-	temperature coefficient

Abbreviations	Dimension(s)	Description
a	m^2/m^3	specific interfacial area
A	m^2	area, surface
A_t	m^2/s	interfacial area produced per unit time
c	g/m^3	gas concentration in water
c_e	g/m^3	gas concentration in the effluent of an aerator
c_g	g/m^3	concentration of a gas in the gaseous phase
c_{gi}	g/m^3	gas concentration in the gaseous phase at the interface
c_{go}	g/m^3	initial concentration of a gas in the gas phase
c_L	g/m^3	gas concentration in a liquid
c_{Li}	g/m^3	gas concentration in the liquid phase at the interface
c_s	g/m^3	saturation concentration of a gas in water
c_s' †	g/m^3	like c_s, but under conditions defined under †

c_{so}	g/m^3	initial saturation concentration of a gas in water
c_{ss}	kg/m^3	concentration of activated sludge suspended solids
c(t, x)	g/m^3	gas concentration in a liquid in dependence of x and t as a consequence of molecular diffusion
D	m^2/s	coefficient of molecular diffusion in a liquid
D_E	m^2/s	coefficient of eddy diffusion
D_g	m^2/s	coefficient of molecular diffusion in a gas
D_t	m^2/s	total coefficient of diffusion: $D+D_E$
D_T	m^2/s	coefficient of diffusion of a gas in water at a temperature of T
D_{10}	m^2/s	coefficient of molecular diffusion of a gas in water at 10°C
d	m	depth (of tank, of packing, etc.)
d_B	m	diameter of gas bubbles in a liquid
d_g	m	thickness of gas film
d_i	m	depth of immersion (or submergence) of an aeration device below the water level
d_L	m	thickness of liquid film
d_o	mm	diameter of the opening of a spray nozzle
G	$m^3/m^3.s$	rate of air flow Q_g (m^3/s) per unit volume of water V (m^3)
h	m	height, head
h_{tot}	m	total head
I	$kmole/m^3$	ionic strength

K	-	efficiency coefficient
k_b	-	Bunsen absorption coefficient
k_B	-	constant, relating bubble diameter to rate of gas flow
k_D	-	distribution coefficient
k_g	m/s	partial coefficient of gas transfer in the gaseous phase
k_H	g/J	Henry's constant
k_L	m/s	partial coefficient of gas transfer in the liquid phase
K_L	m/s	(total) coefficient of gas transfer
k_2	s^{-1}	overall coefficient of gas transfer
l	m	Prandtl mixing length at turbulent flow
m	g/s	average rate of mass (gas) transfer
M	g	mass
MW	-	molecular weight
N_G	W	gross power
OA †	-, %	percent oxygen absorption (amount of oxygen absorbed divided by amount of oxygen contained in the injected air)
oc †	g $O_2/m^3.s$	oxygenation capacity (with reference to the liquid volume)
OC †	g O_2/s	oxygenation capacity (with reference to the aerator)
OD	g O_2/s	oxygen demand
OE †	mg O_2/J	oxygenation efficiency
OU †	g O_2/m^3	oxygen utilization (g O_2 absorbed per m^3 air applied)

† see end of table

P	kPa	(total) pressure
p	kPa	partial pressure
p_o	kPa	standard pressure (101 325 Pa)
p_w	kPa	water vapor pressure
p'	kPa	partial pressure of a gas in water vapor saturated air
Q	m^3/s	liquid flow rate
Q_g	m^3/s	gas flow rate reduced to standard conditions of pressure (101,3 kPa) and temperature (0^oC)
R	-, %	removal efficiency in desorption of gases ($R= (c_o - c_e)/c_o$
r_c	s^{-1}	constant of renewal of the gas-liquid interface
RQ	-	ratio of gas flow rate over liquid flow rate (Q_g/Q)
s	s^{-1}	frequency of renewal of the liquid interface
T	K, ^oC	temperature
t	s	time
t_c	s	(constant) time of exposure of a fluid element to the gas phase
T_o	K, ^oC	standard temperature (0^oC, 273,16 K)
u	m/s	turbulent mixing velocity
V	m^3	volume
v_r	m/s	rising velocity of gas bubbles in a liquid
x	m	distance from gas-liquid interface
x_p	m	depth of penetration

† these terms are defined under the following conditions:

water vapor saturated air
water temperature $10^{\circ}C$
oxygen concentration of the water c = 0 g O_2/m^3
total pressure 101,3 kPa

References

A. Cited References

1. Black, W. M., Phelps, E. B.: Report to the Board of Estimate and Apportionment, New York, 1911

2. Lewis, W. K. & Whitman, W. G.: Principles of Gas Absorption, Ind. Eng. Chem. (1924), p. 1215

3. Higbie, R.: The Rate of Absorption of a pure Gas into a still Liquid during short Periods of Exposure, American Institute of Chemical Engineers May 13-15 (1935), p. 365

4. Danckwerts, P. V.: Significance of Liquid-Film Coefficients in Gas Absorption, Industrial and Engineering Chemistry Vol. 43, No. 6 (1951), p. 1460

5. Dobbins, W. E.: Mechanism of Gas Absorption by Turbulent Liquids, Proceeding of 1. International Conference on Water Pollution Research, paper 2/20 Pergamon Press Ltd., Oxford (1962)

6. Eckenfelder, Jr. W. W., Asce, M.: Absorption of Oxygen from Air Bubbles in Water, Journal of the Sanitary Engineering Division July (1959), p. 89

7. Pöpel, H. J.: Ein einfaches Verfahren zur Auswertung von OC-Versuchen, GWF 109 (1968), p. 307

8. Wilderer, P., Hartmann, L.: Der Einfluss der Temperatur auf die Lösungsgeschwindigkeit von Sauerstoff in Wasser, GWF 110 (1969), p. 707

9. Barrett, M. J., Gameson, A. L. H., and Ogden, C. G.: Aeration studies at four weir systems, Water and Water Engng. 64 (1960), p. 407

10. Kroon, G. T. M. van der, Schram, A. H.: Weir Aeration - part I, H_2O (1969), p. 528

11. Bewtra, J. K., Nicholas, W. R.: Oxygenation from Diffused Air in Aeration Tanks, JWPCF 36 (1964), p. 1195

12. Suschka, J.: Oxygenation in Aeration Tanks, JWPCF 43 (1971), p. 81

13. Horvath, I.: Die Modelldarstellung der Sauerstoffaufnahme in Belüftungsbecken, GWF 107 (1966), p. 946

14. Downing, A. L., Boon, A. G., Bayley, R. W.: Aeration and biological oxidation in activated sludge process, Journ. and Proc. Inst. Sew. Purif. (1962)

15. Kroon, G. T. M. van der, Corstjens, G. H.: Zuurstofoverdracht aan water en kunstmatige actief slib-watermengsel, Water 50 (1966), p. 266

B. Selected Literature

1. Books, Proceedings etc.

16. Baars, J. K., Muskat, J.: Zuurstoftoevoer aan water met behulp van roterende lichamen, Instituut voor Gezondheidstechniek TNO, rapport no. 28,1959

17. Culp, R. L., Culp, G. L.: Advanced Wastewater Treatment, Van Nostrand Reinhold Company, New York-Cincinnati-Toronto-London-Melbourne 1971

18. Eckenfelder Jr., W. W., O'Connor, D. J.: Biological Waste Treatment, Pergamon Press, Oxford 1961

19. Fair, G. M., Geyer, J. C., Okun, D. A.: Water Purification and Wastewater Treatment and Disposal, Vol. 2, John Wiley & Sons, Inc., New York-London-Sydney 1968, Chapter 23 and 24

20. Knop, E., Bischofsberger, W., Stalmann, V.: Versuche mit verschiedenen Belüftungssystemen im technischen Massstab, Vulkan - Verlag Dr. W. Classen, Essen, Vol. I 1964/65

21. Knop, E., Bischofsberger, W., Stalmann, V.: Versuche mit verschiedenen Belüftungssystemen im technischen Massstab, Vulkan - Verlag Dr. W. Classen, Essen, Vol. 2 1964/65

22. Pallasch, O., Triebel, W. (editors): Lehr- und Handbuch der Abwassertechnik Vol 2., Verlag von Wilhelm Ernst & Sohn, Berlin - München 1969

23. Rich, L. G.: Unit Operations of Sanitary Engineering, John Wiley & Sons, Inc., New York - London 1961

24. Sontheimer, H.: Vortragsreihe mit Erfahrungsaustausch über spezielle Fragen der Wassertechnologie Vol. I: Entsäuerung, Enteisenung und Entmanganung, Veröffentlichungen der Abteilung und des Lehrstuhls für Wasserchemie des Instituts für Gastechnik, Feuerungstechnik und Wasserchemie der Technischen Hochschule Karlsruhe, Karlsruhe 1966

25. Derde vakantiecursus in behandeling van afvalwater: De technologie van het beluchtingsproces, Technische Hogeschool, Afdeling der Weg- en Waterbouwkunde, Delft 1968

26. Zesde vakantiecursus in behandeling van afvalwater: De Oxydatiesloot, Technische Hogeschool, Afdeling der Weg- en Waterbouwkunde, Delft 1971

27. Twintigste vakantiecursus in drinkwatervoorziening: Physische technologie van de waterzuivering, Technische Hogeschool, Afdeling der Weg- en Waterbouwkunde, Delft 1968

2. Articles

28. Albrecht, D.: Schätzung der Sauerstoffzufuhr durch Wehre und kaskaden, Die Wasserwirtschaft 11 (1969), p. 321

29. Bewtra, J. K., Nicholas, W. R.: Oxygenation from diffused air in aeration tanks, JWPCF 36 (1964), p. 1195

30. Boelens, A. H. M., Sybrandi, J. C.: Ontzuring door middel van cascades, Water 50 (1966), p. 214

31. Bruijn, J., Tuinzaad, H.: The Relationship between Depth of U-Tubes and the Aeration Process, JAWWA 50 (1958), p. 879

32. Carrière, J. E.: Voorlopige uitkomsten van de door het KIWA verrichte sproeiproeven, N.V. Keuringsinstituut voor Waterleidingartikelen KIWA, Mededeling no. 9, Den Haag 1950

33. Carver, C. E., Asce, F.: Oxygen Transfer from falling water droplets, Journal of the Sanitary Engineering Division (1969), p. 239

34. Eckenfelder Jr., W. W. : Engineering Aspect of Surface Aeration Design, Proceedings of the 22 nd. Industrial Waste Conf. (1967),

p. 279

35. Eckenfelder Jr., W. W., Ford, D. L.: New concepts in oxygen transfer and aeration, in: Gloyna, E. F., Eckenfelder, W. W.: Advances in Water Quality Improvement, Vol. I, University of Texas Press, Austin - London 1968, p. 215

36. Emde, W. von der: Aeration developments in Europe, in:Gloyna, E. F., Eckenfelder, W. W.: Advances in Water Quality Improvement, Vol. I, University of Texas Press, Austin - London 1968, p. 237

37. Emde, W. von der: Belüftungssysteme und Beckenformen, in: München Beiträge zur Abwasser-, Fischerei- und Flussbiologie Band 5, 2. Auflage, (1968), p. 223

38. Franz, B.: Satz von Saugkreiselbelüftern bei der biologischen Reinigung Gaswässern, WWT 18 (1968), p. 165

39. Haberer, K., Baier, R.: Zur Trinkwasserentsäuerung durch Intensivbelüftung im Kreuzstrom, GWF 111 (1970), p. 150

40. Haney, P. D.: Theoretical Principles of Aeration, JAWWA (1954), p. 353

41. Heeb, A., Rau, E.: Die neue Schlammbelebungsanlgae im Hauptklärwerk Stuttgart - Mühlhausen, GWF 101 (1960), p. 437

42. Heeb, A., Rau, E.: Betriebsergebnisse mit der neuen Schlammbelebungsanlage im Hauptklärwerk Stuttgart - Mühlhausen, GWF 101 (1960), p. 758

43. Horvath, I.: Die Modelldarstellung der Sauerstoffaufnahme in Belüftungsbecken, GWF 107 (1966), p. 946

44. Kaelin, J. R., Tofaute, K.: Leistungsfähigkeit von BSK-Turbinen in grossen Belebungsbecken, Wasser Luft und Betrieb 13 (1969), p. 13

45. Kalbskopf, K. H.: Strömungsverhältnisse und Sauerstoffeintragung bei Einsatz von Oberflächenbelüftern, in: Husman, W. (Editor): Vom Wasser XXXIII (1966)

46. Kalinske, A. A.: Turbulence Diffusivity in activated sludge aeration basins, Water Poll. Res. Conf. San Francisco, July (1970), p. II-7/1

47. Kittner, H.: Die mechanische Entsäuerung und Belüftung in der Wasseraufbereitung, WWT 13 (1963), p. 124

48. Kittner, H.: Die mechanische Entsäuerung und Belüftung in der Wasseraufbereitung, WWT 13 (1963), p. 160

49. Kroon, T. M. van der, Schram, A. H.: Weir Aeration - Part II: Step weirs or cascades, H_2O 2 (1969), p. 538

50. Leary, R. D., Ernest, L. A., Katz, W. J.: Full scale oxygen transfer studies of seven diffuser systems, JWPCF (1969), p. 459

51. Louwe Kooymans, L. H.: Aeration and deferrisation, IWSA Congress, London (1955), p. 283

52. Pasveer, A.: Research on activated sludge, VI Oxygenation of Water with Air Bubbles, Sewage and Industrial Wastes, Vol. 27 (1955), p. 1130

53. Pasveer, A.: Untersuchungen über das Belebtschlammverfahren für die Reinigung von Abwasser, G. I. 76 (1955), p. 332

54. Rüb, F.: Oberflächenbelüfter für die biologische Abwasseraufbereitung, Wasser, Luft und Betrieb 15 (1971), p. 397

55. Selm, J. van: Beluchting bij stuwen, Water 51 (1967), p. 355

56. Suschka, J.: Oxygenation in aeration tanks, JWPCF (1971), p. 81

57. Sybrandi, J. C.: Ontzuring door middel van cascades, H_2O 3 (1970), p. 32

58. Westberg, N. K. G.: Intensive Aeration of Water, JAWWA 41 (1949), p. 417

59. Wingrich, H.: Die Verfahren der offenen Belüftung von Rohwasser und ihre Wirtschaftlichkeit, WWT 18 (1968), p. 267

60. Technical Practice Committee - Subcommittee on Aeration in Wastewater Treatment, Aeration in Wastewater Treatment - manual of practice no. 5,
part 1: JWPCF 41 (1969), p. 1863 - 1878
part 2: JWPCF 41 (1969), p. 2026 - 2061
part 3: JWPCF 42 (1970), p. 51 - 76

Aeration and Gas Transfer

1. Introduction

1.1 Definition and terms

Gas transfer is a physical phenomenon, by which gas molecules are exchanged between a liquid and a gas at a gas-liquid interface. This exchange results in an increase of the concentration of the gas(es) in the liquid phase as long as this phase is not saturated with the gas under the given conditions of e.g. pressure, temperature (absorption of gas) and in a decrease when the liquid phase is oversaturated (desorption, precipitation or stripping of gas). In most of the gas transfer operations in sanitary engineering the gaseous phase is represented by "air", the liquid in all cases by water (and its constituents). This gas transfer is brought about by bringing air and water into intimate contact, i.e. by aeration. The goals of aeration and gas transfer cover a wide range and so do the applied operations. Important natural phenomena of gas transfer are the reaeration of surface water, i.e. mainly the transfer of oxygen into surface water, the concentration of which is generally below the saturation value due to the oxygen consumption through bacterial degradation of organic pollutants. On the other hand also desorption of gases from surface water is quite a natural phenomenon:

- release of oxygen produced by algal activities up to a concentration above the saturation concentration;
- release of taste- and odor-producing substances which are volatile and the concentration of which in air is too low to yield a significant saturation concentration in water;
- release of methane, hydrogen sulfide under anaerobic conditions of surface water or of the bottom deposits.

Whereas the mentioned processes of aeration and gas transfer under natural conditions play an important part within the natural stabilization of water pollutants, a wide range of such operations is applied of sanitary engineering for different purposes. This artificialy induced gas transfer by aeration aimes for instance at

- addition of oxygen to groundwaters to oxidize dissolved iron and

manganese to facilitate their removal
- addition of oxygen to sewage within the process of biological treatment, especially activated sludge treatment, in order to supply the oxygen required for aerobic degradation of organic pollutants and in order to maintain the oxygen tension necessary for mentioned aerobic treatment.

Whereas the forementioned processes transfer oxygen into water by aeration, the technique of aeration is also applied for the release of gases from water which may impair the water quality with respect to corrosion problems of storage and distribution facilities or with regard to taste and odor problems. The transfer of oxygen simultaineously brought about during such desorption operations is in this case of minor importance. Specific operations of this kind are
- removal of carbon dioxide to adjust or to approach the carbonate equilibrium with respect to calcium;
- removal of hydrogen sulfide to eliminate taste and odors and to decrease corrosion of metals and disintegration of concrete;
- removal of methane to prevent fire and explosions;
- removal of volatile oils and similar odor- and taste-producing substances;
- removal of ammonia from sewage as a means of reducing eutrophic conditions of receiving waters, especially of lakes.

Finally gas transfer operations have to be mentioned where water is not exposed to air but rather to a specific pure gas, to air enriched with a particular gas or to air or air-gas-mixtures at pressures and temperatures other than those of the normal atmosphere.
The reasons that may lead to the application of the foregoing concepts are, that gases have to be transferred to water that are not present in air or not in sufficiently high concentration to allow for a rapid transfer of the gas in question. Examples are:
- addition of carbon dioxide from flue gas or carbon dioxide generators to water that has been softened by the lime-soda process. Such water is generally supersaturated with $CaCO_3$ and $Mg(OH)_2$ and is stabilized by addition of CO_2;
- the addition of carbon dioxide from flue gas to lime-treated sewage for removal of phosphates. The application is required for economical neutralization of the effluent prior to discharge to a receiving water of low buffer capacity;

- the addition of ozone or chlorine for disinfection of water or for destruction of taste- and odor-producing substances as well as for chemical oxidation of pollutants (e.g. of water in swimming pools).

1.2 Elements of Aeration and Gas Transfer Operations

Since gas transfer occurs only trough the gas-liquid interface, this operation has to be carried out as to maximize the opportunity of interfacial contact between the two phases. In order to have the bulk of the solution also to take part in the transfer, continuous renewal of these interfaces is essential. The engineering goal then is to accomplish this with a minimum expenditure of initial and operational cost (energy).

In principal, four different types of aerators are common for gas transfer operations within the objectives of sanitary engineering:

1. Gravity aerators

1.1 Cascades, by which the available difference of head is subdivided into several steps (fig. 1.1);

1.2 Inclined planes, often equipped with riffle plates to break up the sheet of water for surface renewal (fig. 1.2);

1.3 Vertical stacks through which droplets fall and updrafts of air ascend in countercurrent flow (fig.1.3). The stacks may be subdivided by perforated pans or troughs (fig. 1.4), possibly filled with contact media to create large gas-liquid interfaces (fig. 1.5).

Cokes, stones, plastic tubings ect. are used as contact media. The stacks are either naturally ventilated or the draft is artificially induced.

Gravity aerators are primarily used in water purification plants for desorption of gases. The oxygenation of sewage within trickling filters and ammonia stripping from effluents (fig. 1.6) are examples of application of the gravity principle for gas transfer in the realm of sewage treatment.

2. Spray aerators

By spray aerators the water is sprayed in the form of fine droplets into the air, thus creating a large gas-liquid interface for gas transfer. The fine distribution of the water into the air is

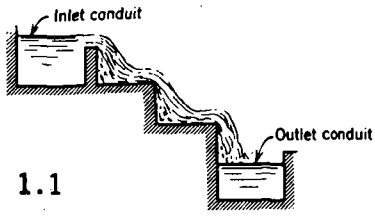

1.1

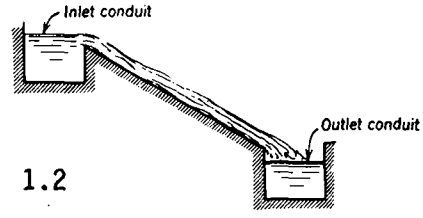

1.2

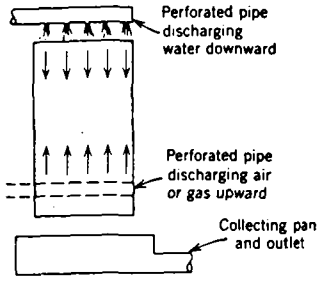

1.3

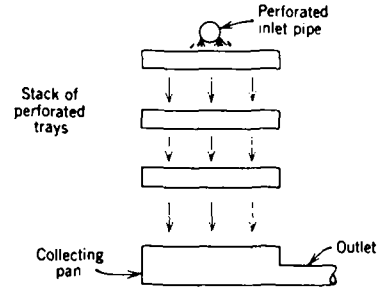

1.4

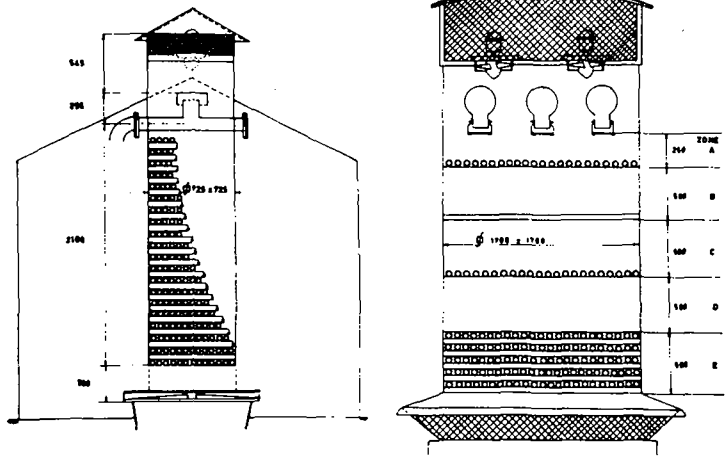

Vertical stack filled with plastic tubes

1.5

Fig. 1.1 - 1.5 GRAVITY AERATORS

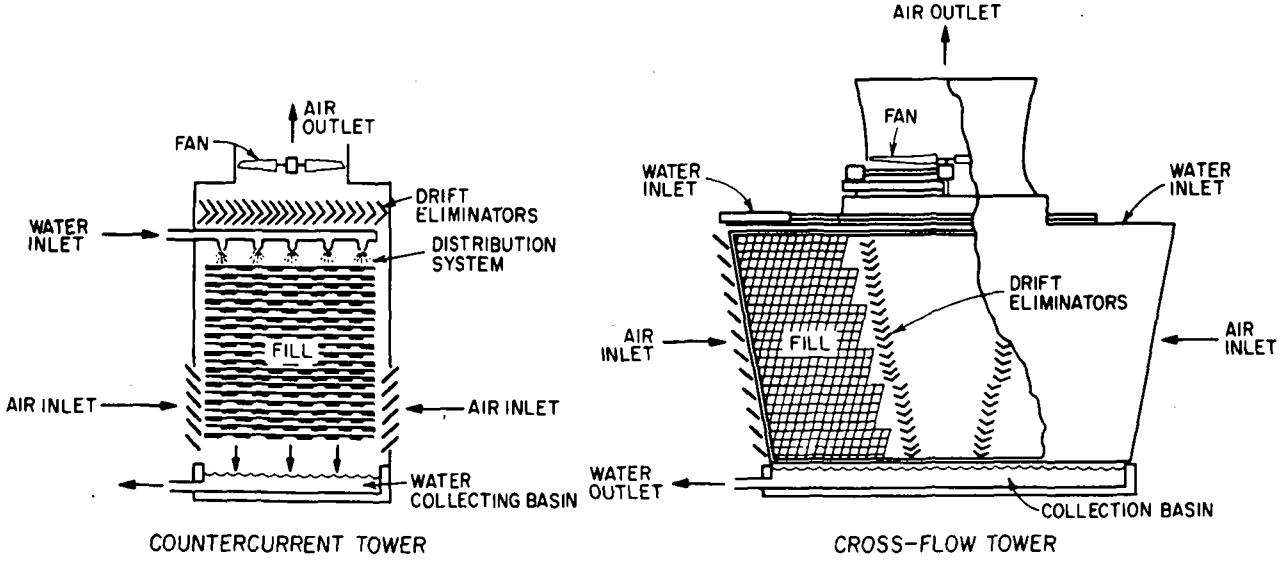

Fig. 1.6 STRIPPING TOWER FOR REMOVAL OF AMMONIA

accomplished by pumping the water through orifices or nozzles mounted upon stationary pipes.

Layout and types of nozzles used for desorption of carbon dioxide in the course of water treatment are sketched in fig. 1.7. In sewage treatment spray aeration is made use of in connection with the distribution of sewage over trickling filters only.

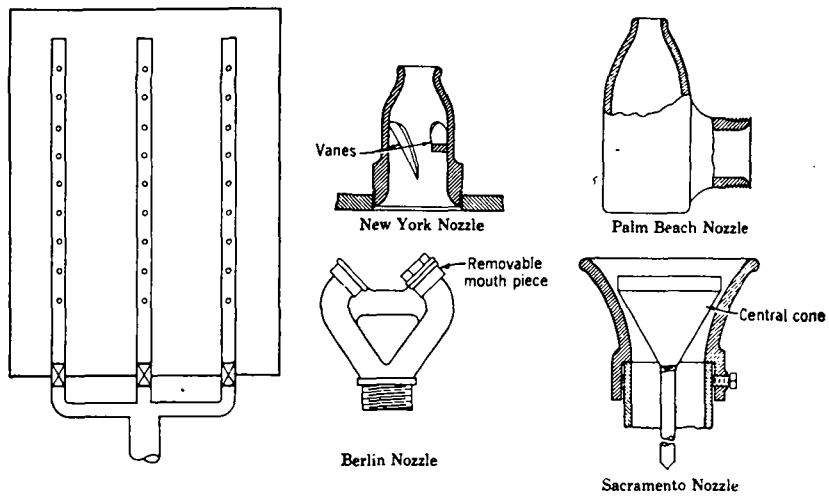

(a) Layout (b) Nozzle types

Fig. 1.7 SPRAY AERATORS

3. Air diffusers (bubble aeration)

By air diffusers compressed air is injected into water through orifices or nozzles in the air piping system (fig. 1.8), through spargers (fig. 1.9), porous tubes, plates, boxes or domes (fig. 1.10) to produce bubbles of various size and hence with different interfacial areas per m^3 of air.

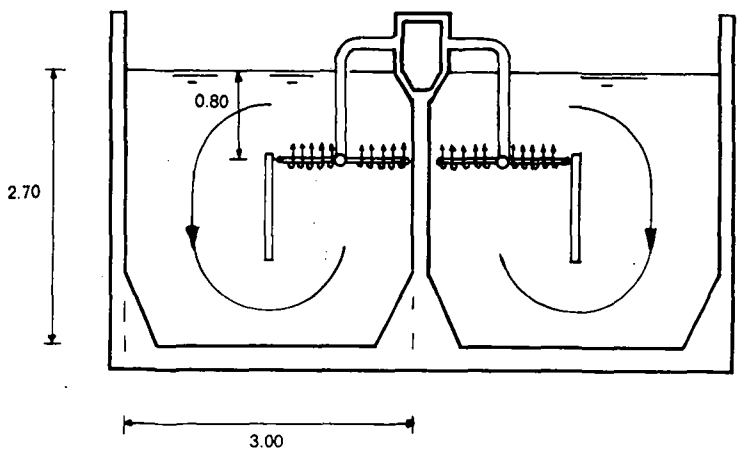

Fig. 1.8 AERATION THROUGH ORIFICES IN THE PIPING SYSTEM (INKA)

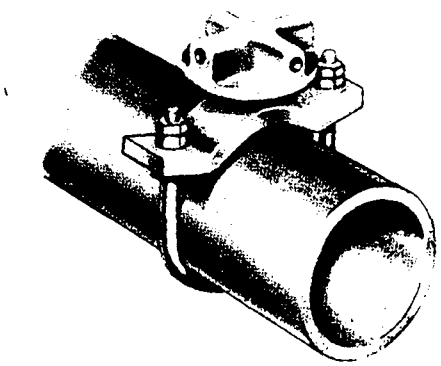

Fig. 1.9 SPARGER-AERATOR

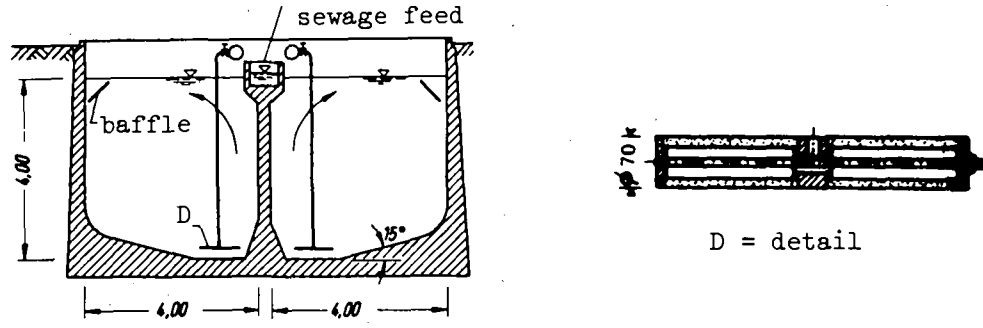

Fig. 1.10 AIR DIFFUSION BY POROUS TUBES (SCHUHMACHER)

The application of air diffusers is more or less restricted to absorption of gases, especially of oxygen. Addition of oxygen to water in the course of purification and especially the oxygen supply of activated sludge treatment units are examples.

A special case of bubble aeration is the venturi aerator and the well aerator. In both systems the streaming velocity of the water is locally enlarged to produce a partial vacuum by which air is sucked into the water in the form of fine bubbles (fig. 3.34). Whereas the venturi aerator creates the increased velocity by narrowing the water transmission pipe (fig. 3.35), the deep well aerator regulates the streaming velocity and hence the amount of air introduced by means of a cone placed on top of the circular well (fig. 3.36). Both types of self-sucking aerators are used for oxygenation of water during the purification process.

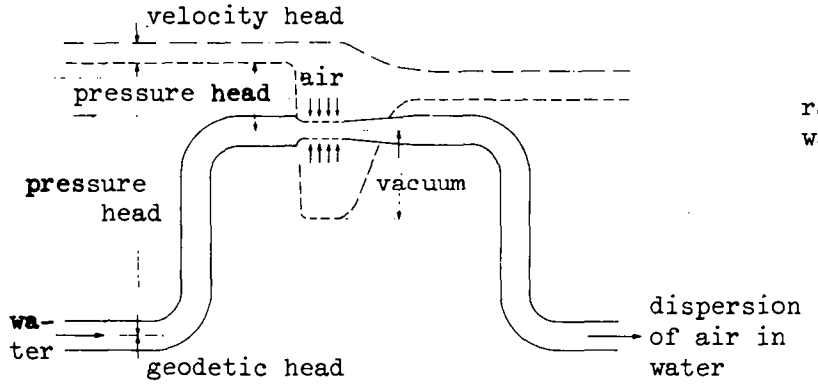

Fig. 3.34 PRINCIPLE OF AERATION BY MEANS OF ENTRAINED AIR

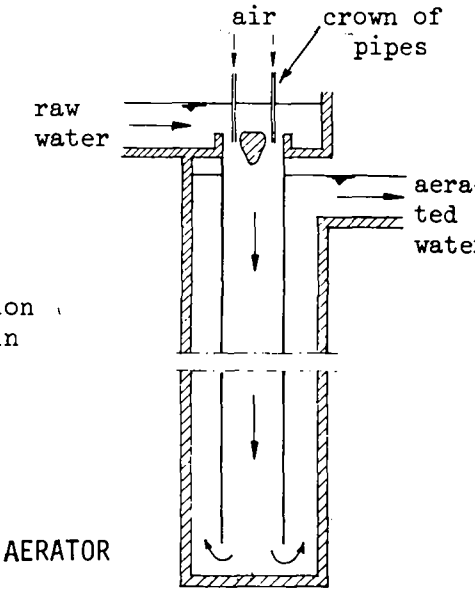

Fig. 3.36 DEEP WELL OR U-TUBE AERATOR

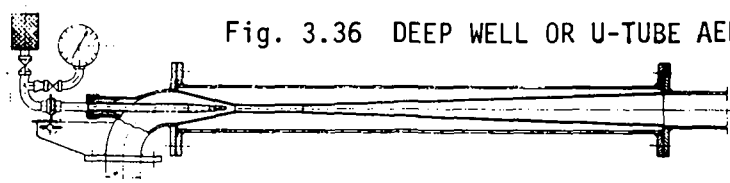

Fig. 3.35 THE VENTURI AERATOR

4. Mechanical Aerators

Mechanical aerators create new gas-liquid interfaces by different means and constructions. Creating of droplets or water aprons above the water level of the tank, entrainement of air due to the pressure falling below normal at great water velocities near the aeration device, renewal of the air-water-interface at the top of the tank and a high degree of turbulence within the tank are mechanisms, that promote the transfer of oxygen. Basically, there are two types of construction:

4.1 Various construction of brushes, consisting of a horizontal revolving shaft with combs, blades or angles attached to it dipping slightly into the water (fig. 3.41 and 3.42);

4.2 Turbine or cone aerators with vertical shaft primarily of the

4.21 Updraft type (surface aerators), by which the rotor pumps large quantities of water at the water surface at low head (fig. 1.11). The aeration by the creation of large water-air interfaces above the water level is enhanced by the entrainement of air bubbles trough the action of the spread water falling upon the water surface of the tank.

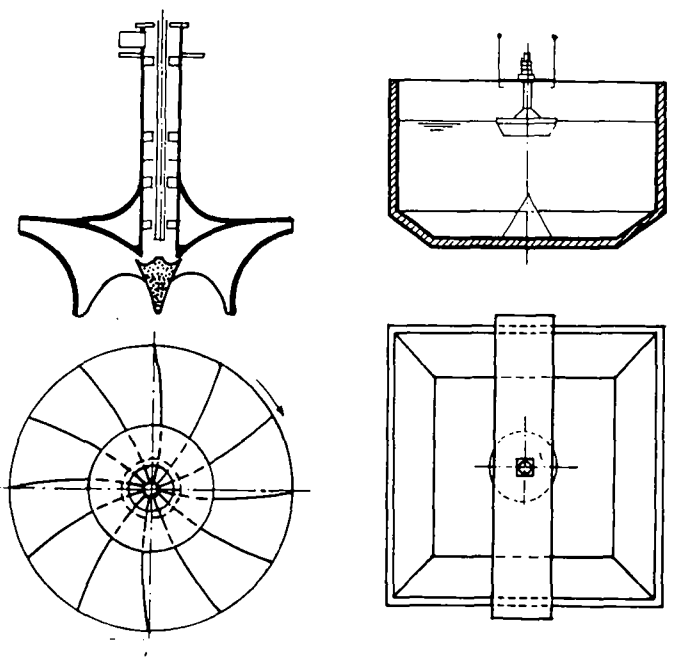

Fig. 1.11 TURBINE AERATOR

4.22 The downdraft type makes use of the negative head produced by the rotating element for aspirating of air.

4.3 Besides these types, rotating impellors are also made use of to disperse coarse air bubbles, induced under pressure, into small ones in order to increase the air-water interface (fig. 3.63)

The purpose of this brief introductory description of the elements of aeration and gas transfer was to give an illustration of the techniques used, that may be of help in understanding the theoretical aspects and engineering applications in the following sections. Although renewal of gas-liquid interfaces has been stressed in the foregoing as the prime factor, other parameters play also an important role in gas transfer operations and will be discussed later.

1.3 Aeration and Gas Transfer within Processes of Water Purification and Sewage Treatment

As mentioned before, aeration and gas transfer serves various purposes in water purification and sewage treatment. In principle, the goal of any of the processes is to either establish a certain concentration of the gas in water or to propagate reactions the gas is involved in. Examples of the first purpose are aeration of water to increase the oxygen content, desorption of carbon dioxide from water to establish or approach the carbonate equilibrium, desorption of taste- and odor-producing gases or volatile substances in order to meet specific quality standards. Examples of the second kind are aeration for oxidation of iron and manganese in water, aeration of activated sludge tanks to supply the oxygen required for aerobic degradation of organic pollutants. The requirements with respect to the gas concentrations to be established or the quantities of gas to be transferred for the propagation of reactions will not be discussed here. The reader is referred to the pertinent literature and textbooks. Nor will alternative processes be covered, that in dependence on the conditions might give a more feasible and more economic engineering solution to the problem than just gas transfer operations. Examples of such alternatives are the application of lime, burned dolomite, soda ash or sodium hydroxide instead of desorption of carbon dioxide; adsorption of taste and odor producing substances on charcoal instead of release by aeration; biological nitrification of ammonia and subsequent denitrification for nitrogen removal from sewage instead of ammonia stripping; ect.

2. Theoretical Aspects of Aeration and Gas Transfer

2.1 Solubility of Gases

The solubility of gases in water (and also in other liquids) depends upon

- the nature of the gas generally expressed by a gas specific coefficient: the distribution coefficient k_D
- the concentration of the respective gas in the gaseous phase (g/m^3) which is related to the partial pressure p of the respective gas in the gas phase
- the temperature of the water T
- impurities contained in the water

2.11 Influence of the Gas Concentration on Solubility

If water is exposed to a gas or gas mixture a continuous exchange of gas molecules takes place from the liquid phase into the gaseous and vice versa. As soon as the solubility concentration in the liquid phase is reached both gas streams will be of equal magnitude such that no overall change of the gas concentrations in both phases will occur. This dynamic equilibrium is generally referred to as the solubility or the saturation concentration of the gas in the liquid. The higher the gas concentration in the gaseous phase is the greater will be the saturation concentration in the liquid phase, obviously. In fact, the relation between the saturation concentration c_s (g/m^3) and the gas concentration in the gas phase c_g (g/m^3) is a linear one:

$$c_s = k_D \cdot c_g \qquad (2.1)$$

with k_D as proportionality constant. Its magnitude depends on the nature of the gas (and of course of the liquid), and - as will be shown later - on the temperature of the water. k_D is generally referred to as distribution coefficient. Values of k_D for various gases are given in table 2.1.

Equation 2.1 can be used for any units for the respective concentrations (g/m^3, moles/m^3, moles/mole etc.). Preferably, mass concentra-

tions are applied (g/m^3). Hence the gas concentration in the gas phase c_g (g/m^3) has to be known for estimating the solubility c_s. c_g may be obtained by application of the universal gas law

$$p \cdot V = n \cdot R \cdot T \qquad (2.2)$$

where

p = partial pressure of the respective gas in the gas phase (Pa)

V = volume occupied by the total gas phase - including all other gases of a gas mixture (m^3)

n = number of moles of the respective gas contained in volume V

R = universal gas constant (8,3143 J/K.mole)

T = absolute temperature (K)

From equation 2.2 it follows, that the molar gas concentration in the gas phase is equal to

$$\frac{n}{V} = \frac{p}{R \cdot T} \qquad (moles/m^3) \qquad (2.3a)$$

Hence the corresponding mass concentration c_g is obtained by multiplication with the molecular weight (MW) of the gas in question:

$$c_g = \frac{p \cdot MW}{R \cdot T} \qquad (g/m^3) \qquad (2.3b)$$

Combination of eq. 2.1 and 2.3b yields

$$c_s = k_D \cdot \frac{MW}{RT} \cdot p \qquad (g/m^3) \qquad (2.4a)$$

and shows the dependence of the solubility c_s on the partial pressure of the gas in the gas phase. Eq. 2.4 is known as Henry's law, formerly widely applied for estimating solubilities. Henry's law is generally written as

$$c_s = k_H \cdot p \qquad (2.4b)$$

with k_H ($g/m^3.Pa = g/J$) being Henry's constant. The relation between the distribution coefficient k_D and Henry's constant follows from eq. 2.4a and b:

$$k_H = k_D \cdot MW/R.T \quad (g/J)$$

Finally, solubilities are estimated by a third approach, the Bunsen absorption coefficient k_b. k_b states, how much gas volume (m^3), reduced to standard temperature (0^oC) and pressure (101,3 kPa), can be absorbed per unit volume (m^3) of water at a partial pressure of p_o = 101,3 kPa of the gas in the gas phase. According to this definition the volumetric saturation concentration at the cited partial pressure would be

$$c_s \ (m^3_{STP} \text{ gas}/m^3 \text{ water}) = k_b \qquad (2.5a)$$

and at any other partial pressure p

$$c_s = k_b \cdot \frac{p}{p_o} \quad (m^3_{STP}/m^3) \qquad (2.5b)$$

Since 1 m^3_{STP} contains according to eq. 2.2 $p_o/R.T_o$ moles of gas and hence a mass of gas equal to $MW.p_o/R.T_o$, the above volumetric gas saturation concentration is converted to the mass solubility by multiplying eq. 2.5b with $MW.p_o/R.T_o$ to give

$$c_s = k_b \cdot \frac{MW}{R.T_o} \cdot p \quad (g/m^3) \qquad (2.5c)$$

The relation between the distribution coefficient k_D and the Bunsen absorption coefficient k_b follows from eq. 2.4a and 2.5b as

$$k_b = k_D \cdot \frac{T_o}{T}$$

The interrelationship between the three discussed coefficients for estimating solubilities is given by

$$k_D = k_H \cdot \frac{R.T}{MW} = k_b \cdot \frac{T}{T_o} \qquad (2.6)$$

When applying any of the three discussed approaches the partial pressure p of the gas in question has to be known. This pressure can be

obtained from the air composition in terms of the percentage volumetric composition (see table 2.1) and the total pressure P on the basis of Dalton's law of partial pressures. According to this law the partial pressure of a gas within a gas mixture is equal to the product of the total pressure P and its volumetric fraction of the gas phase. Dry air, for instance, contains 20,948 % of oxygen (see table 2.1). At standard pressure P_o = 101325 Pa, therefore, dry air has an oxygen partial pressure of p = 101325 . 0,20948 = 21 226 Pa.
In the practice of aeration the gas phase will always be saturated with water vapor exerting a certain partial pressure p_w the magnitude of which depends on the temperature (see table 2.2). Thereby the partial pressures p of the other gases are reduced, such that their sum is $P-p_w$ instead of P. Hence the partial pressures, corrected for water vapor saturation of the gas phase p' amount to

$$p' = p \cdot \frac{P-p_w}{P} \qquad (2.7)$$

At 20°C the oxygen partial pressure of water vapor saturated air is hence not p = 21 226 Pa but rather p' = 21 226.(101 325 - 2 330)/ 101 325 = 20 738 Pa, i.e. 97,7 % of the "dry" value. The solibility is reduced by the same ratio, obviously. Oxygen saturation values of water exposed to air under conditions of water vapor saturation are given in table 2.3.

Example

Compute the solubility of oxygen in pure water of 20°C exposed to air at a pressure of 104 kPa (780 mm Hg). Compute Henry's constant and the Bunsen absorption coefficient for the above conditions.
According to eq. 2.1 the solubility is

$$c_s = k_D \cdot c_g \text{ with } k_D = 0{,}0337 \text{ (table 2.1)}$$

c_g is estimated by means of eq. 2.3b after computing the oxygen partial pressure under conditions of water vapor saturation (eq. 2.7)

$$p' = 0{,}20948 \cdot 104 \cdot \frac{104-2{,}33}{104}$$

$$= 21{,}30 \text{ kPa}$$

$$c_g = \frac{21\,300 \cdot 32}{8{,}3143 \cdot 293{,}16} = 279{,}6 \quad g/m^3$$

$$c_s = 0{,}0337 \cdot 279{,}6 = 9{,}42 \quad g/m^3$$

According to eq. 2.6 Henry's constant at a temperature of 20°C is

$$k_H = k_D \cdot \frac{MW}{R.T} = 0{,}0337 \cdot \frac{32}{8{,}3143.293{,}16} =$$

$$= 4{,}42 \cdot 10^{-4} \quad (g/J)$$

and the Bunsen absorption coefficient amounts to

$$k_b = k_D \cdot \frac{T_o}{T} = 0{,}0337 \cdot \frac{273{,}16}{293{,}16} = 0{,}0314$$

Some of the gases listed in table 2.1 react with water. Equation 2.1 applies but to that part of the absorbate that is present as gas and not to that which is ionized. This holds, for example, for the following gases.

Carbon dioxide:

reactions in water: $CO_2 + H_2O \rightarrow H_2CO_3$ (2.8a)

$$H_2CO_3 \rightarrow HCO_3^- + H^+ \quad (2.8b)$$

$$HCO_3^- \rightarrow CO_3^{-2} + H^+ \quad (2.8c)$$

The equilibrium of eq. 2.8a lies far on the left hand side: but 1 % of the sum of CO_2 and H_2CO_3 is present as carbonic acid, 99 % as carbon dioxide, approximately. In dependence of the pH of the water the reactions 2.8 take place, distributing the total amount of C into bicarbonate and carbonate. Equation 2.1 does apply only to CO_2.

Ammonia:

reaction in water $NH_3 + H^+ \rightarrow NH_4^+$ (2.9)

The protolysis constant for reaction 2.9 at 25°C is given by

$$\frac{(NH_4^+)}{(H^+) \cdot (NH_3)} = 10^{9,25}$$

Thus, the ratio of not ionized ammonia (to which the distribution law is applicable) to that of the ionized form is

$$\frac{(NH_3)}{(NH_4^+)} = \frac{10^{-9,25}}{(H^+)} = 10^{-9,25 + pH} \qquad (2.10)$$

indicating that the gaseous form is predominantly present at pH-values well above 9,25 only.

Hydrogen Sulfide:
reactions in water (constants at 25°C between brackets):

$$H_2S \rightarrow HS^- + H^+ \quad (10^{-7,20}) \qquad (2.11a)$$

$$HS^- \rightarrow S^{-2} + H^+ \quad (10^{-11,89}) \qquad (2.11b)$$

From the cited reactions and the constants it is evident, that the major fraction of sulfide is present in the gaseous form (H_2S) only at pH- values well below neutrality.

2.12 Influence of Temperature on Solubility

When gases dissolve in water, this process is generally accompanied by liberation of heat ΔH. According to the Le Chatelier principle, increase of temperature results in a decrease of solubility, therefore. Since the distribution coefficient k_D represents an equilibrium constant, van 't Hoff's equation may be applied to generalize the temperature dependence:

$$\frac{d\,(\ln k_D)}{dT} = \frac{\Delta H}{RT^2} \qquad (2.12)$$

Where R = universal gas constant
T = absolute temperature K
ΔH = change of heat content accompanying the absorption of 1 mole of gas (J/mole)

By integration of eq. 2.12 between the limits T_1 and T_2, assuming ΔH to be constant over this range, the following expression is obtained

$$\ln \frac{(k_D)_2}{(k_D)_1} = \frac{\Delta H}{R} \cdot \frac{T_2 - T_1}{T_1 \cdot T_2} \tag{2.13}$$

Eq. 2.13 may be simplified due to the fact, that the product $T_1 \cdot T_2$ does not change significantly within the temperature range encoutered in sanitary engineering gas transfer operations. Thus, by assuming $\Delta H/R.T_1.T_2$ = const, the following approximation is obtained:

$$(k_D)_2 = (k_D)_1 \cdot e^{\text{const } (T_2-T_1)} \tag{2.14}$$

Eq. 2.13 and 2.14 are but applicable over a narrow range of temperatures since ΔH is a function of temperature and concentration. They are useful for purposes of interpolation to obtain k_D-values for temperatures other than stated in table 2.1. Since at constant partial pressure (or at constant c_g) of the gas in the gas phase c_s is proportional to k_D, eq. 2.13 and 2.14 may also be applied to approximate the temperature dependence of c_s.

More precise estimates of the solubility may be obtained experimentally only. For oxygen, the saturation concentration of water exposed to water vapor saturated air is given in table 2.3. In this case, application of eq. 2.14 does not result in a good fit of the data of table 2.3, probably because a significant change of ΔH occurs within the temperature range of interest. Better fits are obtained by empirical formulae:

$$c_s = \frac{468}{31{,}6 + T^{\circ}C} \quad (g/m^3) \tag{2.15}$$

for $4 \leq T \leq 30^{\circ}C$

and $$c_s = 14{,}652 - 4{,}1022 \cdot 10^{-1} \cdot T + 7{,}9910 \cdot 10^{-3} \cdot T^2 - 7{,}7774 \cdot 10^{-5} \cdot T^3 \quad (g/m^3) \tag{2.16}$$

2.13 Influence of Impurities on Solubility

The distribution coefficient as defined in eq. 2.1 and as given in table 2.1 is valid only for pure water. Other constituent that may be contained in the water influence the solubility of gases, a fact that may be expressed by an activity coefficient γ:

$$c_s = \frac{k_D}{\gamma} \cdot c_g \tag{2.17}$$

For pure water $\gamma = 1$, whereas γ generally increases as the concentration of substances dissolved in water rises, thus lowering the solubility. This influence of the concentration of impurities c_{imp} on the activity coefficient is represented by the following empirical formulae:

for non-electrolytes

$$\log \gamma = f \cdot c_{imp} \tag{2.18}$$

for electrolytes

$$\log \gamma = f \cdot I \tag{2.19}$$

where f = a constant depending on the matter dissolved in water
I = ionic strength of electrolyte

Whereas c_{imp} and I can be obtained from measurements, f has to be determined experimentally for each solute, limiting the practical use of this approach, especially because little information on f is available. Concerning the influence of salts dissolved in sea water on the solubility of oxygen, an empirical formula has been developed from the data given in table 2.3:

$$\frac{1}{\gamma} = 1 - 9.10^{-6} . c_{imp} \tag{2.20}$$

where c_{imp} = salinity of the sea water expressed in g/m^3 of chloride.

Finally, dissolved substances lower the vapor pressure of water, thus increasing the partial pressure of other gases.
Volatile solutes, however, exert a certain partial pressure in the gas phase, which reduces the partial pressure of other gases in the gas mixture. Often these influences are not of great significance and

hence neglected.

From the many influences on the solubility of gases and their uncertainties (especially impurities) it is evident, that saturation concentrations as obtained from table 2.1 and/or table 2.3 for pure water may not be directly applied to water or especially to sewage with great accuracy. Experimental determination of the solubility is rather required in such cases.

2.2 Diffusion

The phenomenon of diffusion may be described as the tendency of any substance to spread uniformly throughout the space available to it. Obviously, this holds in gas transfer operations for the gaseous phase as well as for the liquid. However, since the diffusion of gases in the gaseous phase is much faster than in the liquid (about 10^4 times) more attention is generally paid to diffusion phenomena in the liquid phase in gas transfer operations in sanitary engineering.

For a quiescent body of water of unlimited depth contacting the gas by an area of A the rate of mass transfer dM/dt as a consequence of diffusion of the gas molecules in the liquid phase defined by Fick's Law

$$\frac{dM}{dt} = -D \cdot A \cdot \frac{\partial c}{\partial x} \quad (g/s) \tag{2.21}$$

where D = coefficient of molecular diffusion (m^2/s)
x = the distance from the interfacial area A
$\partial c/\partial x$ = concentration gradient

Fick's Law is written as partial differential equation because the concentration gradient varies during diffusion. It is important to recognize that solely the concentration gradient determines the rate of diffusion per unit area for a certain gas. The minus sign refers to the fact, that the direction of diffusion is opposite to that of the positive concentration gradient.
Values for the coefficient of molecular diffusion of gases in water are given in table 2.4. In dependence of the gas and the temperature they range from 1 to 7.10^{-9} m^2/s.

As a consequence of the process of molecular diffusion the gas concentration in liquid phase is increasing. The concentrations c(t, x) in the body of water are dependent on the distance x from the interfacial area A and on the time t elapsed. This can quantitatively be described by partial integration of eq. 2.21 assuming an initial gas content of c_o of the bulk of the liquid and immediate saturation (c_s) at the interface A, by

$$c(t, x) = c_o + \frac{c_s - c_o}{\sqrt{\pi Dt}} \int_x^\infty \exp(-x^2/4.Dt) \; . \; dx \qquad (2.22)$$

The practical use of eq. 2.22 is very limited, because the integral cannot be solved directly. Qualitatively, eq. 2.22 is depicted in fig. 2.1 to show the dependency of c on t and x, c(t, x) being expressed in terms of the saturation percentage $c(t, x)/c_s$.

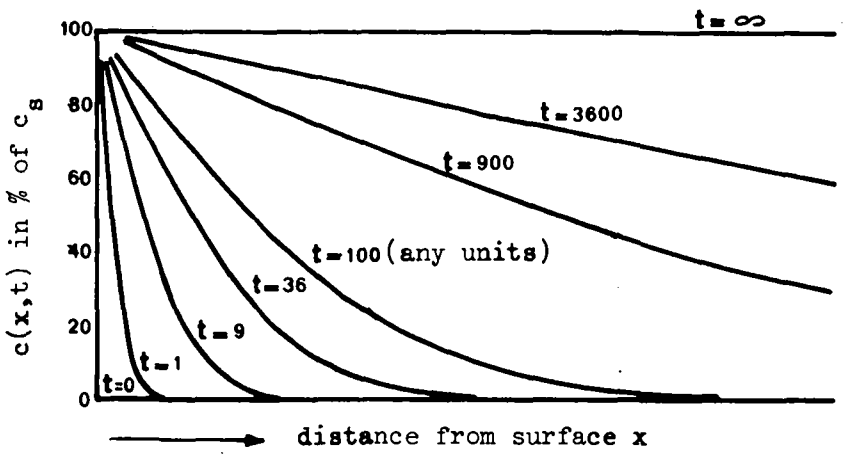

Fig. 2.1 THEORETICAL EFFECT OF TIME ON CONCENTRATION DISTRIBUTION OF DISSOLVED GAS IN A LIQUID DURING ABSORPTION BY MOLECULAR DIFFUSION, t = TIME SINCE EXPOSURE. ALL VALUES ARE RELATIVE.

The total amount of gas M (g), that has been absorbed through the surface area A during the time t, is independent of x, obviously, and amounts to

$$M = 2 \; . \; A \; . \; (c_s - c_o) \sqrt{\frac{Dt}{\pi}} \qquad (g) \qquad (2.23)$$

under conditions of unlimited depth of the water body. Nevertheless, eq. 2.23 can be applied for estimating the absorbed amount of gas M also for limited depth with fair accuracy, if the depth is not too small and the time of diffusion not too long, since diffusion is a very slow process and only very little gas is brought into the deeper layers of the water body (compare fig. 2.1). The rate of gas absorption through A is obtained by differentiation of eq. 2.23 with respect to time t:

$$\frac{dM}{dt} = A \cdot (c_s - c_o) \sqrt{D/\pi t} \quad (g/s) \qquad (2.24)$$

It is infinite at t = o and drops down very quickly to extremely low values.

Example: A quiescent body of oxygen-free water of a depth of 2,0 m and a temperature of 20°C is exposed to air at a pressure of 104,0 kPa. How much oxygen is absorbed during one day? Find the absorption rate after 1 second, 1 minute, 1 hour, and 24 hours.

a) The mass of oxygen absorbed during one day is estimated by means of eq. 2.23 as

$$\frac{M}{A} = 2 \cdot (c_s - c_o) \sqrt{\frac{Dt}{\pi}} \quad (g/m^2)$$

with

$c_o = 0$
$c_s = 9{,}42\ g/m^3$ (see foregoing example)
$D = 1{,}8 \cdot 10^{-9}\ m^2/s$
$t = 86\,400\ s$

Hence

$$M/A = 2 \cdot (9{,}42 - 0) \cdot \sqrt{1{,}8 \cdot 10^{-9} \cdot 86\,400/\pi}$$

$$= 0{,}133\ g/m^2 \text{ during one day}$$

b) The rate of oxygen absorption is computed with eq. 2.24 as

$$\frac{dM}{dt.A} = (c_s - c_o) \cdot \sqrt{D/\pi \cdot t}$$

$$= (9{,}42 - 0) \cdot \sqrt{1{,}8 \cdot 10^{-9}/\pi \cdot t}$$

and amounts after

1 second to	225	$\cdot 10^{-6}$	$g/m^2 \cdot s$
1 minute to	29,1	$\cdot 10^{-6}$	$g/m^2 \cdot s$
1 hour to	3,76	$\cdot 10^{-6}$	$g/m^2 \cdot s$
1 day to	0,767	$\cdot 10^{-6}$	$g/m^2 \cdot s$

In the beginning of this section a quiescent body of water has been assumed: no change of elements of the liquid-gas interface and no mixing within the gas and liquid volume have been presumed. Hence the given equations hold also for laminar flow, where no renewal of the interfacial area A and no eddies are present. With turbulent flow a second mechanism of displacement of solutes within the solution has to be considered, namely the eddy diffusion. Turbulent flow is characterized by the motion of fluid particles, which is irregular with respect to direction, magnitude and time. These properties are described by the Prandtl theory. Eddies are assumed to move with an average velocity u (m/s) perpendicular to the direction of the net flow over an average length, the Prandtl mixing length l. This interchange of fluid particles contributes to equalize the concentration of a solute within the solution and hence shows the same effect as molecular diffusion. In contrast to the phenomeon of the latter type it is called eddy diffusion, the coefficient of eddy diffusion D_E being defined in its most simple form by the product of u and l

$$D_E = u \cdot l \quad (m^2/s) \tag{2.25}$$

Since u and l depend on the hydrodynamic conditions, so does the coefficient of eddy diffusion. Obviously the turbulent hydrodynamic conditions vary over the volume occupied by the liquid, reaching larger values of u.l in the core which diminish at the interfaces, where solely molecular diffusion is responsible for gas transfer.
Molecular and eddy diffusion are additive. Thus, a total diffusion coefficient may be stated as

$$D_t = D + D_E \quad (m^2/s) \tag{2.26}$$

Molecular diffusion is accelerated by increasing the temperature. The temperature dependence of D may be expressed by van 't Hoff's Law analogous to eq. 2.14 as

$$D_2 = D_1 \cdot e^{\text{const.}(T_2-T_1)} \tag{2.27}$$

From the data of table 2.4 the "const." for eq. 2.27 is estimated to cover a range from 0,0255 to 0,0300 for the cited gases.
Another dependence uses the Nernst-Einstein relationship:

$$\frac{D.\mu}{T} = \text{const.} \tag{2.27a}$$

where μ = absolute viscosity (g/m.s)
T = temperature (K)

2.3 Gas Transfer Coefficients

2.31 The Concept of Gas Transfer Coefficients

During the process of gas transfer from a gas phase into water a distribution of the gas concentration in both phases may be imagined as given by figure 2.2. The decrease of concentration in the gas phase

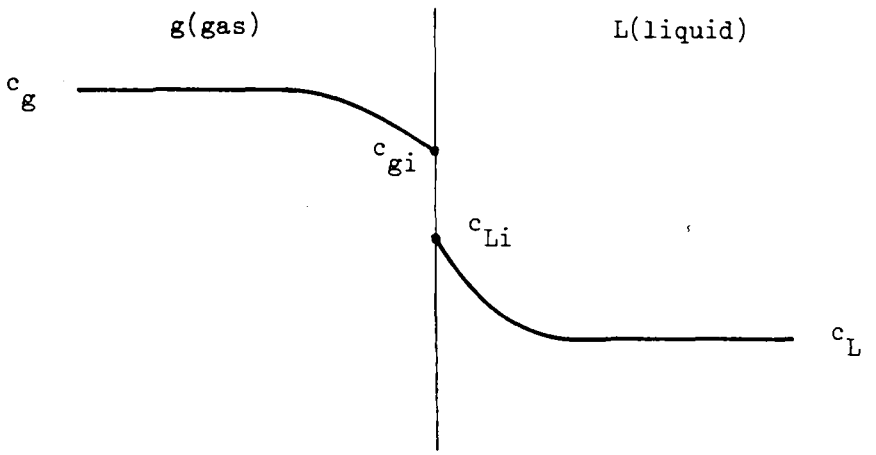

Fig. 2.2 DISTRIBUTION OF THE GAS CONCENTRATION AT A GAS-LIQUID INTERFACE

in direction to the interface from c_g to c_{gi} (concentration in the gas phase at the interface) is induced by absorption of gas in the liquid phase. According to eq. 2.1 c_{gi} is in equilibrium with the gas concentration in the liquid at the interface c_{Li}. The gas concentration in the bulk of the solution is c_L. Since in accordance with Fick's Law (eq. 2.21) the mass transport per unit time (g/s) is proportional to the concentration difference, the following relationship may be stated

for the gas phase $m = k_g \cdot A \cdot (c_g - c_{gi})$ (g/s) (2.28)

and for the liquid phase $m = k_L \cdot A \cdot (c_{Li} - c_L)$ (g/s) (2.29)

where k_g = partial gas transfer coefficient for the gas phase (m/s)

k_L = partial gas transfer coefficient for the liquid phase (m/s)

c_{gi} and c_{Li} are generally not known. They may, however, be eleminated from eq. 2.28 and 2.29 by applying eq. 2.1

$$c_{Li} = k_D \cdot c_{gi}$$

and equating both equations to give

$$m = \left(\frac{1}{k_L} + \frac{k_D}{k_g}\right)^{-1} \cdot A \cdot (k_D \cdot c_g - c_L) \qquad (2.30)$$

Thus it is seen, that the (total) gas transfer coefficient K_L is composed of both the partial coefficients and the distribution coefficient:

$$\frac{1}{K_L} = \frac{1}{k_L} + \frac{k_D}{k_g} \quad (s/m) \qquad (2.31)$$

and eq. 2.30 may hence be rewritten as

$$m = A \cdot K_L \cdot (k_D \cdot c_g - c_L) \qquad (g/s) \qquad (2.32)$$

For the ease of further discussion the result is anticipated, that (in accordance with the penetration theory) the partial coefficients of gas transfer are proportional to the square root of the coefficients of molecular diffusion D of the respective phase. Since the diffusion coefficients of gases in air and in water are in order of 10^{-5} and 10^{-9} m^2/s, respectively, the ratio of the transfer coefficients may be estimated to be of the order of $k_g/k_L = \sqrt{10^4} = 100$. Even with fairly well soluble gases (e.g. ammonia, carbon dioxide, hydrogen sulfide), the value of k_D/k_g will therefore be very small with respect to $1/k_L$. Thus, the influence of the gas transfer coefficient of the gaseous phase may be neglected, which is equivalent to choosing

$$K_L = k_L \qquad (2.33)$$

and consequently

$$m = k_L \cdot A \cdot (k_D \cdot c_g - c_L) \qquad (g/s) \qquad (2.34)$$

Whereas eq. 2.32 and 2.34 describe the overall rate of gas transfer by a more or less arbitrarily chosen parameter - the gas transfer coefficient - a relation between this parameter and the coefficient of diffusion is developed by a theoretical approach of the mechanism of gas transfer. Some of the theories advanced to describe this mechanism will be discussed in the sections to follow.

2.32 Theories on the Mechanism of Gas Transfer

2.321 Film Theory (2)

The model underlying the film theory is the following (fig. 2.3):

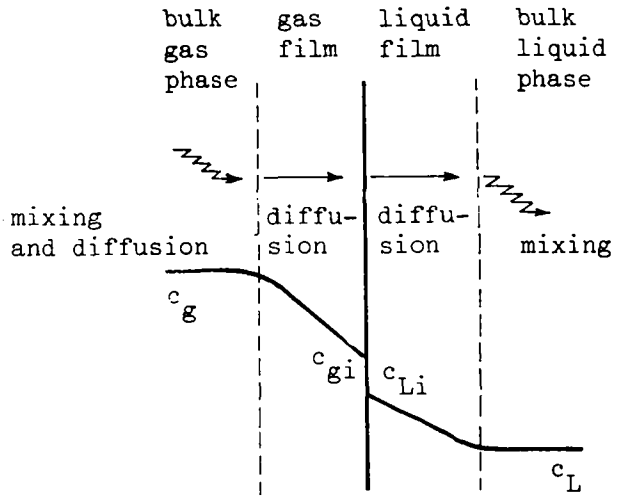

Fig. 2.3 MODEL OF THE FILM-THEORY

by molecular and eddy diffusion and by mixing (convection) the gas to be absorbed is transported into the "gas film" at the interface. This gas film is thought to be stagnant and to have a thickness d_g depending on the degree of turbulence in the gas phase. The same holds for the liquid film with a thickness of d_L. Since the rate controling mechanism of gas transport through both film is only molecular diffusion, which is a very slow process compared with eddy diffusion and convection, it are the films that offer the sole resistance to gas transfer. Applying Fick's Law to the process of diffusion through the films and assuming steady state conditions of turbulence (d_g and d_L are constant) and of gas concentration in the films (c_{gi} and c_{Li} are constant), the following relationships are obtained

$$\text{for the gas films} \quad m = D_g \cdot A \cdot \frac{c_g - c_{gi}}{d_g} \qquad (2.35)$$

$$\text{and for the liquid film} \quad m = D \cdot A \cdot \frac{c_{Li} - c_L}{d_L} \qquad (2.36)$$

A comparison of eq. 2.35 and 2.36 with 2.28 and 2.29, respectively, shows that according to the film theory the coefficients of transfer are proportional to the coefficients of diffusion. Neglecting the influence of k_g on the total coefficient of transfer K_L as proposed in section 2.31, the rate of gas transfer according to the film theory is

$$m = \frac{D}{d_L} \cdot A.(k_D.c_g - c_L) \qquad (2.37)$$

and hence

$$k_L = \frac{D}{d_L} \qquad (2.38)$$

This result is contradictory tc experience, showing a much less pronounced dependency of k_L of D. This fact and reasons to be discussed in the following section have caused the film theory to be largely discredited.

2.322 Penetration Theory (3)

The model of the penetration theory does not proceed from stagnant films but rather from fluid elements which are briefly exposed to the gas phase at the interface of the liquid. During this time of exposure the gas diffuses into the fluid element: it "penetrates" into the liquid. In contrast to the film theory this process of penetration is described by unsteady diffusion, the time of exposure being too short for a steady state of diffusion to develop.

Thus Fick's Law (eq. 2.21), the solution of which has been qualitatively given in fig. 2.1, is applied to describe the mechanism of unsteady diffusion during the time of exposure t. Since this time is generally very short in gas transfer operations (< 0,1 s) an approximation of the solution (eq. 2.22) is used. This approximation is based on replacing the slightly curved depth-concentration relationship by a linear one as stated in figure 2.4. The depth-concentration lines are then defined by the concentration $k_D.c_g = c_s$ at the surface (x = 0) and by the concentration in the bulk of the liquid c_L (= c_o = initial concentration) at some distance x_p from the surface. The distance x_p, the penetration depth, increases with increasing time: $x_p = f(t)$. This function can be obtained by reading the concentration gradient from fig. 2.4 as $\partial c/\partial x = -(c_s-c_L)/x_p$, inserting it into eq. 2.21 and equating with eq. 2.24:

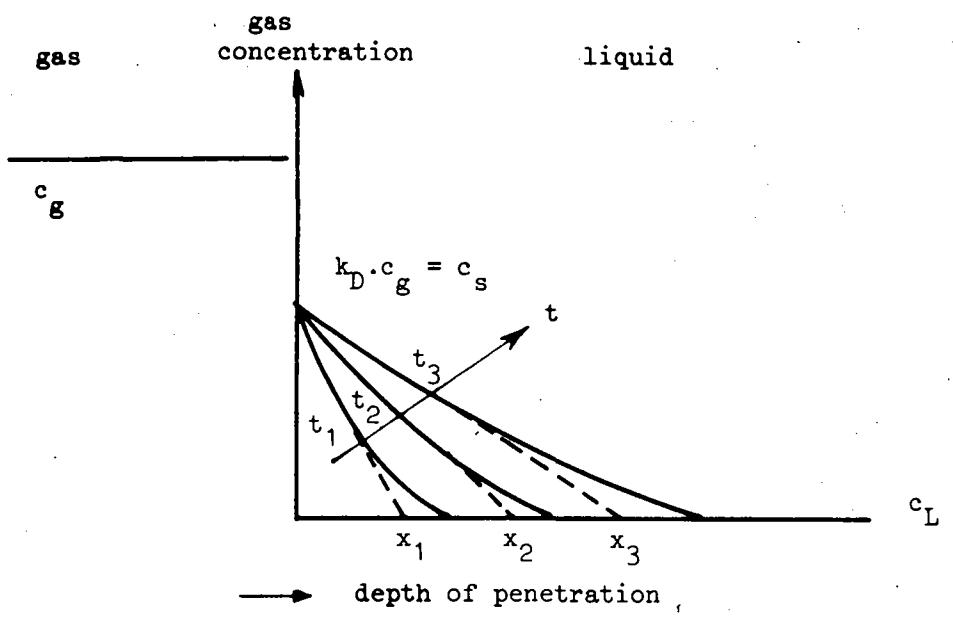

Fig. 2.4 PENETRATION OF A GAS INTO A LIQUID BY UNSTEADY DIFFUSION

$$\frac{dM}{dt} = - D \cdot A \cdot \frac{\partial c}{\partial x} = D \cdot A \cdot \frac{c_s - c_L}{x_p} = A \cdot (c_s - c_L) \cdot \sqrt{D/\pi . t} \quad (2.39)$$

Solving for x_p we get

$$x_p = \sqrt{\pi \cdot D \cdot t} \quad (2.40)$$

Example: In order to get an impression of the magnitude of the depth of penetration in dependence of time, compute the x_p's for the different times of exposure of the example in section 2.2.

According to eq. 2.40 the penetration depth is estimated as $x_p = \sqrt{\pi \cdot 1{,}8 \cdot 10^{-9} \cdot t}$ and amounts after

1 second to $0{,}0752 \cdot 10^{-3}$ m
1 minute to $0{,}582 \cdot 10^{-3}$ m
1 hour to $4{,}51 \cdot 10^{-3}$ m
1 day to $22{,}1 \cdot 10^{-3}$ m

During the time of exposure of the liquid interface to the gas, the gases "penetrate" into the liquid at a diminishing rate, as described by eq. 2.39. The total mass of gas absorbed during this time is given by eq. 2.23 as

$$M = 2 \cdot A \cdot (k_D \cdot c_g - c_L) \cdot \sqrt{\frac{Dt}{\pi}}$$

Hence the average absorption rate m (g/s) during the time t is defined by

$$\frac{M}{t} = m = 2 \cdot A \cdot (k_D \cdot c_g - c_L) \cdot \sqrt{\frac{D}{\pi t}} \quad (g/s) \tag{2.41}$$

The only unknown parameter of eq. 2.41 is now the time of exposure t. The penetration theory assumes it to be constant

$$t = t_c \tag{2.42}$$

for a gas transfer process operated under steady state condition. As will be shown later, t_c can be estimated in some cases. Inserting the constant time of exposure t_c into eq. 2.41 we get the final form of the rate expression for gas absorption as proposed by the penetration theory:

$$m = 2 \cdot \sqrt{\frac{D}{\pi . t_c}} \cdot A \cdot (k_D \cdot c_g - c_L) \quad (g/s) \tag{2.43}$$

Thus it is seen (compare eq. 2.43 and 2.34) that according to the penetration theory

$$k_L = 2 \cdot \sqrt{\frac{D}{\pi . t_c}} \tag{2.44}$$

stating that the coefficient of gas transfer is proportional to the root of the coefficient of diffusion.

Assumption of a constant time of exposure of fluid elements to the gas phase implies that there is also a constant rate r_c (s^{-1}) of renewal of the surface

$$r_c = 1/t_c \quad (s^{-1}) \tag{2.45}$$

Taking r_c instead of t_c, the coefficient of gas transfer becomes

$$k_L = 2 \cdot \sqrt{\frac{D . r_c}{\pi}} \tag{2.46}$$

2.323 Surface Renewal Theory (4)

The model underlying the surface renewal theory is equal to that of the penetration theory: unsteady diffusion (penetration) of the gas into liquid elements exposed to the gas phase. Thus eq. 2.39 is being used to describe the time dependence of mass transfer during the exposure. However, this theory does not assume this time to be constant but rather to follow a frequency distribution f(t) with ages of the fluid elements (= time of exposure) ranging from zero to infinity. More specific, the theory is based on the assumption, that the fraction of the surface having ages between t and t + dt is given by $f(t)dt = s.e^{-s.t}dt$. This is true if a surface element of any age always has the chance of s.dt of being replaced; in other words, if each surface element is being renewed with a frequency s, independent of its age. Inserting the frequency distribution of ages into eq. 2.39, the average rate of gas transfer is

$$m = \int_0^\infty A \cdot (k_D.c_g - c_L) \cdot \sqrt{\frac{D}{\pi.t}} \cdot s.e^{-st}\, dt$$

$$= \sqrt{D.s} \cdot A \cdot (k_D.c_g - c_L) \qquad (2.47)$$

Thus it is seen that the surface renewal theory forecasts

$$k_L = \sqrt{D.s} \qquad (2.48)$$

2.324 Film-Surface-Renewal Theory (5)

This theory attempts a combination of the film theory and the surface renewal theory in principle, i.e. a combination of steady and unsteady diffusion. The reasoning, that led to this approach lies in the fact that at conditions of very low turbulence (e.g. stagnant or very slow streaming rivers) the exposure of surface elements to the gas phase may be sufficiently long for a steady type of diffusion to develop. Moreover, the theory argues that during unsteady diffusion under these conditions the penetration depth may theoretically reach into the region of constant gas concentration where molecular and eddy diffusion and mixing processes govern the dispersion process and not solely molecular diffusion. Applying the surface renewal concept the theory is

able to state the gas transfer coefficient as a function of the average rate of surface renewal s and max $x = d_L$

$$k_L = \sqrt{D.s} \cdot \coth \sqrt{\frac{s.d_L^2}{D}} \qquad (2.49)$$

The properties of this function are such, that at low turbulence ($s \to o$) the film theory applies ($k_L = D/d_L$), whereas at high turbulence the second term of eq. 2.49 approaches 1 and k_L is governed by the rate of surface renewal s.

2.325 Comparison of the Discussed Theories

The difference of the theories with respect to the underlying model of diffusion (steady and/or unsteady) and the hydrodynamic properties of the liquid at the surface (stagnant films or continuous renewal of surface) has been discussed in the foregoing sections and is summarized in the following table.

theory	properties of liquid surface	type of diffusion	k_L =
film	stagnant	steady	D/d_L
penetration	renewal of surface, constant time of exposure of fluid elements to surface	unsteady	$2.\sqrt{D/\pi.t_c}$
surface renewal	renewal of surface, frequency distribution for time of exposure to gas phase	unsteady	$\sqrt{D.s}$
film-surface-renewal	stagnant and continuously renewed surface depending on degree of turbulence	steady and/or unsteady	$\sqrt{D.s}\coth\sqrt{\frac{s.d_L^2}{D}}$

The table also contains the relationship between k_L and the parameters determining the gas transfer coefficient according to the respective theory. The prime difference is that the film theory forecasts k_L to be proportional to D, whereas both the following theories state k_L proportional to $\sqrt{D}$. The last theory basically shows k_L to be pro-

portional to D^n, n varying from 1 (s = o) to 0,5 at high turbulence. Deviations from n = 0,5 are less than 5 % for $\sqrt{s.d_L^2/D} > 1,86$, less than 1 % for > 2,56, and less than 0,5 % for > 3,0.

With the exception of the combined film-surface-renewal theory each theory contains one unknown parameter, which is basically dependent on the hydrodynamic conditions of the fluid. The experience, that k_L increases slightly with increasing turbulence, is explained by the theories on the basis of changing this factor. Thus, increase of turbulence would

a) decrease the film thickness d_L

b) decrease the time of exposure of the fluid elements t_c to the gas phase

c) increase the average rate of surface renewal s

d) decrease d_L and increase s

Although the physical interpretation of k_L differs from theory to theory, a relation between the unknown parameters may be obtained by numerically equalizing the k_L's. This yields for the first 3 theories the following relationship, which may be useful when interpreting k_L-data by some of the theories.

$$d_L = \sqrt{D.\pi.t_c} = \sqrt{D/s} = x_p \qquad (2.50)$$

$$t_c = d_L^2 / D.\pi = 1/s.\pi \qquad (2.51)$$

$$s = D/d_L^2 = 1/t_c.\pi \qquad (2.52)$$

As already mentioned, the film theory has largely been discredited due to its assumption of stagnant films and steady diffusion, a process that cannot develop within the brief time of exposure of fluid elements to the gas phase, generally encountered in transfer operations in sanitary engineering. Applying unsteady diffusion, the penetration theory may be more useful than the surface renewal theory, because the time of interfacial contact t_c may be estimated in some cases. The average rate of surface renewal s, however, cannot be measured but rather recomputed from k_L-values and the coefficient of diffusion (eq. 2.48). Thus, the penetration theory would deserve predominant application in gas transfer operations in the realm of sanitary engineering.

2.33 Some Applications of the Penetration Theory

As already mentioned the coefficient of gas transfer k_L may be estimated for transfer operations when the time of interfacial contact of a fluid element with the gaseous phase can be assessed. In bubble aeration t_c may be computed from the rising velocity with respect to water v_r and the bubble diameter d_B as $t_c = d_B/v_r$. Then the coefficient of gas transfer becomes

$$k_L = 2 \sqrt{\frac{D.v_r}{\pi.d_B}} \qquad (2.53)$$

In figure 2.5 the rising velocity of bubbles in stagnant water is given as a function of d_B. The corresponding times of interfacial contact $t_c = d_B/v_r$ range from 0,003 to 0,1 seconds as may be seen from the figure. Application of eq. 2.53 then gives the k_L-values in dependance of d_B.

The solid lines apply to pure water, the dashed lines (for bubbles of approximately $0{,}5.10^{-3} \leq d_B \leq 10.10^{-3}$ m) to tap water. It is interest-

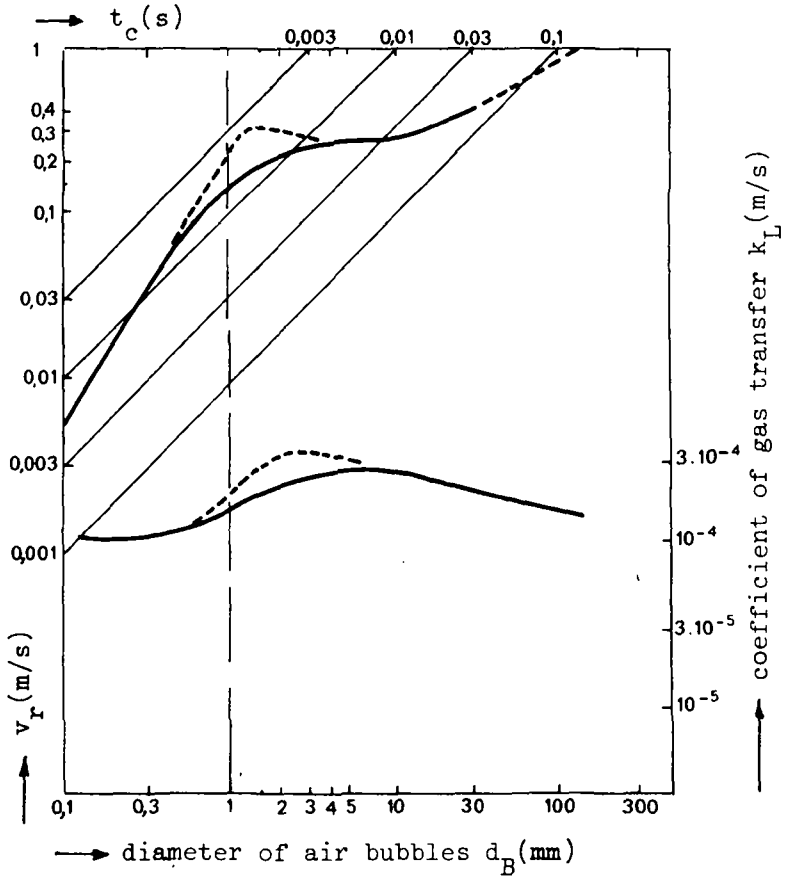

Fig. 2.5 RISING VELOCITY OF AIR BUBBLES IN WATER AND THE COEFFICIENT OF GAS TRANSFER AND TIME OF EXPOSURE ACCORDING TO THE PENETRATION THEORY

ing to note that the coefficient of gas transfer (for oxygen in this case) varies but over a narrow range of approximately $10^{-4} \leq k_L \leq 3.10^{-4}$ m/s, averaging $1,5.10^{-4}$ m/s. This includes that the gas transfer per unit area A (compare eq. 2.34) does not differ greatly but that the total gas transfer is mainly determined by the total bubble surface area present in the liquid phase. This area is proportional to d_B^2. Since, however, the size and size distribution of d_B in practical diffusion operations is difficult to estimate exactly, only empirical relationships can be applied to forecast the rate of gas transfer.

Spray aeration is considered as a second example. Assume droplets to be formed of 6 mm diameter falling with a velocity of 7 m/s over a length of 3,5 m. The time of contact is 3,5/7 = 0,5 s giving a value for k_L at 20°C for oxygen of $k_L = 2\sqrt{1,8.10^{-9}/\pi.0,5} = 0,68.10^{-4}$ m/s and for carbon dioxide with D = $1,68.10^{-9}$ m^2/s of.

$k_L = \sqrt{1,68.10^{-9}/\pi.0,5} = 0,65.10^{-4}$ m/s.

Again, k_L lies in the same order of magnitude as for bubble aeration, being somewhat less, however. Both examples are realistic and show that in gas transfer operation the time of exposure is very short (< 0,5 s). The corresponding penetration depths are less than 5.10^{-5}m (0,05 mm) when applying an average coefficient of diffusion for gases of $1,5.10^{-9}$ m^2/s in connection with eq. 2.40. This thin layer is hardly influenced by increasing the turbulence of the liquid phase, so that k_L is primarily determined by molecular and not by eddy diffusion. Increase of turbulence will, however, increase the interfacial area (for instance by producing smaller bubbles or droplets) and decrease the time of exposure t_c and thus thus promote the rate of gas transfer.

2.34 Factors Affecting the Gas Transfer Coefficient

The main factors affecting the gas transfer coefficient are the temperature and the concentration and nature of hydrophobic substances. Whereas temperature influences all gas transfer operations, the presence of hydrophobic matter is of importance only in connection with the oxygenation of sewage and sewage-sludge mixtures (activated sludge process), where significant concentrations of hydrophobic matter, especially surface active agents, are to be expected.

The temperature dependence of the coefficient of gas transfer may be seen from eq. 2.44, stating k_L as a function of D and t_c, and from eq. 2.27 and 2.27a giving the influence of temperature on the coefficient of diffusion. Thus there are two temperature influences to be conceived: first the coefficient of diffusion increases with increasing temperature and secondly, the viscosity is decreased with increasing temperature, thus increasing the rising velocity of bubbles and thereby decreasing the time of exposure $t_c = d_B/v_r$. Finally the local hydrodynamics of the interface are altered (Brownian movement) in such a fashion as to augment the coefficient of gas transfer. Moreover the rate of gas transfer (eq. 2.34) is influenced by a change of temperature through alteration of the total interfacial area A and the driving force $(k_D.c_g - c_L)$. Although these factors do not refer to the temperature dependence of k_L, they are briefly discussed here.

The increase of A is mainly caused by the temperature dependence of the surface tension. In bubble aeration, for instance, the diameter of spherical bubbles is $d_B = 4\sigma/p$, σ being the surface tension and p the local pressure at the bubble surface. Thus by decreasing the surface tension by increasing the temperature, the average bubble diameter is decreased giving rize to a greater interfacial area A.

The temperature dependence of k_D results in a decrease of the saturation value of a gas with increasing temperature, thus lowering the driving force and thereby the rate of gas transfer for absorption processes and increasing the driving force and rate for stripping.

Combining all mentioned effects of temperature on the rate of gas transfer (effects on k_L and A), the following function may be principally applied for generalization

$$(k_L.\frac{A}{V})_{T_2} = (k_L.\frac{A}{V})_{T_1} \cdot \theta^{T_2-T_1} \qquad (2.54)$$

The temperature coefficient θ for oxygenation of sewage, for instance, has been found to be in the range of 1,016 to 1,047.

The influence of hydrophobic constituents and surface active agents on the rate of gas transfer is manifold. Such matter has the tendency to accumulate at interfacial surfaces, a process which is quantitavely described by the "Gibbs adsorption equation":

$$S = -\frac{c}{RT} \cdot \frac{d\sigma}{dc} \qquad (2.55)$$

where in this case

c = concentration of hydrophobic substance in the bulk of the solution (g/m^3)

S = excess concentration of hydrophobic substance at the surface (g/m^2) as compared with that of the bulk of the solution

R = universal gas constant

$d\sigma/dc$ = rate of increase of surface tension with increasing the concentration of the hydrophobic substance.

Since hydrophobic substances, especially surface active agents lower the surface tension ($d\sigma/dc < o!$) it is seen from eq. 2.55 that there is an excess concentration at the surface, the magnitude of which depends on the rate of decrease of the surface tension. By this excess the properties of the interfacial area are changed:

a) the rate of diffusion is generally lowered, due to the surface being covered with the hydrophobic substance

b) the hydrodynamic properties of the surface are changed by rendering the surface layer, normally strongly influenced by random motion, into a viscous layer. This phenomenon of "surface stagnation" or "quiescence" reduces the magnitude of k_L by lowering the rate of surface renewal. An example for the effect of the surface active agent AEROSOL O.T. on the oxygen transfer coefficient for bubble aeration (laboratory scale) is shown in figure 2.6.

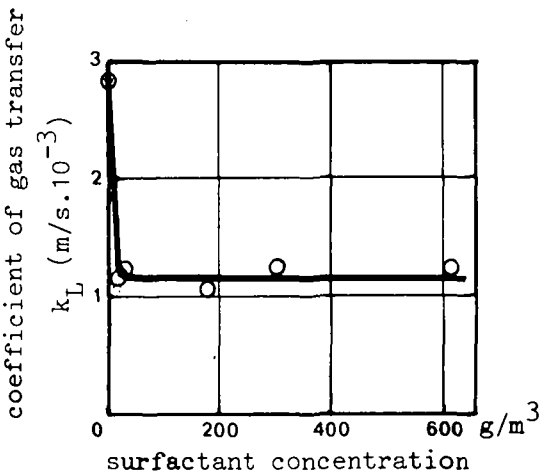

Fig. 2.6 EFFECT OF THE SURFACTANT AEROSOL O.T. ON THE COEFFICIENT OF GAS TRANSFER

The magnitude of the excess concentration at the gas-liquid interface is of dynamic nature. When an interface is being formed it takes a certain time t_E until the equilibrium between the bulk concentration is established. If now the average time of exposure of the interface t_c is smaller than t_E, the influence of the surface active agents on k_L is much less than for the case where $t_c > t_E$. Figure 2.7 gives an example for this type of dynamic surface concentration. It is seen that with a bulk concentration of 800 g/m^3 of the SAA Dodecyltrimethylammonium chloride it takes about 0,01 seconds to establish the equilibrium completely, whereas with a bulk concentration of 400 g/m^3 it is not reached within 0,05 seconds under the hydrodynamic conditions of the experiment.

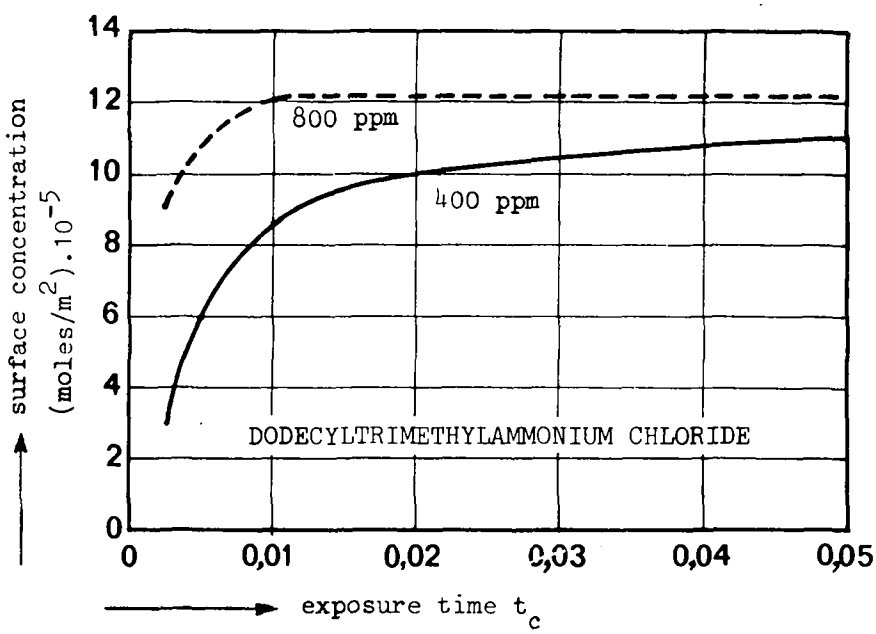

Fig. 2.7 DYNAMIC NATURE OF SURFACE CONCENTRATION

Finally, also the total rate of gas transfer (eq. 2.34) is influenced by the presence of surface active agents or hydrophobic matter by giving rise to a larger interfacial area A due to the lowering of the surface tension σ. Summarizing the effects of hydrophobic matter on the rate of gas transfer it may be stated that

a) a reduction of the rate via the coefficient of diffusion and the alteration of the hydrodynamic properties of the interface is to be expected, the magnitude of which depends on the time of exposure of these interfaces or on the rate of surface renewal (influences on k_L)

b) an increase of the rate is to be expected due to the increase of the interfacial area as a consequence of the reduction of the surface tension.

The magnitude of the influence (a) and/or (b) depends greatly on the system of gas transfer operation and moreover on the physical and chemical structure of the hydrophobic matter. Thus, no general rules can be put foreward and the effect can be determined experimentally only.

2.4 Practical Approach to Gas Transfer Rate Formulations

The disadvantage of the cited rate formulation is that the diffusion coefficient D and the time of exposure of the interfacial area t_c have to be known to forecast the coefficient of gas transfer.
To finally determine the rate of gas transfer also the size of the interfacial area A has to be estimated.
Methods to determine these parameters are available. In bubble aeration for instance, the bubble size and its velocity can be measured to yield information on k_L and A. The same holds for spray aeration. Such estimates are of limited accuracy since they do not account for the rapid change of interfacial area during their information. It has been found for instance, that during the formation of bubbles or droplets a significant gas transfer take place which is not included in formulations as eq. 2.43. Although an evaluation of these effects by stating a seperate k_L-value for the formation period could be conceived of, this would give rise to intricate formulations of little practical value. In some cases, mechanical aeration for instance, it seems impossible to accurately determine the required parameters for an estimate of k_L. Consequently, other more practical approaches to the formulation of the rate of gas transfer have become quite common, which will be discussed in the sections to follow.

2.41 The Overall Gas Transfer Coefficient or Aeration Coefficient

Under steady state conditions of gas transfer operation the coefficient of diffusion D and the time of exposure t_c may be assumed constant, also for the process of formation of interfacial area, yielding a constant gas transfer coefficient k_L. Furthermore, the size of the interfacial area A and the specific surface area a = A/V may be taken constant. Thus under steady state conditions of operation a constant k_2 may be defined as

$$k_2 = 2 \cdot \frac{A}{V} \cdot \sqrt{\frac{D}{\pi . t_c}} = \frac{A}{V} \cdot k_L = a \cdot k_L \quad (1/s) \tag{2.56}$$

where k_2 or $k_L.a$ is the overall gas transfer coefficient. In accordance with eq. 2.43 the rate of gas transfer, expressed as the rate of concentration change, may then be written as

$$\frac{m}{V} = \frac{dc}{dt} = k_2.(c_s - c) \quad (g/m^3.s) \tag{2.57}$$

which integrates with c_o at $t = o$ to

$$c = c_s - (c_s - c_o).e^{-k_2.t} \tag{2.58}$$

or

$$\frac{c_s - c}{c_s - c_o} = e^{-k_2.t} \tag{2.59}$$

From eq. 2.57 and 2.58 it is seen that the difference between the saturation concentration and that at $t = o$ (c_o) decreases exponentially towards zero under steady state conditions of operation.
The overall gas transfer coefficient k_2 can easily be determined experimentally by measuring the change of concentration as a function of time and by plotting $\log (c_s - c)/(c_s - c_o)$ versus time according to eq. 2.58:

$$\log \frac{c_s - c}{c_s - c_o} = \log e^{-k_2.t} = -k_2.t.\log e$$

$$= - 0{,}4343.k_2.t \tag{2.60}$$

In evaluating gas transfer experiments knowledge of the saturation concentration c_s under the experimental steady state conditions is required. Temperature, dissolved substances, pressure (partial pressure of the examined gas in air!) are factors which influence c_s and may cause deviations from tabulated values. If c_s is not estimated correctly there will be deviations from the expected straight-line relationship. Numerical evaluation of k_2 and c_s under experimental conditions is facilitated by statistical methods (e.g. 7), being more powerful than graphical try and error procedures.

Example: In an oxygenation experiment the oxygen concentration was determined in intervals of 120 seconds as stated in the following table. Determine the overall gas transfer coefficient k_2.

t(s)	0	120	240	360	480	600	720	840
$c(g/m^3)$	3,8	5,2	6,3	7,2	7,9	8,4	8,8	9,2
$e^{-k_2 \cdot t}$	1,000	0,791	0,627	0,493	0,388	0,313	0,254	0,194

Assuming c_s = 10,5 g O_2/m^3 the third line of the table ($e^{-k_2 \cdot t}$) is calculated by means of eq. 2.59 and plotted in figure 2.8 versus time. The obtained straight line indicates a correct assumption of c_s. From the slope of the line 0,000840 (1/s) it follows, that k_2 = 0,00193 (1/s). From the data of c in figure 2.8 the influence of the driving force (c_s - c) is readily seen: the higher the oxygen (gas) concentration the lower is the rate of absorption by transfer.

2.42 The Efficiency Coefficient

With some transfer operations, e.g. cascades, weir aeration, it is difficult or impossible to determine the parameter time t contained in eq. 2.57 to 2.60. If now a constant time t_k is assumed for the aeration step under steady state conditions of operation, a generalization of the above formulations is arrived at by the following reasoning.

Let c_o be the gas constant at the inlet of the aerator and c_e that of the effluent. Then, according to equation 2.58

$$\frac{c_s - c_e}{c_s - c_o} = e^{-k_2 \cdot t_k} = \text{constant} = 1 - K \qquad (2.61)$$

From eq. 2.61 the rise (or decrease) in gas concentration (c_e - c_o) may be deducted to be

$$\frac{c_s - c_e}{c_s - c_o} = 1 + \frac{c_o - c_e}{c_s - c_o} = 1 - K$$

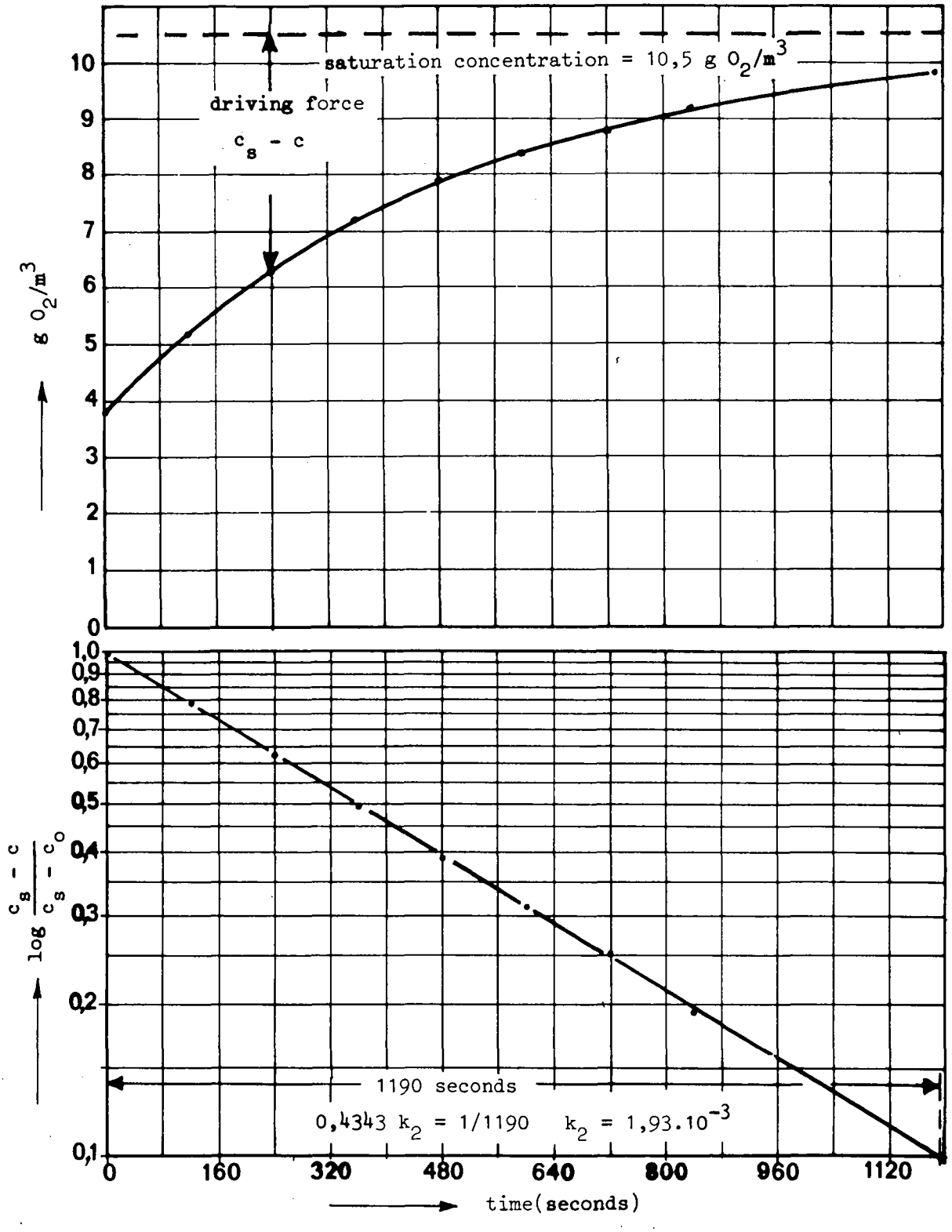

Fig. 2.8 GRAPHICAL REPRESENTATION OF AN OXYGENATION EXPERIMENT

yielding

$$(c_e - c_o) = K.(c_s - c_o) \tag{2.62}$$

Thus, the increase $(c_e - c_o)$ is proportional to the initial degree of undersaturation $(c_s - c_o)$, the proportionality constant K being according to eq. 2.61

$$K = 1 - e^{-k_2.t_k} \tag{2.63}$$

K can be designated as efficiency coefficient of the system.
A graphical representation of eq. 2.62 is given in figure 2.9, giving c_e at the ordinate versus c_o at the abscissa. The dashed line is represented by the equation $c_e = c_o$, the solid line by

$$c_e = K.c_s + c_o.\frac{c_s.(1-K)}{c_s}$$

The distance between the two lines is then given as

$$c_e - c_o = K.c_s + c_o(1-K) - c_o$$

$$= K.(c_s - c_o)$$

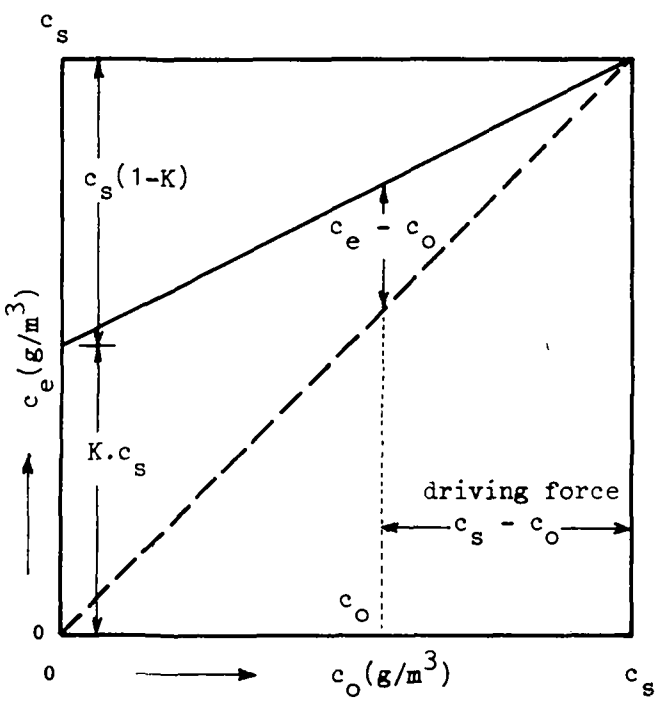

Fig. 2.9 APPLICATION OF THE EFFICIENCY COEFFICIENT K

Thus for a given c_o the increase in gas concentration can easily been read from the figure. Again this figure clearly shows the great influence of the driving force $(c_s - c_o)$ on the concentration increase. For the case $c_s = 0$ the rise in gas concentration will be $c_e - c_o = K.c_s$. Thus K states the fraction of the saturation concentration that will be gained when aerating gas-free water.

Example: A spray aerator was found to remove 10 g/m^3 of CO_2 at an initial CO_2 content of 26 g/m^3. Determine (a) the efficiency coefficient K and (b) the effluent concentration of water containing 41 g CO_2/m^3 when sprayed under the same hydraulic conditions. Assume a saturation concentration of c_s = 1 g CO_2/m^3.

a) According to eq. 2.62

$$K = (c_e - c_o)/(c_s - c_o) = -10/(1-26) = 0,4$$

b) From eq. 2.62 it follows

$$c_e = c_o + K.(c_s - c_o) = 41 + 0,4.(1-41)$$
$$= 41 - 16 = 25 \text{ g/m}^3$$

2.43 The Oxygenation Capacity

A third common approach to describe the rate of gas transfer is used in the field of oxygenation of water or of the mixed liquor of activated sludge tanks. Due to the consumption of oxygen by microbial degradation of the organic substances present in sewage, aeration does not lead to an increase of oxygen concentration but rather an equilibrium between the oxygen supply and consumption is established, leading to a certain oxygen concentration. The oxygenation capacity of an aeration system is then commonly defined as the rate of oxygen transfer at

a) a temperature of 10°C; to take into account the influence of temperature on c_s, D, t_c, and A/V;

b) a pressure of 101,3 kPa to take into account the influence of p on c_s;

c) an oxygen concentration of c = 0, which leads to a driving force of c_s.

Thus the oxygenation capacity oc is defined according to equation

2.57 and the cited conditions, as the rate of increase of oxygen concentration and is expressed by

$$oc = k_2 \cdot c_s' \qquad (g\ O_2/m^3.s) \tag{2.64}$$

where c_s' = oxygen saturation concentration in pure water at $T = 10^oC$ and $P = 101,3$ kPa, amounting to $11,3\ g/m^3$

Whereas the above definition refers to the possible increase of the oxygen content of a volume of water of $V(m^3)$, the oxygenation capacity OC (g/s) of an aeration system is given by the product

$$OC = V \cdot oc = k_2 \cdot V \cdot c_s' \qquad (g\ O_2/s) \tag{2.65}$$

The extensive use of this parameter in sewage treatment practice requires further detailed consideration.
The oc may be determined after estimating k_2 or after observing the increase in oxygen concentration from c_1 to c_2 within a time period from t_1 to t_2.
According to eq. 2.60 and 2.64 the oc-value is obtained by

$$oc = k_2 \cdot c_s' = 2,303 \cdot c_s' \cdot \frac{1}{t_2 - t_1} \cdot \log \frac{c_s - c_1}{c_s - c_2} \tag{2.66}$$

The two last terms of the right hand side of eq. 2.66 are identical to $0,4343.k_2$ and are commonly designated by tg α, tg α hence representing the overall coefficient of gas transfer (k_2) on the basis of log(10) rather than on ln(e) and being defined by

$$tg\ \alpha = \frac{1}{t_2 - t_1} \cdot \log \frac{c_s - c_1}{c_s - c_2} = 0,4343 \cdot k_2$$

Frequently, the oc is then defined on the bases of tg α as

$$oc = 2,303 \cdot c_s' \cdot tg\ \alpha = 2,303 \cdot 11,3 \cdot tg\ \alpha$$
$$= 26,0 \cdot tg\ \alpha \tag{2.67}$$

It has to be kept in mind, that the saturation value c'_s refers to that in pure water at 10°C and 101,3 kPa of pressure, whereas c_s in eq. 2.66 refers to the saturation value under the experimental conditions.

The influence of temperature on the oc is commonly accounted for by the following formule 2.68, which is based on actual experimental data (including all possible influences on k_2 as discussed in section 2.34) but which relates these results solely to the temperature influence on the coefficient of diffusion, applying the penetration theory. Thus the rate of oxygen transfer measured at a temperature T - expressed by $(k_2)_T$ - can be converted to that at T = 10°C - expressed by $(k_2)_{10}$ - by

$$(k_2)_{10} = (k_2)_T \sqrt{\frac{D_{10}}{D_T}} \tag{2.68}$$

The correction factor has been deducted from experimental data as

$$\sqrt{\frac{D_{10}}{D_T}} = 1{,}038^{\,0{,}5\,.\,(10^\circ C - T)} = 1{,}0188^{\,(10^\circ C - T)} \tag{2.69}$$

Thus the oc-value is finally

$$oc = 26{,}0 \;.\; tg\,\alpha \;.\sqrt{\frac{D_{10}}{D_T}} \tag{2.70}$$

The correction factor $\sqrt{D_{10}/D_T}$ is given in table 2.5. A more comprehensive discussion of the temperature influence on the oxygenation capacity is found in (8).

Example: Determine the oxygenation capacity of the example given in section 2.41 under the assumption of an experimental temperature of 15°C.

The foregoing example gave $(k_2)_{15} = 2{,}303 \;.\; tg\,\alpha = 0{,}00193$ (1/s) or $tg\,\alpha = 0{,}00193/2{,}303 = 0{,}00084$. The correction factor for temperature is taken from table 2.5 as 0,911. Thus

$$\begin{aligned} oc &= 26{,}0 \;.\; 0{,}00084 \;.\; 0{,}911 \\ &= 0{,}0199 \text{ g } O_2/m^3.s \\ &= 71{,}6 \text{ g } O_2/m^3.h \end{aligned}$$

Although the oxygenation capacity is a useful and convenient concept in sewage treatment, a word of caution against careless application is necessary. First of all, the definition (eq. 2.64 and 2.65) contains the saturation value of oxygen in pure water at 10°C. In sewage this value is generally lower than 11,3 g/m^3 due to the impurities contained in the sewage. Furthermore the magnitude of k_2 is decreased in comparison to pure or tap water, especially by the presence of hydrophobic substances and surface active agents as discussed in section 2.34. This is commonly taken account of by a factor α, relating the oc determined in tap water to that in the mixed liquor under operating conditions:

$$(oc)_{\text{mixed liquor}} = \alpha \cdot (oc)_{\text{tap water}} \qquad (2.71)$$

The magnitude of α depends on the type and concentration of the surfactant and the dynamics of surface renewal induced by the aerator (see section 2.34).

In redetermining the oxygenation capacity for temperatures other than 10°C two influences have to be considered: first, the saturation values in eq. 2.64 decreases with increasing temperature: secondly, the overall transfer coefficient k_2 increases. Although the second influence is somewhat greater than the first, temperature has no significant influence on the oxygenation capacity, as may be seen from the following example.

Example: Estimate the oxygenation capacity of the foregoing example at 5°C and 25°C.
Since

$$oc_T = c_s \cdot (k_2)_T \text{ and}$$

$$(k_2)_T = (k_2)_{10} / \sqrt{D_{10}/D_T} \qquad \text{(compare eq. 268)}$$

it follows that

$$oc_T = oc \cdot \frac{c_s}{c'_s} \cdot \frac{1}{\sqrt{D_{10}/D_T}} \qquad (2.72)$$

From the values given in table 2.3 and 2.5 it is seen that

$$oc_{5^oC} = 0{,}0199 \cdot \frac{12{,}8}{11{,}3} \cdot \frac{1}{1{,}098} = 0{,}0199 \cdot 1{,}032 = 0{,}0205 \text{ g/m}^3\text{.s}$$

$$oc_{25^oC} = 0{,}0199 \cdot \frac{8{,}2}{11{,}3} \cdot \frac{1}{0{,}756} = 0{,}0199 \cdot 0{,}960 = 0{,}0191 \text{ g/m}^3\text{.s}$$

From the correction factors it is obvious that the oxygenation capacity is likely to change by less than 10 % when increasing the temperature from 5°C to 25°C. It has, however, to be taken in mind that the oc refers to an oxygen content of zero. In practice, a certain minimum oxygen concentration in the aeration tank has to be maintained (e.g. 2 g/m^3) giving rise to a temperature dependence of the driving force (c_s - c) and thus of the oxygen transfer capacity. Maintaining 2 g O_2/m^3 the transfer capacity at 5°C would be

$$oc_{5^oC} \cdot \frac{c_{s,5}-2}{c_{s,5}} = 0{,}0205 \cdot \frac{12{,}8-2}{12{,}8} = 0{,}0205 \cdot 0{,}844 = 0{,}0173 \text{ g } O_2/\text{m}^3\text{.s}$$

whereas the influence of temperature at 25°C is more pronounced

$$oc_{25^oC} \cdot \frac{c_{s,25}-2}{c_{s,25}} = 0{,}0191 \cdot \frac{8{,}2-2}{8{,}2} = 0{,}0191 \cdot 0{,}756 = 0{,}0144 \text{ g } O_2/\text{m}^3\text{.s}$$

Finally, the pressure influences the oxygenation capacity by increasing the saturation value with increasing pressure; hence

$$oc_p = oc \cdot \frac{P - p_w}{101{,}3 - p_w} \qquad (2.73)$$

Again, this influence is of minor importance. A pressure drop of some 3 kPa (22,5 mm Hg) at 10°C (p_w = 1,23 kPa), for instance, will reduce the oc according to eq. 2.73 to (101,3 - 3 - 1,23)/(101,3 - 1,23) = 97 % of its original value.

The relation of the oxygenation capacity to the overall gas transfer coefficient is obvious from eq. 2.64. Its relation to the efficiency coefficient K may be deducted from eq. 2.63 and 2.64 assuming t_k to be equal to the detention time τ of the water in the areation tank.

This yields

$$K = 1 - e^{-k_2 \cdot \tau} = 1 - e^{-oc.\tau/c_s} \qquad (2.74)$$

or

$$oc = - \frac{c_s}{\tau} \cdot \ln (1-K) \qquad (2.75)$$

The relation between K and the oxygenation capacity OC (g O_2/s) as defined by eq. 2.65 may be stated by assuming a flow of Q (m^3/s) being oxygenated as

$$K = 1 - e^{-OC/Q.c_s} \qquad (2.74a)$$

$$OC = - Q \cdot c_s \cdot \ln (1-K) \qquad (2.75a)$$

Example: Determine the efficiency coefficient K under the assumption that the oxygenation capacity of the foregoing example is utilized to increase the oxygen content of ground water of T = 5°C and of c_o = 2 g O_2/m^3, when a detention time of τ = 5 minutes is provided. What is the effluent oxygen concentration?

$$oc_{5^oC} = 0{,}0205 \text{ g } O_2/m^3.s$$

$$c_{s,5^oC} = 12{,}8 \text{ g}/m^3$$

According to eq. 2.74

$$K = 1 - e^{-oc.\tau/c_s} = 1 - e^{-\frac{0{,}0205.(5.60)}{12{,}8}} = 1 - e^{-0{,}480} = 0{,}381$$

According to eq. 2.62

$$c_e = c_o + K(c_s - c_o) = 2 + 0{,}381 \cdot (12{,}8 - 2)$$

$$= 2 + 4{,}1 = 6{,}1 \text{ g}/m^3$$

2.5 Change of the Gas Phase in Gas Transfer Operations

In the foregoing sections it has tacitly been assumed, that the driving force ($c_s - c$) during gas transfer operations is influenced only by a change in the gas concentration in the liquid phase c. When absorbing, however, a certain gas from air, its concentration in the air is decreasing during the process of absorption and the saturation value $c_s = k_D \cdot c_g$ is decreasing correspondingly. Hence the driving force ($c_s - c$) is steadily decreasing (a) by an increase of c and (b) by a decrease of c_g. In stripping operations, c is decreasing and c_g increasing during desorption, giving rise to a decrease of the absolute magnitude of the driving force. The magnitude of the change of c_g and hence c_s depends on the amount of air supplied for gas transfer. To quantitatively describe these effects an input-output balance is set up. Consider an aerator being fed with Q_g (m^3/s) of air with c_{go} (g/m^3) of the gas in question and Q (m^3/s) of water containing c_o (g/m^3) of the same gas. Assuming no significant change of Q_g during operation (which might be caused by desorption or absorption of gases), the balance is written with c_{ge} and c_e as effluent concentrations as

$$Q_g \cdot c_{go} + Q \cdot c_o = Q_g \cdot c_{ge} + Q \cdot c_e$$

After defining the ratio of air to water flow as $RQ = Q_g/Q$, the above equation is rearranged as

$$RQ = - \frac{c_e - c_o}{c_{ge} - c_{go}} = - \frac{\Delta c}{\Delta c_g} \qquad (2.76)$$

Hence the negative ratio of the concentration change in the liquid phase Δc over that in the gaseous phase Δc_g is equal to the air to liquid flow ratio RQ.

Δc and Δc_g influence the driving force during transfer operation and hence the rate of gas transfer. These interrelationships depend on the type of aerator: intermittent (e.g. cascades, plate towers); or complete mix conditions (bubble aeration) and moreover on the direction of air and water flow with respect to each other (co-current, counter-

current, cross flow). To quantitatively illustrate these consideration, three examples are treated in the following

a) complete mix system of bubble aeration;
b) packed tower (continuous plug flow) with co-current flow of air and water;
c) packed tower with counter-current flow of air and water.

The preconditions for eq. 2.76 are assumed to apply, which would be true for dilute systems (low concentration in the liquid phase, low to moderate solubility of the gas), conditions hence, which are generally met in sanitary engineering gas transfer operations.

a) Complete Mix Bubble Areation:

Assume a reactor of volume V, being fed with Q and Q_g and providing a theoretical detention time for the water flow of $T = V/Q$. Due to complete mix conditions the liquid in the reactor has a gas content of c_e at any place and the air of c_{ge}, the respective incoming concentrations being c_o and c_{go}. The effluent gas concentration in the air follows from eq. 2.76:

$$c_{ge} = c_{go} - \frac{c_e - c_o}{RQ}$$

and the corresponding saturation value in the liquid amounts to $c_s = k_D \cdot c_{ge}$, such that the driving force $df = c_s - c_e$ is given by

$$df = k_D . c_{go} - c_e . (1 + \frac{k_D}{RQ}) + c_o . \frac{k_D}{RQ} \qquad (2.77)$$

Under steady state conditions of operation the driving force is constant, therefore. The concentration change dc follows from combining eq. 2.57 and 2.77:

$$dc = k_2 \cdot df \cdot dt \qquad (2.78)$$

The left-hand side of eq. 2.78 is integrated between the limits of c_o and c_e, the right-hand side between zero and $t = T$ to give

$$c_e = \frac{c_{so} + c_o.(1/k_2.T + k_D/RQ)}{1 + (1/k_2.T + k_D/RQ)} \tag{2.79}$$

or written in a form similar to eq. 2.62

$$\frac{c_e - c_o}{c_{so} - c_o} = \frac{1}{1 + 1/k_2.T + k_D/RQ} = K_1 \tag{2.80}$$

The left-hand side of eq. 2.80 has previously been referred to as efficiency coefficient K of the system (comp. eq. 2.62). The term k_D/RQ clearly shows the reduction of K_1 by the change of the gas concentration in the gas phase during operation. Also at conditions of $k_D/RQ \to 0$ (very low solubility, very great RQ) K_1 is smaller than predicted by eq. 2.62. This is caused by eq. 2.62 being based on plug flow conditions, whereas complete mix conditions are assumed in the derivation K_1, yielding a smaller average driving force.

b) Packed Tower, Co-Current Flow

Assume a packed tower being co-currently fed at its top with Q_g and Q, having initial concentrations of c_{go} and c_o of the interesting gas, respectively. Eq. 2.76 can be applied for any section of the tower, starting from the top and reaching until some tower depth (smaller than the total tower obviously. Let c_g and c be the effluent concentrations of the section under considerations. Assuming plug flow of Q_g and Q of the same velocity, the relation between c_g and c is given by eq. 2.76 as

$$c_g = (c_{go} + \frac{c_o}{RQ}) - \frac{c}{RQ} \tag{2.81}$$

In a graph with c_g as ordinate and c as abscissa, eq. 2.81 plots as a straight line, which is referred to as "operating line", indicating the course of change of c_g and c through the tower (fig. 2.10). The diagram contains also the "equilibrium line", given by eq. 2.1 as $c_g = c/k_D$, indicating the saturation concentration c_s corresponding to any c_g. c_s can be obtained by multiplication of eq. 2.81 with k_D as

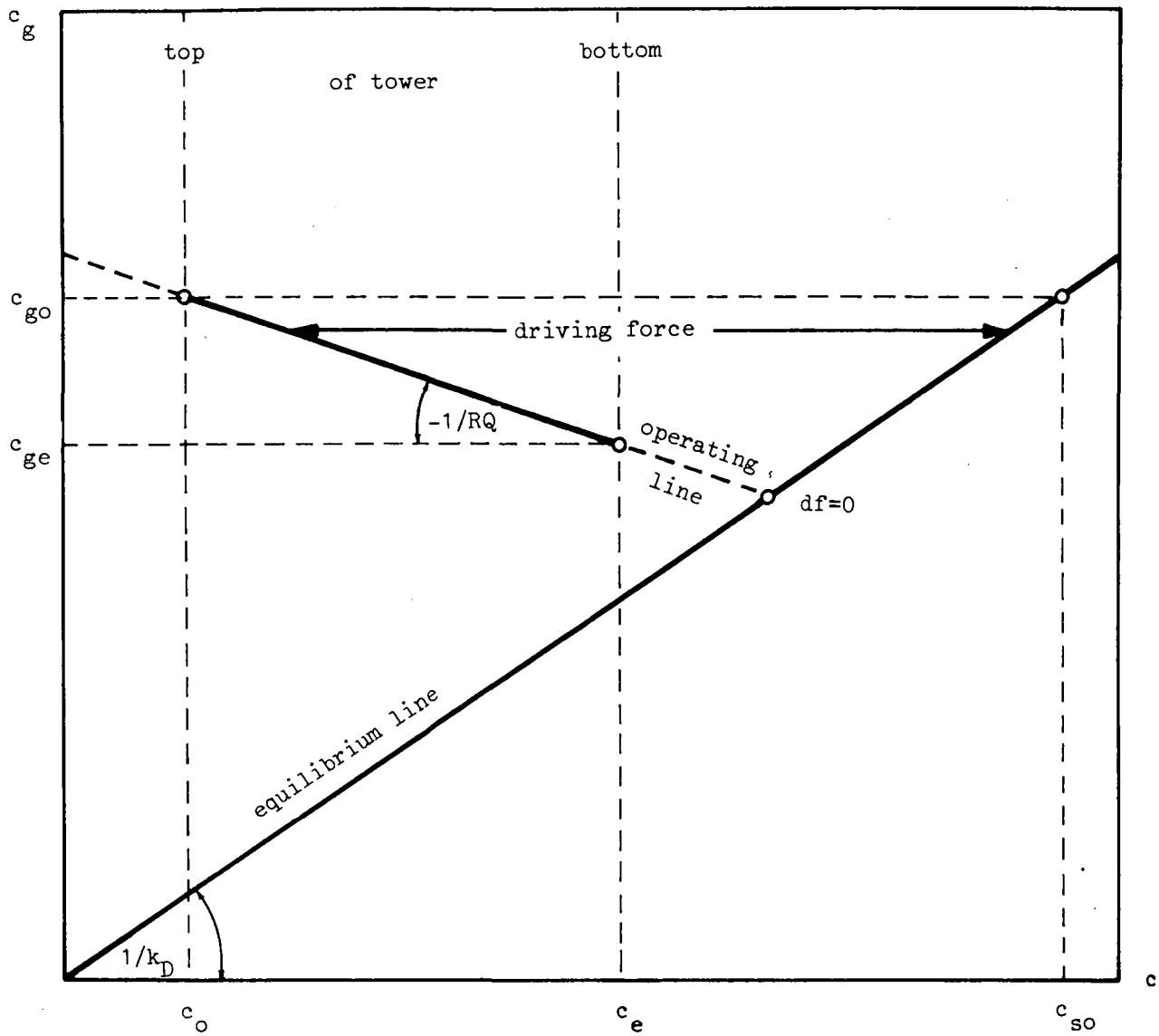

Fig. 2.10 CHANGE OF c_g, c AND DRIVING FORCE IN A PACKED TOWER. CO-CURRENT FLOW.

$$c_s = k_D \cdot c_g = k_D \cdot c_{go} + c_o \cdot \frac{k_D}{RQ} - c \cdot \frac{k_D}{RQ} \qquad (2.82)$$

The driving force $df = c_s - c$ is described, therefore, by

$$df = k_D \cdot c_{go} + c_o \cdot \frac{k_D}{RQ} - c \cdot \left(1 + \frac{k_D}{RQ}\right)$$

$$= c_{so} + c_o \cdot \frac{k_D}{RQ} - c \cdot \left(1 + \frac{k_D}{RQ}\right) \qquad (2.83)$$

with c_{so} being the saturation value under natural conditions (= on top of the tower). The rate of concentration change in the liquid phase dc/dt is given by eq. 2.62 as

$$dc/dt = k_2 \cdot df$$

which integrates after inserting eq. 2.83 and solving for the boundary condition t = 0 with $c = c_o$ to

$$c = c_o + (c_{so} - c_o) \cdot \frac{1 - \exp\left(- k_2 . t . (1 + k_D/RQ)\right)}{1 + k_D/RQ} \qquad (2.84)$$

The time t in eq. 2.84 can be related to tower height (starting at top) by h = t . v, v being the velocity of water and gas flow through the tower.

c) Packed Tower, Counter-Current Flow

In counter-current operation (water flowing from the tower top to its bottom, air in the opposite direction) the operating line is defined by the following two points (see figure 2.11):

at tower top : $c_g = c_{ge}$ $\qquad c = c_o$

at tower bottom: $c_g = c_{go}$ $\qquad c = c_e$

The slope of this line amounts to

$$\frac{c_{go} - c_{ge}}{c_e - c_o} = + \frac{1}{RQ} \qquad \text{(compare eq. 2.76)}$$

Hence the operation line is given by

$$c_g = (c_{go} - \frac{c_e}{RQ}) + \frac{c}{RQ} \qquad (2.85)$$

and the corresponding driving force $df = k_D . c_g - c$ amounts to

$$df = c_{so} - c_e . \frac{k_D}{RQ} - c . (1 - \frac{k_D}{RQ}) \qquad (2.86)$$

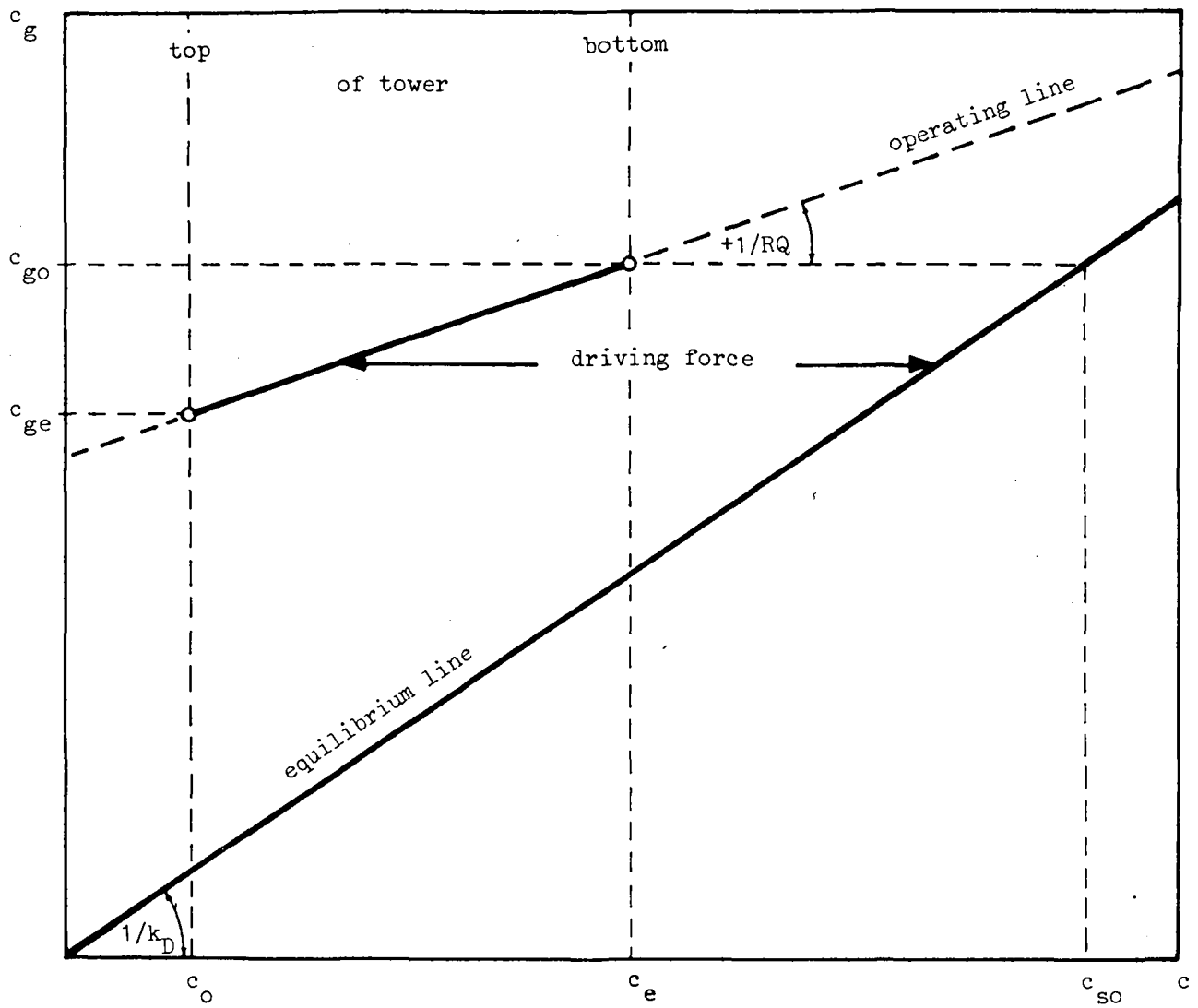

Fig. 2.11 CHANGE OF c_g, c AND DRIVING FORCE IN A PACKED TOWER. COUNTER-CURRENT FLOW.

Integrating $dc/dt = k_2.df$ under the boundary condition $t = 0$ with $c = c_o$ one gets

$$c = c_o.\exp + (c_{so} - c_e.k_D/RQ) \cdot \frac{1 - \exp}{1 - k_D/RQ} \qquad (2.87)$$

$$\text{with } \exp = \exp\left(-k_2.t.(1 - k_D/RQ)\right)$$

Eq. 2.87 describes the relation between the c and time (or tower height). At the tower bottom, i.e. at $c = c_e$, eq. 2.87 states for c_e after rearranging

$$c_e = c_o + (c_{so} - c_o) \cdot \frac{1 - \exp}{1 - \exp.k_D/RQ} \qquad (2.88)$$

Eq. 2.87 and 2.88 are not defined for $k_D = RQ$ with exp = 1. In this case the driving force remains constant throughout the tower and amounts to $df = c_{so} - c_e$ (eq. 2.86), whereas the relation between c and c_e with respect to time are given, respectively, by

$$c = c_o + (c_{so} - c_e).k_2.t \qquad (2.89)$$

and

$$c_e = c_o + (c_{so} - c_o).\frac{k_2.t}{1+k_2.t} \qquad (2.90)$$

The foregoing considerations are summarized by rewriting the respective equations for the effluent concentrations c_e (i.e. eq. 2.62; 2.80; 2.84; and 2.87) in a form similar to eq. 2.62 for

a) plug flow conditions at $k_D/RQ \to 0$ (eq. 2.62):

$$\frac{c_e - c_o}{c_{so} - c_o} = 1 - \exp(-k_2.t) = K \qquad (2.91)$$

b) complete mix conditions (eq. 2.80):

$$\frac{c_e - c_o}{c_{so} - c_o} = \frac{1}{1 + 1/k_2.t + k_D/RQ} = K_1 \qquad (2.92)$$

c) plug flow conditions, co-current flow (eq. 2.84):

$$\frac{c_e - c_o}{c_{so} - c_o} = \frac{1 - \exp\left(-k_2.t.(1+k_D/RQ)\right)}{1 + k_D/RQ} = K_2 \qquad (2.93)$$

d) plug flow conditions, counter-current flow (eq. 2.87):

$$\frac{c_e - c_o}{c_{so} - c_o} = \frac{1 - \exp\left(-k_2.t.(1-k_D/RQ)\right)}{1 - \frac{k_D}{RQ} \cdot \exp\left(-k_2.t.(1-k_D/RQ)\right)} = K_3 \qquad (2.94)$$

The left-hand sides of the above equations state the fraction of the initial degree of over- or undersaturation that has been de- or absorbed during the transfer operation. It has previously been designated as efficiency coefficient K of the system (eq. 2.62). K_1, K_2, and K_3 hence, state the efficiency coefficient of the respective systems (b) through (c), i.e. under different conditions of flow taking the change of the gas phase during transfer into consideration.
Two factors, obviously, determine the above efficiency coefficients
- the product $k_2.t$ and
- the ratio k_D/RQ, i.e. the solubility of the gas (k_D) and air to water flow ratio (RQ).

The properties of the functions 2.92 through 2.94 are such that
- with increasing ratio k_D/RQ - i.e. with increasing solubility of the gas and/or with decreasing ratio RQ - the efficiency coefficients decrease (and vice versa)
- the rate of these changes is comparetively high at great magnitude of $k_2.t$ and correspondingly low at small k_2. t-values. Hence the magnitude of k_D/RQ is of particular significance at great k_2-values and/or long aeration times .

These properties are illustrated by the following

Example: Estimate the efficiency coefficients $(c_e - c_o)/(c_{so} - c_o)$ for a complete mix aeration system (K_1), for a co-currently operated tower (K_2), and for a counter currently operated tower (K_3), all providing a k_2-value of $k_2 = 2.10^{-2}$ (1/s) with aeration times of (a) t_1 = 80,5 s and (b) t_2 = 25,5 s (K amounts to 0,8 and 0,4, respectively) and being operated at RQ-values of 10; 1; 0,1; 0,01; 0,001; and zero.
Express the computed efficiency coefficients also as a percentage of $K = 1-e^{-k_2.t}$.

The efficiency coefficients K_1, K_2, and K_3 are computed by means of eq. 2.92, 2.93, and 2.94, respectively. The results are summarized in figure 2.12 and in the following table, which also contains the required percentages. Fig. 2.12 clearly shows the previously discussed properties of the respective functions.

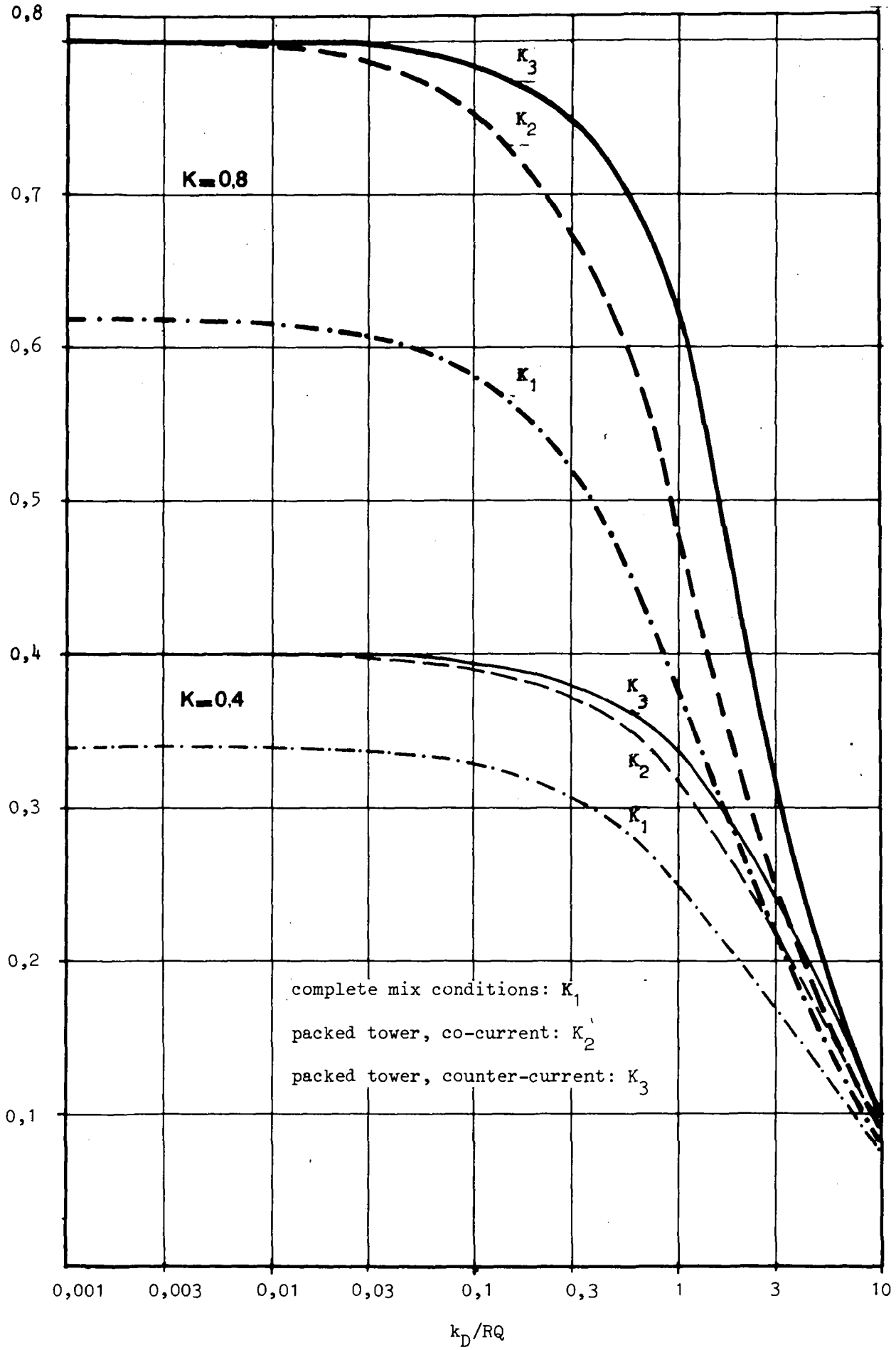

Fig. 2.12 INFLUENCE OF THE RATIO k_D/RQ ON THE EFFICIENCY COEFFICIENT AT DIFFERENT OPERATIONAL CONDITIONS.

$\frac{k_D}{RQ}$	K_1 $K_1/K(\%)$		K_2 $K_2/K(\%)$		K_3 $K_3/K(\%)$	
	K=0,8	K=0,4	K=0,8	K=0,4	K=0,8	K=0,4
10	0,086	0,077	0,091	0,091	0,100	0,099
	10,8	19,3	11,4	22,6	12,5	24,8
1	0,381	0,253	0,480	0,320	0,617	0,338
	47,9	63,2	60,0	80,0	77,1	84,5
0,1	0,581	0,327	0,754	0,391	0,783	0,393
	72,6	81,8	94,3	97,7	97,9	98,3
0,01	0,613	0,337	0,795	0,399	0,798	0,399
	76,6	84,2	99,4	99,8	99,8	99,8
0,001	0,616	0,338	0,7995	0,3999	0,7998	0,3999
	77,0	84,5	99,9	99,98	99,98	99,98
0	0,617	0,338	0,800	0,400	0,800	0,400
	77,1	84,5	100	100	100	100

From the foregoing considerations and example the following conclusions may be drawn. For gases of different solubility having the same coefficient of diffusion D, i.e. having under the same conditions of A/V and t_c also the same overall transfer coefficient k_2, the extent of gas exchange will be the same when applying the equal ratios k_D/RQ. To prevent a significant change of the gas concentration in the gas phase which would reduce the transfer rate and hence call for long transfer times, the ratio k_D/RQ should be well below one and approach zero. For carbon dioxide and oxygen, for instance, the coefficients of diffusion are almost the same but the solubility differs significantly. The ratio of the respective k_D-values varies within the temperature range of $0^oC < T < 30^oC$ from 35 to 25. Hence the air to water flow ratio RQ for removal of carbon dioxide should be 25 to 35 times that for oxygenation, provided the same extent of transfer $(c_e - c_o)/(c_{so} - c_o)$ is required.

The second conclusion concerns the most efficient means of increasing the rate and extent of gas transfer: transfer time t (or $k_2.t$) or RQ. Sparingly soluble gases (small k_D) show at low RQ-values already small ratios k_D/RQ. An increase of RQ is very ineffective in increasing the rate and extent of gas transfer. Increase of k_2 and/or aeration time t are the only means, therefore, to promote gas transfer of slightly soluble gases and low air to water flow ratios RQ can be applied economically. With more soluble gases, the air to water flow ratio RQ becomes the most significant parameter determining the rate and extent of gas transfer. As previously stated, this is especially the case great at magnitude of $k_2 \cdot t$, i.e. at long aeration times. Obviously, an economic optimum for a preset extent of gas exchange $(c_e - c_o)/c_{so} - c_o)$ can be found, when unit costs for providing aeration time (size of reactor) and air flow are known.

Example: Groundwater with a carbon dioxide content of 61 g/m^3 and an oxygen content of 1 g/m^3 is aerated by means of a co-currently operated packed tower to achieve a CO_2-content of 13 g CO_2/m^3. Estimate different combinations of packing height h and air to water flow ratio RQ to obtain this result and the corresponding oxygen content of the effluent.

Assume a k_2-value of the packing independent of RQ of $k_2 = 2.10^{-2}(1/s)$ for both gases. The saturation concentration c_{so} and the distribution coefficient k_D are for CO_2 1 g/m^3 and 1,2 and for oxygen 11 g/m^3 and 0,04, respectively. The hydraulic load of the tower amounts to $v_F = 0{,}025\ m^3/m^2.s$.

From the above information the required efficiency coefficient K_2 is computed for CO_2

$$K_2 = (13-61)/(1-61) = 0{,}8$$

For estimating h-RQ-combinations, eq. 2.93 is rearranged to give

$$t = - \frac{\ln\left(1-K_2(1 + k_D/RQ)\right)}{k_2 \,.\, (1 + k_D/RQ)}$$

and with $k_2 = 2.10^{-2}$ and $h = t \,.\, v_F$

$$t = - \frac{\ln(0{,}2 - o{,}8.1{,}2/RQ)}{0{,}02(1 + 1{,}2/RQ)}$$

$$h = 0{,}025 \,.\, t$$

The above equations are evaluated for various RQ-values, starting from the lowest possible to obtain $K_2 = 0{,}8$, following from the condition

$$0{,}2 - 0{,}8.1{,}2/RQ \geq 0$$

$$RQ \geq 4{,}8$$

The results are given in the following table

RQ	t	h	g O_2/m^3
4,8	∞	∞	11,00
5	194,7	4,87	10,72
10	101,0	2,53	9,65
20	88,7	2,22	9,29
50	83,5	2,09	9,11
100	81,9	2,05	9,05
∞	80,5	2,01	9,00

The corresponding oxygen concentrations, also contained in the above table, are estimated by means of eq. 2.84

$$c = 1 + (11-1) \cdot \frac{1 - \exp\left[-2.10^{-2}.t(1 + 0{,}04/RQ)\right]}{1 + 0{,}04/RQ}$$

Note the important parameter time for the extent of gas exchange of the sparingly soluble gas oxygen: with decreasing the aeration time (or the packing height) the effluent oxygen concentration decreases, whereas the effluent CO_2-content is 13 g/m^3 for all given combinations!

In the foregoing considerations and examples a constant value of k_2 has been assumed. At large air to water flow ratios, however, a greater interfacial area per unit volume (A/V) is created, such that an increase of k_2 with increasing RQ has to be expected.

Obviously, highly soluble gases can optimally be exchanged only with aerators providing large RQ-values at low energy input, i.e. basically aerators which disperse water into air (e.g. spray aeration, packed towers), whereas gases of low solubility are transfered most expediently by dispersing air into water at low RQ-ratios (e.g. bubble aeration). These facts may sometimes be applied when deciding upon the aeration equipment. If, for instance a raw water is in the carbonate equilibrium but is deficient in oxygen, some type of bubble aeration (deep well, ventury aerator, air diffusors) are more appropriate than

spray aeration. The former types will increase the oxygen concentration but not significantly change the CO_2 content, thus preserving the carbonate equilibrium.

3. Practical Aspects of Aeration and Gas Transfer

In this section the devices for aeration and gas transfer, applied in sanitary engineering practice, are covered according to their working principle as mentioned in section 1: gravity aerators, spray aerators, air diffusers, and mechanical aerators. A short description of the aeration system is followed by known attempts to apply theoretical aspects for describing and designing the process. In some cases the design criteria of proprietary aerators are appended.
The effectiveness for ab- or desorption of gases in sanitary engineering is discussed as well as advantages and drawbacks from technical, operational and economical point of view.

3.1 Gravity Aerators

The principle of gravity aeration is to utilize the potential energy of water to create interfaces for efficient gas transfer. The most simple case is given by weir aeration, which leads to the cascade principle when the available fall is subdivided into several steps. Placing of the different steps of a cascade vertical below each other yields stacks of perforated pans, which may be filled with contact media. When the available space is completely filled with such contact media, the bottom constructions between the steps may be omitted and the principle of a packed tower is attained, the extreme of which, using fine packing material, is given by the dry filter.
Frequently, these vertical gravity aerators are referred to as cascades too.

Although spray aeration makes use of the gravity principle too, it is covered seperately in section 3.2.

3.1.1 Weir Aeration and Cascades

When water is passed over a weir submerging into the tail water two different mechanisms of gas transfer may be differentiated:

a) during the free fall of water a certain surface area A is created. From the weir height h the average time of exposure of the surface A to air could be estimated ($t_c = \sqrt{2\,h/g}$), allowing an estimate

of the coefficient of gas transfer k_L. The size of the contact area depends on the configuration of the weir: partition of the nappe into several jets will obviously increase A/V. Increase of the flow is likely to decrease the specific interfacial area of the jets. Although these factors could be taken account of when estimating k_L, the second mechanism, being of far greater significance, is less susceptible to an approach of this kind:

b) when the nappe or its jets submerge into the receiving body of water significant amounts of air are entrained. The entrained air is then dispersed in the form of bubbles throughout the receiving body of water, which leads to an intense transfer of gases. The amount of air entrained depends primarily on the velocity ($\sqrt{2gh}$) of the nappe when passing the surface of the tail water. Hence the mechanism of gas transfer is mainly determined by the weir height, contrary to the first mentioned. Finally, the depth of the receiving water influences the amount of gas transfered: the deeper the nappe with the entrained air is able to enter into the tail water, the greater is the specific surface area A/V and the contact time between bubbles and water. For optimum utilization of this effect, the depth should be chosen in such a manner that the final velocity of the jets within the tail water before reaching its bottom is equal to the rising velocity of the bubbles produced. Empirical estimates recommend a depth equal or greater than 2.h/3.

Due to the predominance of the second mechanism ("bubble aeration"), weir aeration is an excellent means for oxygenation of water. Removal of CO_2 or taste and odor producing substances is limited more or less to transfer actions described by the first mechanism (comp. section 2.5). Thus the application of the gravity principle in connection with weirs is primarily restricted to oxygenation of water in water treatment practice and partially for reaeration of streams.

3.111 Single Free Fall in Weir Aeration

Since a variety of influences effect the gas transfer in weir aeration, the application of the efficiency coefficient K is appropriate to describe the process. For the oxygenation of water, also of polluted

water, the following formula has been advanced (9), relating K to the parameters weir height (of a straight weir) and temperature (^{o}C) for

$$\begin{aligned} &\text{unpolluted water} && K = 0{,}45\ (1 + 0{,}046.T)\ .\ h \\ &\text{polluted water} && K = 0{,}36\ (1 + 0{,}046.T)\ .\ h \\ &\text{sewage} && K = 0{,}29\ (1 + 0{,}046.T)\ .\ h \end{aligned} \qquad (3.1)$$

Other investigations confirmed this linear relationship between K and h (10), but gave a smaller proportionality constant of about 0,4, being almost independent of temperature and of flow variations between $6{,}5.10^{-3}$ $m^3/m.s$ and $26{,}0.10^{-3}$ $m^3/m.s$. Partitioning of the nappe by rectangular notches into at least 4 jets per meter weir length increased the proportionality constant up to 0,64 for heights below 0,70 m. Above this height the influence of h on K is less pronounced (fig. 3.1).

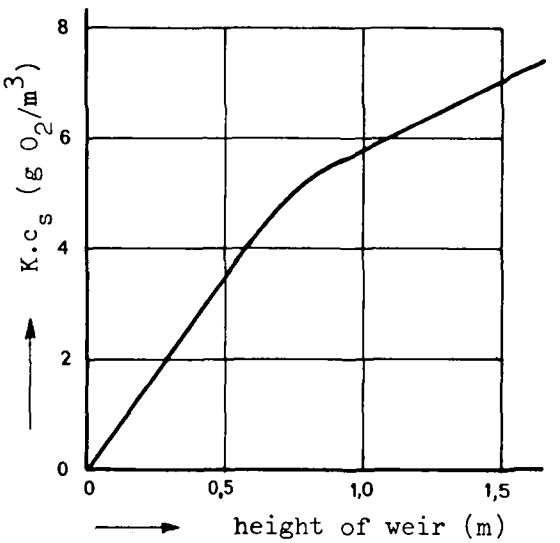

Fig. 3.1 EFFICIENCY COEFFICIENT IN DEPENDENCE OF THE HEIGHT OF FALL OVER WEIRS

Example: Raw water with 2 g O_2/m^3 and a temperature of $10^{o}C$ is passed over a straight weir of a height of 0,65 m. Estimate the down stream oxygen content.

According to eq. 3.1

$$K = 0{,}45.(1 + 0{,}046.10).0{,}65 = 0{,}427$$

Application of eq. 2.62 yields with $c_s = 11{,}3\ g/m^3$

$$c_e = c_o + K.(c_s - c_o) = 2{,}0 + 0{,}427.(11{,}3-2{,}0) = 6\ g/m^3$$

The oxygenation efficiency OE in terms of mg O_2 absorbed per Joule at zero oxygen content may be computed for a flow of Q (m^3/s) passing over the weir from

a) the amount of oxygen transferred per unit time which is according to eq. 2.62 at $c_o = 0$ equal to $Q.K.c_s$ and

b) the power $Q.h.\rho.g$ exerted by the flow when passing over the weir height h as

$$OE = \frac{Q.K.c_s.10^3}{Q.h.\rho.g} \quad (\frac{mg\ O_2}{J}) \tag{3.2a}$$

Hence, with $\rho = 1000\ kg/m^3$,

$$OE = \frac{1}{9,807} \cdot \frac{K.c_s}{h} \quad (\frac{mg\ O_2}{J}) \tag{3.2b}$$

Thus the oxygenation efficiency of a weir, applying K/h-values in the range of 0,4 to 0,7, is expected to be in the order of 0,4 to 0,7 mg O_2/J (1,5 to 2,5 kg O_2/kWh).

3.112 Step Weirs or Conventional Cascades

Frequently the available head difference of a weir is subdivided into to several steps, expecting an increase of the amount of gases transferred.

For desorption of CO_2 this increase is accomplished, because each step of a cascade leads to the formation of new interfacial area, promoting the desorption efficiency.

Since the rate of oxygenation is primarily determined by the velocity of the nappe or its jets when submerging into the tail water, subdivision into several steps is likely to decrease the rate of oxygen transfer. Inspection of fig. 3.1, however, shows, that due to the modest increase of K for weir heights above 0,70 m, subdivision of only a great head difference into several steps of 0,60 to 0,70 m will have an positive effect on the rate of oxygenation.

A mathematical analysis of the oxygen transfer by cascades may be based on eq. 2.62, assuming the height of the weir being subdivided into n equal steps, each having an efficiency coefficient of $K_n = K/n$. Then the effluent concentration of the first step c_1 may be based on that of the influent c_o:

$$c_1 = c_o.(1-K_n) + K_n.c_s$$

and for the following steps

$$c_2 = c_1.(1-K_n) + K_n.c_s$$

$$= c_o.(1-K_n)^2 + K_n.(1-K_n)c_s + K_n.c_s$$

$$c_3 = c_2.(1-K_n) + K_n.c_s$$

$$= c_o.(1-K_n)^3 + K_n.(1-K_n)^2.c_s + K_n.(1-K_n).c_s + K_n.c_s$$

.

.

.

$$c_n = c_o.(1-K_n)^n + K_n.c_s.\left[1 + (1-K_n) + (1-K_n)^2 + \ldots + (1-K_n)^{(n-1)}\right]$$

$$c_n = c_o.(1-K_n)^n + K_n.c_s \;.\; GS$$

GS is a geometrical series the sum of which is

$$GS = \frac{1 - (1-K_n)^n}{1 - (1-K_n)} = \frac{1 - (1-K_n)^n}{K_n}$$

Hence, after inserting this expression into the above equation and rearranging

$$c_n = c_s - (c_s - c_o).(1 - \frac{K}{n})^n \qquad (3.3)$$

Since the factor $(1 - \frac{K}{n})^n$ increases with increasing n, reaching e^{-K} as n approaches infinity, it becomes evident that subdivision of a weir is reducing the final oxygen content c_n, as long as K is proportional to the weir height as has been assumed by setting $K_n = K/n$.

Example: Determine the number of steps of a cascade to achieve maximum oxygenation, assuming an available head of 1,5 m, an efficiency coefficient K depending on the weir height h as stated by figure 3.1, $c_s = 10\ g/m^3$ and $c_o = 2\ g/m^3$

a) one step:

h = 1,50 $\quad K.c_s = 7,0 \quad K = 7,0/10 = 0,7$

K/n = 0,7

$c_1 = c_s - (c_s - c_o).0,3 = 0,7.c_s + 0,3.c_o = 7,6\ g/m^3$

b) two steps:

h = 0,75 per step $K.c_s = 5,0$ $K = 5,0/10 = 0,5$

K/n = 0,5

$$c_2 = c_s - (c_s - c_o).(1-0,5)^2 = 0,75.c_s + 0,25.c_o = 8,0\ g/m^3$$

c) three steps:

h = 0,50 m per step $K.c_s = 3,5$ $K = 3,5/10 = 0,35$

K/n = 0,35

$$c_3 = c_s - (c_s - c_o).(1-0,35)^3 = 0,726 \cdot c_s + 0,274 \cdot c_o = 7,8\ g/m^3$$

d) further subdivision will further decrease c_n. For step heights below 0,6 m fig. 3.1 states $K.c_s = 7,0.h$ or with $c_s = 10\ g/m^3$ and n steps: $K/n = 0,7.h/n = 0,7.1,50/n = 1,05/n$. Thus further subdivision would theoretically ($n \to \infty$) lead to

$$c_\infty = c_s - (c_s - c_o) \cdot e^{-1,05} = 0,65 \cdot c_s + 0,35 \cdot c_o = 7,2\ g/m^3$$

Although 2 steps show the greatest final oxygen concentration, the influence of subdivision on c_n is of little significance and economic considerations would finally determine the chcice in this case.

A special construction of the convential cascade is to arrange the steps vertically below each other (fig. 3.2). The water then has to

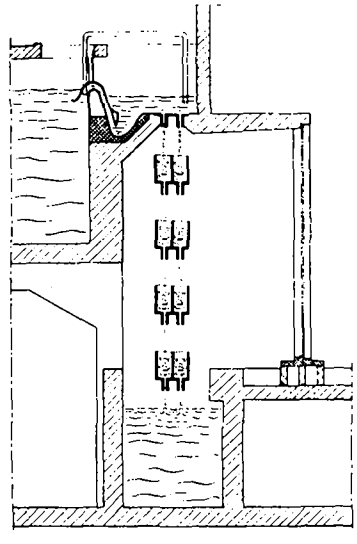

Fig. 3.2 CASCADE CONSISTING OF SLOTTED TROUGHS ARRANGED ONE BELOW EACH OTHER

be drawn from the bottom of the slotted troughs instead of being passed over a weir. The mechanisms of gas transfer, however, are the same as mentioned for weir aeration. Fig. 3.3 shows results of oxygen

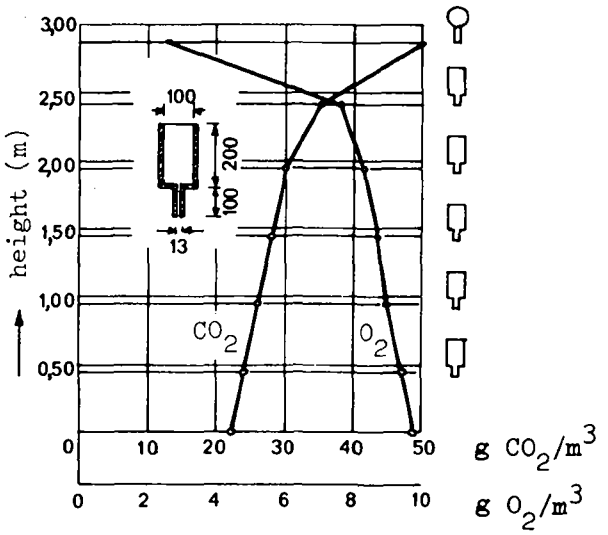

Fig. 3.3 CO_2 AND O_2 TRANSFER OF A TROUGH CASCADE

absorption and CO_2-desorption, applying troughs of 0,10 m width and of 0,20 m height with slots 0,013 m wide at a hydraulic loading of 0,02 $m^3/m.s$. Assuming a saturation value for oxygen of 10 g/m^3 and for CO_2 of 1 g/m^3 the K-values of the first step may be computed from fig. 3.3 for

$$CO_2: \quad K = \frac{c_e - c_o}{c_s - c_o} = \frac{35 - 50}{1 - 50} = 0,306$$

$$O_2: \quad K = \frac{7,6 - 2,6}{10 - 2,6} = 0,676$$

This again shows the minor efficiency of cascades in removing CO_2 as compared to absorption of oxygen.
Summarizing it may be stated that weirs and conventional cascades are an efficient means for oxygenating water in the course of water treatment, the efficiency coefficient K ranging from 0,4 to 0,7 per meter weir height, the oxygenation efficiency from 0,4 to 0,7 mg O_2/J (1,5 to 2,5 kg O_2/kWh). Variation of flow between 5.10^{-3} and 25.10^{-3} $m^3/m.s$ is of neglegible influence on K.

Subdivision into steps of a height of less than 0,6 m will decrease the oxygenation efficiency but promote desorption of CO_2 and odor and taste producing volatile substances. Nevertheless, step heights of 0,20 to 0,40 m are quite common. Cascades require little space within the process of water treatment (approximately 50 to 200 m^2 per m^3/s treatment capacity) and neglegible maintenance.

3.12 Stacks of Perforated Pans or Tower Cascades

The construction of tower cascades aims at renewing the interfacial area between the liquid and the gaseous phase as frequently as possible in order

a) to produce a large specific surface area A/V and a frequent renewal of it;
b) to allow an intense exchange of the gaseous phase, i.e. large ratios of air to water flow RQ. Thus tower cascades are primarily intended to desorb gases from water of low to moderate solubility as discussed in section 2.5 (e.g. CO_2, NH_3, H_2S, and many taste and odor producing volatile substances).

The most simple construction are stacks of perforated pans, which may be placed in open air or housed (fig. 3.4). To create large A/V-ratios

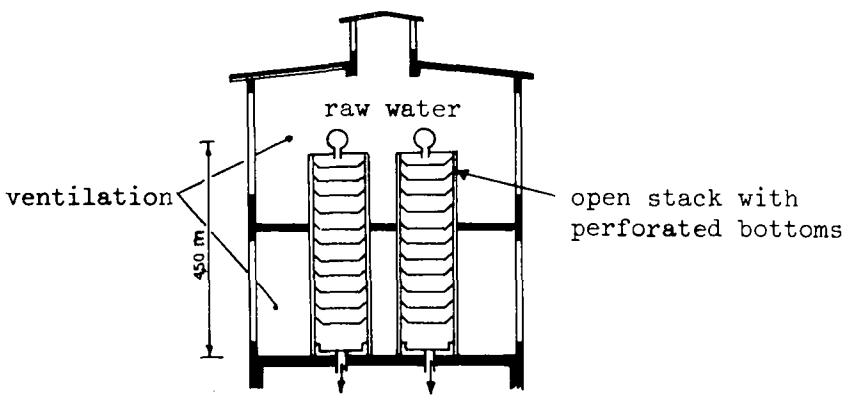

Fig. 3.4 STACK OF PERFORATED PANS

also within the pans, they may be filled with contact media like coke, stone, ceramic or plastic rings or balls. The distance between the trays may vary from 0,30 to 0,45 m, the size of the contact media from 0,025 to 0,15 m. Although contact media of smaller size would increase the specific surface area A/V and the frequency of surface renewal, they are to be avoided because they easily lead to clogging (e.g. by precipitation of iron or impurities) and furthermore impair the exchange of the gaseous phase by ventilation.

Finally the whole tower may be filled with contact media, omitting seperate trays. This includes, in principle, designs as

- towers filled with crosswise arranged plastic tubes of a diameter of 0,025 to 0,05 m (fig. 3.5), preferably applied for desorption of carbon dioxide;
- towers filled with red wood, hemlock or plastic bars, used for stripping of ammonia from treated sewage;
- closed tanks filled with ceramic or plastic tube pieces (Raschig rings) of 0,001 to 0,05 m of size or coarse sand, used for desorbtion of CO_2 or absorption of ozone for the oxidation of organic impurities in the course of water treatment and of purification of water in swimming pools;
- this design approaches the concept of dry filtration (fig. 3.6).

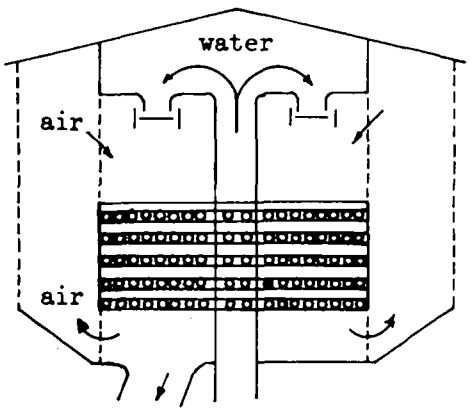

Fig. 3.5 TOWER CASCADE FILLED WITH PLASTIC TUBES

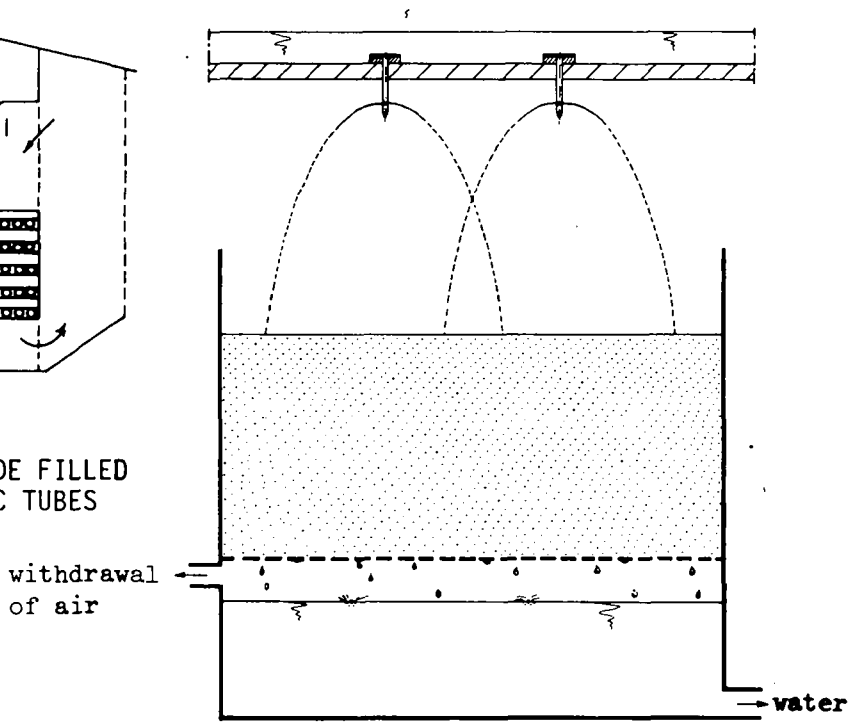

Fig. 3.6 SCHEMATIC REPRESENTATION OF A DRY FILTER

Mention should be made, that the selection of contact media is frequently done with regard to iron removal. Iron precipitants on the surface of the filling is catalytically promoting the removal efficiency, the discussion of which is beyond the scope of aeration.

Gas transfer by means of tower cascades requires ventilation, which may be accomplished by natural means, also with housed towers, or may be artificially induced. The draft may be in the same direction as the water flow, counter-current or vertical to the water flow (cross flow).

Factors influencing the transfer efficiency of tower cascades are

- the type, size and spacing of fill, which primarily determines the specific surface area A/V and the frequency of surface renewal;
- the tower height, which determines the time of interfacial contact between the gaseous and the liquid phase;
- the water and air flow in m^3 applied per m^2 of crosssectional area and unit time and the direction of this flows with respect to each other.

The influence of these parameters on the transfer efficiency is discussed in the following sections for removal of CO_2 from groundwater and of NH_3 from sewage. In both cases the stripping process is accompanied by an oxygenation of the water up to almost the saturation value. Thus oxygen transfer will not further be discussed.

3.121 Tower Cascades for Removal of Carbon Dioxide

Tower cascades filled with crosswise arranged plastic tubings have succesfully been applied for removal of carbon dioxide in water treatment practice. The different designs consist of towers subdivided into 4 to 6 sections, each some 0,50 m high, filled with up to 10 layers of plastic tubes as well as completely filled towers (fig. 1.5)

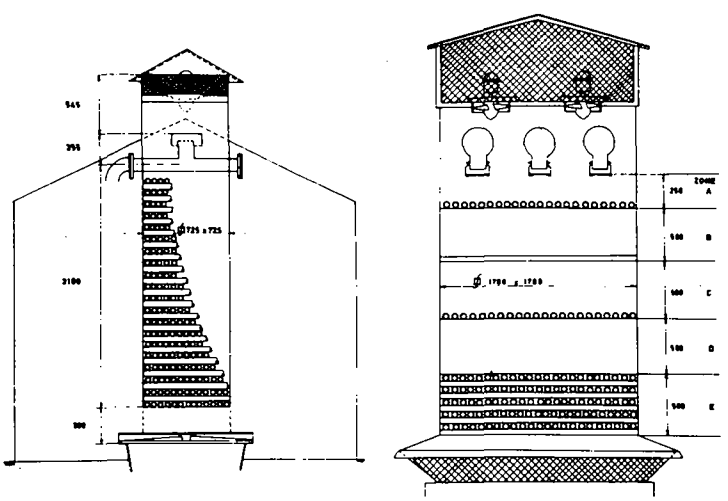

Vertical stack filled with plastic tubes

Fig. 1.5 GRAVITY AERATOR

of a height of 2 to 3 m. Water is fed onto the fill by spraying, the air draft is generally induced into the same direction by a fan on top of the tower.

The influence of some of the design and operational characterstics on the percentage carbon dioxide removal

$$R = \frac{c_o - c_e}{c_o} \qquad (3.4)$$

usually taken as parameter to describe the removal efficiency, is discussed in the following.

Size and spacing of fill: variations of the tube diameter from 0,0125 to 0,025 m and of the horizontal clear distance between the tubes from 0,003 to 0,025 m does not affect the removal efficiency R significantly. Hence the most economical design are tubes of a diameter of 0,025 with slot widths of the same magnitude of 0,025 m. Subdivision of the tower into several sections of approximately 0,50 m, each section being filled with 10 layers of tubes (height of packing 0,25 m, equal to half the height of the section), will generally give excellent removal results.

Hydraulic load: the hydraulic load of tower cascades in m^3 applied per m^2 cross-sectional area per unit time ranges from about 0,01 to 0,07 m/s. The influence of the hydraulic load on the removal efficiency R is seen from fig. 3.8, giving the results of two Dutch water works (Engelse Werk and Denekamp). Increase of the hydraulic load above 0,01 m/s (36 m/h) decreases R significantly from about 90 % to lower values between 75 and 80 % at loadings above 0,04 m/s (150 m/h).

Air to water flow ratio: the decrease of removal efficiency going along with an increase of the hydraulic load, as mentioned above, is

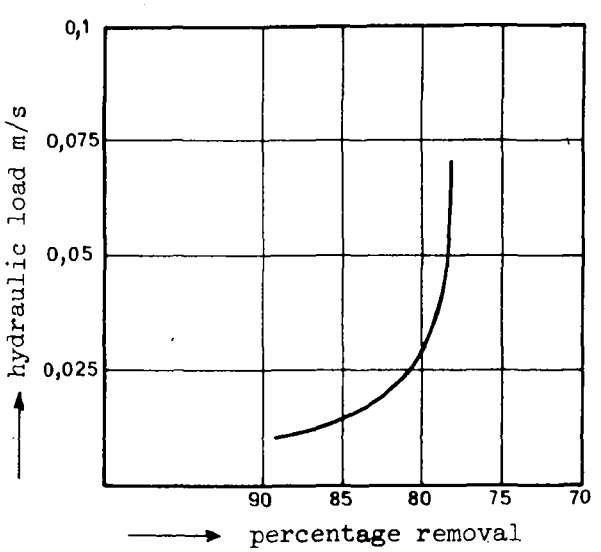

Fig. 3.8 EFFECT OF THE HYDRAULIC LOAD ON THE PERCENTAGE REMOVAL OF CARBON DIOXIDE

caused not only by the decreasing A/V-ratio within the tower cascade. Besides this effect, the increased load causes the resistance for the induced air draft to increase, yielding less ventilation. Thus the air to water flow ratio RQ generally decreases more than proportional to the increase of the hydraulic load at a constant head of the fans applied for ventilation. The accompanied increase of the CO_2 content of the gas phase reduces the driving force $(c_o - c_s)$ and thus the efficiency.

Fig. 3.9 clearly shows this effect, stating the percentage removal efficiency R at 3 different hydraulic loads and various air to water flow ratios as measured at the tower cascade Denekamp.

At the highest hydraulic load (0,050 m/s) an air to water flow ratio of RQ = 42 could be obtained, giving R = 80 %, whereas the same fan led to RQ = 190 at a hydraulic load of 0,015 m/s, yielding 90 % removal efficiency.

Based on figure 3.9, the most economical air to water flow ratio decreases from about 60 to 20 with increasing flow rates as commonly applied (0,01 to 0,07 m/s). Within this ranges removal efficiencies are to be expected increasing from about 75 to 90 % with decreasing hydraulic load.

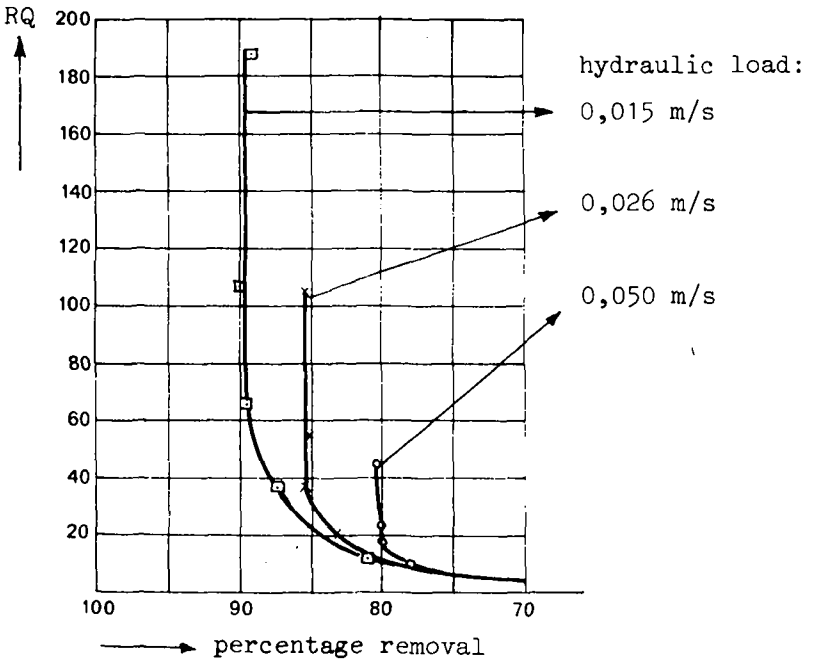

Fig. 3.9 EFFECT OF HYDRAULIC LOAD ON AIR TO WATER FLOW RATIO AND PERCENTAGE REMOVAL OF CARBON DIOXIDE

These efficiencies could be increased by reversing the direction of the air flow, i.e. by applying the counter-current principle. This, however, would require more powerful and hence more expensive ventilators, since counter-current air flow causes much higher a resistance. Fans can be used counter-currently until uneconomical hydraulic loads of some 0,015 m/s only. To nevertheless overcome a significant increase of the carbon dioxide content in the gaseous phase, ventilation may be applied in two stages, one stage serving the upper half, the second stage the lower half of the tower cascade (fig. 3.10). In this case, the spray action between the two stages will considerably assist the carbon dioxide removal.

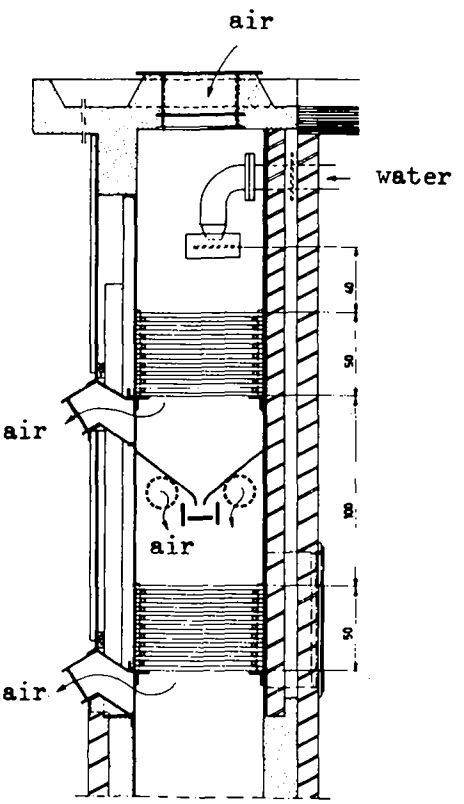

Fig. 3.10 TWO-STAGED CASCADE

Although there is at present not sufficient information on the interaction of the forementioned influences available to enable a rational design of tower cascades, theoretical aspects may be useful in interpreting experimental results and in comparing the efficiency of minor variations of design. This is illustrated by the following example.

Example: Estimate the removal efficiency of a tower cascade with a hydraulic load of 0,04 m/s and an air to water flow ratio of 15, assuming an efficiency coefficient K of the sprayers feeding the cascade of 0,3 and of 0,35 for each section of 0,50 m height (consisting of 10 layers of plastic tubes of 0,025 m and a clear distance of 0,025 m) fed with groundwater with 60 g/m^3 of carbon dioxide when

a) 4 section are built into a single stage
b) 2 stages are designed, each consisting of two sections, with seperate ventilation.

Assume a saturation value under natural conditions of c_{so} = 1 g CO_2/m^3. Determine the CO_2-content of the effluent air also.

For determining the effluent concentration eq. 2.84 is applied. The basic parameters to be applied are k_D/RQ = 1,2/15 = 0,08 and $k_2.t$, which can be obtained from the given K-values by means of eq. 2.63:

for spraying $k_2.t = -\ln(1-0,3) = 0,357$

for one tube section $k_2.t = -\ln(1-0,35) = 0,431$

Obviously, the $k_2.t$-values of several sections are additive. Hence $k_2.t$ for the total tower amounts to 0,357+4.0,431 = 2,081, which would correspond to a K-value of $K = 1-e^{-2,081} = 0,875$. For the two stages $k_2.t$ is 0,357+2.0,431 = 1,219 (K = 0,704).

Application of eq. 2.84 for the total tower then gives

$$c_e = 60 + (1-60) \cdot \frac{1 - \exp\{-2,081(1+0,08)\}}{1 + 0,08}$$

$$= 60 - 59.0,828 = 60 - 48,9$$

$$= 11,1 \text{ g } CO_2/m^3$$

and a removal efficiency of

$$R = \frac{60 - 11,1}{60} = 81,5\ \%$$

For the two staged tower the effluent concentration of the first stage amounts to

$$c_e = 60 + (1-60)\,\frac{1 - \exp[-1{,}219(1+0{,}08)]}{1 + 0{,}08}$$

$$= 60 - 59.0{,}678 = 60 - 40{,}0 = 20{,}0 \text{ g/m}^3$$

and for second stage

$$c_e = 20{,}0 + (1-20{,}0).0{,}678 = 20{,}0 - 12{,}9$$

$$= 7{,}1 \text{ g } CO_2/\text{m}^3$$

giving a removal efficiency of

$$R = \frac{60 - 7{,}1}{60} = 88{,}2\ \%$$

The effluent CO_2-content of the air is estimated by means of eq. 2.81 with $c_{go} = c_{so}/k_D = 1/1{,}2 = 0{,}8$ g/m^3.
For the total tower we get

$$c_{ge} = 0{,}8 + \frac{60}{15} - \frac{11{,}1}{15} = 4{,}1 \text{ g/m}^3$$

to which a saturation concentration of

$$c_s = k_D \cdot c_{ge} = 1{,}2.4{,}1 = 4{,}9 \text{ g/m}^3$$

would correspond. The first stage of the two staged tower has a c_{ge} of

$$c_{ge} = 0{,}8 + \frac{60 - 20}{15} = 3{,}5 \text{ g/m}^3$$

the second stage of

$$c_{ge} = 0{,}8 + \frac{20 - 7{,}1}{15} = 1{,}7 \text{ g/m}^3$$

3.122 Packed Towers for Ammonia Stripping

Stripping of ammonia from sewage, generally from biologically treated sewage, requires a pH-adjustment to convert the NH_4^+-ion to the volatile NH_3-molecule, as was pointed out in section 2.11. The protolysis constant of this reaction depends strongly on temperature (figure 3.11). Hence pH and temperature determine the percentage fraction of

the sum of NH_4^+-N and NH_3-N, that can be removed from sewage by aeration. The total ammonia nitrogen content in sewage ranges from 25 to 45 g/m^3. Effluent concentration of 1 to 2 g/m^3 are aimed at in order to prevent eutrophication of receiving waters as far as possible. Hence percentage removal efficiencies in the order of magnitude of 90 to 98 % should possibly be accomplished, requiring almost complete conversion of NH_4^+ to NH_3, i.e. pH-values in the range of 10,8 to 11,5 by means of lime addition. Nevertheless, the efficiency of ammonia stripping will significantly decrease with decreasing temperature, firstly because the conversion gets more and more incomplete (fig. 3.11), secondly because the rate of diffusion and of renewal of the interfacial area between air and water decreases, thirdly, because the saturation value increases giving rise of a reduction of the driving force. This can partially be compensated by applying high air to water flow ratios and low hydraulic surface loads as compared to removal of carbon dioxide.
However, application of high RQ-values is likely to decrease the temperature of the sewage, thus decreasing the efficiency of the process again.

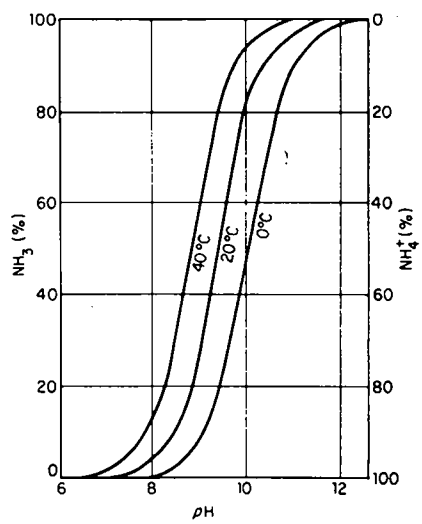

Fig. 3.11 EFFECTS OF pH AND TEMPERATURE ON THE DISTRIBUTION OF AMMONIA AND AMMONIUM ION IN WATER

The influence of some significant design and operational criteria is discussed in the following, based on completely filled towers (no subdivision into sections), counter current or cross-flow ventilation

(figure 1.6), pH-values of the influent about 11, and a temperature of some 20°C.

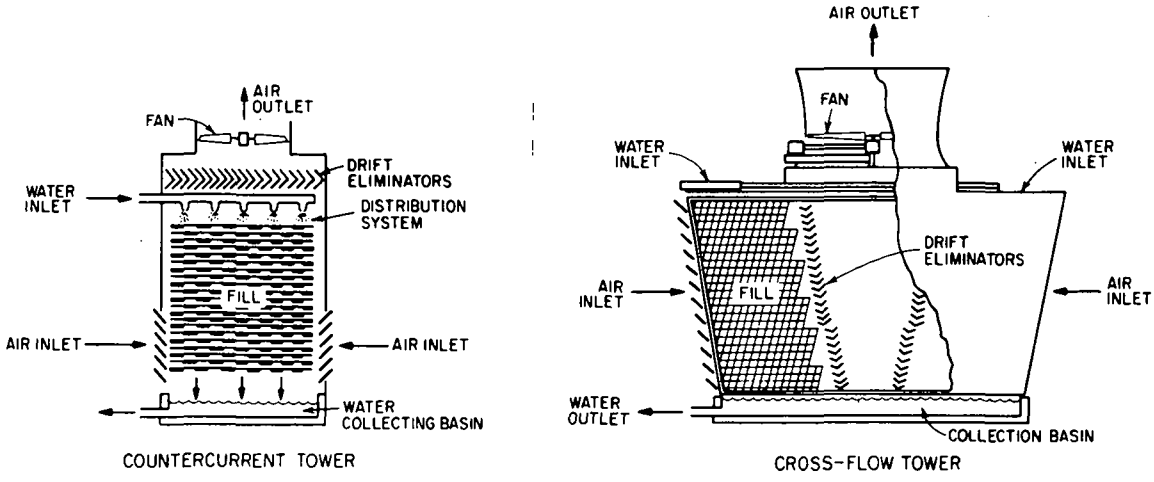

Fig. 1.6 STRIPPING TOWERS FOR REMOVAL OF AMMONIA

The combined effect of packing depth and air to water flow ratio RQ is shown in figure 3.13, varying the packing depth from 3,90 m to 7,90 m. The efficiencies of the 6,60 m and 7,90 m packing depth are essentially the same up to 90 % efficiency, requiring a RQ = 2000. Removals above 90 % cannot be obtained with a packing height of 6,60 m and require prohibitively large ratios of air to water flow at 7,90 m depth of fill.

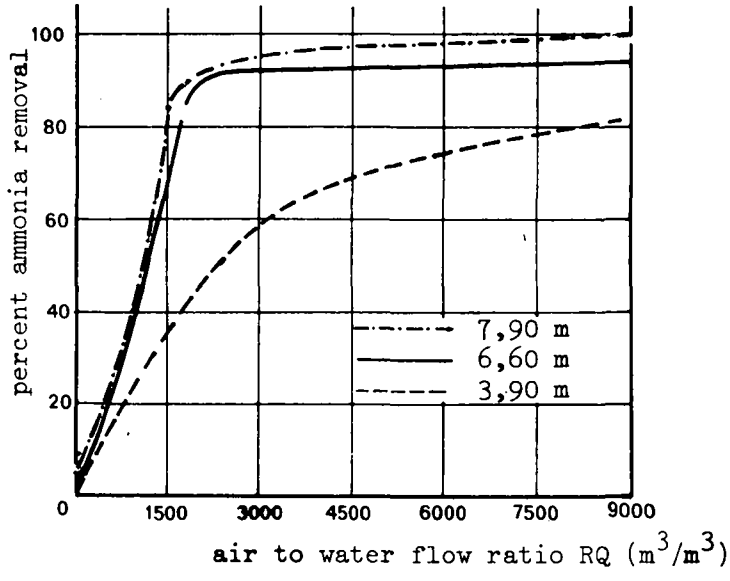

Fig. 3.13 INFLUENCE OF THE AIR TO WATER FLOW RATIO RQ ON THE PERCENT REMOVAL OF AMMONIA

The effect of hydraulic surface loading and height of fill is depicted in figure 3.14. Again, their is no significant difference in efficiency between depths of 6,60 and 7,90 m. At loads above 0,002 m/s the removal efficiency rapidly decreases due to formation of water sheets instead of droplets, providing less specific interfacial area A/V.

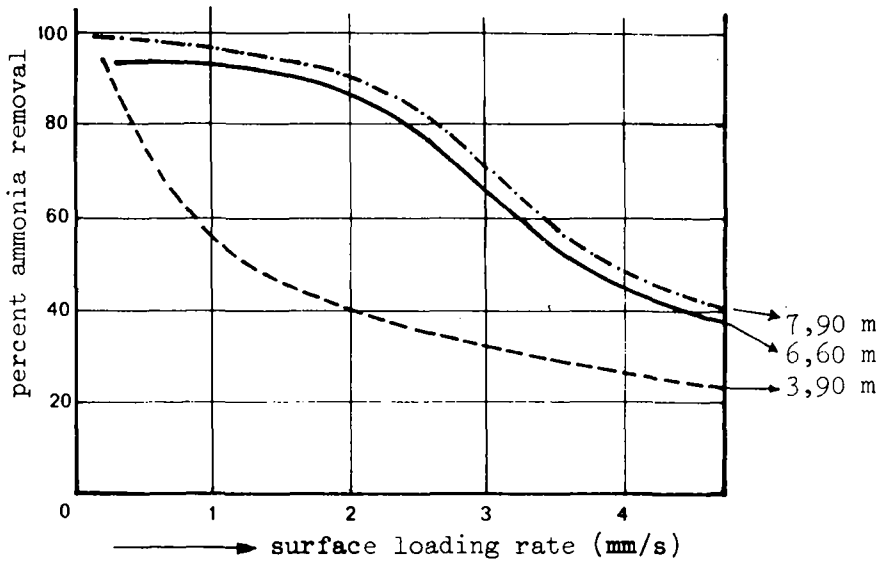

Fig. 3.14 PERCENT AMMONIA REMOVAL VERSUS SURFACE LOADING RATE FOR VARIOUS DEPTHS OF PACKING

Figure 3.15 finally shows the influence of the spacing of the tower fill on the removal efficiency at various RQ-values. Red wood slats, spaced at 38 mm vertical and 51 mm horizontal distance are less susceptible to formation of water sheeting than plastic truss bars, spaced at 100 x 100 mm and accomplish higher removal efficiencies at the same air to water flow ratio, therefore.

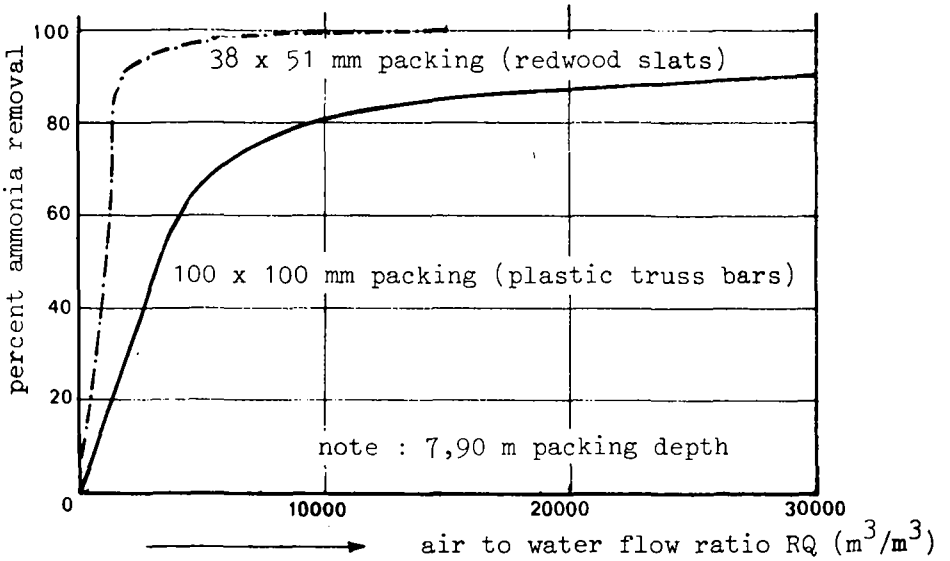

Fig. 3.15 EFFECT OF PACKING SPACING ON AIR REQUIREMENTS AND EFFICIENCY OF AMMONIA STRIPPING

Combining the discussed effects, the following operational criteria must be met to achieve percentage removals between 80 and 98 percent with a red wood slat fill spaced at 38 x 51 mm. The recommendations hold for a pH-value about 11 and a temperature of 20°C.

Percent ammonia-N removal	6,60 m packing		7,90 m packing	
	hydraulic load (mm/s)	RQ (m^3/m^3)	hydraulic load (mm/s)	RQ (m^3/m^3)
80	2,5	1700	2,7	1500
85	2,2	1800	2,4	1600
90	1,7	2100	2,0	1900
95	-	-	1,4	3000
98	-	-	0,5	6000

Decrease of temperature will substantially lower the given removal efficiencies. At winter conditions the above range has to be expected to decrease to 50 to 60 %. At temperatures below 0°C the removal efficiency is further reduced to some 30 %. Furthermore, freezing is likely to occur, which requires termination of operation. By reversing the draft fan, a slight ice build up on the outside of the tower may be removed by action of the escaping air, being warmed up by the sewage.

A second operational problem reducing the removal efficiency is scale formation on the packing due to precipitation of calcium carbonate. The scale may be soft and washed out by normal operation, or somewhat harder, such that hosing is required for removal, or extremely hard, such that cleansing is accomplished only by application of dilute acid in combination with organic dispersants. The chemical or physical factors accounting for the hardness of the scale and for the amount formed are not known at this time.

3.2 Spray Aeration

Spray aeration is applied in the course of water treatment for absorption of oxygen and/or desorption of carbon dioxide.
Spray aeration achieves the transfer of these gases by distributing water into air in the form of small droplets by means of orifices or nozzles mounted on a stationary pipe system. The orifices and nozzles may be constructed and arranged to discharge the water vertically or at an angle in upward or downward direction. The water is collected by an apron, collecting tank or a contact bed.
Nozzles have been depicted in fig. 1.7; some other types are given in figure 3.16:

a) the Amsterdam nozzle: two jets of water impinge at an angle of 90°C and are dispersed;
b) the Marley and Binks nozzle: by means of a tangential inlet in the head of the nozzle a revolving flow of the water is obtained, resulting in a fine uniform spray distribution;

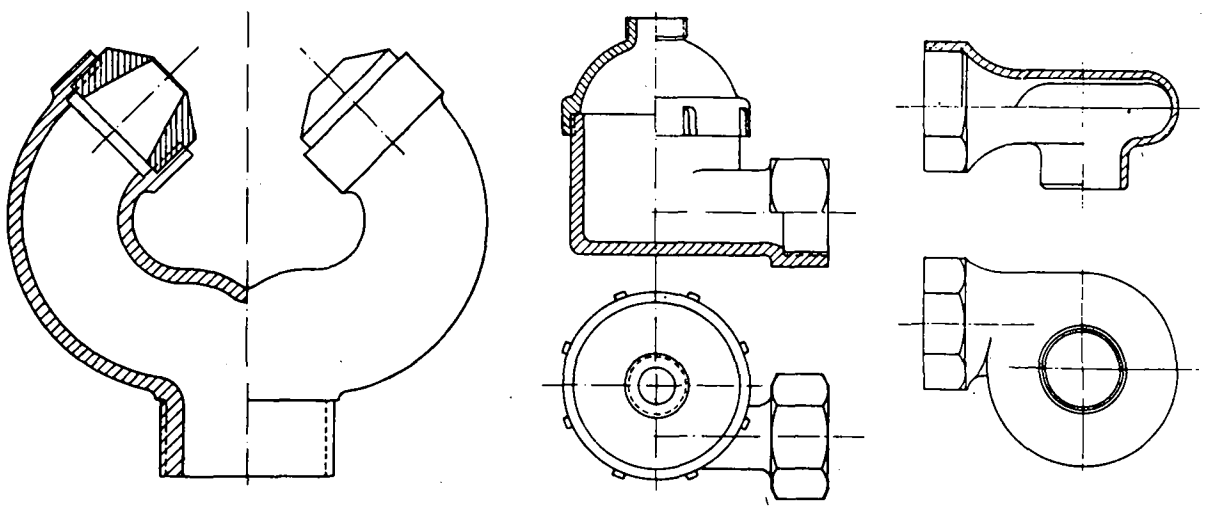

Amsterdam nozzle Marley nozzle Binks nozzle

Fig. 3.16 NOZZLE TYPES

c) Talford nozzle: by means of inclined channels a rotating movement of the water is achieved, which leaves the nozzle by an opening being controlled by an adjustable cone;
d) Patterson nozzle: the water is discharged through two slots in the shape of a snail-shell, facing each other at 180°;

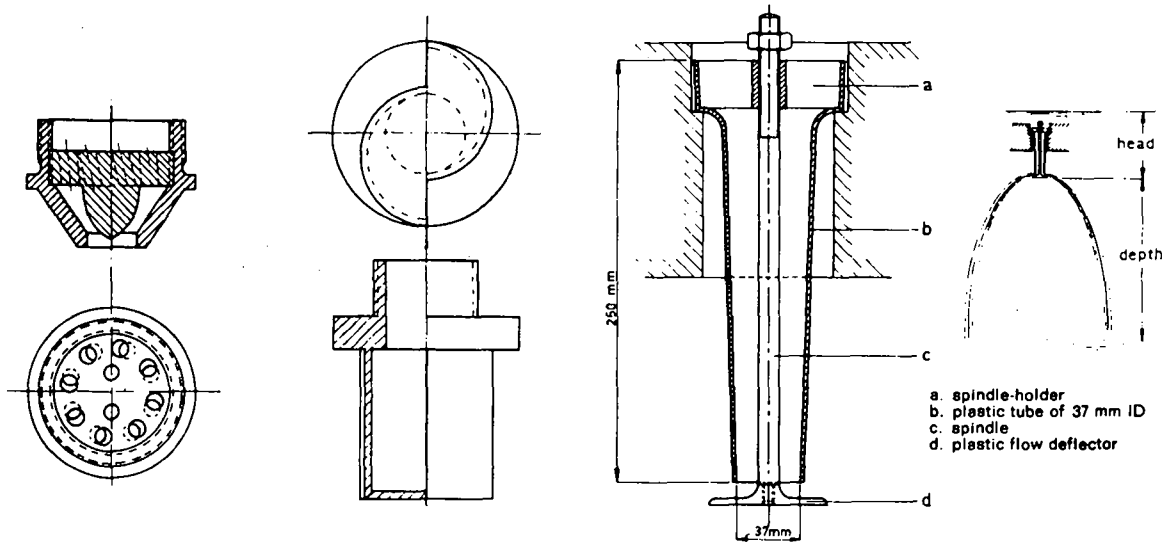

Talford nozzle Patterson nozzle Dresden nozzle

Fig. 3.16 NOZZLE TYPES

e) Dresden nozzle (only for downwards spraying): the water flowing out of a plastic tube strikes a disc (plastic flow deflector), and is spread to assume the shape of an umbrella, eventually disintergrating into droplets.

Generally, the efficiency of gas transfer is increased by applying small openings of the nozzles, producing fine droplets with a large specific interfacial area A/V and by applying a high nozzle head, giving rise to long contact times between water and air. Small nozzle openings, however, are likely to clogg. Hence, depending on the nozzle construction, openings (d_o) between 5 and 37 mm are in use, discharging at water heads h (m) between 5,0 and 0,5 m, respectively. The discharge Q from n nozzles, each having an opening area of $A = \pi d_o^2/4.10^6$ (m^2), may be obtained from the initial spray velocity $v_s = C_v . \sqrt{2.gh}$, C_v being the velocity coefficient, generally close to 0,95:

$$Q = C_d . n . A.\sqrt{2.gh} \quad (m^3/s) \qquad (3.5)$$

The coefficient of discharge C_d is the product of C_v and the coefficient of contraction C_c, thus $C_d = C_v . C_c$. The coefficient of discharge, of velocity and contraction vary with the shape and other characteristics of the nozzle.

The time of exposure t_c of an upward spray at an angle of α between the initial velocity vector and the horizontal may be estimated by

$$t_c = 2 \cdot C_v \cdot \sin \alpha \cdot \sqrt{2h/g} \qquad (3.6)$$

which ranges for initial heads between 1 and 3 m and angles between 45° and 90° from 0,6 to 2,6 seconds for $C_v = 0,95$. Application of eq. 2.44 with $D = 1,8.10^{-9}$ m^2/s shows the gas transfer coefficient to vary but between the limits of $0,3.10^{-4} < K_L < 0,6.10^{-4}$ m/s.
The radius of the spray circle r_s, neglecting wind effects amounts to

$$r_s = 2 \cdot C_v^2 \cdot h \cdot \sin 2\alpha \qquad (3.7)$$

and extends under the above assumptions up to 5,40 m. To prevent interference of sprayers, which would lead to a decrease of the efficiency by coalescence of droplets, the sprayers should be spaced at a distance of approximately $2.r_s$. Thus, nozzles spacing generally varies from 0,50 to 5 m, requiring large areas to be allocated to upward spray aeration, ranging from 350 to 700 m^2 per m^3/s treatment capacity. Furthermore, the energy consumption is quite high as indicated by the oxygenation efficiency OE, ranging from 0,14 to 0,33 mg O_2/J (0,5 to 1,2 kg O_2/kWh).

In connection with the large space requirement spray aeration is mostly performed in open air, providing good ventilation. Thus, the CO_2-content of the gaseous phase is not significantly increased when removing carbon dioxide. Hence the efficiency for desorption of CO_2 is expected to be almost equal to that for absorption of oxygen.
If spray aerators are housed (e.g. to prevent freezing or contamination) proper ventilation has to be provided by means of blinds (fig. 3.17), possibly by an induced draft.

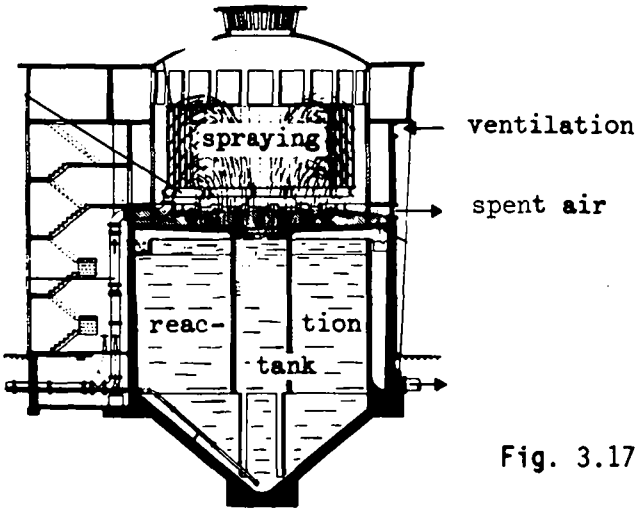

Fig. 3.17 HOUSED SPRAY AERATION

Finally, oxygenation by means of spray aeration may be performed in pressurized tanks, when the water is planned to remain under pressure in the course of treatment (fig. 3.18). The saturation concentration and hence the driving force and the rate of oxygen transfer is increased proportional to the pressure thereby, obviously.

In the following sections two types of sprayers are discussed somewhat more quantitatively.

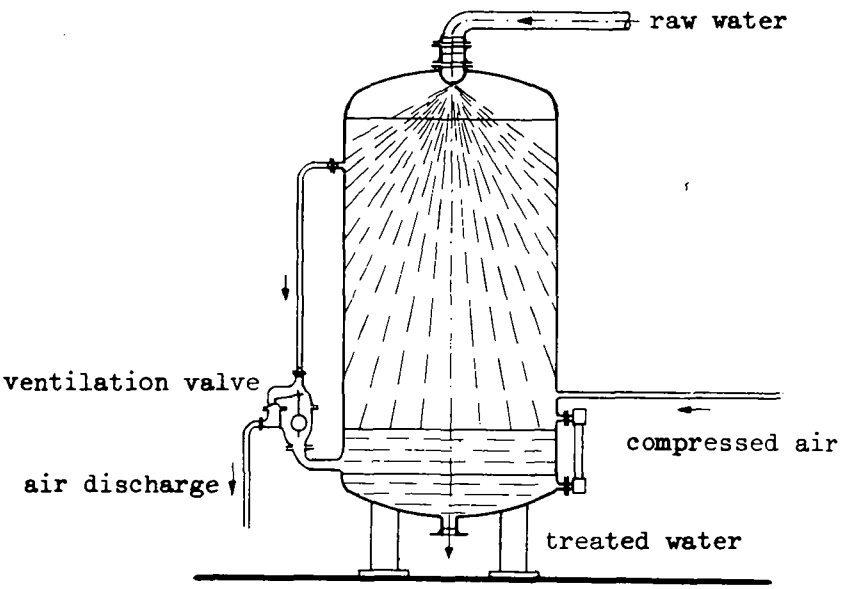

Fig. 3.18 SPRAY AERATION IN PRESSURE VESSEL

3.21 The Dresden Nozzle

The flow rate discharged by a Dresden nozzle depends on the internal diameter of the plastic tube (19 mm, 25 mm, or 37 mm), the applied head and the distance between the flow deflector and the end of the tube, being adjustable from about 0,02 to 0,03 m (see figure 3.16). Depending on the rate of flow, the discharged film of water extends to some 0,25 to 0,30 m below the deflector and then disintegrates into droplets due to gravity. During this passage an intense gas exchange takes place, the rate of which decreases with increasing depth of fall due the driving force declining as a result of gas exchange. Thus, with increasing depths of fall diminishing increases are to be expected. As an illustration of this effect, fig, 3.19 states the efficiency coefficient K for desorption of CO_2 by means of a 37 mm Dresden nozzle, discharging $0{,}8.10^{-3}$ m^3/s at a head of h_d = 0,35 m,

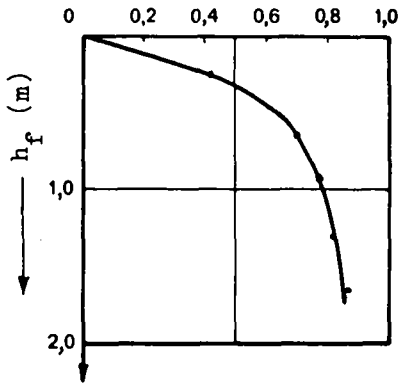

Fig. 3.19 EXAMPLE OF PERFORMANCE OF THE DRESDEN NOZZLE

as a function of the depth of fall h_f at 16°C. It is seen that up to h_f = 0,65 K increases significantly (almost proportional to h_f), whereas depths of fall above 1,0 m do not substantialy promote the desorption of CO_2. The above curve can mathematically be expressed when assuming a horizontal discharge of the water above the flow deflector. Then the relationship between time of interfacial contact t_c and the height of fall is given by

$$t_c = \sqrt{2h/g}$$

which combines with eq. 2.63 to

$$K = 1 - \exp(-k_2 \cdot \sqrt{2h/g}) \qquad (3.8)$$

$$= 1 - \exp(-0,4516 . k_2 . \sqrt{h})$$

Increasing the rate of flow will generally lower the efficiency coefficient K. Principally, the flow may be regulated by either varying the head of discharge h_d or by adjusting the distance between the end of the tube and the deflector. The latter is more reasonable, since at a given total head difference (h_d+h_f), as much height as possible should be utilized for the depth of fall in order to obtain a maximum efficiency coefficient K. The following table shows the influence of the flow rate on K for CO_2-removal for a 37 mm Dresden nozzle fed at a constant head of 0,35 m.

Influence of Flow Rate and Depth of Fall on the Efficiency Coefficient K for Removal of CO_2 at 16°C.

Flow rate 10^{-3} m^3/s	Depth below flow deflector			
	0,65 m	0,95 m	1,30 m	1,65 m
0,80	0,70	0,77	0,82	0,86
1,03	0,65	0,76	0,80	0,83
1,33	0,61	0,65	0,75	0,76
1,61	0,62	0,70	0,73	0,74

It is seen from these K-values, that increase of flow rate gradually decreases the efficiency of removal for all depths of fall.

Finally the following table proves, that desorption of CO_2 and absorption of oxygen are almost equally efficient in spray aeration with the Dresden nozzle. The data for K refer to a 37 mm nozzle at $0{,}8.10^{-3}$ m^3/s.

Comparison of Efficiency for CO_2-Removal and O_2-Uptake at 16°C.

Efficiency coefficient	Depth below flow deflector		
	0,65 m	0,95 m	1,30 m
K (CO_2)	0,70	0,77	0,82
K (O_2)	0,75	0,78	0,83
K (O_2)/K (CO_2)	1,07	1,01	1,01

The slightly greater coefficients for oxygen uptake as indicated by the ratio $K(O_2)/K(CO_2)$ may be attributed to the difference of the diffusion coefficients of both gases, the square root of the ratio of the respective coefficient being $\sqrt{D(O)_2/D(CO_2)} = 1{,}035$.

The oxygenation efficiency OE may be obtained from eq. 3.3 and the total loss of head h_d+h_f. For small heads of discharge (< 0,50 m) and depths of fall between 0,65 and 1,50 m OE will range from 0,7 to 0,4 mg O_2/J (2,5 to 1,5 kg O_2/kWh), respectively.

3.22 The Amsterdam Nozzle

The performance of the Amsterdam nozzle (fig. 3.16) with respect to CO_2-removal in dependence of the applied head and the diameter of the nozzle opening is illustrated in the following table, containing also

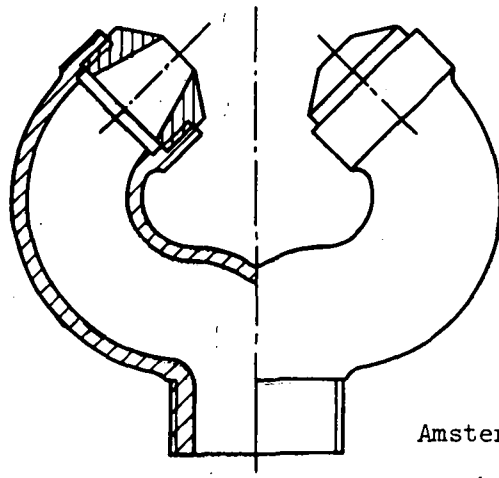

Amsterdam nozzle

the discharge capacity at the applied heads. The performance is expressed as percentage removal efficiency R (compare eq. 3.4), which, however, comes close to the efficiency coefficient, when c_s is very small as compared to c_o (eq. 2.62):

$$K = \frac{c_o - c_e}{c_o - c_s} \xrightarrow{c_s \to o} R = \frac{c_o - c_e}{c_o} \qquad (3.9)$$

Efficiency Coefficient K for CO_2-Removal by the Amsterdam Nozzle

Head in m	nozzle diameter 6 mm		nozzle diameter 7 mm		nozzle diameter 8 mm	
	Q 10^{-3} m^3/s	R (%)	Q 10^{-3} m^3/s	R (%)	Q 10^{-3} m^3/s	R (%)
1,75	0,31	76,5	0,42	74,0	0,55	75,5
2,75	0,39	81,5	0,53	85,0	0,69	76,0
3,75	0,46	82,0	0,61	79,5	0,80	79,0

It is seen that increase of the applied head and decrease of the opening diameter slightly increases the removal efficiency.
A comparison of these results with those for the Dresden nozzle, shows the latter to be more effective. This advantage holds also for

the oxygenation efficiency OE which may be approximated from the above data to range under the cited hydraulic conditions to vary from 0,22 to 0,44 mg O_2/J (0,8 to 1,60 kg O_2/kWh). This result is obtained, when assuming that the given R-values for CO_2-removal are close to the K-values for oxygen absorption.

Example: Determine the effluent carbon dioxide and oxygen content of a water with 60 g CO_2/m^3 and 2 g O_2/m^3 being aerated by

a) Dresden nozzles of 37 mm opening

b) Amsterdam nozzles of 8 mm opening

when a total head of 1,75 m is applied.

Assume

- a water temperature of 16°C
- an increase of the CO_2-concentration in the air, applied for ventilation, to give a saturation value of 3 g CO_2/m^3
- the efficiency coefficients K to be equal for absorption of oxygen and desorption of CO_2.

a) Applying a head of discharge of 0,35 m, the depth of fall is 1,75 - 0,35 = 1,40 m. From fig. 3.19 the efficiency coefficient is obtained as $K(CO_2)$ = 0,84 for a depth of fall of 1,40, the discharge being 0,8 . 10^{-3} m^3/s per nozzle.

Hence for

CO_2 $\quad c_e = c_o + K(CO_2).(c_s - c_o)$

$= 60 + 0{,}84.(3-60) = 12$ g CO_2/m^3

O_2 $\quad c_e = c_o + K(O_2).(c_s - c_o)$

$= 2 + 0{,}84.(9{,}8-2) = 8{,}6$ g O_2/m^3

b) The removal efficiency of the Amsterdam nozzle at h_d = 1,75 m amounts to some R = 75,5 %. Thus with c_o = 60 g/m^3 the effluent concentration is

CO_2 $\quad c_e = 60(1-0{,}755) = 14{,}7$ g CO_2/m^3

from which the efficiency coefficient is obtained as

$$K = (c_e - c_o)/(c_s - c_o) = (14{,}7-60)/(3-60) = 0{,}79$$

Applying this value to the transfer of oxygen the effluent oxygen concentration will be

$$O_2 \qquad c_e = c_o + K.(c_s - c_o) = 2{,}0 + 0{,}79.(9{,}8-2) = 8{,}2 \text{ g } O_2/m^3$$

Summarizing, it may be stated, that depending on the operational conditions (type of nozzle, head of discharge, flow per nozzle) the efficiency of spray aeration in terms of the efficiency coefficient ranges from 0,50 to 0,85. Removal of CO_2 and uptake of oxygen are equally efficient. The percentage gas transfer efficiency R for CO_2-removal, however, is much more influenced by temperature changes than that for oxygen uptake (see section 2.5)

Since spray aeration requires much area, its sole application is generally restricted to small treatment works.

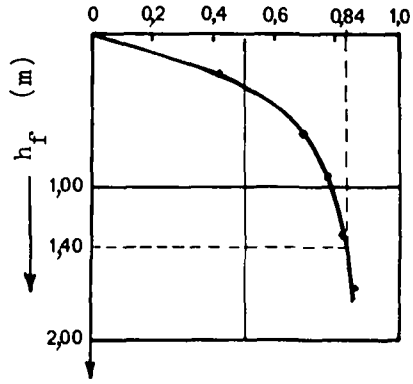

efficiency coefficient K for removal of CO_2

Fig. 3.19 EXAMPLE OF PERFORMANCE OF THE DRESDEN NOZZLE

3.3 Bubble Aeration or Air Diffusion

3.31 General Considerations

The transfer of gas by means of air diffusion is accomplished by injecting compressed air through orifices of various size into the water contained in an "aeration tank". Gas transfer occurs as the bubble emerges from the orifice, as the bubble rises through the liquid (section 2.33) and as it bursts at the surface, shedding an oxygen saturated film into the surface layers. Additional aeration occurs by velocity gradients at the surface induced by the turbulence of the rising bubbles. To all three mechanisms of gas transfer different coefficients of gas transfer may be assigned. Generally however, the share of the surface effects is small and almost negligible in comparison to the effects of bubble formation and rise. Inspection of eq. 2.53 and 2.56 then shows, that the prime parameters affecting the rate of gas transfer are the bubble size (d_B) as correlated with the rising velocity (v_r) relativ to the liquid (see also figure 2.5). Both factors determine the coefficient of gas transfer k_L (eq. 2.53) and the specific surface area A/V.

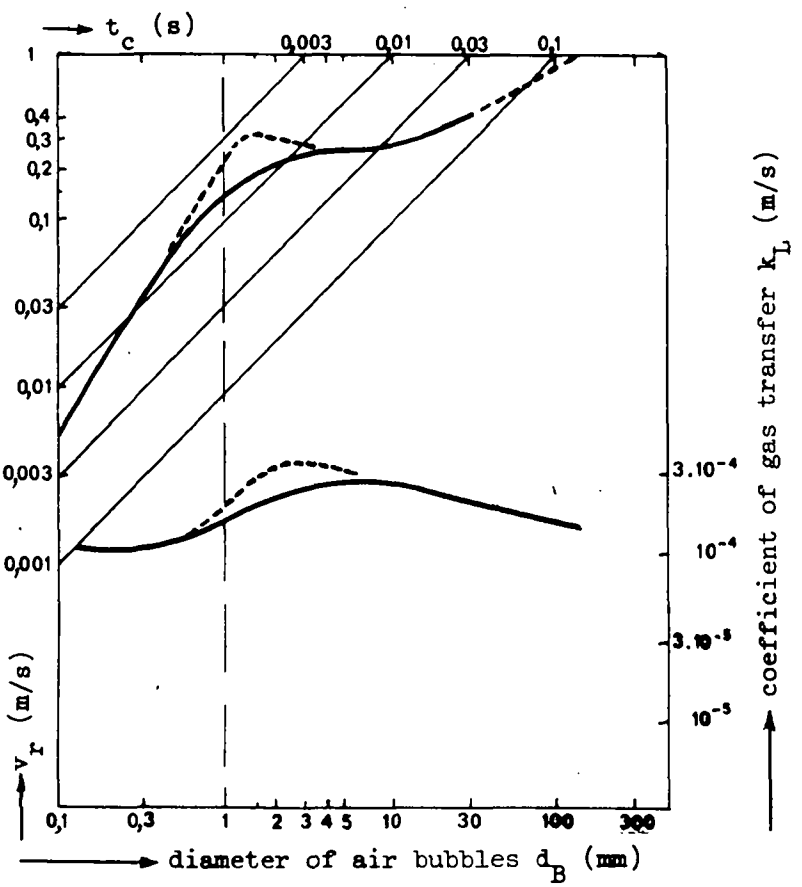

Fig. 2.5 RISING VELOCITY OF AIR BUBBLES IN WATER AND THE COEFFICIENT OF GAS TRANSFER AND TIME OF EXPOSURE ACCORDING TO THE PENETRATION THEORY

The bubble size is related to the orifice diameter and the rate of air flow. At low air rates, the bubble volume is proportional to the orifice diameter and the surface tension and inversely proportional to the liquid density. The bubble size results from a balance of the boyant forces separating the bubble from the orifice and the shearing forces required to overcome the surface tension across the orifice. In this case the bubble size is independent of the air rate and the frequency of bubble release is proportional to the air rate.

At high air rates, the bubble diameter increases as a function of the air rate, the frequency of release remaining constant.
Within the intermediate range, generally uncountered in practice, bubble size and frequency of release depend on the air rate. The mean bubble diameter then is a exponential function of the air rate Q_g:

$$d_B = k_B \cdot Q_g^n \qquad (3.10)$$

where k_B is related to the orifice diameter and the air discharge velocity through the orifice.
Bubble size d_B and velocity v_r, together with the immersion depth of the diffuser d_i and the air rate Q_g determine the total interfacial area A. Assuming spherical bubbles, the total surface area produced per unit time (A_t) is obtained by dividing the air rate Q_g by the bubble volume ($d_B^3.\pi/6$) and multiplication with the bubble surface (πd_B^2), giving

$$A_t = Q_g \cdot \frac{d_B^2.\pi}{d_B^3.\pi/6} = \frac{6.Q_g}{d_B} \quad (m^2/s) \qquad (3.11)$$

The detention time of the bubbles within the liquid t_B may be estimated as

$$t_B = d_i/v_r \qquad (3.12a)$$

for stagnant water and as

$$t_B' = d_i/(v_r + v_w) \qquad (3.12b)$$

when the water has an upward velocity, induced by the rising bubbles of v_w.

Hence the total surface area A present at any time will be

$$A = A_t \cdot t_B = \frac{6.Q_g \cdot d_i}{d_B \cdot v_r} \qquad (3.13a)$$

or

$$A' = A_t \cdot t'_B = \frac{6.Q_g \cdot d_i}{d_B.(v_r+v_w)} \qquad (3.13b)$$

and after combination with eq. 3.10

$$A = \frac{6.Q_g^{(1-n)}.d_i}{v_r \cdot k_B} \qquad (3.14a)$$

or

$$A' = \frac{6.Q_g^{(1-n)}.d_i}{k_B(v_r + v_w)} \qquad (3.14b)$$

Thus the rate of gas transfer will increase with decreasing bubble size and increasing depth of immersion and air rate, primarily by increasing the total surface area A by two mechanisms: firstly a greater surface per unit air volume injected is produced (eq. 3.11) and secondly, the detention time t_B is increased by smaller bubbles having a smaller rising velocity (fig. 2.5).

Besides the discussed parameters bubble size, air rate and depth of immersion the following factors will effect the rate of gas transfer by air diffusion:

- size and shape of the aeration tank
- arrangement of diffusers within the aeration tank
- air rate per diffuser unit, or for a given rate of air flow Q_g the number of diffuser units applied.

The size and shape of the aeration tank and the arrangement of diffuses primarily determine the pattern of flow of the water within the tank and hence v_w. Examples are given in fig. 3.20. The figures indicate that depending on the above factors a circulatory motion of water of diffirent extent and intensity is induced due to the air-water mixture near the diffusers being of less specific density than the bulk of the tank content.

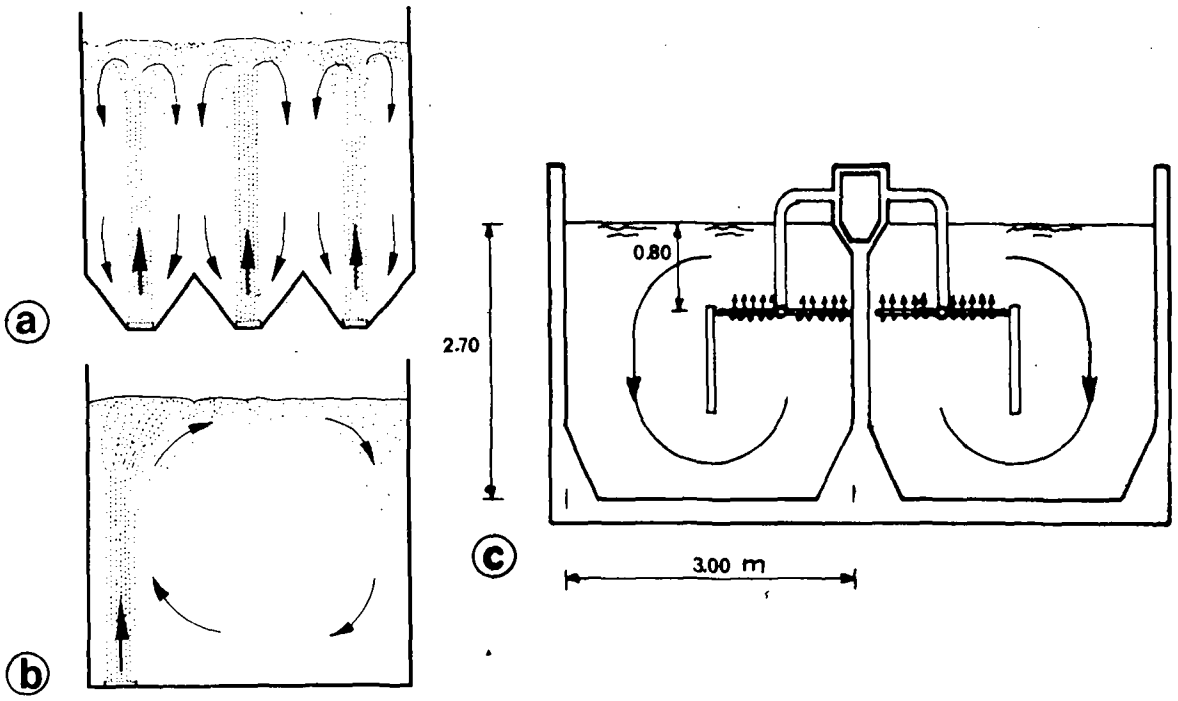

Fig. 3.20 ARRANGEMENT OF DIFFUSERS WITHIN AN AERATION TANK AND THE CORRESPONDING PATTERN OF FLOW

Above the diffusers, the rising velocity of the liquid and of the bubbles with respect to the liquid add, the vertical vectorial sum of both determining the detention time of the bubble within the liquid. This obviously decreases the total interfacial area A (compare eq. 3.13). On the other hand, some of the bubbles will be transported downwards on the tank side opposite to the diffusers, increasing the air liquid interface again. Generally the decreasing effect of the circulatory motion on A/V is more significant. Hence arrangements of diffusers which induce small, locally confined rotations (fig. 3.20a) are more efficient for gas transfer than systems, affecting a general circulation of the total tank content (spiral flow). Principally, an arrangement of the diffusers is likely to be most efficient which produces the smallest average streaming velocity of the water v_w.

The last mentioned factor influencing the rate of gas transfer, the air rate per diffuser unit, is seen from eq. 3.10. Since a diffuser unit provides a certain total orifice area, the air rate per unit should be as low as possible in order to produce small bubbles of greater transfer efficiency. The lowest air rate that may practically be applied is determined by the air pressure required for all orifices of the diffuser units to release bubbles. Obviously, this depends on the structure and hence on the commercial type of diffuser applied.

Although numerous factors, partially not numerically expressible , influence the rate of gas transfer by bubble aeration, the aeration coefficient (and oc) can be related to the important process variables. Assuming a fairly constant coefficient of gas transfer k_L (comp. section 2.33) and inserting eq. 3.14 b into the basic equation $k_2 = k_L \cdot A'/V$ we get

$$k_2 = \frac{6 \cdot k_L}{k_b} \cdot \frac{Q^{(1-n)}}{v_r + v_w} \cdot \frac{d_i}{V} \qquad (3.15a)$$

and with eq. 2.64

$$oc = \frac{6 \cdot k_L \cdot c'_s}{k_b} \cdot \frac{Q^{(1-n)}}{v_r + v_w} \cdot \frac{d_i}{V} \qquad (3.15b)$$

The first factor of eq. 3.15 may be interpreted as a „constant", whereas the remaining two describe the influence of the important process variables.

Since sufficient information on the constants of eq. 3.15 is not available, eq. 3.15 can only be used for interpreting oxygenation experiments by air diffusion and is less suitable for designing purposes. Other models for oxygenation by bubble aeration have been proposed by Bewtra and Nicholas (11), Suschka (12), and Horvath (13), which do not overcome this drawback either. Hence, the rate and efficiency of some of the air diffusers applied in practice are discussed in the following sections. Depending on the size of the orifices of the diffusion devices, three basic types of bubble aeration may be differentiated:

1. fine bubble aeration, achieved by small orifices of an order of magnitude of 0,1 mm in porous filter media;
2. medium bubble aeration, through orifices of 2 to 5 mm diameter;
3. large bubble aeration through orifices of more than 5 mm diameter or open tubes of some 25 mm diameter. In either case special constructions for breaking up of the large bubbles into smaller ones are often applied to increase the gas transfer efficiency.

Although bubble aeration is sometimes used for oxygenation and removal of taste and odor producing substances in the course of water treatment, it is the domain of oxygen transfer in sewage treatment by the activated sludge treatment. Hence the following sections are primarily restricted to oxygen transfer. The system of medium bubble aeration at low depths of immersion for removal of carbon dioxide from water is covered seperately, therefore.

Finally, special attention is paid to systems of bubble aeration not by means of compressed air but rather by air drawn into the water by a partial vacuum induced by locally increased streaming velocities (venturi aerator, deep well aerator). Both systems are used in the course of water purification.

Before discussing the systems of air diffusion the customary parameters for expressing the rate and efficiency of oxygen transfer in bubble aeration are commentated. Most of them are directly related to the overall transfer coefficient k_2, as will be shown.

- the oxygenation capacity oc (g $O_2/m^3.s$) is widely used as a rate parameter. It has been discussed in section 2.43. Generally, the oc of bubble aeration is correlated to the air flow Q_g per unit tank volume V (= water volume V of the air-water mixture):

$$G = \frac{Q_g}{V} \quad (m^3 \text{ of air / } m^3 \text{ of water volume . s}) \qquad (3.16)$$

The air flow Q_g is to be stated at standard conditions of temperature (0°C; in the U.S. often 16°C = 60°F) and pressure (101,3 kPa) for dry air. The rational basis of this approach is seen from eq. 3.15, taking into account the definition of $oc = k_2.c'_s$ (eq. 2.64). An example is given in figure 3.21.

- the oxygen utilization (OU) states, how much oxygen is absorbed per standard m^3 air applied, and is obtained by

$$OU = \frac{oc}{G} = \frac{k_2 \cdot c'_s}{G} \quad (g\ O_2 \text{ absorbed / } m^3 \text{ of air applied}) \qquad (3.17)$$

and thus is an indication of the efficiency of the diffuser system.

- Frequently, this efficiency is expressed as "percent oxygen absorption" (OA). Since dry air contains 20,95 % of oxygen by volume, 1 m^3 of air at standard conditions contains c_g = 0,2095.32/0,0224 = 299 g O_2 and the percent oxygen absorption may be obtained from the oxygen utilization by

$$OA = 100 \cdot \frac{OU}{c_g} = 100 \cdot \frac{OU}{299} = 0{,}334\ OU\ \% \qquad (3.18)$$

$$= 100 \cdot \frac{k_2 \cdot c'_s}{G \cdot c_g} = 100 \cdot \frac{k_2 \cdot k_D}{G} \qquad (k_D \text{ at } 10^\circ C\ !)$$

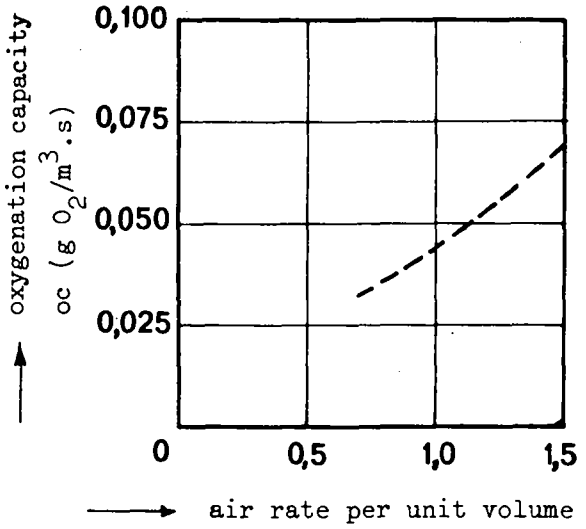

Fig. 3.21 INFLUENCE OF THE AIR RATE PER UNIT VOLUME (G) ON THE OXYGENATION CAPACITY (oc)

- To allow for the influence of the depth of immersion d_i, not contained in the above parameters, the oxygen utilization may be related to d_i. The appropriate parameter then is oxygen utilization per m of d_i, which is equal to OU/d_i (g $O_2/m^3.m$).
- The oxygenation efficiency OE (g O_2/J; kg O_2/kWh) may be computed from the gross power N_G (W) used by the blower and the oxygenation capacity OC (g O_2/s) of the system:

$$OE = OC/N_G \qquad (g\ O_2/J) \tag{3.19}$$

$$= oc \cdot V/N_G$$

The gross power N_G is estimated from the air flow Q_g (m^3/s), the air pressure P (Pa) and the efficiency η of motor and blower

$$N_G = P \cdot Q_g/\eta \quad (W) \tag{3.20a}$$

The pressure P is composed of the pressure drop ΔP in the air distribution system and in the diffusers plus the pressure against the water depth in the aeration tank amounting to $d_i.\rho.g$ (Pa). Thus

$$N_G = Q_g.(\Delta P + d_i.\rho.g)/\eta \qquad (W) \tag{3.20b}$$

Frequently, also ΔP is expressed as Δh (m water column). Then eq. 3.20b is rewritten with $\Delta h = \Delta P/\rho.g$ and $\Delta h + d_i = h_{tot}$ as

$$N_G = Q_g \cdot h_{tot} \cdot \rho \cdot g/\eta \tag{3.20c}$$

Example: An aeration tank contains 540 m^3 of water which is aerated at a rate of $G = 10^{-3}$ $m^3/m^3.s$ at an immersion depth of the diffusers of $d_i = 2,70$ m. The oxygenation capacity has been found as $oc = 0,025$ g $O_2/m^3.s$. The head loss in the total tubing system and the diffusers $\Delta h = 0,36$ m, the efficiency of the motor and blower is $\eta = 0,60$.

Compute the oxygen utilization, also per m of d_i, the percent oxygen absorption, the oxygenation efficiency, and the gross power dissipated per unit volume.

According to eq. 3.17 the oxygen utilization is

$$OU = oc/G = 0,025/10^{-3} = 25 \text{ g } O_2/m^3 \text{ of air}$$

which gives an oxygen utilization per m of d_i of

$$OU/d_i = 25/2,70 = 9,26 \text{ g } O_2/m^3.m$$

The percent oxygen absorption is (eq. 3.18)

$$OA = 0,334 \cdot OU = 0,334 \cdot 25 = 8,35 \%$$

Since the total rate of air flow amounts to $Q_g = V.G = 540.10^{-3}$ m^3/s the gross power is (eq. 3.20c)

$$N_G = 0,540 \cdot 1000 \cdot 9,81 \cdot (2,70 + 0,36)/0,60 = 27\,000 \text{ W}$$

Hence

$$OE = \frac{OC}{N_G} = \frac{oc.V}{N_G}$$

$$= 0,025 \cdot 540/27000 = 5 \cdot 10^{-4} \text{ g } O_2/J = 0,5 \text{ mg } O_2/J$$

$$= 5 \cdot 10^{-4} \cdot 3600 = 1,8 \text{ kg } O_2/kWh$$

The gross power dissipated per unit volume is

$$\varepsilon_G = N_G/V \qquad (3.21)$$

$$= 27000/540 = 50 \text{ W/m}^3$$

3.32 Fine Bubble Aeration

3.321 Types of Diffusers and Their Arrangement

The diffusers applied for fine bubble aeration consist of porous media providing different orifice diameters in order of magnitude of 0,1 mm. The size of the bubble produced ranges under operational conditions from about 1 to 6 mm. The porous media may be formed in the shape of tubes, plates covering a box, or domes.
The porous media may be of the filter type, consisting of granular material bound by synthetic resins (Brandol-diffuser), or of plastic foam (Flygt-diffuser), sometimes of ceramic nature. Small orifices are also obtained by winding a Saran plastic cord around a tube of corrugated sheet metal, into which holes of some 3 mm of diameter are drilled (Saran tube). Examples are given in figure 3.22.
For efficient gas transfer the air flow per diffuser unit may be varied within certain limits only. The lower limit is determined by the air rate required to release bubbles all over the diffuser surface in order to prevent water or pollutants from entering into it. The upper limit is set by the increase of the resistance against air flow and by the fact, that increasing air rates increase the bubble size. Finally, the bubble concentration (number of bubbles per unit tank volume) increases as does the chance of two or more bubbles to collide and coalesce to one great bubble. All effect reduce the interfacial area and hence the rate of gas transfer. The optimum air rate ranges from 0,01 to 0,02 m^3 air per m^2 diffuser surface per second. Since the effective aerating surface of the commercial diffusers ranges from 0,15 to 0,30 m^2, optimum air flow rates vary between $1{,}5.10^{-3}$ and $6{,}0.10^{-3}$ m^3/s per unit (5 to 22 m^3/h per unit).

70 mm Ø, 1085 mm long, equipped with 2 filter tubes "Brandol" granulation as requested, each 70/40 mm Ø, 500 mm long, fixed with tie rod, 2 flanges, central piece for admission of air with inside thread 1",nut and washers. Steel and cast iron mountings coated with stoved lacquer. Weight about 7 kilos. Effective aerating surface 0,22 m^2

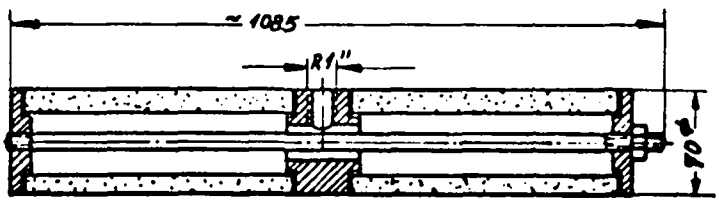

Pressure loss of cylindrical aerator 70 mm Ø with "Brandol" tubes of different granulation in relation to volume of air. Distribution of air into water.

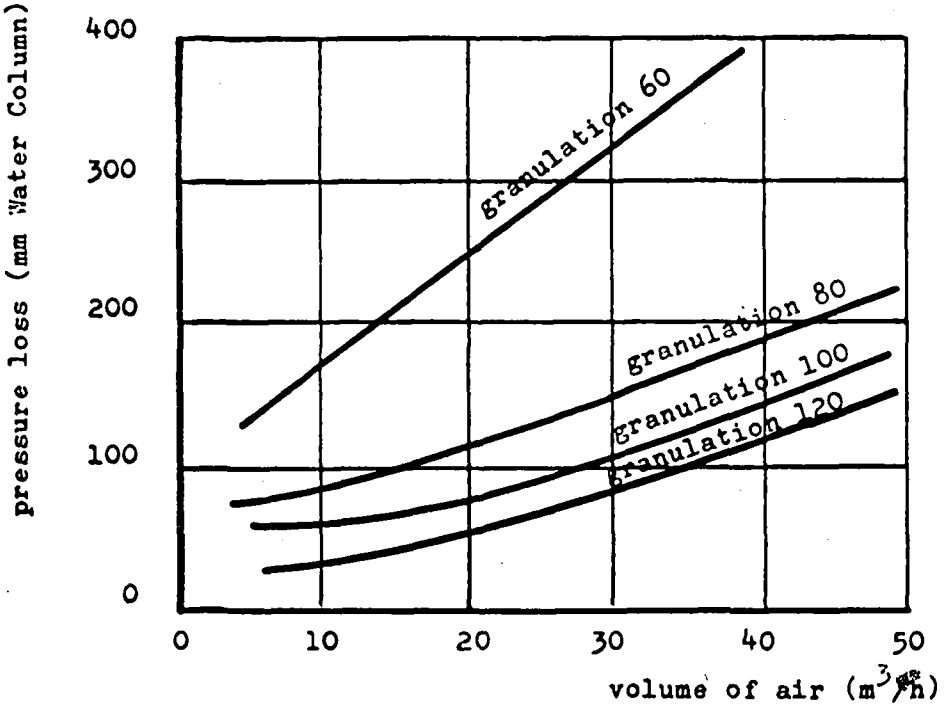

The indicated volume of air is the intake volume at 20°C. The pressure losses indicated are to be understood for complete cylindrical aerators with wet "Brandol" tubes without consideration of the liquid column above the aerators.

Fig. 3.22 a DIFFUSER FOR FINE BUBBLE AERATION - SCHUMACHER-TUBE (70 mm diam.)

100 mm Ø, about 1100 mm long, equipped with 2 filter tubes "Brandol" granulation as requested, each 100'60 mm Ø, 500 mm long, fixed with tie rod 2 flanges, central piece for admission of air with inside thread 1", nut and washers. Steel and cast iron mountings coated with stoved lacquer. Weight about 13,3 kg
Effective aerating surface 0.314 m^2

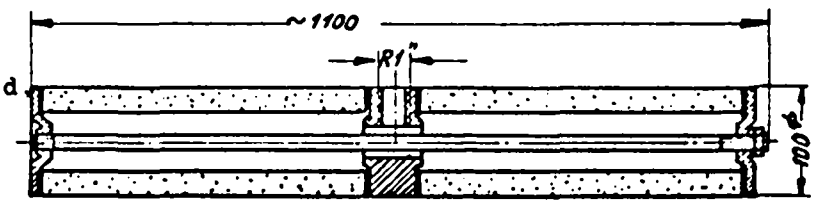

Pressure loss of cylindrical aerator 100 mm Ø with "Brandol tubes of different granulation in relation to volume of air. Distribution of air into water.

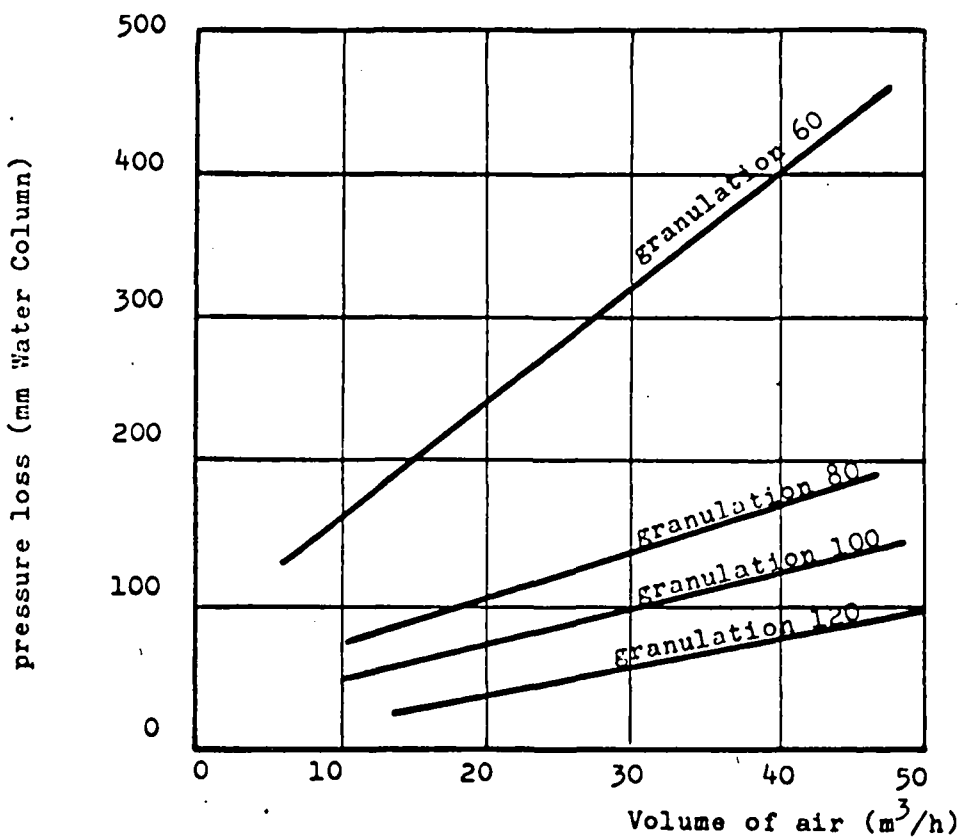

The indicated volume of air is the intake volume at 20°C. The pressure losses indicated are to be understood for complete cylindrical aerators with wet "Brandol" tubes without consideration of the liquid column above the aerators.

Fig. 3.22 b DIFFUSER FOR FINE BUBBLE AERATION - SCHUMACHER-TUBE (100 mm diam.)

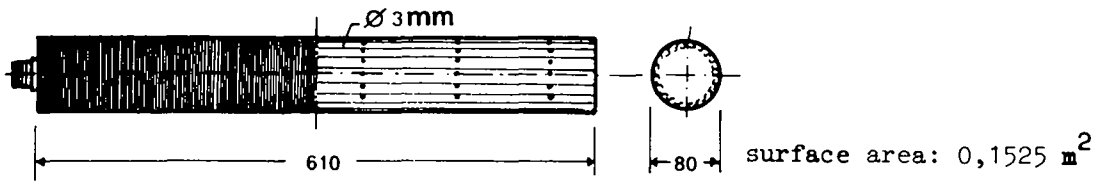

Fig. 3.22 c DIFFUSER FOR FINE BUBBLE AERATION - SARAN-TUBE

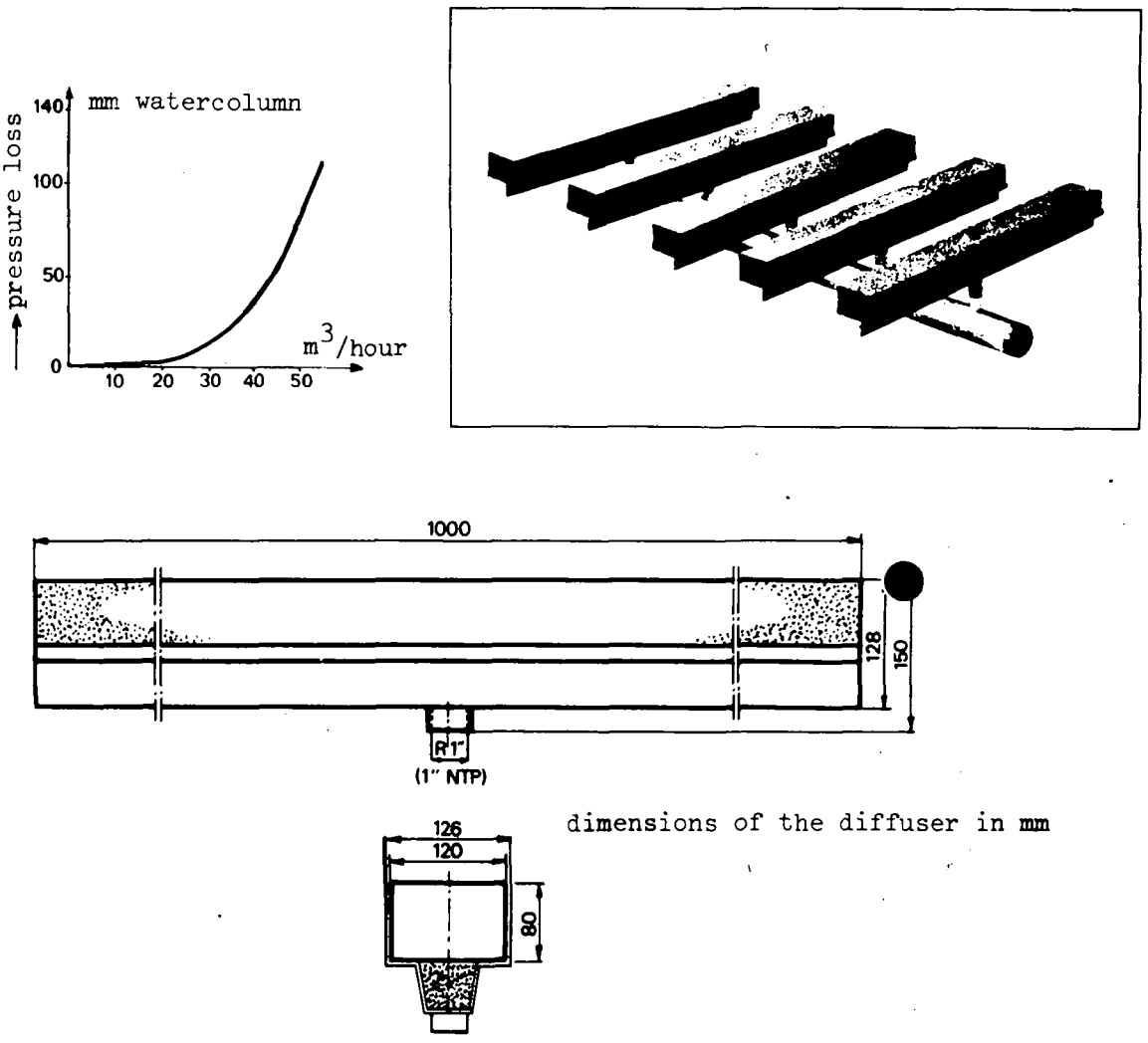

Fig. 3.22 d DIFFUSER FOR FINE BUBBLE AERATION - FLYGT-DIFFUSER

The following table gives an indication of the loss of head of the forementioned diffuser types

Diffuser Type	air rate per unit	loss of head	
	10^{-3} m^3/s	kPa	mm column of water
Brandol	2,8	1,96	200
	5,6	2,94	300
	8,3	3,92	400
	11,1	4,90	500
Saran	1,7	1,50	153
	3,3	1,57	160
	5,0	1,70	173
Flygt	5,6	0,10	10
	8,3	0,15	15
	11,1	0,34	35
	13,9	0,59	60

Generally the diffusers are placed as near to the tank bottom as possible to make full use of the tank depth for the bubble rise. The diffusers may be arranged as follows:

a) near one side wall of the tank, producing a spiral flow of the tank content, which is facilitated by a quadratic cross section of the tank. Diffuser tubes may be arranged parallel to the side wall ("narrow band") or rectangular to it ("wide band") as shown in figure 3.23. A dubble spiral flow is obtained by arranging the narrow or wide band system at both sides of a tank, which is preferably twice as wide as deep. Reducing this width leads to the arrangement generally referred to as

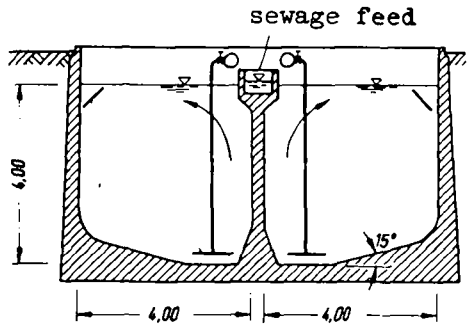

Fig. 3.23 WIDE BAND ARRANGEMENT OF DIFFUSER TUBES

b) "longitudinal pattern". This system is achieved by placing three or more diffuser bands within a tank of optional width (fig. 3.20a)

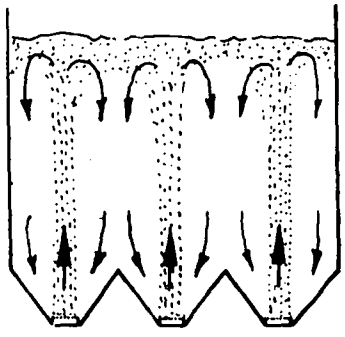

Fig. 3.20 a ARRANGEMENT OF DIFFUSER WITHIN AN AERATION TANK AND THE CORRESPONDING PATTERN OF FLOW

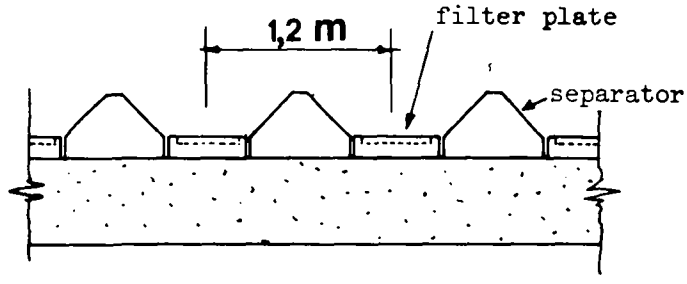

Fig. 3.24 CROSS-SECTION OF TANK BOTTOM WITH RIDGE-AND-FURROW DIFFUSER ARRANGEMENT

or with the well known "ridge- and -furrow" system (fig. 3.24), consisting of the ridge for seperating the bubble streams produced by filter plates placed in the furrows at the bottom of the tank. Filter domes spread over the tank bottom also produce a longitudinal pattern.

3.322 Factors Influencing the Rate and Efficiency of Oxygen Transfer

In the following, results of experiments on the influence of the important parameters air rate, depth of immersion and arrangement of diffusers on the rate and efficiency of oxygen transfer by fine bubble aeration are given. These will finally lead to guide values for the design of oxygen transfer by fine bubble aeration.

The combined influence of diffuser submergence and air rate (per diffuser and m^3 of air per m^3 water volume per second) is seen from figure 3.25. It follows, that the percent oxygen absorption (eq. 3.18) increases almost linearly with the depth of immersion d_i. Extrapolating the lines to $d_i=0$ shows, that the high rate of oxygen transfer during bubble formation accounts for some 2 to 3 % of oxygen absorption. Although the oxygen utilization does not increase strictly proportional to d_i, the amount of oxygen transferred per meter of d_i is frequently used as a convenient measure of an aeration system. This approach is justified, since d_i influences the gas transfer more significant than other parameters. For a chosen depth of d_i = 3,0 m the percent oxygen absorption varies within the stated G-values from 9 to 12 %, which, according to eq. 3.18, corresponds to an oxygen utilization of 27 to 36 g O_2/m^3 of air, respectively, which yields per m depth of submergence OU/d_i = 9 to 12 g O_2/m^3.m and OA/d_i = 3 to 4 %/m.

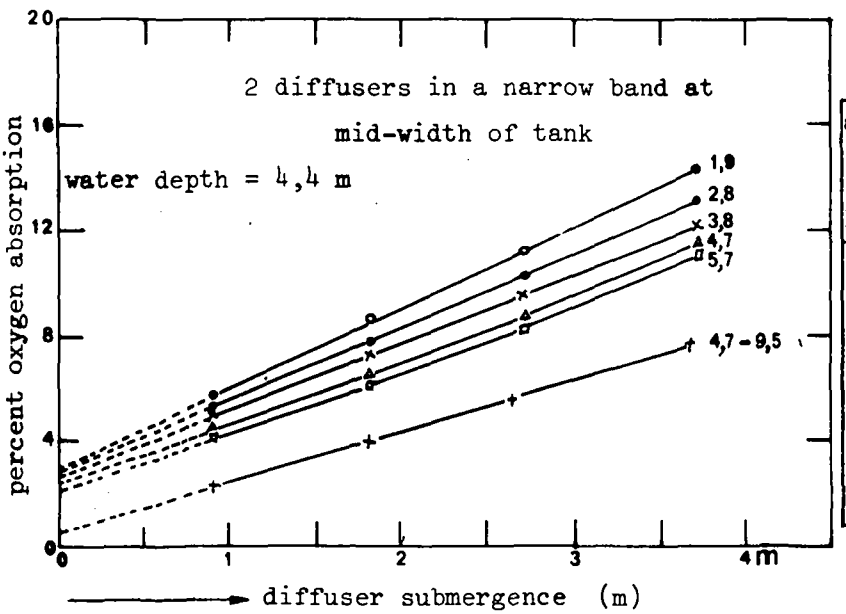

air rate 10^{-3} m^3/s per diffuser	G (10^{-3} $m^3/m^3.s$)
1,9 (Saran tube)	0,10
2,8 ,,	0,15
3,8 ,,	0,20
4,7 ,,	0,25
5,7 ,,	0,30
4,7-9,5(Sparger)	0,25 - 0,50

Fig. 3.25 EFFECT OF DIFFUSER SUBMERGENCE AND AIR-FLOW RATE ON THE PERCENTAGE OXYGEN ABSORPTION

Similar results can be read from figure 3.26, where the oxygenation capacity oc (g O_2/m^3.s) is given as a function of the air rate G (m^3/m^3.s) in dependence of the diffuser arrangement.

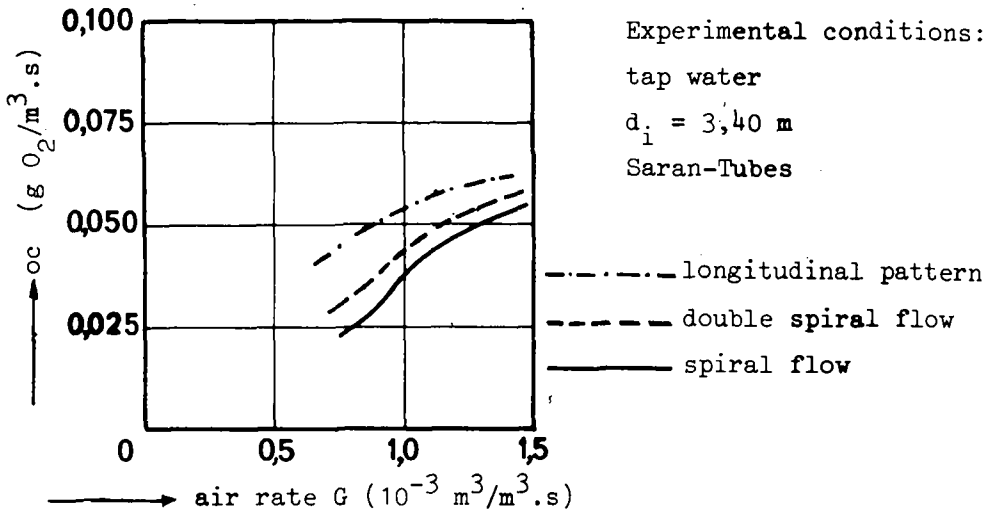

Fig. 3.26 EFFECT OF DIFFUSER ARRANGEMENT ON THE OXYGENATION CAPACITY

Application of eq. 3.17 then indicates the following ranges of oxygen utilization:

diffuser bands per tank width	range of oxygen utilization		
	OU (g O_2/m^3)	OU/d_i (g O_2/m^3.m)	
		range	average
1	33 - 40	9,7 - 11,8	11,0
2	35 - 45	10,3 - 13,2	11,8
3	45 - 55	13,3 - 16,3	15,3

Summarizing, it may be stated, that the oxygen transfer by small bubble aeration can be characterized by the oxygen utilization per m of diffuser submergence (OU/d_i) which amounts for common tank depth (2 to 5 m) to some 8 - 15 g O_2/m^3.m. Within this range,

a) the arrangement sequence narrow - wide band - longitudinal pattern will increase OU/d_i caused by a reduction of the upward water velocity v_w (comp. eq. 3.13 and 3.14);

b) an increase of G within the common range of 0,5 to $1{,}8.10^{-3}$ m^3/m^3.s will lower OU/d_i, due to the accompanied increase of the air rate per diffuser unit, which gives rise to the formation of bubbles of greater size and of coalescence of bubbles.

The cited values are applicable to tap water only. The presence of hydrophobic and surface active matter in sewage will strongly reduce the oxygen transfer by small bubble aeration (see sections 2.34 and eq. 2.71). The reduction (factor α) for biologically treated sewage ranges in dependence of the type and concentration of surface active matter from 0,5 to 1,0, whereas values as low as 0,2 to 0,6 have been reported for settled sewage. The influence of the suspended solids concentration c_{ss} on oxygen transfer is controversial. On the one hand it has been found that a variation of the suspended solids concentration between 0,3 and 6 kg/m^3 did not significantly affect α (14), on the other hand, more recent investigations (15) postulate the following quantitative relationship between α and c_{ss}:

$$\alpha = 1 - 0{,}16.c_{ss}^{2/3} \qquad (3.22)$$

Within the common range of $2 < c_{ss} < 6$ kg SS/m^3 eq. 3.22 yields values for α between 0,75 and 0,53, respectively. Despite many factors influencing the magnitude of α, it is general practice to apply a value of $\alpha = 0{,}7$ to operational condition of fine bubble aeration.

The oxygenation efficiency to be expected in fine bubble aeration may be estimated from the stated OU/d_i-values (8 to 15 g O_2/m^3.m) after combining eq. 3.19 with eq. 3.17 and 3.20b, in which ΔP is neglected in comparison to $d_i.\rho.g$:

$$OE = \frac{oc \cdot V}{N_G} = \frac{oc \cdot V}{d_i \cdot Q_g} \cdot \frac{\eta}{\rho \cdot g} = \frac{OU}{d_i} \cdot \frac{\eta}{\rho \cdot g}$$

With $\eta = 0{,}6$; $\rho = 1000$ kg/m^3; $g = 9{,}81$ m/s^2 and $OU/d_i = 8$ to 15 g O_2/m^3.m, the oxygenation efficiency is likely to vary between 0,5 and 0,9 mg O_2/J (1,8 to 3,3 kg O_2/kWh). Figure 3.27 states the oxygenation efficiency obtained from the experiments given in figure 3.26 as an illustration.

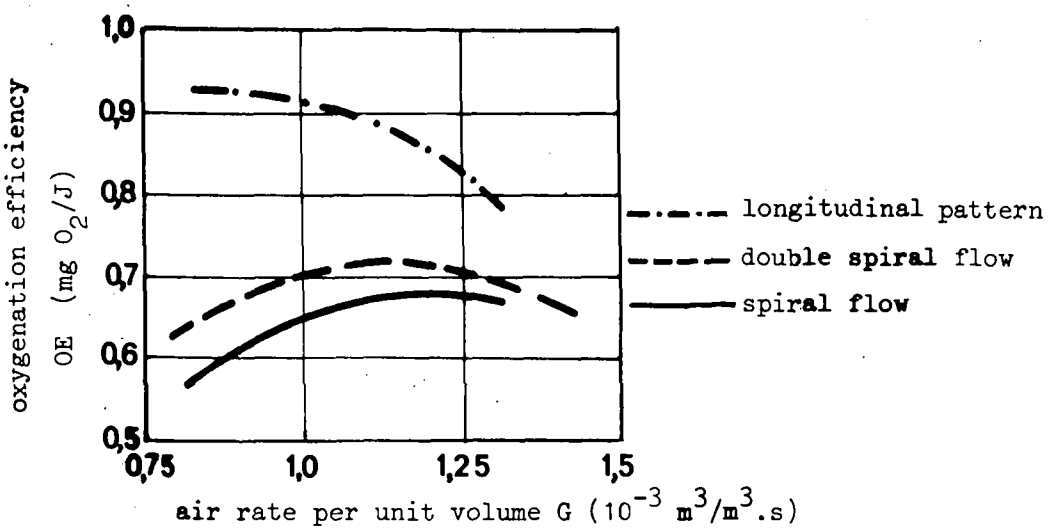

Fig. 3.27 THE INFLUENCE OF THE AIR RATE G ON THE OXYGENATION EFFICIENCY OE

The following table summarizes the most important guide values for designing oxygen transfer by fine bubble aeration in the activated sludge treatment process.

Guide Values for Oxygenation by Fine Bubble Aeration

	optimum conditions			average conditions		
	OU/d_i	OE		OU/d_i	OE	
	g O_2/m^3.m	mg O_2/J	kg O_2/kWh	g O_2/m^3.m	mg O_2/J	kg O_2/kWh
tapwater operational conditions (α = 0,7)	12	0,6	2,2	10	0,47	1,7
	8,5	0,42	1,5	7	0,33	1,2

3.323 Practical Aspects

The advantage of a great oxygen transfer efficiency by fine bubble aeration has to be paid for by a careful control of operation to prevent clogging of the fine pores of the diffusers.
Clogging may be caused by pollutants in the compressed air like dust, soot from the environment, or oil particles from the blowers, corrosion of the air distribution system. From outside, the diffusers can be clogged by matter contained in the water or sewage (carbonates, high pH-values, metal ions which precipitate, grease, oil, fine sand) or by penetration of sludge particles when the blowers do not work (break down of electricity supply etc.).

Cleansing of the diffusers is brought about by lowering of the water level in order to significantly increase the air rate per unit. More convenient in this respect are swing diffusers (fig. 3.28): a battery of some 4 to 10 diffusers are mounted at one or two pipes fixed to the air distribution main by movable joints. This construction allows to increase the air rate for cleaning by lifting one battery or facilitates replacing of a clogged unit. Partial replacing of units, however, leads to unequal restistance of the diffuser units and consequently to an uneven distribution of the diffused air over the aeration tank. Throttling of the air rate for replaced diffuser batteries may overcome this drawback, but leads to an increased power consumption again.

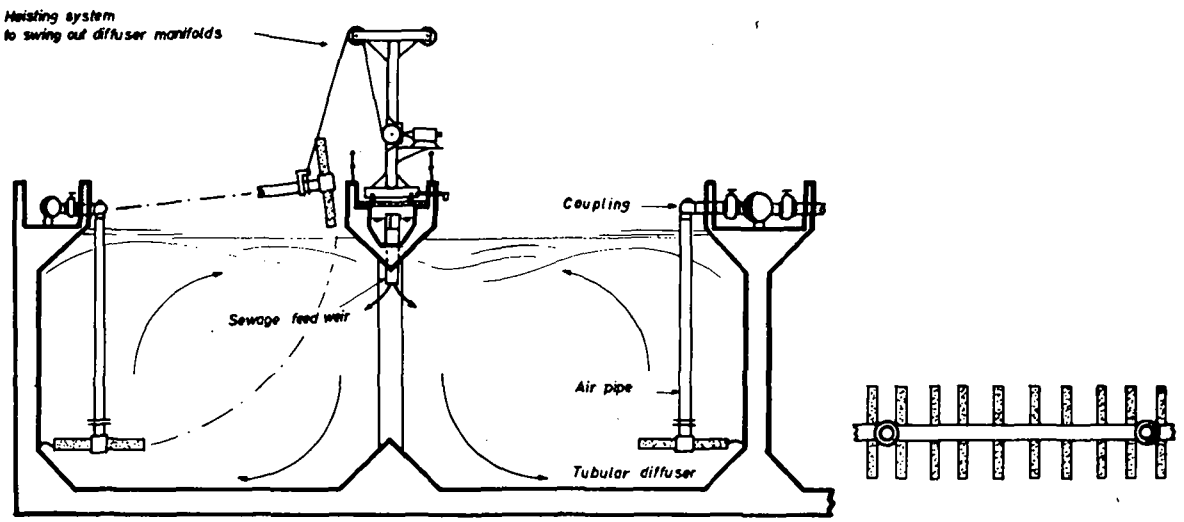

Fig. 3.28 SWING DIFFUSER ARRANGEMENT (SCHUMACHER)

Thus, fine bubble aeration requires skilled maintenance and is hence applied in great installations only, treating water or sewage not likely to give rise to diffuser clogging.
The air has carefully to be filtered and blowers discharging oil free air have to be applied.

Example: The maximum oxygen demand of an activated sludge treatment unit (d_i = 3,70 m) has been found to be max OD = 70 g O_2/s, the minimum value min OD = 20 g O_2/s. Estimate the maximum and minimum air rate required and the number of Saran tubes to be installed (operation range for Saran tube according fig. 3.22 is 1,5 to 5,5 . 10^{-3} m^3 of air per second, optimum rate is 3,3 . 10^{-3} m^3/s) when the oxygen saturation concentration under operational conditions is c_s = 10,5 g/m^3 and a oxygen concentration of c = 1,5 g/m^3 has to

be maintained in the mixed liquor.
What is the maximum gross power consumption?
At zero oxygen content in the tank, the oxygenation capacity of the aeration system OC has to be equal to the oxygen demand OD:

$$oc \cdot V = OD$$

Inserting eq. 3.17 and 3.16 into this expression yields

$$OU \cdot G.V = OU \cdot Q_g = OD$$

or

$$Q_g = \frac{OD}{OU/d_i} \cdot \frac{1}{d_i} \quad (m^3 \text{ of air/s}) \qquad (3.23)$$

To allow for the required oxygen concentration c = 1,5 g/m^3 the air rate has to be increased by $c_s/(c_s - c)$ to give

$$Q_g = \frac{OD}{(OU/d_i)} \cdot \frac{1}{d_i} \cdot \frac{c_s}{c_s - c}$$

Hence, with OU/d_i = 7 g O_2/m^3 for average operational conditions:

$$\max Q_g = \frac{70}{7} \cdot \frac{1}{3,70} \cdot \frac{10,5}{10,5-1,5} = 3,15 \text{ m}^3/\text{s}$$

$$\min Q_g = \frac{20}{7} \cdot \frac{1}{3,70} \cdot \frac{10,5}{10,5-1,5} = 0,90 \text{ m}^3/\text{s}$$

Since increased air rates reduce the oxygen transfer efficiency, the number of tubes is estimated by comparing min Q_g with the lower limit of the air rate per tube ($1,5.10^{-3}$ m^3/s):

Number of tubes = min $Q_g/1,5.10^{-3} = 0,9/1,5.10^{-3} = 600$
For max Q_g the air rate per tube equals to
max $Q_g/600 = 3,15/600 = 5,2.10^{-3}$ m^3/s which is below the upper limit of $5,5.10^{-3}$ m^3/s.

Assuming an oxygenation efficiency of OE = 0,33 mg O_2/J, the maximum gross power is obtained from max OD = 70 g O_2/s as 70.1000/0,33 J/s = 212 kW at c = 0 g O_2/m^3. Thus, the actual maximum gross power is 212.10,5/(10,5-1,5) = 247 kW.

3.33 Medium Bubble Aeration (High Pressure)

3.331 Types of Diffusers and Their Arrangement

Medium bubble aeration at high pressure is performed by means of

- perforated pipes with openings of 2 to 5 mm diameter at the bottom side of the pipe arranged in one or more rows. The pipes may be combined to an aeration grid. A grid-like effect is obtained by application of perforated plates. The units may be connected to the header by joints (swing-type) similar to figure 3.28.
- small tube pieces, crosswisely arranged in a casting of iron or plastic, which is saddle mounted on the air distribution headers (sparger: fig. 3.29)

As with fine bubble aeration, the aeration units are placed as near

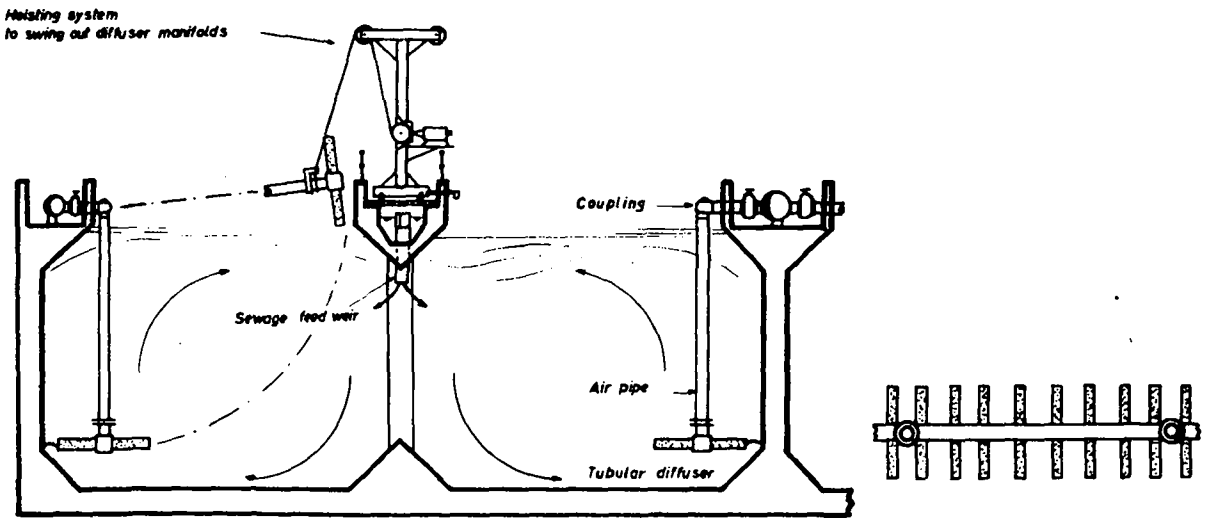

Fig. 3.28 SWING DIFFUSER ARRANGEMENT (SCHUMACHER)

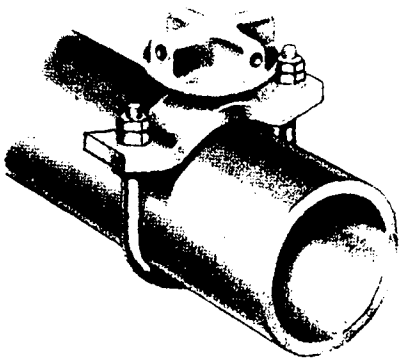

Fig. 3.29 SPARGER SADDLE MOUNTED ON HEADER

to the tank bottom as possible to make full use of the tank height for contact between air and water. High pressure blowers are required therefore. On the other hand perforated pipes or grids are applied at shallow submergence (combined with low pressure fans). This system is covered in section 3.334.
Generally, the wide or narrow band type of arrangement of the diffuser units is applied.

3.332 Factors Influencing the Rate and Efficiency of Oxygen Transfer

The main difference of rate and efficiency of medium bubble aeration as compared to oxygen transfer by fine bubble is caused by 2 factors:

1. The larger bubbles provide a smaller total interfacial area;
2. The bubbles are not formed by a slow increase of their size, but are released in a chain-like manner. Partly, the formed bubbles are to great to withstand the hydraulic shear imposed on them by the high water velocity around the place of bubble formation. Breaking into a number of smaller bubbles in the consequence, then.

The firstly mentioned decrease of the total interfacial area obviously leads to a decrease of the rate of oxygen transfer as compared to fine bubble aeration.
Due to the difference in bubble formation, mentioned under item 2, the oxygen transfer during formation is much less pronounced than with fine bubbles. This is evident from figure 3.25. Whereas the process of bubble formation accounts to some 2 to 3 % of oxygen absorption with Saran tubes, this effect is decreased to about 0,5 % when applying medium bubble aeration by spargers. The figure also reveals, that variation of the air rate per diffuser unit or per tank volume is of neglegible influence on the gas transfer efficiency. Moreover, the size of the orifices within the stated range of 2 to 5 mm is of no significant influence. This has been shown by applying various opening diameters within this range and air discharge velocities from 3 to 100 m/s. No significant differences concerning the oxygen utilization had been obtained.
Finally medium bubble aeration is less susceptible than fine bubble

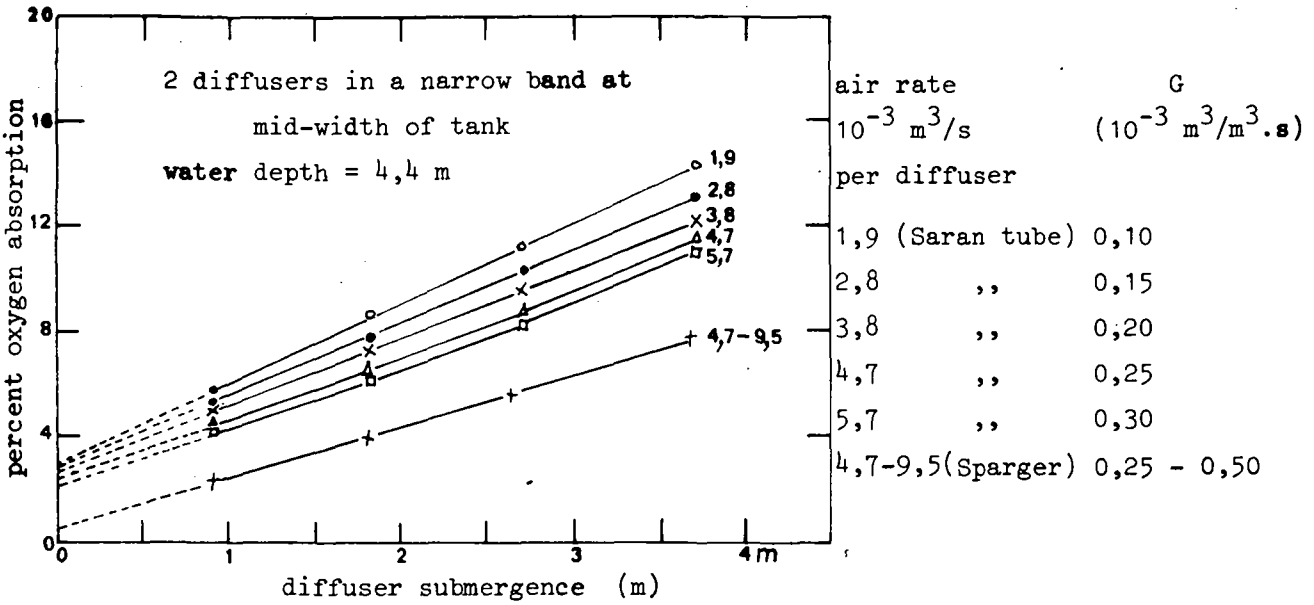

Fig. 3.25 EFFECT OF DIFFUSER SUBMERGENCE AND AIR-FLOW RATE ON THE PERCENTAGE OXYGEN ABSORPTION

diffusion to hydrophobic or surface active matter. On the average a reduction factor of $\alpha = 0,8$ represents the experience of practice for operational conditions as compared to 0,7 for fine bubble aeration.

Concerning the guide values, refering to the oxygen utilization per meter of submergence, a first estimate may be taken from figure 3.25, which shows for the cited experiment with spargers a percent oxygen absorption of some 6 % for 3 m of submergence, or 2% per m submergence. Applying eq. 3.18, this is equivalent to $OU/d_i = 6/0,334.3 = 6$ g $O_2/m^3.m$. This result corresponds very well to the guide values on OU/d_i for medium bubble aeration in activated sludge treatment given in the following table. This table states also the oxygenation efficiency to be expected.

Guide Values for Oxygenation by Medium Bubble Aeration

	optimum conditions			average conditions		
	OU/d_i	OE		OU/d_i	OE	
	g $O_2/m^3.m$	mg O_2/J	kg O_2/kWh	g $O_2/m^3.m$	mg O_2/J	kg O_2/kWh
tap water operational conditions ($\alpha = 0,8$)	7	0,39	1,4	6	0,31	1,1
	5,5	0,31	1,1	4,5	0,22	0,8

3.333 Practical Aspects

The main advantage of medium bubble aeration lies in the fact that air-side clogging of the diffusers does not occur. The air needs but rough cleaning by coarse screening to prevent larger particles from entering into the aeration system. Water-side clogging happens equally often as with porous diffusers but is eliminated more easily. Cleaning is, of course facilitated by the swing arrangement of the diffuser units.

Due to the small resistance of air flow imparted by the diffusers, they have to be constructed almost perfectly horizontal in order to guarantee a uniform air distribution all over the tank area. The uniform distribution is also achieved by arranging throttle-valves between header and diffuser unit.

Since medium bubble aeration requires less skilled maintenance it is preferably applied for small and medium large treatment works handling primarily domestic sewage. Efficient primary sedimention, however, is then a prerequisite to help in preventing the diffusers from clogging. Medium bubble aeration is used also for large treatment works in case the energy cost are low.

3.334 Medium Bubbles Aeration (Low Pressure)

Medium bubble aeration at low depth of submergence is used for oxygenation of the mixed liquor in activated sludge plants as well as for oxygenation and primarily carbon dioxide removal in water treatment works. This aeration system is known under the commercial name of Inka (it has been developed by INDUSTRIKEMISKA AB, Sweden) for sewage treatment, whereas the somewhat different design, applied for water treatment is referred to by Inka-Intensive aeration.

3.3341 The Inka Aeration System

The main features of the Inka aeration system applied for oxygen transfer within the activated sludge treatment process are an aeration grid made from stainless steel or plastic with orifices of 2,5 to 4,5 mm diameter placed at about 0,80 m depth of submergence, covering one half of the aeration tank, the other half being separated by a vertical wall extending until about again 0,80 m above the tank bottom (see figure 3.30). Aeration enforces a rotational movement of the tank content at high velocity by an action, similar to that of a mammoth pump. Thereby a fair portion of the bubbles is

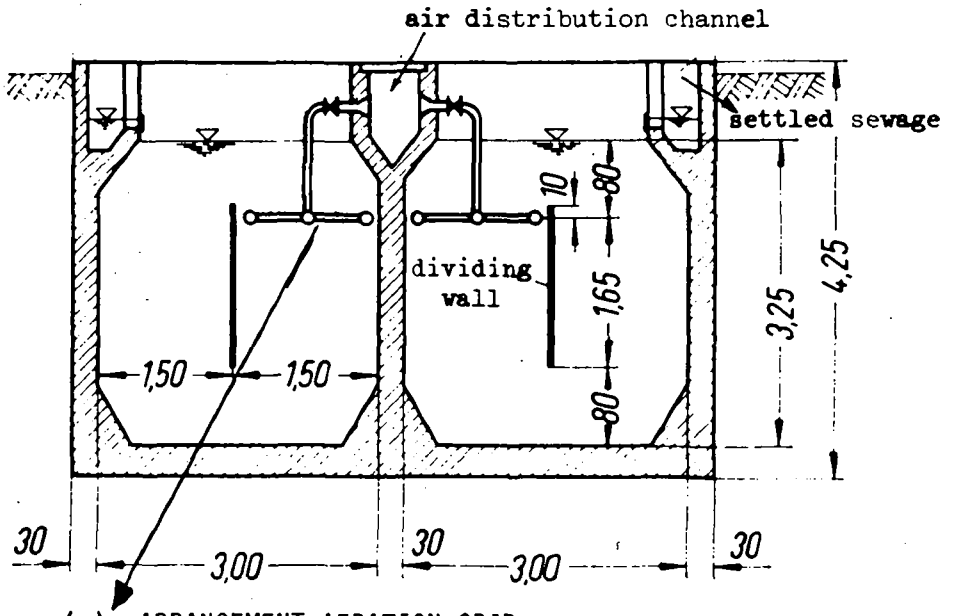

(a) ARRANGEMENT AERATION GRID

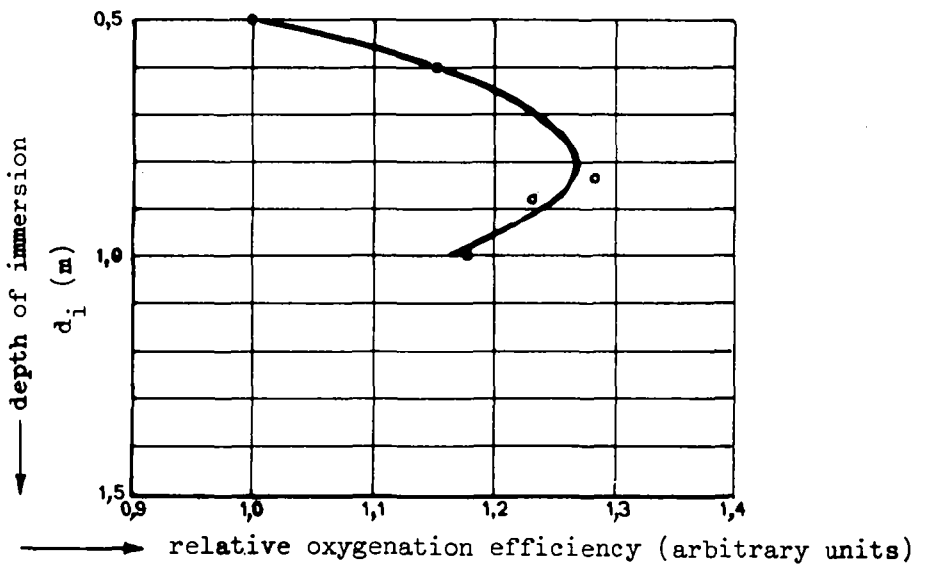

(b) INFLUENCE OF THE DEPTH OF IMMERSION ON THE OXYGENATION EFFICIENCY OE

Fig. 3.30 INKA-AERATION

forced to move downwards into the compartment opposite to the aeration grid, increasing the average detention time of the bubble within the liquid and hence the total interfacial area.
Increase of the air rate (which is commonly 5 times as high as with conventional fine or medium bubble aeration) generally leads to an increase in percent oxygen absorption. This is evident, since increase of the air rate enhances the rotational movement and thus enforces a greater portion of the bubbles into the not aerated division of the

tank.

Since the grids are manufactured at a width of 1,50 m and since a depth of submergence of 0,80 m has been evaluated to be optimal (see figure 3.30), the tank dimensions as given by figure 3.30 are appropriate. Although the aeration grids are generally placed at 0,80 m of submergence, the guide values for oxygen utilization are given per meter of submergence for easy comparison with other bubble aeration systems. The amount of energy to be spent for diffusing the air is small, firstly because of the low depth of immersion, secondly because of the low resistance to air flow, the air being distributed by wide air channels above the water level of the tank (see figure 3.30), and thirdly because the fans applied for aeration generally reach a higher efficiency than high-pressure blowers.

Guide Valves for Oxygenation by Low Pressure Medium Bubble Aeration (Inka)

	optimum conditions			average conditions		
	OU/d_i	OE		OU/d_i	OE	
	g $O_2/m^3.m$	mg O_2/J	kg O_2/kWh	g $O_2/m^3.m$	mg O_2/J	kg O_2/kWh
tap water operational conditions (α = 0,8)	9	0,50	1,8	8	0,40	1,5
	7,5	0,40	1,5	6,5	0,32	1,2

Concerning practical aspects of the Inka aeration system it has to be mentioned that the aeration grating has to be carefully placed horizontally. The same holds for the outlet weir to guarantee a horizontal water surface. Small deviations in either respect will lead to an uneven distribution of the air over the tank surface. This is of special importance for the Inka system since the total pressure (sum of head loss, head loss of discharge through orifices, and water head) amount to only some 0,90 to 0,95 m of water column, so that small head differences will have a significant effect. Partial waterside clogging of the aeration grid will lead to an uneven distribution of the air also. Moreover, any increase of the resistance due to clogging will significantly decrease the air rate since pressure increase strongly reduces the capacity of the fan. Thus, efficient primary sedimention is a prerequisite for the application of the

Inka low pressure aeration. Especially filamentous material has to be completely removed in order to prevent formation of pig-tails at the grating.

3.3342 The Inka Intensive Aeration

The basic Inka principle, namely aeration through a grid of orifices at a pressure low enough to enable the application of fans, is used also in the course of water treatment for oxygenation and removal of carbon dioxide (and possibly taste and odor producing volatile matter). The design of this system, referred to by Inka Intensive Aeration, differs significantly from that used for oxygenation of sewage, however (compare fig. 3.30 and 3.31). Hence, the principal features are a plate of stainless steel, perforated with orifices of some 2 mm diameter, covering about 2 to 3 % of the "grid" area, which is placed horizontally on a foundation consisting of a concrete chamber. The water is uniformly distributed over the front width of the plate by a sprinkle pipe. To stabilize the bubble layer above the plate, a foam screen is placed at the discharge end of the plate, the slot width controlling the foam thickness. Air is supplied by a fan, passes through the water and is carried off by an exhaust stack.

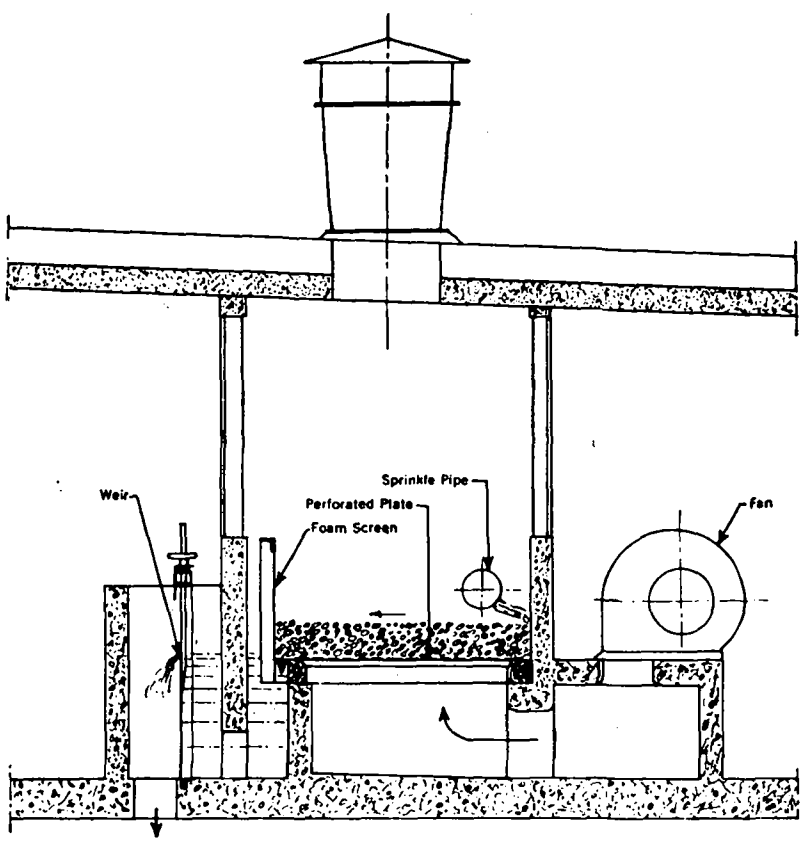

Fig. 3.31 THE INKA INTENSIVE AERATION

By proper choice of number, size and location of the plate holes, of the water and air rate and of the slot width controlling the thickness of the foam layer, the water is distributed in a continuous layer of almost uniform polyhedral bubbles. The bubbles consist of a thin water film, thus providing a large air-water interface. A continuous vertical up and down movement of the liquid has been ascertained, which leads to a continuing renewal of the interfacial area. Both facts give rise to a great rate of gas transfer.

Depending on the desired degree of oxygenation or carbon dioxide removal, the air to water flow ratio RQ is varied from 25 to 500. With such large ratios no significant increase of gases to be removed within the gaseous phase will occur which might decrease the rate of stripping (compare section 2.5).

Due to the interaction of the operational variables the optimum operation can be established experimentally only. Important interactions are the following:
the narrower the slot width of the foam screen is chosen, the more water is retained on the plate and the higher is the foam layer which leads to a longer time of contact between air and water, promoting the exchange of gases. On the other hand, however, this increases the total resistance against air flow and is reducing the air rate discharged by the fan which will decrease the gas exchange efficiency. The same effects are observed when increasing the flow rate of water at constant slot width of the foam screen. Finally, the described interdependencies are influenced by the size and the arrangement of the holes of the plate.

Despite the difficulties met in optimalization, the Inka intensive aeration system is an very efficient process for removing carbon dioxide. At high ratios of air to water flow carbon dioxide can almost fully be stripped from the water. Hard water and water containing appreciable amounts of iron and/or manganese may cause operational troubles by clogging of the holes by precipitates of calcium, iron, and manganese.

Although the oxygenation of the treated water is excellent too, the process is not very efficient in this respect from an economical point of view:
the oxygenation efficiency OE does not reach values of larger than 0,19 to 0,28 mg O_2/J (0,7 to 1,0 kg O_2/kWh).

3.34 Coarse Bubble Aeration

3.341 Types Diffusers and Their Arrangement

Coarse bubble aeration is performed by means of slotted or perforated pipes or plates with orifices greater than 5 mm diameter, or of open pipes of 25 to 50 mm diameter which are vertically arranged within the aeration tank.

The size of the produced bubbles may be reduced by additional devices near the air discharge openings. In principle these devices create a locally increased turbulence, excerting shear forces on the bubbles large enough to subdivide them. Two typical constructions are depicted in figure 3.32. Figure 3.32a shows a deflecting plate mounted at the lower end of a 57 mm diameter pipe. The plate is inclined in the directions of the spiral flow to induce a high shearing velocity upon the discharged coarse bubble. Ribs are welded on the plate to assist in breaking up the coarse bubbles. Figure 3.32b shows the shear box

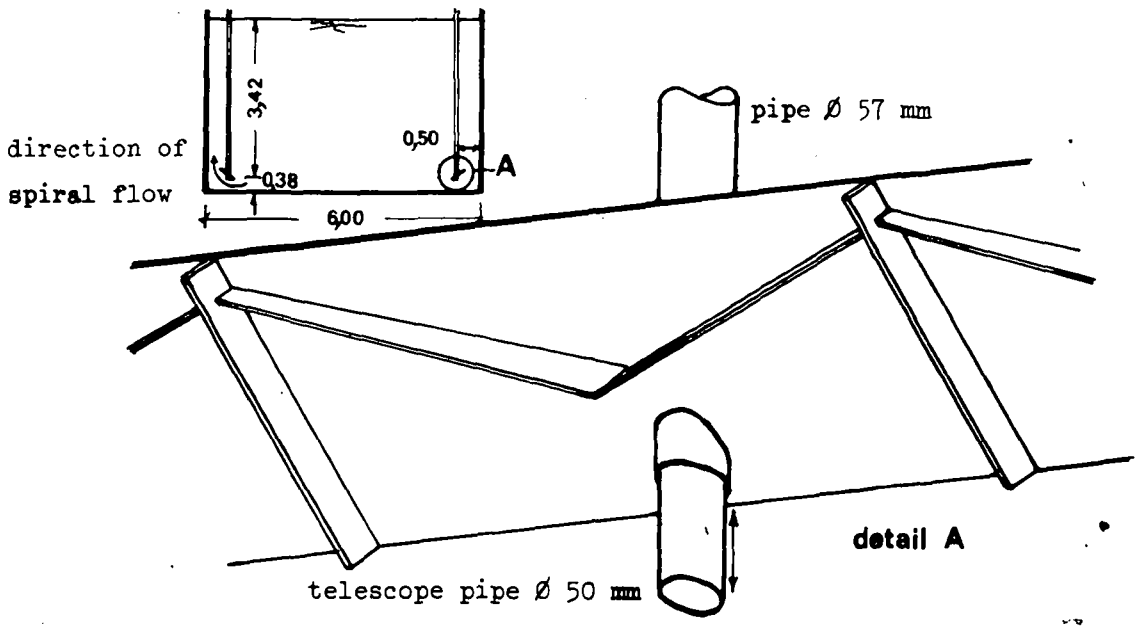

Fig. 3.32 a DEFLECTING PLATE FOR DISINTEGRATION OF COARSE BUBBLES

construction, a square shaped box with a closed bottom and an open top mounted on the header. Air is introduced through a nozzle with a large opening. Induced counter flowing air-liquid streams shear large bubbles released from the nozzle into fine bubbles.

Tank dimensions and the arrangement of the diffusers within the tank are similar to those reported for fine and medium bubble aeration.

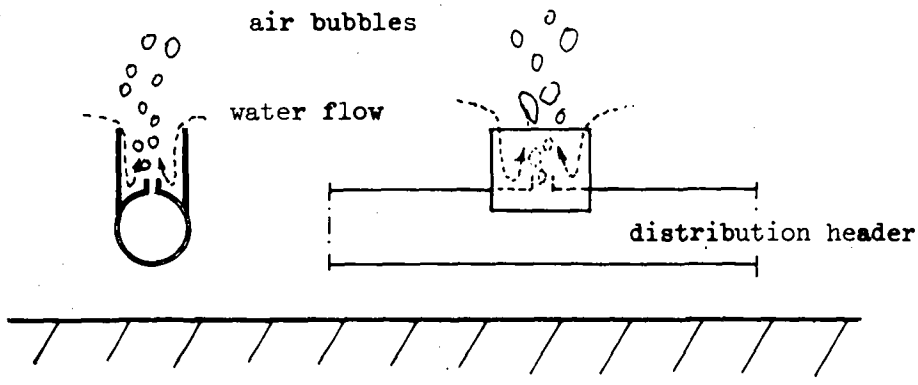

Fig. 3.32 b SHEAR BOX FOR DISINTEGRATION OF COARSE BUBBLES

3.342 Factors Influencing the Rate and Efficiency of Oxygen Transfer

Due to the large size of the bubbles and the corresponding small total interfacial area, coarse bubble aeration shows the least oxygen utilization OU of all air diffusion systems. As with medium bubble aeration the oxygenation during formation of the bubbles is almost negligible. Hence the oxygen utilization increases linearly with increasing water depth. The application of deflecting plates or shear devices for breaking up the large bubbles significantly increases the efficiency of aeration. This is seen from a comparison of the guide values for oxygen utilization with and without deflecting plates given in the two following tables, respectively.
Although it is general practice to consider a α value of 0,8 for operational conditions, hydrophobic and surface active matter has but little influence on the oxygen utilization as is seen from a comparison of fine and coarse bubble aeration in figure 3.33.

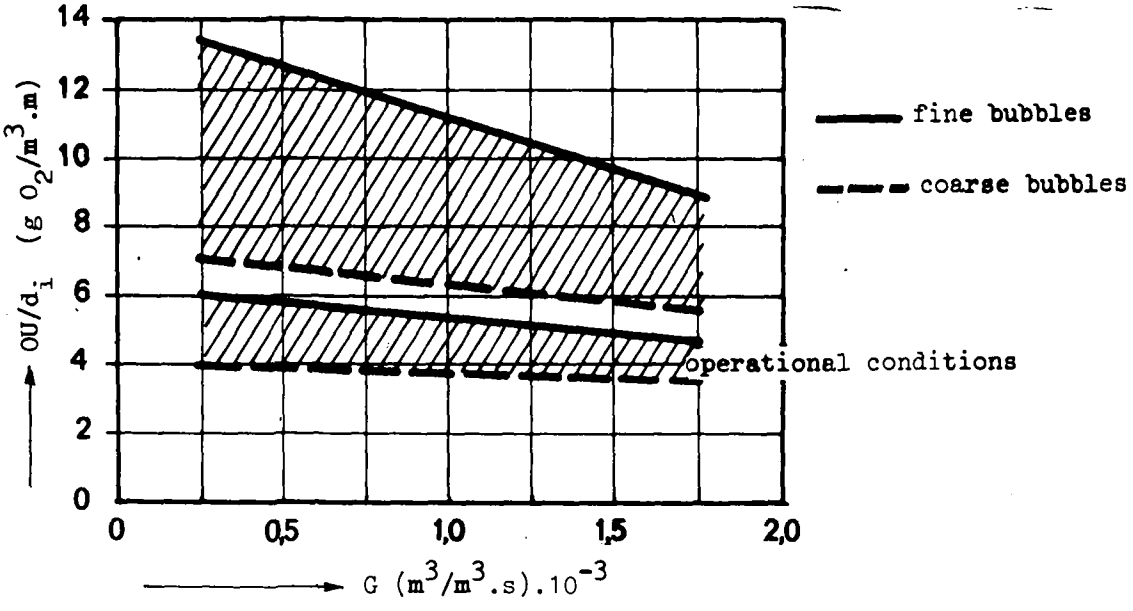

Fig. 3.33 EFFECT OF SEWAGE CONSTITUENTS ON THE OXYGEN UTILIZATION USING FINE AND COARSE BUBBLE AERATION

Guide Values for Oxygenation by Coarse Bubble Aeration						
	optimum conditions			average conditions		
	OU/d_i	OE		OU/d_i	OE	
	g $O_2/m^3.m$	mg O_2/J	kg O_2/kWh	g $O_2/m^3.m$	mg O_2/J	kg O_2/kWh
without deflectors						
tap water operational conditions	6	0,33	1,2	5	0,25	0,9
(α = 0,8)	4,5	0,25	0,9	4,0	0,20	0,7
with deflecting plates						
tap water operational conditions	7,5	0,45	1,6	7	0,42	1,5
	6,5	0,36	1,3	5,5	0,28	1,0

3.343 Practical Aspects

The main advantage of coarse bubble aeration is an operational one: clogging of the diffusers cannot happen because of their large dimensions. Their domain, therefore, are small plants without skilled maintenance, aeration without primary sedimentation (when energy cost are low) and possibly the aeration of industrial wastes which tend to clogg fine and medium diffusers.
Since the large orifices applied in coarse bubble aeration do not exert any controlling resistance against the air flow, the air discharge openings have to be carefully arranged horizontally. This may be facilitated by a short piece of pipe which is placed in a telescope like manner into the aeration pipes (see figure 3.32a).

3.35 Air Diffusion by Means of Entrained Air

For the oxygenation of water in the course of water treatment two processes of air diffusion by means of entrained air have been developed. Both make use of the venturi tube principle, i.e. by locally

increasing the streaming velocity of water the velocity head $v^2/2.g$ is increased as to let the pressure head fall below the geodetic head.

This principle is shown for the venturi aerator as example in figure 3.34. It is evident that at the point of high velocity a vacuum is produced. This will cause air to be entrained if the tube is perforated.

In the following the venturi aerator and the deep well aerator (U-tube aerator), both being based on this principle, will be discussed.

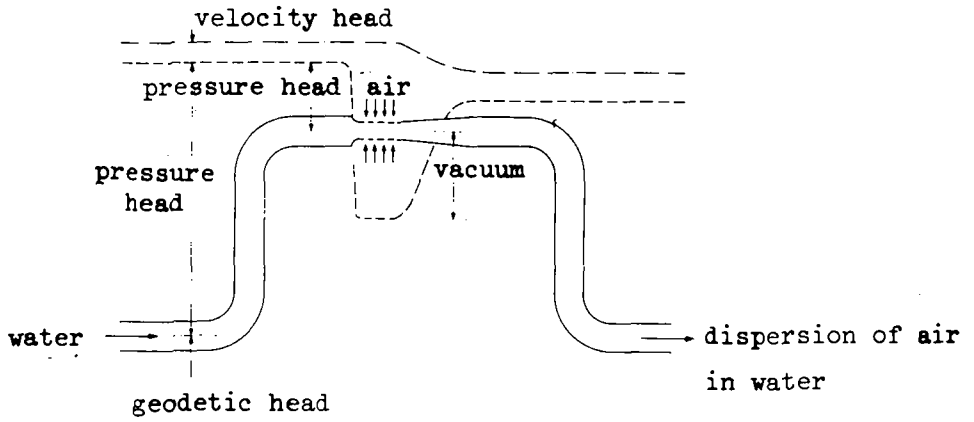

Fig. 3.34 PRINCIPLE OF AERATION BY MEANS OF ENTRAINED AIR

3.351 The Venturi Aerator

Figure 3.35 gives a schematic representation of a venturi aerator. The air is entrained in the inlet throat of the venturi tube. The strong turbulence at water velocities between 6 and 12 m/s causes an intensive mixing of the entrained air with the water which leads to a dispersion of fine bubbles. The dispersion is carried away with the water stream, also when this is directed downwards. Thus, a great interfacial area between air and water and a large time of contact is provided. Since there is almost no difference to be observed in the velocities of water and air bubbles, the renewal of the interfacial surface is low, which partially offsets the above mentioned positive effects with regard to the rate of oxygen transfer.

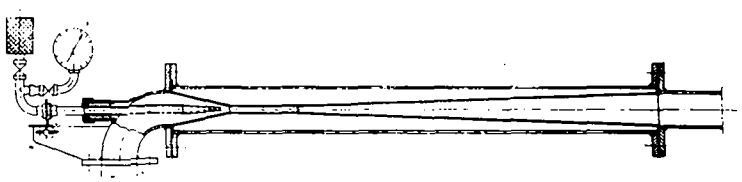

Fig. 3.35 THE VENTURI AERATOR

Since the rate of air to water flow, that may be obtained by the venturi aerator, is well below RQ = 1, the carbon dioxide content of the water is not significantly decreased.

Important constructional details are the great length of the venturi tube, which is chosen to reduce the loss of energy as far as possible. In the back part of the tube the angle of the cone does not exceed $7{,}5^{\circ}$, therefore.
The air to be entrained is purified by a filter; a pressure meter controls the produced vacuum.

3.352 The Deep Well Aerator (U-Tube Aerator)

An ingenious application of the venturi principle is the deep well aerator which is depicted in figure 3.36. A well of some 10 to 20 m

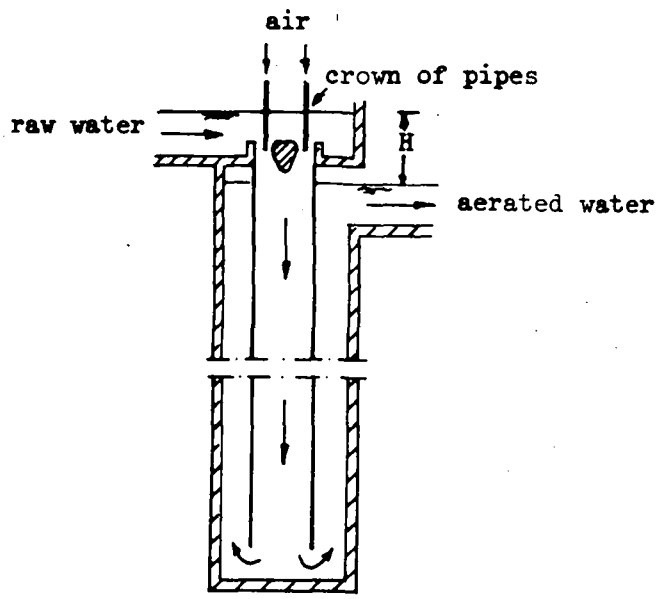

Fig. 3.36 DEEP WELL OR U-TUBE AERATOR

of depth and 1,5 m of diameter is divided into two sections by inserting a steel tube of some 0,60 m diameter extending to about 0,30 m above the well bottom. The water is fed into the inner tube. The inlet velocity is controlled by a cone which is adjustable with respect to height. A crown of pipes is submerged into the annular space between cone and inner tube through which air is entrained. As the water and the entrained air bubbles pass downwards the pressure is increased in proportion to the depth as is the saturation value c_s. At a depth of 20 m, for instance, the saturation value amounts to 3 times that under normal conditions. This obviously will significantly increase the driving force and hence the rate of gas absorption.

The downwards velocity should be 0,50 m/s at least in order to guarantee that the air bubbles cannot rise. The maximum downwards velocity is below 1,5 m/s to prevent loss of energy which would reduce the oxygenation efficiency. For the same reasons the upwards velocity in the outer annular space has to be chosen as small as possible. Generally it is designed to be 1/3 to 2/3 of the downwards velocity.

The flow rate may be controlled by either adjusting the height of the cone or by changing the pressure head H. The first measure has no influence on the oxygenation capacity of the system, whereas variation of the head and the well depth are the prime parameters controlling the amount of gas absorbed. Figure 3.37 indicates the influence of these parameters on the efficiency coefficient $K = (c_e - c_o)/(c_{so} - c_o)$, where c_{so} refers to atmospheric pressure. It is seen that with a depth of 15 m an efficiency coefficient of greater than 0,9 is obtained. With deeper wells (depth some 20 m) a K-value of greater than 1,0 may be obtained even, indicating that supersaturation will be reached. Referring to the small heads applied (see figure 3.37) it is evident, that the deep well aeration seems to be the most efficient system for oxygenation of water. The oxygenation efficiency varies depending on the well depth and the rate of flow from 0,7 to 1,8 mg O_2/J (2,5 to 6,5 kg O_2/kWh).
Since the ratio of air to water flow RQ is very small, deep well aeration is not efficient in removing gases. The efficiency coefficient K for removing carbon dioxide, for instance, has been found as low as some 0,1 to 0,15.

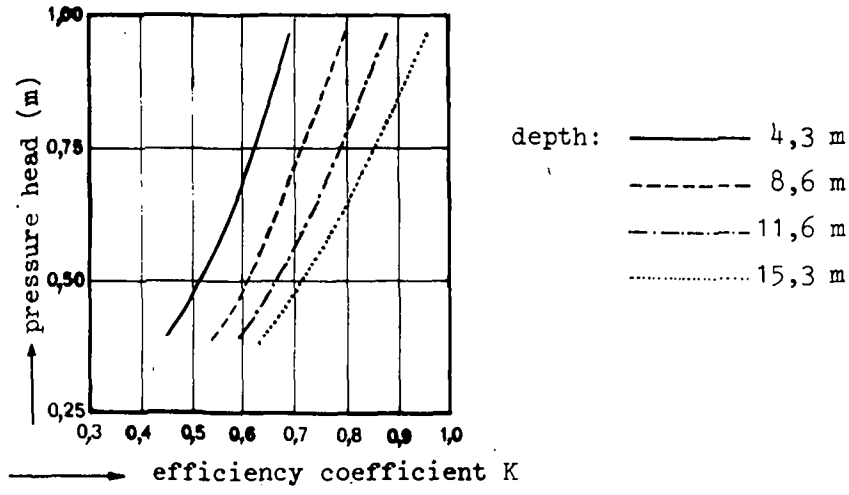

Fig. 3.37 RELATIONSHIP OF TUBE DEPTH TO EFFICIENCY

3.4 Mechanical or Surface Aeration

3.41 General Considerations

Mechanical aeration is performed by rotating devices which are slightly submerged into the water and thereby effect spreading of the water above the water surface. This action at the same time enforces a spirally shaped flow of the water within the tank, the pattern of which depends on the geometry of the aeration device and the tank. The exchange of gases by the described action of mechanical aerators is achieved by several mechanism:

1. By spreading of the water in the form of droplets and/or water films above the water surface a large interfacial area is created.
2. By reentering of the spread droplets and films of water into the bulk of the tank content the gases absorbed at their surfaces are mixed with the bulk of the water. Furthermore bubbles are entrained when the spread water submerges into the tank content, an effect similar to that observed in weir aeration (section 3.11), however less pronounced due to the low height of fall.
3. An entrainement of bubbles into the water is achieved by the rotating aeration device itself. At certain points of the device the velocity of the water is great enough as to locally produce a partial vacuum by which the entrainement is caused. Some devices are especially equipped to promote this additional effect of gas transfer.
4. The pattern of flow in the tank induced by the aerator furnishes a steady renewal of the water surface of the tank, assisting in gas exchange. Moreover the spiral like flow pattern is frequently of a velocity great enough to carry the entrained bubbles downwards, which leads to a longer time of contact between bubbles and water. High streaming velocities of the water in the same direction as the peripheral motion of the aerating device are to be avoided. Thereby the velocity difference between water and aerator decreases, may eventually approach zero, and the above major mechanisms of gas transfer are minimized.

Thus it is seen, that a variety of mechanisms cause the exchange of gases in mechanical aeration. The alternative term of "surface aeration" refers only to the mechanisms mentioned under 1 and partially

under 2. The greater the share of the total gas transfer by these mechanisms is, the more is the term "surface aeration" justified. A quantitative measure for this effect may be the flow of water (m^3/s) spread by the aerators by its "pumping action". The other mechanisms causing gas transfer are strongly dependent on the size and shape of the aeration tank which mainly determine the flow pattern.

Mechanical aeration is primarily used for oxygenation of the mixed liquor in activated sludge treatment. Comparing mechanical aeration with air diffusion, some of the more obvious advantages of mechanical aerators are the elimination of several appurtenances of the diffused air system such as piping, branching of pipes, valves, blowers or fans, air filters etc. Moverover the mechanical aerator is also generally more maintenance free and does not need the high degree of attention that is required for cleaning of the diffusers. These advantages have led to almost an explosion of marketed types of mechanical aerators, the end of which seems not yet to be within sight. This development has been promoted by the fact, that mechanical aerators can easily be float mounted and thus conveniently be applied in larger tanks or for aeration of lagoons or surface waters.

Basically, the types of mechanical aerators may be differentiated as follows (compare section 1.2)

1. Rotor aerators (formerly referred to as "brushes"), consisting of a horizontal revolving shaft with combs, blades or angles attached to it which are slightly dipping into the water.

2. Cones, impellers or turbines revolving round a vertical shaft. The cones may be further subdivided into the following types:

   2.1 Plate types

   discharging the water in radial direction at the tank surface at high velocity which leads to a peripheral hydraulic jump. Both effects cause a rapid renewal of the air-water interface and partially also air entrainement.

   2.2 Updraft types

   actually acting like a pump, discharging large quantities of water at the surface at relatively low heads.

   2.3 Downdraft types

   a unit where oxygen is supplied by air selfinduced from a negative head produced by the rotating element. Due to this entrainement of air, being the prime mechanism of gas transfer, the downdraft types are no surface aerators.

The oxygen transfer efficiency of mechanical aerators is generally stated in g of oxygen transferred per aerator per second, (or kg O_2/h), being equivalent to the oxygenation capacity (OC) as defined by eq. 2.65. Prime factors influencing the oxygenation capacity are the size of the aerator, the depth of submergence; the speed of rotation. Concerning the size, the diameter gives sufficient information for cone-type aerators, mentioned under 2, whereas the oxygenation capacity for rotors is generally related to their diameter and a rotor length of 1 m.

Increasing these controlling parameters will generally increase the oxygenation capacity (OC), but will vary the oxygenation efficiency OE (mg O_2/J) in such fashion as to provide optimum conditions at a certain magnitude of rotational speed and submergence as is qualitatively shown in figure 3.38. At magnitudes of the controlling parameter below the optimum values, the oxygenation capacity OC generally increases with increasing the size of the aeration device, expressed by its diameter D_c, the depth of immersion d_i, and its peripheral speed v_p. Generally, this increase may be approximated by the following relations concerning

a) the size of the aerator $OC \propto D_c^2$

b) the depth of immersion $OC \propto d_i$

c) the peripheral speed $OC \propto v_p^n$

with $2,5 < n < 3,0$

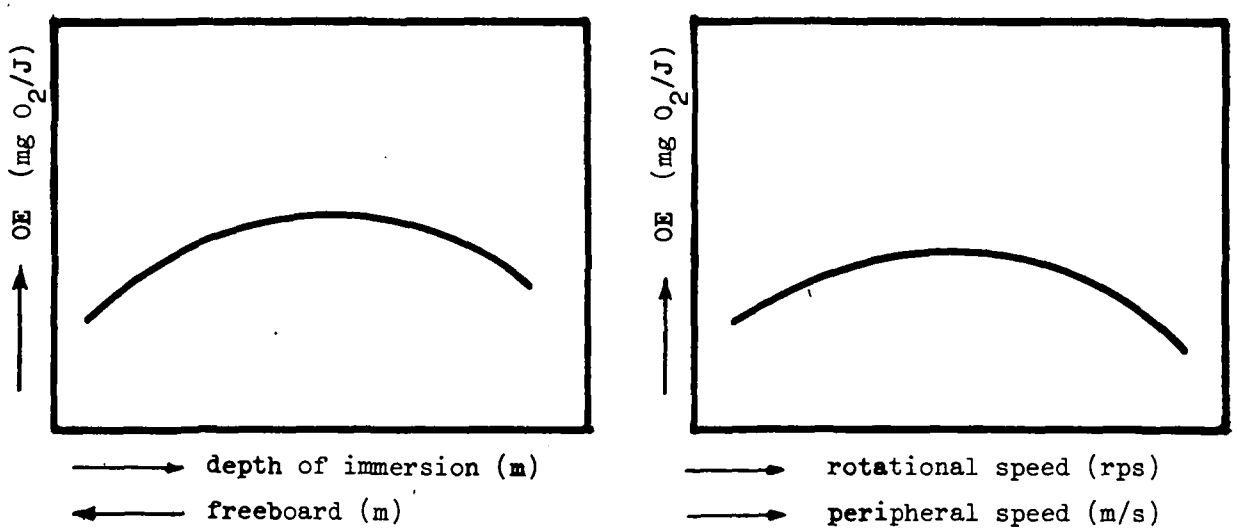

Fig. 3.38 SCHEMATIC SHOWING EFFECT OF SPEED AND SUBMERGENCE ON OXYGENATION EFFICIENCY

As already has been mentioned, also the pattern of flow and its velocity are of significant influence on the oxygenation capacity. Both parameters are primarily modified by the size and the geometry of the tank, keeping the size of the cone, its rotational speed and depth of immersion constant. Quantitative measures for these influences are the velocity difference between water and the aerator periphery and the ratios of aerator diameter D_c over the tank width w (D_c/w) and over the tank depth d (D_c/d).

Applying well shaped aeration tanks, the size then will have a great influence on the oxygenation capacity achieved with a surface unit. Generally speaking, the larger the tank is, the smaller are the velocities of the induced spiral flow and the less pronounced are the transfer mechanisms mentioned under point 4.

A quantitative measure for this influence is the amount of energy dissipated per unit tank volume ε_G (W/m^3) which will be seen to be of significant influence on the oxygenation efficiency OE (mg O_2/J).

Concerning the influence of hydrophobic and surface active matter on the oxygenation capacity of mechanical aerators it may be stated, that the turbulence in the region of the aerator is generally large enough to prevent reformation of a layer of such substances at the produced air-water interfaces (compare section 2.34). Thus the positive effects of surface active agents on gas transfer will prevail and cause an increase of the oxygenation capacity with increasing content of surfactants. On the other hand, the effect of the entrained air bubbles on gas exchange will generally be lowered by the presence of surfactants, as was evident for air diffusion systems. The sum of both effects leads generally to a much less pronounced decrease of the rate of gas transfer by surface active matter than in bubble aeration; frequently such substances will even increase the oxygenation capacity of a surface aerator.

In the following sections the mentioned types of mechanical aerators are covered in detail giving due attention to their construction and operation, to their oxygenation capacity, to the commonly applied tanks, and to practical aspects of operation.

3.42 Rotor Aerators

3.421 Types of Rotor Aerators and Their Arrangement

The predecessor of the rotor aerators are the Haworth or Sheffield paddles (fig. 3.39), developed as early as 1916 in England, which where used in combination with snakewise arranged channels of some 1 m of width and 1 to 1,5 m of depth. By rotation of the paddles of 2 m of diameter some transfer of oxygen was achieved, but mainly the induced streaming velocity of some 0,5 m/s provided aeration of the mixed liquor.

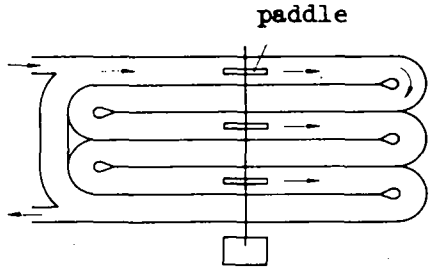

Fig. 3.39 HAWORTH PADDLES

A further step of development was the introduction of the "Kessener Brush" (1926), a rotor equipped with piassave brush material of some 0,60 to 0,70 m of diameter rotating at about 1 rps (60 rpm).
Later developments include a variety of "brush"-materials, like fraised stainless-steel combs caulked into longitudonal grooves cut into the steel line shaft; or steelbars and angle irons of different size and spacing, attached to the shaft.
At present, basically 2 types of rotors are available

1. The cage-rotor, consisting of two steel discs attached to the central shaft at both ends with T-shaped bars are attached to the discs (hence being placed parallel to the shaft). To each of the 12 T-bars a series of short steel plates each about 0,15 m long and 0,05 wide are bolted at right angles, spaced at about 0,05 m clear distance. The overall diameter amounts to 0,70 m, the maximum length is some 3,0 to 5,0 m (fig. 3.40).
2. The plate rotor consists of a shaft onto which short lengths of steel plates are clamped in a star-like manner. The total diameter is some 0,5 m, the maximum length about 2,5 m (fig. 3.41).
   A recent development of the plate rotor is the so-called mammoth rotor. The constructional principle is the same, however the total diameter is increased up to 1,0 m, which allows total lengths of some 9,0 m (fig. 3.41).

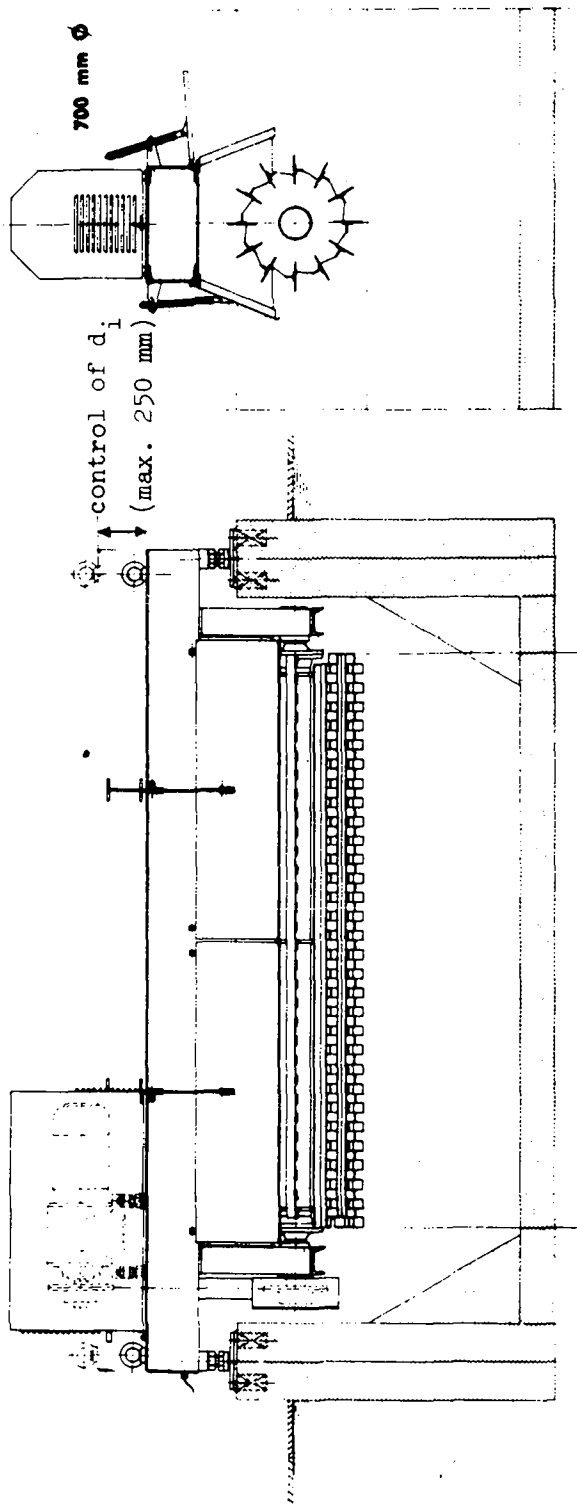

Fig. 3.40 a BRIDGE MOUNTED CAGE-ROTOR

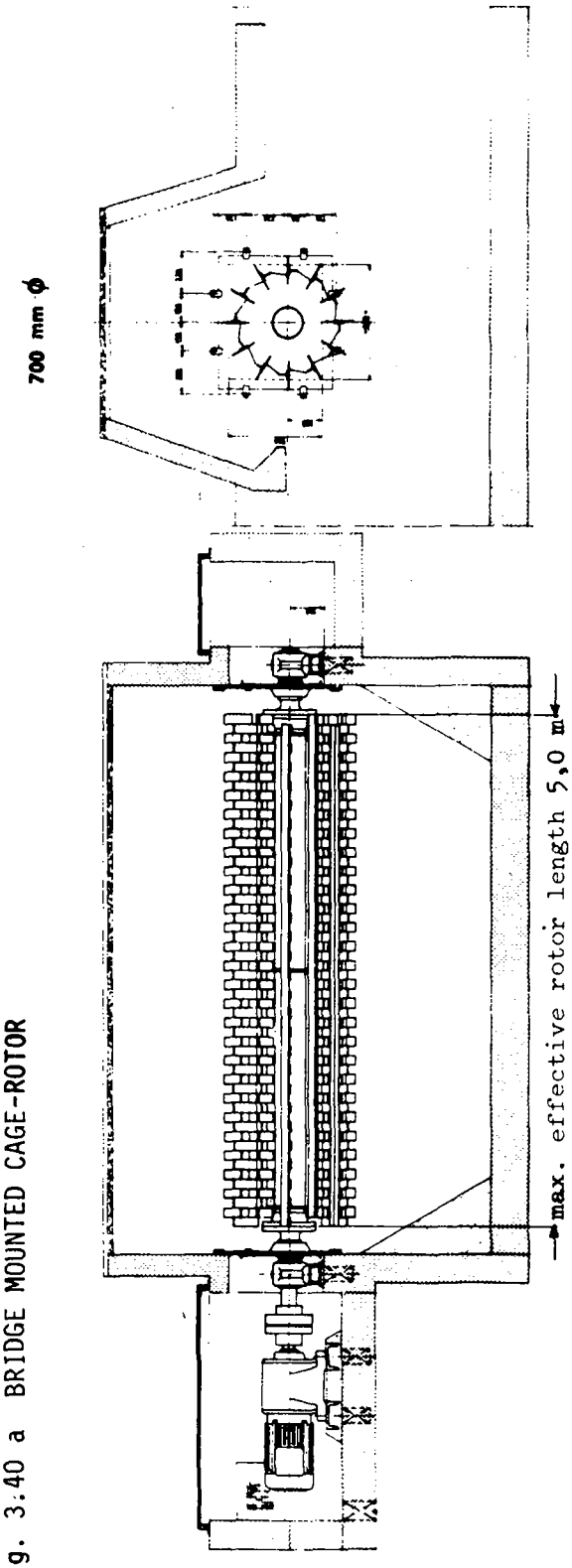

Fig. 3.40 b CAGE-ROTOR WITHOUT BRIDGE

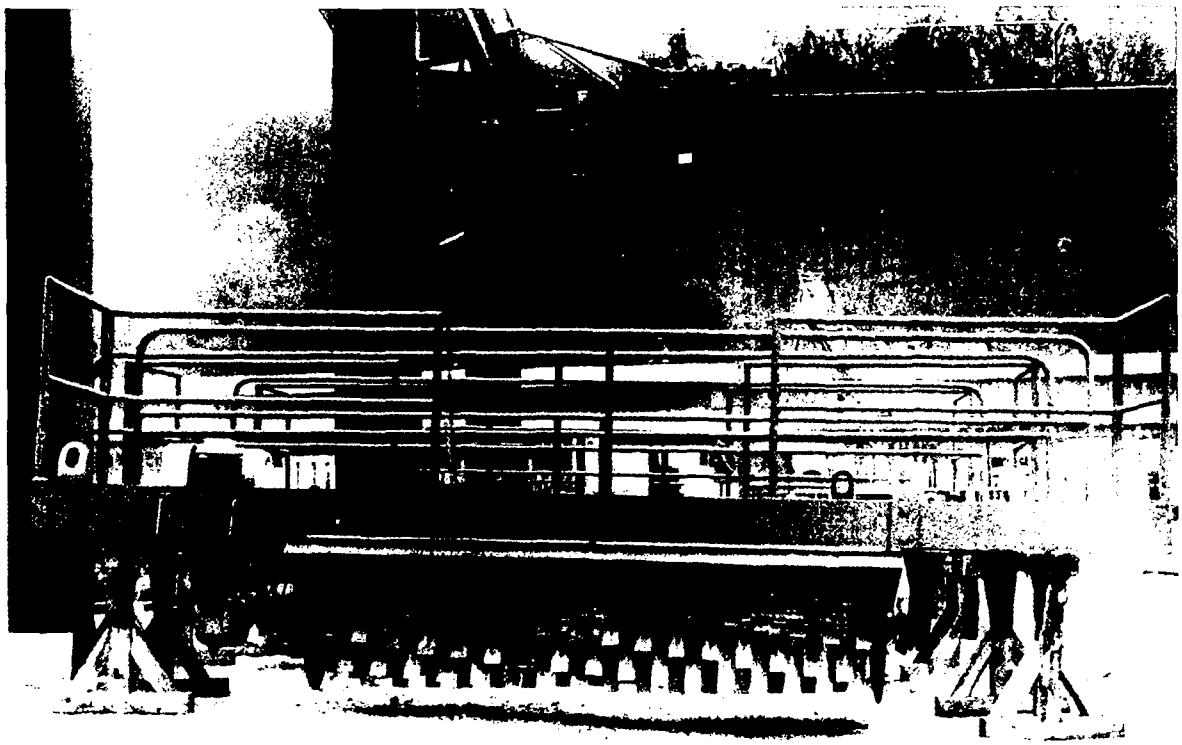

Fig. 3.41 a PLATE-ROTOR

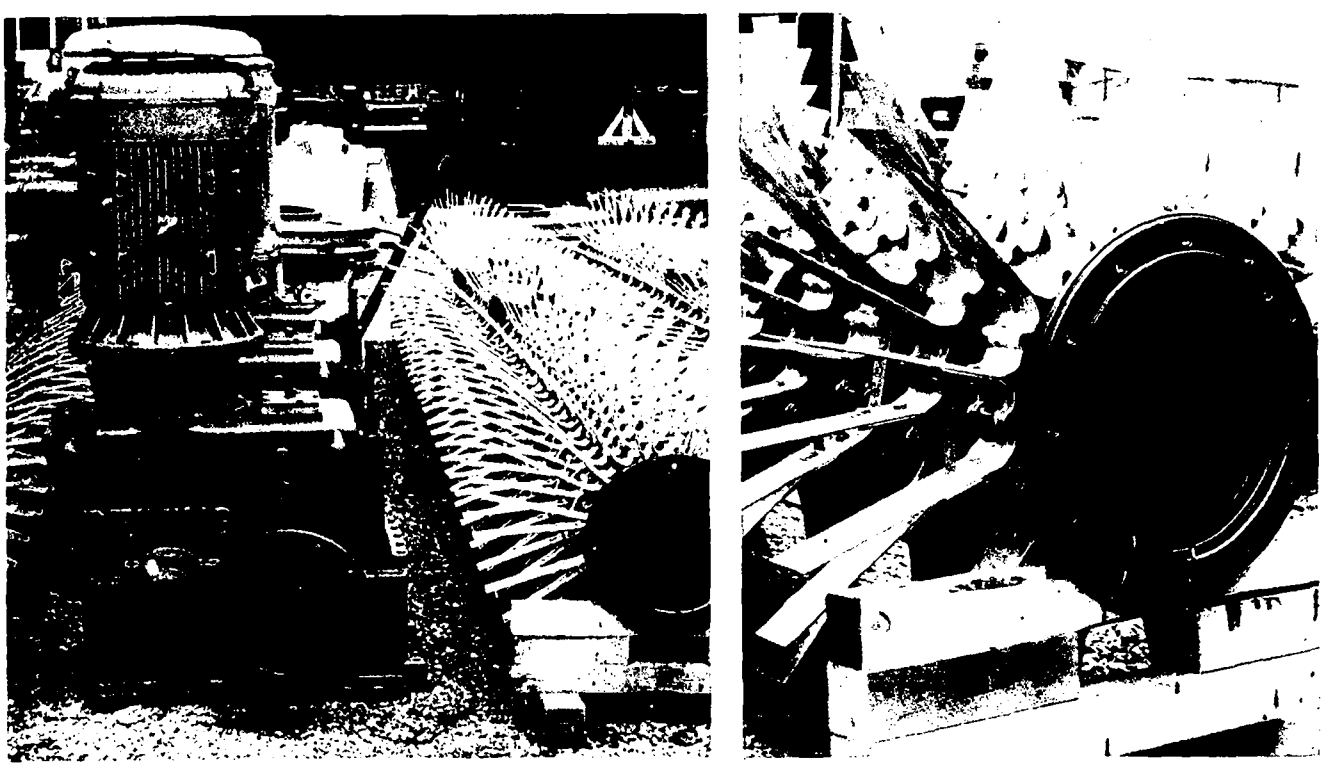

Fig. 3.41 b MAMMOTH-ROTOR

Rotors are applied in connection with two types of tanks:

1. A tank of rectangular or round cross-section with the brushes placed along one side of the tank length. The rotors then induce a spiral flow which is rectangular to the displacement velocity of the mixed liquor through the tank (fig. 3.42). For this type of tank generally plate rotors or mammoth rotors are applied although cage-rotors have been used also.

   To achieve thorough mixing all over the cross-section guide baffles are frequently required which force the water velocity induced at the tank surface into the deeper parts of the tank (fig. 3.42 a + b with so-called pressure baffles). Rectangular tanks are additionaly equipped suction baffles under the rotor, (fig. 3.42 c + d) which assist in achieving a good mixing also with this type of cross-section.

   With plate rotors the cross-section is generally square, whereas with mammoth rotors the width may be increased to twice the depth without serious decrease of proper mixing conditions.

   The rotors may be covered with easily removable splash-guards.

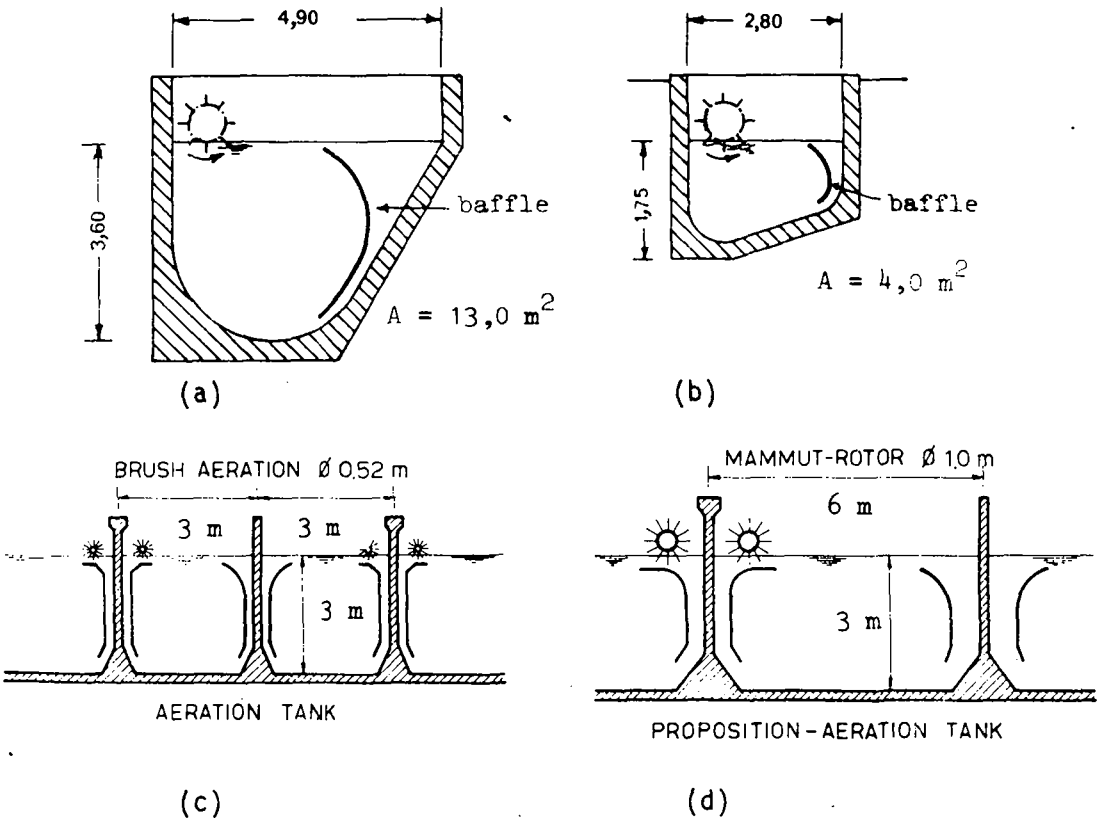

Fig. 3.42 ARRANGEMENT OF ROTOR AERATORS (ROTOR SHAFT IN DIRECTION OF DISPLACEMENT VELOCITY)

2. A long circuit-like tank of rectangular or trapezoidal cross-section. One or more rotors are arranged across the circuit channel and induce a longitudinal velocity great enough for proper mixing of the mixed liquor (fig. 3.43a). Classical examples of this types of tank are the Haworth channel (although without rotors) and the oxidation ditch (fig. 3.43b). For this type of tank the cage rotor and the mammoth rotor are primarily applied.

In order to achieve proper mixing all over the cross-sectional area the depth of either tank type has to be limited to some 3,50 m. The ditch-type tank, when operated with cage-rotors, should not exceed a depth of 1,50 to 1,60 m.

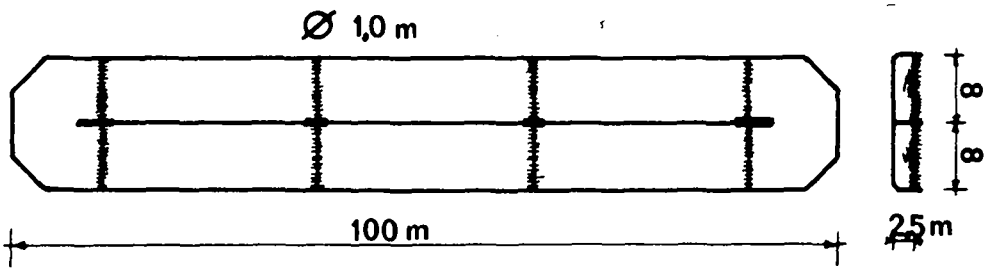

Fig. 3.43 a CHANNEL-LIKE TANK WITH MAMMOTH-ROTORS

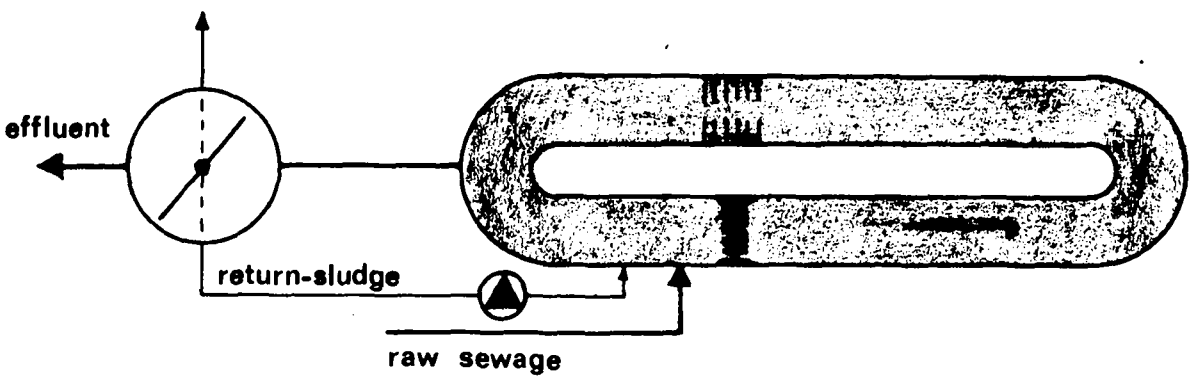

Fig. 3.43 b OXYDATION DITCH WITH CAGE ROTOR

3.422 Factors Influencing the Rate and Efficiency of Oxygen Transfer

The main mechanisms of gas transfer by rotor aeration are:
- whipping of air bubbles into the water by the blades of the rotor;
- spreading of the water in the form of droplets over the water surface in front of the rotor;
- inducing a circular or longitudinal streaming velocity possibly guided by baffles, which renews the water surface and submerges the entrained air bubbles.

The main factors which determine the oxygenation capacity achieved by these mechanisms are the peripheral speed of the rotor v_p (m/s), the depth of submergence of the blades of the rotor d_i (m). Generally the oxygenation capacity per m of rotor length (OC_l) increases in proportion to the depth of immersion d_i and to some power of the peripheral speed v_p:

$$OC_l = K_r \cdot v_p^{\beta} \cdot d_i \quad (g\ O_2/s.m \text{ of rotor length}) \qquad (3.24)$$

where K_r = a constant depending on the specific rotor construction and the tank geometry

β = exponent

For a tank of square cross-sectional area (3,0 m width and 3,0 m depth) equipped with pressure and suction baffles, for instance, the above constants for a plate type rotor of 0,52 m total diameter were found to be $K_r = 1{,}33$ and $\beta = 2{,}6$ at depths of immersion of $0{,}04 \leq d_i \leq 0{,}14$ m and peripheral velocities of $1{,}8 \leq v_p \leq 2{,}4$ m/s. From further investigations it may be concluded that especially K_r is strongly dependent on the specific conditions of rotor and tank construction, whereas much less variation of the exponent β is to be expected.

Since the gross power required generally increases in proportion to the depth of immersion d_i and to the second power of the peripheral speed (v_p^2), it is evident from equation 3.24 that variation of the depth of immersion d_i will not alter the oxygenation efficiency OE significantly, whereas the difference of the exponents of v_p refering to OC_l and the gross power indicates, that the oxygenation efficiency

OE will increase with increasing peripheral speed v_p. This would call for very high numbers of revolution of the rotor. In practical operation, however, an upper limit is set due to the fact that hydrophic and surface active matter reduce the spiral velocity of the tank at high rotational speeds.

Frequently the spiral flow is confined to the upper part of the tank, the content of which renders into a dispersion of fine bubbles in the water, rotating above the water of the lower part of the tank. This effect may be strongly reduced by the baffles, but nevertheless an "optimum" peripheral speed can be established in terms of maximum oxygenation efficiency. An example is given in figure 3.44, indicating v_p = 2,4 m/s to be optimum for a square tank.

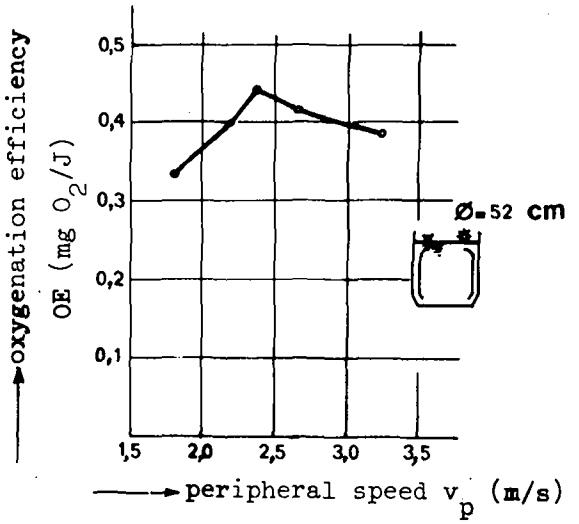

Fig. 3.44 OXYGENATION EFFICIENCY OF A PLATE ROTOR ARRANGED IN A TANK OF QUADRATIC CROSS-SECTION

The rotational speed nowedays applied is generally set by the manufacturers. Plate rotors with a total diameter of 0,50 m are mostly designed for 2,0 rps (120 rpm), giving v_p = 3,14 m/s, the depth of immersion being varied from 0,05 to 0,15 m; cage rotors for 1,25 to 1,33 rps (75 to 80 rpm), with $2{,}75 \leq v_p \leq 2{,}93$ and a range for d_i of some 0,10 to 0,20 m; whereas large rotors of 1 m of diameter are manufactured for 0,88 rps (53 rpm) corresponding to v_p = 2,77 m/s and for 1,20 rps (72 rpm) which is equivalent to v_p = 3,77 m/s, with a depth variation from 0,10 to 0,30 m.

Within the variations caused by the size and geometry of the tank the following empirical equations are given to estimate the oxygenation capacity per m length of rotor.

a) Plate rotor (see figure 3.45; data taken from large municipal plant, tank according to figure 3.42b with a cross-sectional area of 6,5 m^2 and a rotor length of 0,82 m per m of tank length):

$$OC_1 = - 0{,}070 + 3{,}8 \cdot d_i \quad g\ O_2/m.s \qquad (3.25)$$

$$= - 0{,}25 + 13{,}7 \cdot d_i \quad kg\ O_2/m.h$$

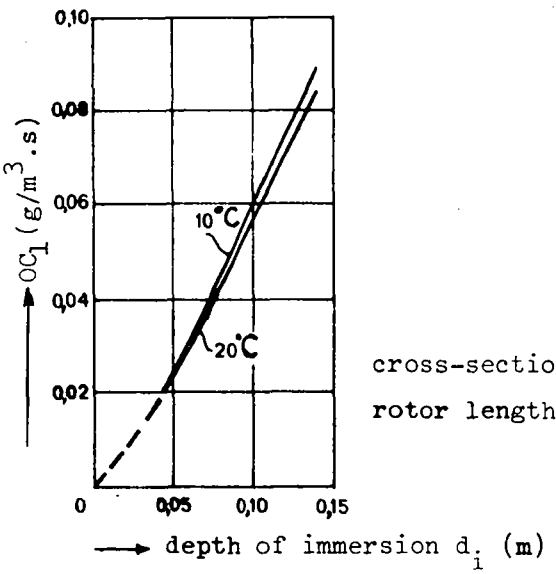

cross-sectional area: 6,5 m^2

rotor length: 0,82 m per meter of tank length

Fig. 3.45 OXYGENATION CAPACITY OF PLATE ROTORS (diam. 0,5 m, 2 rps) AS MEASURED AT A LARGE MUNICIPAL PLANT

b) Cage rotors (see figure 3.46; data from manufacturer for 1,25 rps = 75 rpm)

$$OC_1 = - 0{,}61 + 9{,}1 \cdot d_i \quad g\ O_2/m.s \qquad (3.26)$$

$$= - 2{,}2 + 32{,}8 \cdot d_i \quad kg\ O_2/m.h$$

c) Large rotor (see figure 3.47, data for mammoth rotor given by manufacturer for 72 rpm)

for $0{,}10 \leq d_i \leq 0{,}20$ m

$$OC_1 = - 0{,}11 + 11{,}7 \cdot d_i \quad g\ O_2/m.s \qquad (3.27)$$

$$= - 0{,}4 + 42{,}0 \cdot d_i \quad kg\ O_2/m.h$$

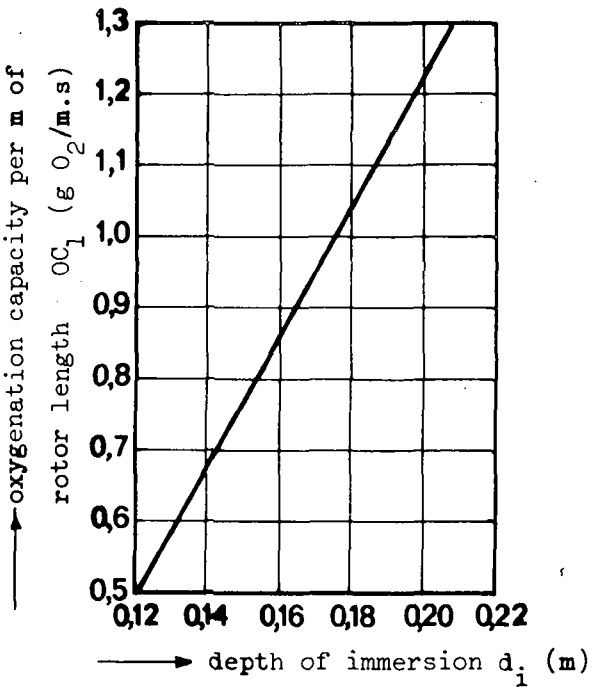

Fig. 3.46 OXYGENATION CAPACITY PER METER LENGTH OF A CAGE-ROTOR (data from manufacturer for 0,70 m diam. and 1,25 rps = 75 rpm)

As is seen from fig. 3.47, the oxygenation capacity increases less than proportional to d_i for depths of immersion above 0,20 m. The oxygenation efficiency for all three types is about 0,55 mg O_2/J (2 kg O_2/kWh).

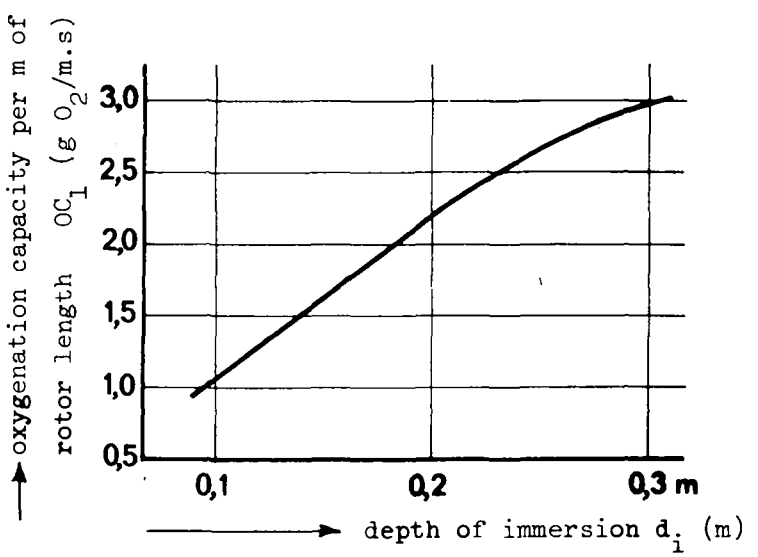

Fig. 3.47 OXYGENATION CAPACITY OF A MAMMOTH-ROTOR (data from manufacturer for 1,0 m diam. and 1,2 rps = 72 rpm at depths of 2,5 to 3,0 m)

The presence of detergents or hydrophobic matter generally increases the oxygenation capacity OC_1 and the efficiency OE. Depending on the depth of immersion and the induced pattern flow the increase of the oxygenation capacity may be as high as some 80 %, that of the oxygenation efficiency somewhat less.

Example: Estimate the total length of
a) plate rotors and b) mammoth rotors to supply the oxygen requirement of an activated sludge treatment plant, which amounts to 45 g O_2/s as daily average. Select the depth of immersion in order to meet the expected hourly variations of the oxygen demand ranging from 0,70 to 1,30 of the daily average. Assume c_s = 10 g/m^3, 2 g O_2/m^3 to be maintained in the aeration tank and α = 1,0. Estimate the average power dissipation ε_G (W/m^3), assuming an average oxygenation efficiency of 0,55 mg O_2/J (2 kg O_2/kWh) and a total tank volume of 1000 m^3.

a) Plate rotors

The maximum oxygen demand is 1,3 . 45 = 58,5 g O_2/s for which d_i is chosen at max d_i = 0,15 m. At operational conditions the $(OC_1)_{op}$ of the rotor is $(OC_1)_{op} = OC_1 \cdot \alpha\,(c_s - c)/c_s = OC_1 \cdot 1{,}0 \cdot (10-2)/10$ = 0,8 OC_1. The total rotor length l_R may be obtained by using eq. 3.25:

$$58{,}5 = 0{,}8 \cdot OC_1 \cdot l_R = 0{,}8 \cdot l_R \cdot (-0{,}070 + 3{,}8 \cdot 0{,}15)$$

$$l_R = 147 \text{ m}$$

With the maximum rotor length of 2,5 m this would require 147/2,5 = 58,8, hence 59 rotors, each 2,5 m long.
Similarly, the depth of immersion at minimum oxygen demand of 0,7 . 45 = 31,5 g O_2/s may be estimated from

$$31{,}5 = 0{,}8 \cdot 147\,(-0{,}070 + 3{,}8 \cdot d_i)$$

which yields

$$d_i = 0{,}089 \text{ m}$$

Since the construction length including bearings of the rotor is some 3,0 m, the 59 rotors require a tank length of 59 . 3,0 = 177 m, which corresponds to a cross-sectional area of 1000/177 = 5,6 m^2. The tank may be shaped according to figure 3.42b.

b) Mammoth rotor

For the peak oxygen demand of 58,5 g O_2/s a depth of immersion of d_i = 0,30 is chosen. According to figure 3.47 the OC_1 amounts to 2,9 g O_2/m.s.
Hence

$$2,9 \cdot 1,0 \cdot \frac{10-2}{10} \cdot l_R = 58,5$$

which yields

$$l_R = 25,2$$

To estimate d_i for the minimum oxygen demand eq. 3.27 is applied:

$$31,5 = 0,8 \cdot 25,2.(-0,11 + 11,7 \cdot d_i)$$

from which follows

$$d_i = 0,14 \text{ m}$$

The design would include 6 mammoth rotors of 4,5 m length each, arranged in a channel-like tank according to figure 3.43a with a total width of 2.(4,5+1,0) = 11 m. Taking a depth of 2,5 m the length of the tank would be 1000/11 . 2,5 = 37 m.

The average power dissipation, based on 0,55 mg O_2/J and 45 g O_2/s amounts to $45/0,55.10^{-3}$= 82000 J/s = 82 kW.
Hence the power dissipation per unit volume is
$\varepsilon_G = N_G/V = 82 \cdot 1000/1000 = 82$ W/m^3.
From the oxygen demand and per unit volume (45 mg/m^3.s) and the power dissipation ε_G = 82 W/m^3 it is evident that the example is based on a high-rate activated sludge process. With low-rate or extended aeration installation ε_G may be as low as 10 W/m^3.

3.423 Practical Aspects

The great advantage of rotor aerators, as compared to air diffusers for instance, is the fact, that due to the simple and open construction clogging cannot occur. On the contrary, the intensive mechanical action of the rotor works somewhat like a comminutor, disintegrating solid matter with exception of rubber, plastic and leather pieces. Hence, rotor aeration may be applied without primary sedimentation

(oxidation ditch). A disadvantage of the rotor construction are mainly the bearings, which require careful maintenance. Water (or mixed liquor) lubricated bearings, primarily used in former times, are nowedays replaced by fat-pressure bearing. Since moreover the development of large rotors with construction lengths up to 9 m reduced the number of bearings significantly, the maintenance problem of bearings seems to be solved.

The variation of the oxygenation capacity by changing the depth of immersion of the rotors is generally achieved by an adjustable outlet weir of the aeration tank, although adjusting the height of the total rotor construction is also been used in connection with cage rotors for oxidation ditches. The number of revolutions is generally kept constant. But motors with pole changing windings have also been applied to enable two different peripheral speeds to be applied. Furthermore the oxygenation capacity may be adjusted to the oxygen demand by switching off or on of rotor units, in case several are installed. Care should be taken then, however, to maintain a streaming velocity and mixing conditions which prevent solids from settling. Appropriate baffling may assist such efforts by diverting the velocity primarily induced at the surface region of the tank into its lower parts. This will generally increase the oxygenation efficiency OE somewhat, at the same time.

3.43 Cone Aeration

3.431 Types of Cones and Their Arrangement

Contrary to rotors cones are mounted on a vertical shaft. Therefore, they are generally arranged within a tank of square or round horizontal cross-section. Several tank units may be combined to a large tank. This arrangement induces two spiral motions overlapping each other to a complex pattern of flow. The first type is caused by the "pumping" and/or radial discharge action of the cone, producing an upward flow in the tank center and a downward flow near the tank walls (vertical spiral flow). The second type of motion is a slow rotation of the total tank content induced by the rotation of the impeller (horizontal spiral flow). From the previous discussion of the mechanism of gas transfer by mechanical aeration it is obvious,

that the vertical spiral flow significantly controls the rate of gas transfer, whereas an increase of the horizontal spiral flow decreases the velocity difference between water and cone periphery and thus decreases the oxygenation capacity and efficiency. Frequently, the tank is equipped with baffles in order to minimize the horizontal spiral flow.

Cone aeration is also applied in connection with a special type of oxidation ditch (type carrousel, fig. 3.48). The basic principle is also a round or square tank, but to one side two long channels are connected, which provide the large tank volume required for oxidation ditches. This, obviously, then leads to a longitudinal flow pattern rather than to a spiral one. In other words: The horizontal spiral flow induced by the cone is transformed to a longitudinal flow by means of the middle wall extending up to the cone periphery.

Finally cone aeration is extensively used in aerated lagoons and for reaeration of surface waters. For this purpose the aerators are frequently float mounted, whereas for the other types of application bridge mounting is the design of preference, although some of the cone types used in large tanks are float mounted.

The tank dimensions for optimum oxygen transfer and operation depend primarily on the size of the cones, ranging from some 0,40 m to 4,50 m; and secondly on the type of cone. These aspects will more fully be covered in section 3.432.

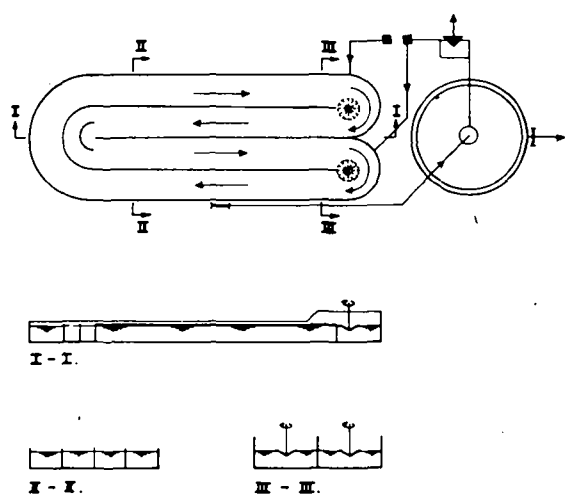

Fig. 3.48 LARGE OXIDATION DITCH (TYPE CARROUSEL) OPERATED WITH CONE AERATORS

In the following section some of the marketed aerators are described. Although it is tried to mention the cones in the order of types (plate-, updraft-, downdraft type), these underlaying principles overlap and are sometimes used in combination.

3.4311 Plate Aerators

The best known plate aerator is the Vortair-Cone which consists of a circular flat plate with 20 to 30 vertical blades attached at the periphery of the plate (fig. 3.49). The angle of the plates with the radius is adjustable from 0° to 25°. Openings behind the blades facilitate entrainement of air.

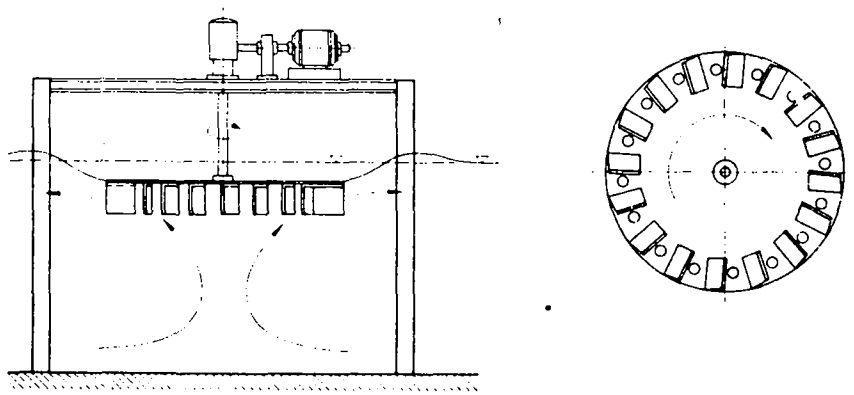

Fig. 3.49 SCHEMATIC REPRESENTATION OF A PLATE TYPE AERATOR (VORTAIR-CONE)

The Vortair-Cone is manufactured in 16 different sizes ranging from 0,40 to 4,5 m in diameter. The cone uses a standard motor and gear drive unit. The gross power input varies within the above range of sizes from 0,75 to 75 kW.

As already mentioned, the oxygen transfer is basically achieved by two mechanisms. At rotation of the cone slightly below the water level, the water is radially discharged which leads to a peripheral hydraulic jump. At optimum rotational speed the top plate is clear of water and air is entrained through the openings due to the low pressure behind each of the blades. This second effect accounts for some 10 % of the oxygenation capacity.

Although the Vortair-Cone has originally been developed for aeration of ponds and lagoons, it has sucessfully been applied in conventional activated sludge treatment at tank depths 2,0 to 3,5 m depending on the cone size. At greater depths the oxygenation capacity generally decreases.

3.4312 Updraft Aerators

The updraft type is the most common cone aerator. The variety of updraft types marketed requires a further subdivision into types working according to somewhat different principles: although the common principle is a pumping action, there is a certain difference in the way of discharging the water: either the water is issued in the form of large jets onto the water surface at low head (jet aerators) or it is sprayed. In the first case the cone somewhat resembles an impeller of a centrifugal pump, in the second case a vane-type pump is submerged issuing the water at an orifice in an exposure pattern formed by the diffuser. The jet aerators apply open and closed impeller cones. The pumping action of the closed units is somewhat superior but they are more likely to clogg. Finally, the updraft may be guided by draft tubes which permits greater tank depths to be applied.

The following updraft aerators will be discussed:

Simcar-Cone : an open impeller (jet aerator without draft tube)

Gyrox-Cone : open and closed impeller (jet aerator) without draft tube

Simplex-Cone : 3 closed types of impellers (jet aerators) with draft tube, partially combined with plates peripherally mounted on the impeller to produce a hydraulic jump

BSK-Turbine : a open and closed impeller unit (jet aerator) without draft tube

Hamburg-Rotor: a rotating draft tube with 6 to 10 radially mounted discharge tubes (jets) and plates for inducing a peripheral hydraulic jump

Aqua-Lator : a closed spray aerator

Simcar-Cone

The Simcar-Cone consists of a cone-shaped disc with square bar blades radiating outwards from almost the center. At the periphery the blades are horizontal (fig. 3.50).
The depth of submergence may be varied from the point when the horizontal blades just touch the water surface (minimum d_i) up to the 1,4 times the height of the blades. For the cone depicted in figure 3.50 the total variation then would be 1,4 x 133 = 186 mm. Taking the upper plane of the cone as reference the depth of submergence is varied between -133 mm and + 0,4.133 = 53 mm. Frequently, the depth of submergence of cones is referred to by "freeboard", (fb) which is defined by

$$+ \text{ freeboard (fb)} = - \text{ depth of submergence } (d_i)$$

The cone is manufactured in the size range from 0,4 m to 3,6 m of diameter. The oxygenation capacity OC ranges from some 0,3 to 50 g O_2/s (1,0 to 180 kg O_2/h), respectively (see table 3.1, appendix). The optimum dimensions of a square tank are established at a ratio of width over depth of 2 to 4 with a maximum depth of 5 m.

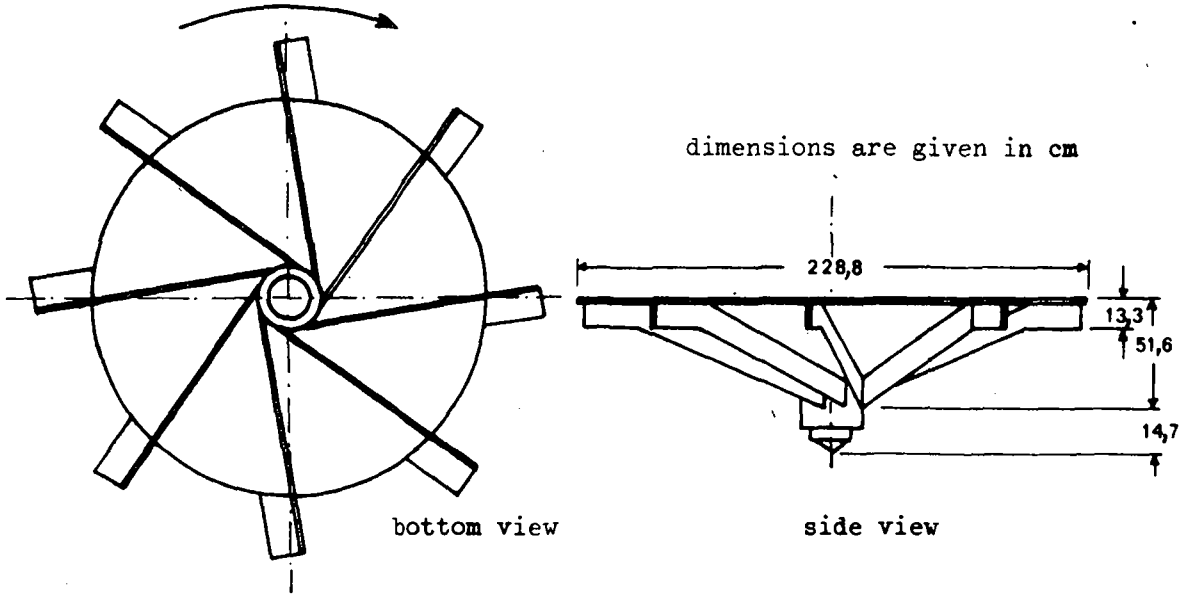

Fig. 3.50 SIMCAR-CONE (No.90 = 90 inch Ø)

Gyrox-Cones:

Gyrox-Cones may be looked at as a further development of the Vortair-Cone: The open Gyrox-Cone (type SE) consists of a circular plate onto which curved impeller vanes are attached (fig. 3.51a). Openings in the top plate behind the vanes increase the entrainement of air. The closed type of the Gyrox-Cone (fig. 3.51b) is based on the same construction. A part of the vanes is, however, covered by a truncated cone, which extends at the lower end into a short draft tube.
The closed construction provides a somewhat more intensive circulation of the tank content, requires, however, primary sedimention to prevent clogging.
Like many of the cones with curved vanes, the Gyrox-Cones may be operated at both directions of rotation. The normal rotation in direction of the concavity of the vanes is frequently referred to as "dragging", whereas the opposite direction, when the convex parts of the vanes "bite" or "push" into the water, is generally called the "opposite", "biting",or "pushing direction". The latter obviously achieves a greater oxygenation capacity.

The range of cone sizes, the corresponding average oxygenation capacity and the optimum tank dimensions are stated in table 3.2.

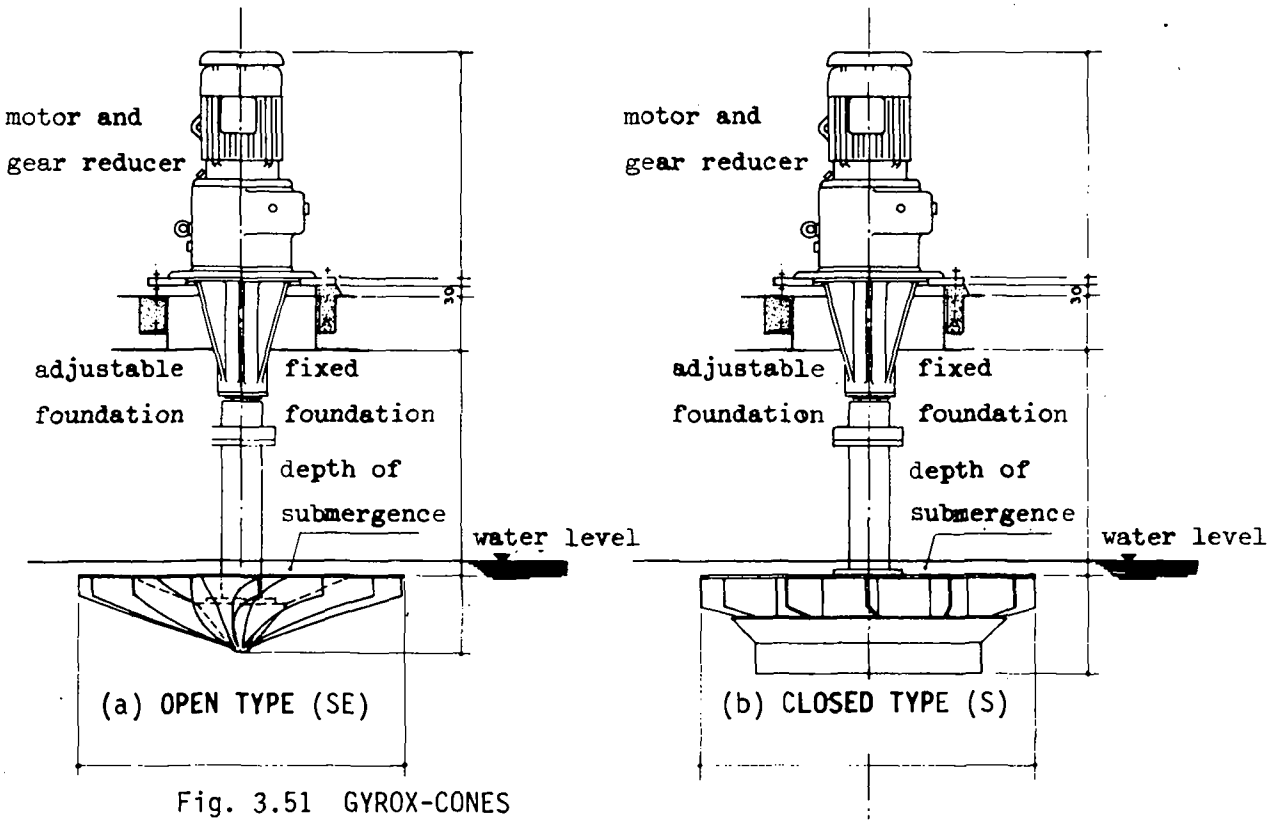

Fig. 3.51 GYROX-CONES

Simplex-Cones:

The basic type (type HL) consists of an open-ended conical shell formed out of steel plate, to the inner face of which a number of specially shaped blades are attached. The conical shell extends at the lower end into a ring, which covers the stationary draft tube of the tank. On the top of the vanes an annular ring is welded. Into this ring a number of short stays are fitted, which support the cone from the driving ring attached to the gear head (see figure 3.52). The type Simplex-S is essentially like the HL-type but a number of steel blades are fixed to the outer part of the conical shell additionally (fig. 3.53). Thereby, not only the pumping action of the inner construction but also the turbulence of the water surface induced by the outer ribs assists in transferring oxygen. Obviously, the oxygenation capacity of the S-type is superior to that of the HL-type.

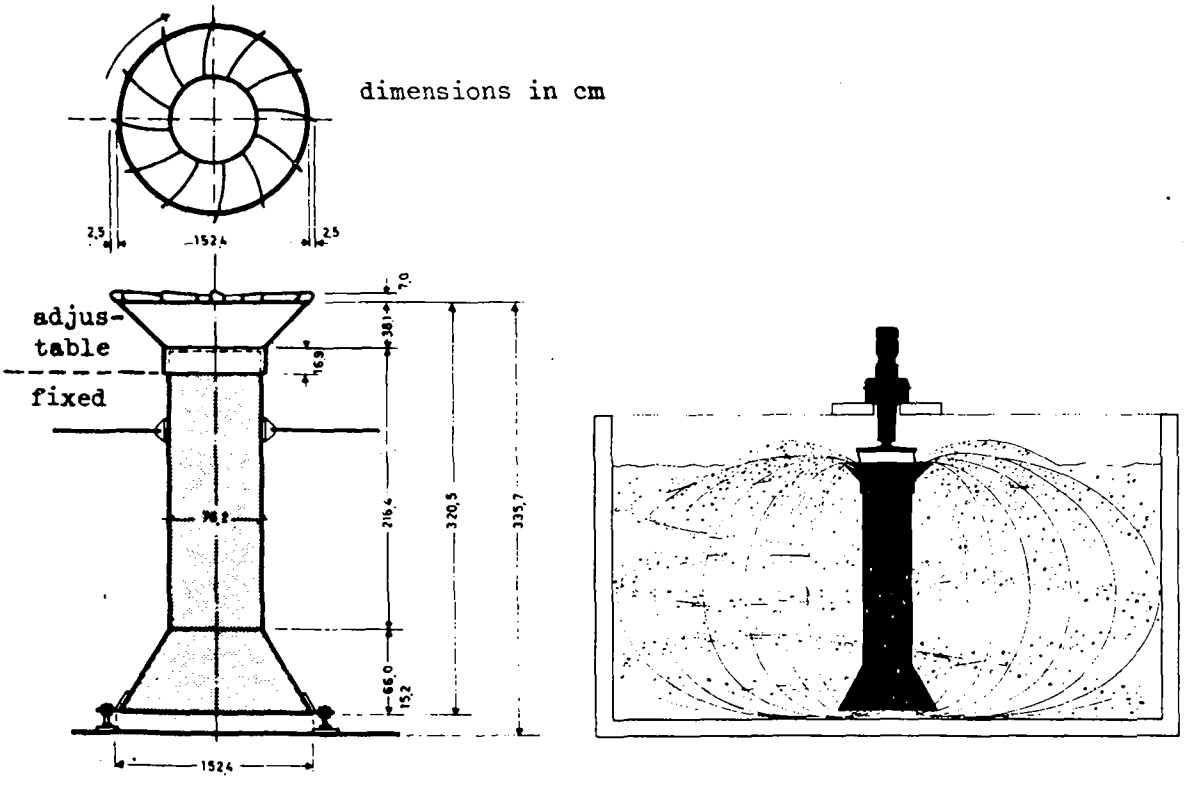

(a) SIMPLEX-CONE WITH DRAFT TUBE

(b) SCHEMATIC REPRESENTATION OF THE SPIRAL FLOW INDUCED BY AN UPDRAFT-CONE (SIMPLEX)

Fig. 3.52 SIMPLEX-CONE

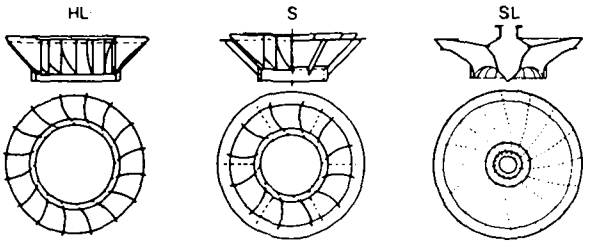

Fig. 3.53 TYPES OF SIMPLEX-CONES

A further increase of the oxygenation capacity is achieved by the SL-type, which is mainly a completely closed impeller (fig. 3.53), discharging water jets at low head. The channels of the impeller are large to prevent clogging.

The E-type is based again on the HL-type, however a circular plate of a diameter greater than the cone covers the blades (see figure 3.54). This plate disintegrates the discharged water jets to some degree, creating a larger interfacial area between air and water. The Simplex types are manufactured in sizes from 0,6 to 3,0 m of diameter. They may be arranged to adjust the freeboard or fixed (fig. 3.54). The range of variation of the depth of submergence is limited by stationary draft tube (see also table 3.3, appendix).

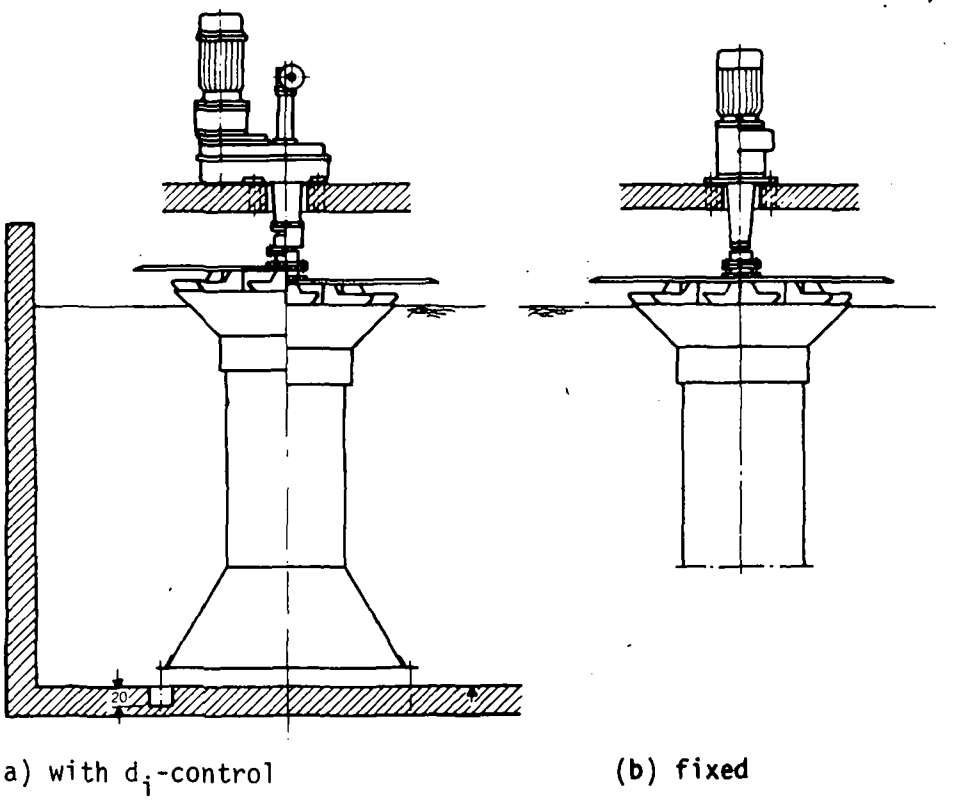

Fig. 3.54 SIMPLEX-CONE TYPE E

Due to the action of the draft tube tanks equipped with Simplex-Cones are generally deeper than with other cones. The optimum ratio of width to depth for square tanks ranges from 2 to 3. With very shallow tanks or for aeration of lagoons or surface waters the stationary draft tube may be omitted.

BSK-Turbines:

The BSK-Turbine is a cone-like impeller made out of glasfiber reinforced polyester. With the open type, named Gigant, the impeller channels are formed by open T-like beams situated at the bottom side of the cone (figure 3.55a), whereas with the closed type (Favorit), the channels are covered (fig. 3.55b) giving rise to an increased pumping action of the impeller. The top plate of the closed type contains holes for entrainement of air.
Both turbines are operated in the normal directions of rotation as well as in the "biting" direction for achieving higher oxygenation capacities.

The open type is produced in sizes from 0,75 to 2,0 m of diameter with a range of oxygenation capacities from some 0,3 to 28 g O_2/s (1 to 100 kg O_2/h), the closed type from 0,5 to 3,15 m and 0,3 to 100 g O_2/s (1 to 370 kg O_2/h), respectively (see table 3.4, appendix).

For optimum oxygen transfer the ratio of width to depth of square tanks should be in the range of 2,5 to 4,5. At greater depths a cone situated at the tank bottom under the aerator is installed to provide

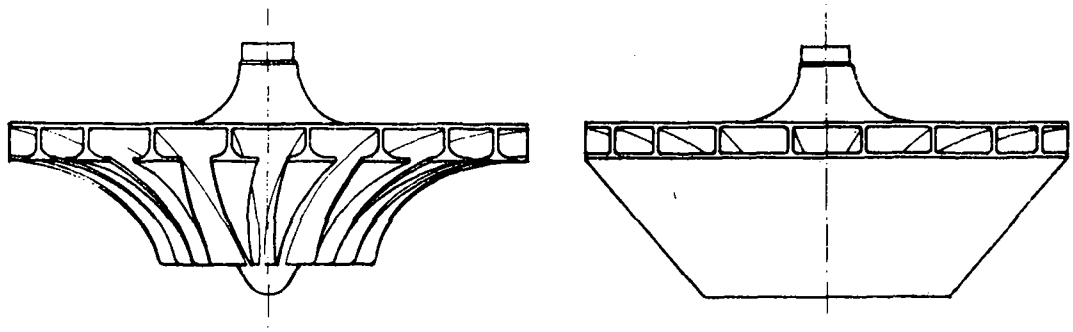

(a) OPEN TYPE (GIGANT) (b) CLOSED TYPE (FAVORIT)

Fig. 3.55 BSK-TURBINES

proper circulation of the water content; at smaller depths baffles are designed near the side walls to brake the horizontal circular motion of the tank content.

Hamburg-Rotor:

The Hamburg-Rotor consists of a short rotating draft tube with a number of radially mounted discharge tubes, leaving the central tube at a slight angle upwards. Into the angle under each discharge tube a triangular steel plate is welded (figure 3.56). In its normal position the lower edge of the discharge tubes is at the height of the water level.

When rotating, the discharge tubes jet the water over the tank surface thus producing an updraft which induces a spiral motion of the tank content.
The triangular plates and the outer side of the tubes cause - like the plates of the Vortair-Cone - a peripheral hydraulic jump.

The Hamburg-Rotor is manufactured in size from 1,0 to 3,6 m total diameter, with oxygenation capacities from 1,7 to 70 g O_2/s (6 to 250 kg O_2/h).
For optimum oxygenation in square tanks the ratio of width to depth to rotor diameter is advised to range from 3 : 1 : 0,6 to 4 : 1 : 0,67 (see also table 3.5, appendix).

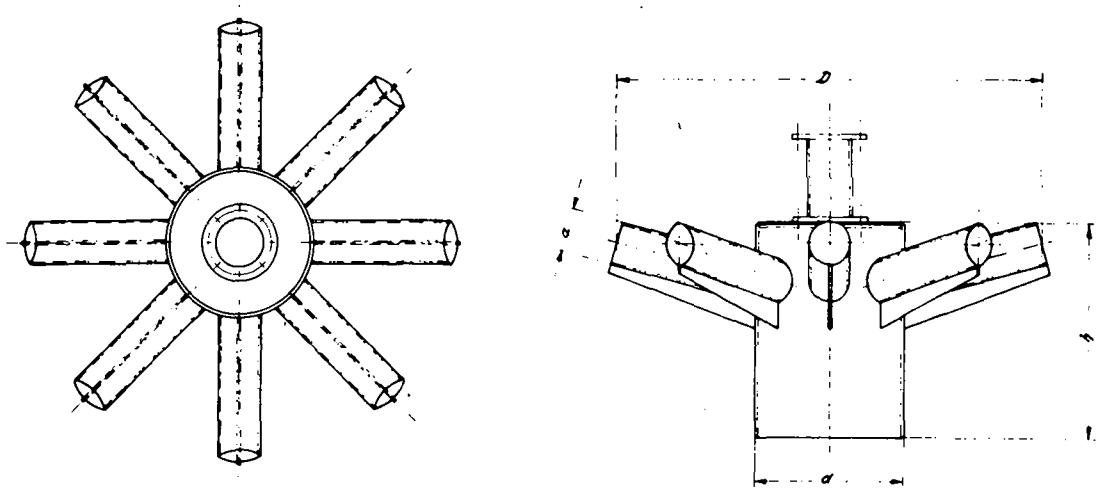

Fig. 3.56 HAMBURG-ROTOR

Aqua-Lator:

The Aqua-Lator consists of a float mounted high speed impeller which sucks the water through a short draft tube and sprays it through a discharge cone over the tank surface. The circular float unit (see figure 3.57) is made out of glasfiber inforced polyester, filled with plastic foam.
The Aqua-Lator is available on various sizes up to some 3,50 m diameter of the total unit with oxygenation capacities from about 2 to 25 g O_2/s (7 to 90 kg O_2/h) (see also table 3.6, appendix).

Although preferably used for the aeration of lagoons, ponds and surface waters, the Aqua-Lator may also be applied in large activated sludge tanks.
Due to the intense updraft the minimum depth of lagoons and ponds is

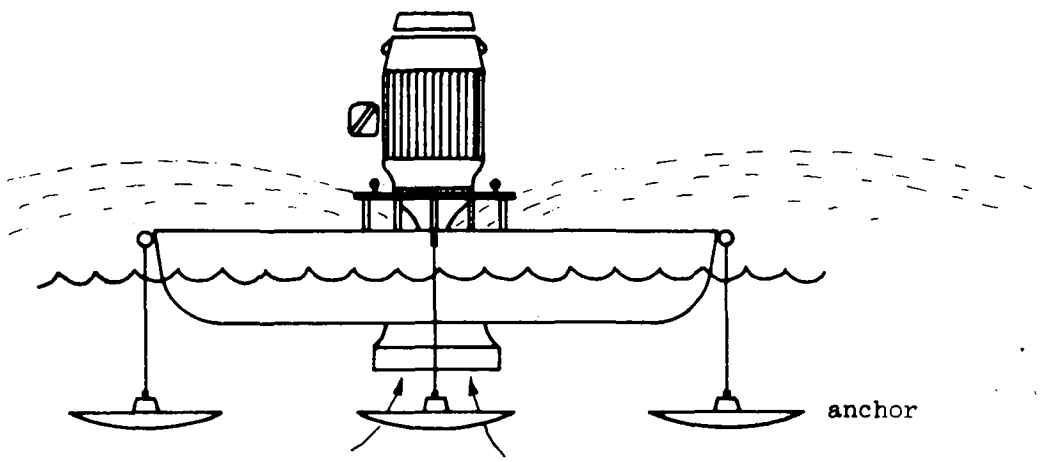

Fig. 3.57 AQUA-LATOR

2 to 3 m to prevent erosion of the bottom, whereas the maximum depth is already reached at 3,5 to 4,2 m, depending on the size of the turbine. To the lower end of the draft tube a flat cone may be attached to prevent erosion by inducing a vertical input velocity. The depths then can be reduced to 0,8 to 1,2 m, respectively.

3.4313 Downdraft Aerators

The common principle of all downdraft aerators is a turbine placed at or near the bottom of a square or round tank. The high speed turbine induces a downdraft followed by a circular motion of the tank content in a direction opposite to that of the updraft types. The high water

velocities near the impeller produce a partial vacuum entraining air through the hollow drive shaft extending into the air. A small additional effect of gas transfer is achieved by the constant renewal of the water surface. Most of the dissipated energy is used, however, for creating turbulence, not of air-water interfaces, giving rise to low oxygenation capacities and efficiencies.
Since moreover the oxygenation capacity cannot be varied in a simple manner under operational conditions, it is obvious that downdraft aerators have more and more been displaced by updraft types.

3.432 Factors Influencing the Rate and Efficiency of Oxygen Transfer

Referring to the discussed mechanisms of oxygen transfer by mechanical aeration (section 3.41) it is evident that the oxygenation capacity of cones is primarily determined by the flow (m^3/s) pumped by the aerator and by the size of the jets or droplets spread onto the surface.
The flow is strongly influenced by the size of the cone or its diameter D_c, the rotational speed or peripheral speed v_p, its direction, and the depth of submergence d_i or freeboard. These factors and furthermore the construction of the cone itself determine the air-liquid interface of the discharged water.

The additional effects of gas transfer by air entrainement, previously discussed, are basically determined by the tank size: the smaller the tank is, the greater are the spiral velocities and the more significant are these "secondary" effects. In an infinitely large tank volume (pond, lagoon, surface water) these effects will almost approach zero. Hence it is reasonable to relate the oxygenation capacity and oxygenation efficiency to the power dissipation per unit volume ε_G (W/m^3). Qualitatively, a greater ε_G will yield a higher oxygenation capacity OC and a greater oxygenation efficiency OE. The power dissipation (N_G) again, is determined by the before mentioned factors of D_c, v_p, d_i and direction of rotation.

The forementioned considerations will be discussed in the following by means of a few examples referring to updraft aerators.
The influence of the cone diameter D_c, the peripheral speed v_p and the depth of immersion on the oxygenation capacity has been shown to follow the relationship

$$OC = k_c.(1 + k_i.d_i) \cdot D_c^{\,n} \cdot v_p^{\,m} \quad (g\ O_2/s) \qquad (3.28)$$

where in this case

k_c = a constant dependent on the shape of the tank and the construction of the cone

k_i = a constant to account for the depth of immersion of the cone d_i

n = a constant signifying the influence of the cone diameter

m = a constant signifying the influence of the peripheral speed.

For the BSK-Turbine and the Simcar-Cone the constants have been found in tank volumes of 1200 m^3 (BSK) and from 110 to 600 m^3 (Simcar) as follows

	D_c	k_c	k_i	n	m
BSK	2,0	0,028	2,9	2	3
BSK	3,0	0,028	3,3	2	3
Simcar	2,3	0,015	3,1	2	3
Simcar	3,6	0,015	1,9	2	3

The above information is of limited value, however, since especially the constant k_c is strongly dependent on the chosen condition of tank size and shape and the type of aerator.

The linear influence of the depth of immersion and peripheral speed on the oxygenation capacity is shown in figure 3.58 for the Simplex-HL-Cone (a) for the Simcar-Cone (b) and for the Vortair-Cone (c). For both updraft types the linear influence is seen, whereas the plate type (Vortair) has a pronounced optimum d_i.

Variation of d_i and v_p, therefore, is an effective means for controlling the oxygenation capacity. According to eq. 3.28 the variation of v_p is more effective.

Generally, the oxygenation capacity of all updraft types may be adjusted by variation of the depth if immersion over a range from about 40 % to 100 % of the maximum capacity. Concerning the peripheral speed v_p, cones are operated from about 2 to 7 m/s, the optimum v_p with regard to the oxygenation efficiency ranging between 3,5 to

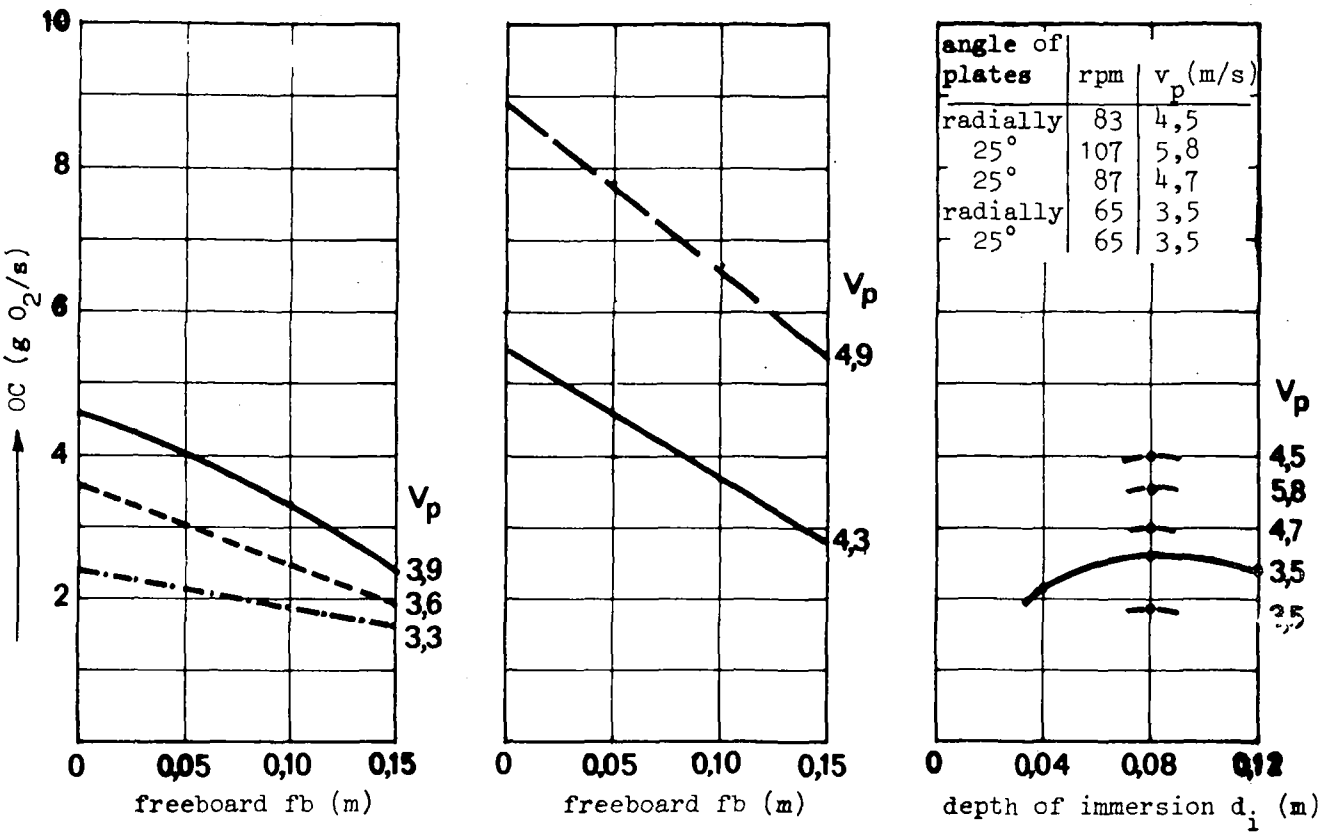

(a) SIMPLEX
D_c = 1,524 m
V = 120 m^3

(b) SIMCAR
D_c = 2,288 m
V = 115 m^3

(c) VORTAIR
D_c = 1,04 m
V = 135 m^3

Fig. 3.58 INFLUENCE OF d_i AND v_p ON THE OXYGENATION CAPACITY

5 m/s. Within these ranges the greater velocities refer to smaller cones and vice versa.

Changing v_p by means of motors with pole changing windings (e.g. doubling of rotational speed) would allow to reduce the oxygenation capacity according to eq. 3.28 from 100 % to $(\frac{1}{2})^3$ = 12,5 % of the maximum capacity. In practice, however, a gradual control is required to meet the variation of the oxygen demand. This is most effectively attained by variation of the depth of immersion d_i of the cone. On the other hand, an alteration of the rotational speed also influences the "secondary effects" of surface aeration. Hence the range of control is generally less than would be expected from the above consideration. By combining both control mechanisms (d_i and v_p) the oxygenation capacity may commonly be varied from about 15 % to 100 % of the maximum capacity.

As already mentioned, the influence of the tank size may be accounted for by relating the power dissipation per unit volume ε_G (W/m^3) to the oxygenation capacity. Since the power requirement of a mixing device generally increases with the second power of the diameter and

the third power of the peripheral speed one would expect a straight line relationship between the oxygenation capacity OC and the power input with reference to eq. 3.28. Since, however, increasing the power input per unit volume generally increases the turbulence of the tank content and hence also the "secondary effects" of gas transfer, the oxygenation capacity is likely to increase more than proportional to the power dissipation per unit volume.

For illustration purposes an example is given in figures 3.59 and 3.60 for the BSK-Turbines, based on measurement with all diameters produced and tank volumes from 50 m^3 to 2220 m^3. Figure 3.59 refers to the closed type (Favorit) and shows also the effect of reversing the direction of rotation from biting to dragging; figure 3.60 is a logarithmic plot for both BSK-types at biting direction (data from manufacturer).
Both graphs show the discussed effect of ε_G on OC and furthermore also an increase of the oxygenation efficiency with increasing power dissipation per unit volume, as may be seen from the given lines of equal OE. As with almost all surface units the oxygenation efficiency varies between the limits of some 0,4 to 1,0 mg O_2/J (1,5 to 3,5 kg O_2/kWh), averaging about 0,55 mg O_2/J (2 kg O_2/kWh).
The increase of the oxygenation efficiency with increasing power input per unit volume has been investigated for several surface aerators and has been generalized by the following equation

$$OE = OE_o + k_{OE} \cdot \varepsilon_G \qquad (3.29)$$

where

OE_o = oxygenation efficiency at infinite tank volume (ponds, lagoons); i.e. at $\varepsilon_G = 0$

k_{OE} = constant characteristic of the aerator.

OE_o at $\varepsilon_G = 0$ does obviously not refer to a not-operating surface aerator, but rather to a surface unit working in a very large tank volume. Thus, OE_o states the oxygenation efficiency obtained by the liquid spray solely, whereas the increase with ε_G, as given by the second term of eq. 3.29, mainly signifies the influence of the "secondary effects".

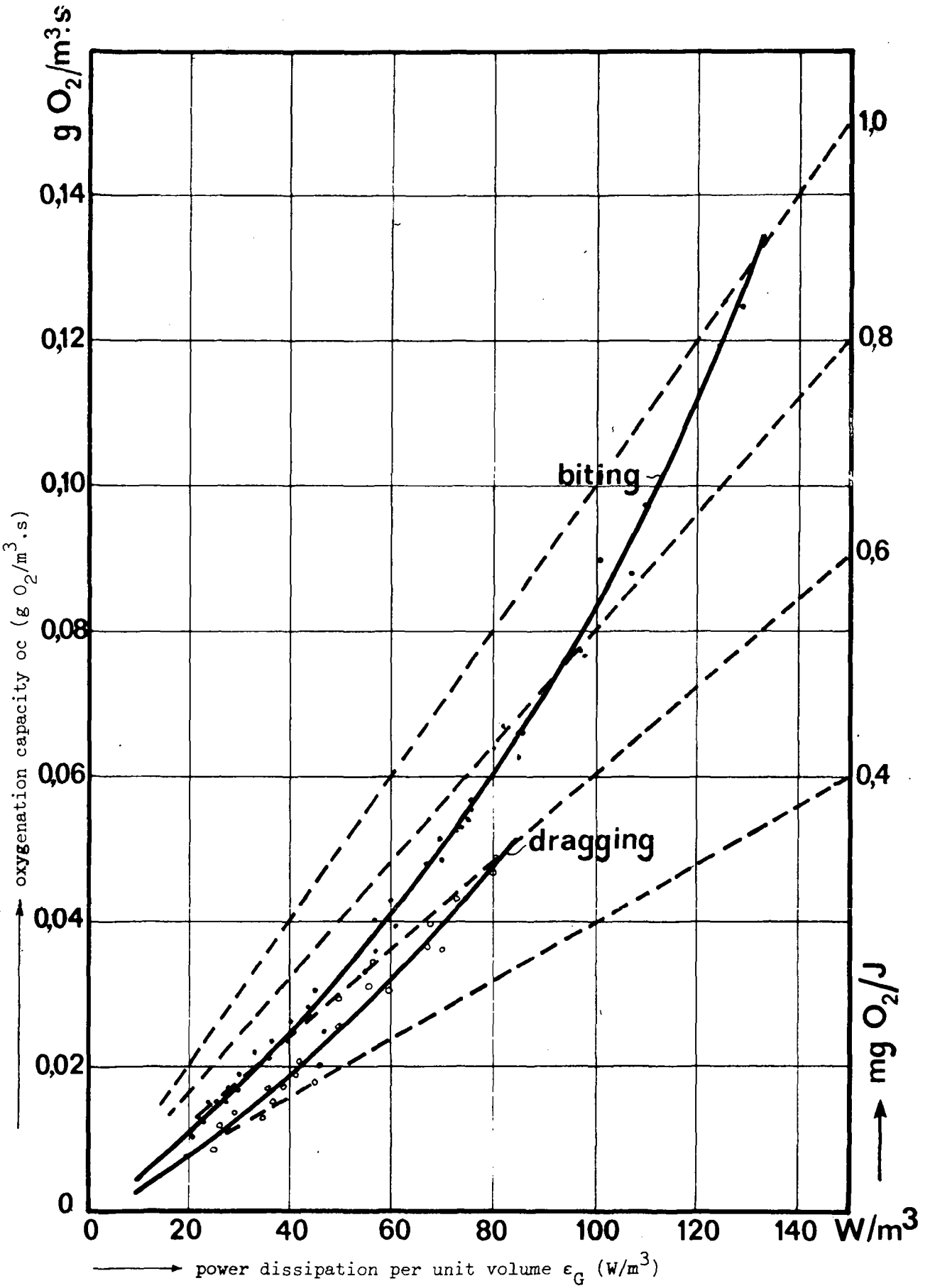

Fig. 3.59 OXYGENATION CAPACITY oc AND EFFICIENCY OE OF CLOSED BSK-TURBINES (FAVORIT) AS A FUNCTION OF THE POWER DISSIPATION PER UNIT VOLUME ε_G

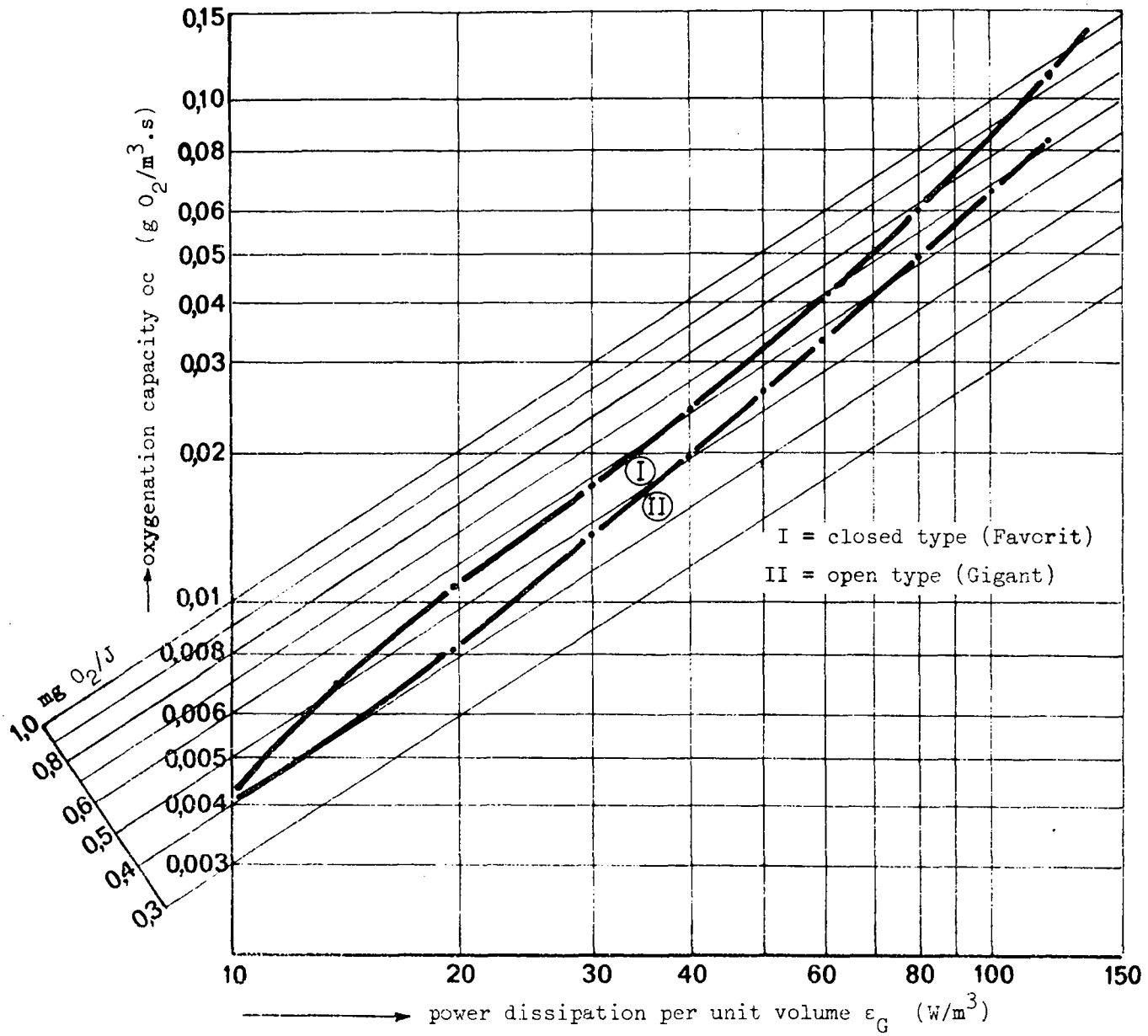

Fig. 3.60 OXYGENATION CAPACITY oc AND EFFICIENCY OE OF BSK-TURBINES AS A FUNCTION OF THE POWER DISSIPATION PER UNIT VOLUME ε_G

Figure 3.61 states an example for eq. 3.29. The following table summarizes the constants thusfar determined and the respective expermental conditions.

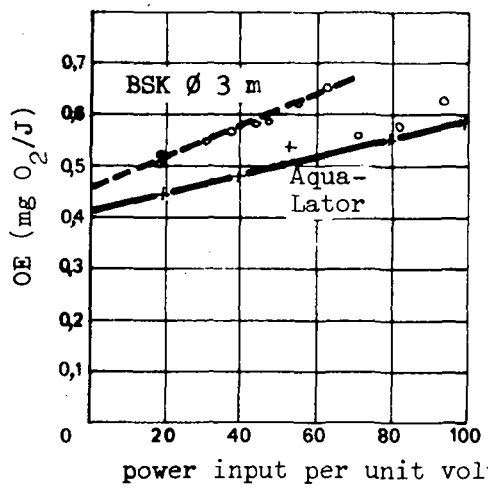

$$OE = OE_o + k_{OE} \cdot \varepsilon_G$$

	OE_o	k_{OE}
Aqua-Lator	0,42	0,0017
BSK Ø 3 m	0,44	0,0033

Aqua-Lator: V = 200 - 2000 m^3
N_G = 4 - 40 kW
BSK Ø 3 m : V = 1200 m^3

Fig. 3.61 INFLUENCE OF THE POWER INPUT PER UNIT VOLUME(ε_G) ON THE OXYGENATION EFFICIENCY OE IN CONE AERATION

Experimental conditions	OE_o	k_{OE}	dimension of OE
Various surface aerators			
V = 110-1200 m^3	0,33	0,0089	mg O_2/J
N_G = 4-55 kW	1,2	0,032	kg O_2/kWh
ε_G = 10-60 W/m^3			
Aqua-Lator			
V = 200-2000 m^3	0,42	0,0017	mg O_2/J
N_G = 4-40 kW	1,5	0,006	kg O_2/kWh
ε_G = 20-100 W/m^3			
BSK, 3 m diameter			
V = 1200 m^3	0,44	0,0033	mg O_2/J
N_G = 25-80 kW	1,6	0,012	kg O_2/kWh
ε_G = 20-65 W/m^3			

The variability of the constants, also of those given for eq. 3.28, clearly shows, that the equations are able to account for only a part of the factors influencing the rate and efficiency of oxygen transfer by cone aeration. For a certain type of cone applied in connection with a certain range of tank dimensions they may, however, provide a useful means of interpreting measurements and forecasting oxygenation capacities and efficiencies under varied operational conditions.

Concerning the effect of surface active and hydrophobic matter on the oxygenation capacity and efficiency, it follows from what has been stated in section 3.41 for mechanical aeration, that in regions of high turbulence (e.g. near the blades of the cones) an increase is to be expected, whereas at places of low turbulence (e.g. entrained bubbles in the bulk of the tank content) a reduction is encountered. Thus, the overall influence varies with the type of aerator and furthermore with the power input per unit volume.
A reduction of the OC and OE in comparison to tap water is rare and never reaches the values encountered in air diffusion. α-values as high as 1,44 have been reported but should obviously not be applied within a conservative design. Unless their is no evidence of a serious reduction of the rate of oxygen transfer, a value of $\alpha = 1$ should be chosen, therefore.

For illustration purposes the design information as given by the manufacturer is appendixed in the tables 3.1 to 3.6 for the Simcar-Cone, the Gyrox-Cone, the Simplex-Cone (type E), the BSK-Turbine (type Favorit), the Hamburg-Rotor and the Aqua-Lator.
Unless otherwise stated, the values refer to the maximum attainable oxygenation capacity. This also includes the direction of rotation.

3.433 Practical Aspects

Generally closed cones are susceptible to clogging and require primary sedimentation therefore, whereas the open types can be used without any pretreatment and are hence primarily applied in connection with extended aeration and large oxydation ditches. The tendency of clogging of the closed types obviously depends on the dimensions of the cone channels. If they are large enough, also closed types may be used without pretreatment. Following these principles will reduce maintenance to a minimum.

At proper shaping of the tanks and sufficient power input per unit volume (e.g. $\varepsilon_G \geq 10\ W/m^3$) the cones commonly provide a bottom velocity of the water which will prevent the activated sludge from settling. Proper shaping of the tanks includes additional structures as a hopper-like bottom or a solid cone situated on the bottom in the center of the tank. The requirement of sufficient bottom velocities ($v \geq 0{,}15$ m/s) limits the tank depth. In this connection updraft types generally allow greater depths than plate types; with draft

tubes (used in connection with Simplex-Cones) still greater depths may be designed.

Cones are normally bridge mounted in activated sludge tanks. Although several cones may be driven by one motor and gear reducer, there is a trend to drive each unit seperately. Normally, conventional motors, horizontal or vertical are used. The motor is directly connected to the gear reducer. An example of a vertical mounting is seen in figure 3.51, whereas figure 3.62 shows a horizontal assembly. As already

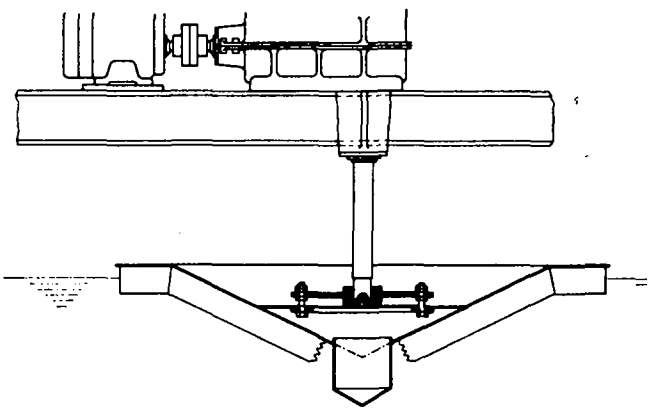

Fig. 3.62 SIMCAR-CONE WITH HORIZONTAL MOTOR AND GEAR REDUCER

mentioned, the cones may also be float mounted for application in large tanks, lagoons, ponds, or for aeration of surface waters.

The control of the oxygenation capacity by means of varying the depth of submergence is achieved by either an adjustable weir or by directly controlling the depth of submergence of the cone (fig. 3.54). Control of the peripheral velocity is obtained by applying motors with pole changing winding, control of the direction of rotation by reversable motors.

Example: Design on the basis of the oxygen demand given in the example in section 3.422 an aeration tank of V = 2000 m^3 for cones of 2,5 m of diameter equipped with a 30 kW motor, the oxygenation capacity of which follows the relation $OC = 0{,}014.(1 + 3{,}3.d_i).D_c^2.v_p^3$ (g O_2/s). Estimate the oxygenation efficiency on the basis of $OE = 0{,}4+0{,}003.\varepsilon_G$ (mg O_2/J) at conditions of maximum oxygenation capacity.

The oxygenation capacity of x cones will be at

$d_i = 0$ and $v_p = 4{,}5$ (chosen)

$$OC = x \cdot 0{,}014 \cdot 2{,}5^2 \cdot 4{,}5^3$$
$$= x \cdot 8 \text{ g } O_2/s$$

At an oxygen concentration of c = 2 and $\alpha = 1$
the oxygenation capacity is

$$OC_{c=2} = x \cdot 8 \cdot (10 - 2)/10 = x \cdot 6{,}4 \text{ g } O_2/s$$

The number of cones is determined by equalizing this oxygenation capacity with the minimum oxygen demand of 45.0,7 g O_2/s:

$$45 \cdot 0{,}7 = x \cdot 6{,}4$$
$$x = 4{,}9$$

i.e. 5 cones of the above specification are required. The maximum oxygen demand of 45.1,3 g O_2/s can be met by increasing the depth of submergence.
The required d_i may be obtained by setting the maximum demand equal to the oxygenation capacity of the 5 cones at operational conditions (5.6,4 g O_2/s) and multiplication with the term accounting for the influence of d_i:

$$45 \cdot 1{,}3 = 5 \cdot 6{,}4 \cdot (1 + 3{,}3.d_i)$$
$$d_i = 0{,}25 \text{ m}$$

The oxygenation efficiency is obtained from the power input per unit volume at maximum oxygenation capacity, which amounts to

$$\varepsilon_G = 5 \cdot 30 \text{ kW}/2000 \text{ m}^3$$
$$= 75 \text{ W/m}^3$$

Hence

$$OE = 0{,}4 + 0{,}003 \cdot 75$$
$$= 0{,}62 \text{ mg } O_2/J$$
$$= 2{,}2 \text{ kg } O_2/kWh$$

Since the rectangular tank should comprise 5 square units, the tank dimensions are designed at about a ratio of length : width : depth = 5 : 1 : 0,25 to give a length of 60 m, a width of 12 m and a depth of 2,80 m.

3.5 Combined Aerator Types

Combined aeration is a combination of bubble aeration and mechanical means for dispersion of the bubbles and creating turbulence, also assisting in transfer of gases. Since both mechanisms may be controlled seperately, the oxygenation capacity may be varied over wide limits to meet the variations of oxygen demand in activated sludge treatment. Their application in water treatment is rare.

The DO-Turbine (Dorr Oliver) is depicted in figure 3.63. It consists of a sparge ring releasing air bubbles of medium size through orifices of 1 to 2 mm of diameter and a centrally arranged vertical shaft with one or two bladed impellers, one closely above the sparge ring. DO-Turbines are preferably used in deep tanks of square cross-sectional area.

For efficient oxygen transfer the rotational speed of the impeller(s) should be adjusted to the air flow. An example is given in the following table (recommandation of manufacturer).

air flow 10^{-3} m^3/s	16	28	39	51
rotational speed rps	0,9	11,3	12,6	14,0

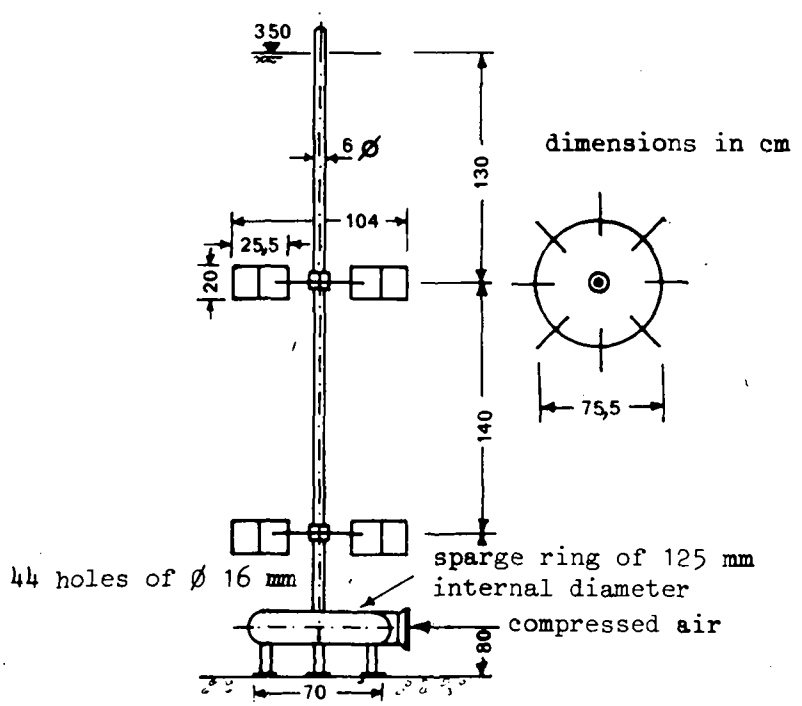

Fig. 3.63 DO-TURBINE

The given rotational speeds indicate that a geared drive is required. Two thirds of the total power are taken by the turbine, one third by the air diffusion on the average. The oxygenation efficiency is generally less than with mechanical aeration, amounting to about 0,4 mg O_2/J (1,5 mg O_2/kWh).

A somewhat different design is the Permeator, using a sparge ring also, but two seperately driven impellers, one just above the sparge ring, the other near the surface to act as an surface aerator.

The Vogelbusch-Disperser (fig. 3.64) has primarily been developed for aeration in connection with industrial processes (fermentation processes, oxidation of dye-stuff) but has also been used for oxygenation and carbon dioxide removal in water treatment.
The aerator consists of a sickle-like impeller, with slots on the back side, mounted on a hollow shaft, through which compressed air is diffused.

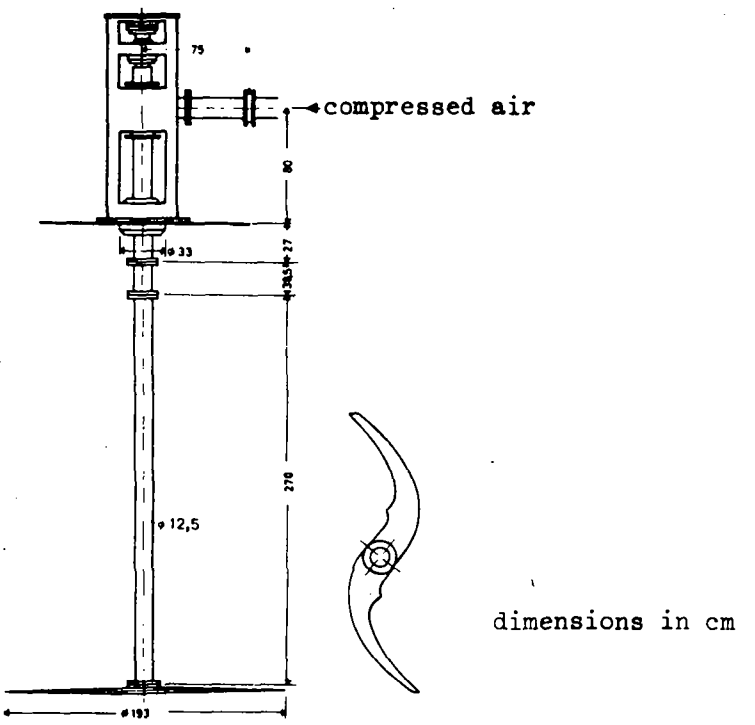

Fig. 3.64 VOGELBUSCH - DISPERSER

The air discharged by the slots is dispersed into fine bubbles of 2 - 4 mm of diameter by the turbulence and shear action induced by the rotation of the impeller. The air-pressure to be applied is generally less than the depth of submergence due to a partial vacuum being produced at the reverse side of the impeller.

Hence deep tanks of square or circular cross-section are appropriate, in which the rising air bubbles induce an upwards velocity in the center region of the tank and a downwards motion at the side walls, effecting sufficient mixing of the tank content. To prevent a high horizontal circular velocity, depreciating the oxygenating and mixing conditions, the tanks are generally baffled.

It is evident that - like with the other combined types also - the mechanical action accounts for the dispersion of the air bubbles, whereas the injected air primarily determines the oxygenation capacity. The oxygen utilization per unit depth of submergence has been found in the order of 6 to 7 g $O_2/m^3.m$, the oxygenation efficiency ranging from but 0,3 to 0,4 mg O_2/J (1 to 1,5 kg O_2/kWh). Since the system is basically fine bubble aeration at high turbulence, the gas transfer is somewhat less reduced by surface active agents than air diffusion: α-values of 0,8 to 0,95 have been reported.

Table 2.1 Distribution Coefficient for Gases in Water k_D

Gas	Mol. wt.	density at 0°C and 101,3 kPa	Distribution Coefficient k_D				Boiling point
	g/mole	kg/m^3	0°C	10°C	20°C	30°C	°C
Hydrogen, H_2	2,016	0,08988	0,0214	0,0203	0,0195	0,0189	- 253
Methane, CH_4	16,014	0,7168	0,0556	0,0433	0,0335	0,0306	- 162
Nitrogen, N_2	28,01	1,251	0,0230	0,0192	0,0166	0,0151	- 196
Oxygen, O_2	32,00	1,429	0,0493	0,0398	0,0337	0,0296	- 183
Ammonia, NH_3	17,03	0,771	1,300	0,943	0,763	...	- 33,4
Hydrogen sulfide, H_2S	34,08	1,539	4,690	3,65	2,87	...	- 61,8
Carbon dioxide, CO_2	44,01	1,977	1,710	1,23	0,942	0,738	- 78,5
Ozone, O_3	48,00	2,144	0,641	0,539	0,395	0,259	- 112
Air	...	1,2928	0,0288	0,0234	0,0200	0,0179	...

At sea level dry air contains 78,084 % N_2, 20,948 % O_2, 0,934 % A, 0,032 % CO_2, and 0,002 % other gases by volume. For ordinary purposes it is assumed to be composed of 79 % N_2 and 21 % O_2.

Table 2.2 Vapor Pressure of Water

Temperature	Vapor Pressure	
°C	kPa	mm Hg
0	0,611	4,58
5	0,872	6,54
10	1,23	9,21
15	1,71	12,8
20	2,33	17,5
25	3,17	23,8
30	4,24	31,8

Table 2.3 Solubility of Oxygen in Water Exposed to Water-Saturated Air at a total pressure of 1013 mbar (760 mm Hg)

Temperature in °C	Chloride Concentration in Water g/m³					Difference per 100 mg Chloride
	0	5.000	10.000	15.000	20.000	
	Dissolved Oxygen g/m³					
0	14,6	13,8	13,0	12,1	11,3	0,017
1	14,2	13,4	12,6	11,8	11,0	0,016
2	13,8	13,1	12,3	11,5	10,8	0,015
3	13,5	12,7	12,0	11,2	10,5	0,015
4	13,1	12,4	11,7	11,0	10,3	0,014
5	12,8	12,1	11,4	10,7	10,0	0,014
6	12,5	11,8	11,1	10,5	9,8	0,014
7	12,2	11,5	10,9	10,2	9,6	0,013
8	11,9	11,2	10,6	10,0	9,4	0,013
9	11,6	11,0	10,4	9,8	9,2	0,012
10	11,3	10,7	10,1	9,6	9,0	0,012
11	11,1	10,5	9,9	9,4	8,8	0,011
12	10,8	10,3	9,7	9,2	8,6	0,011
13	10,6	10,1	9,5	9,0	8,5	0,011
14	10,4	9,9	9,3	8,8	8,3	0,010
15	10,2	9,7	9,1	8,6	8,1	0,010
16	10,0	9,5	9,0	8,5	8,0	0,010
17	9,7	9,3	8,8	8,3	7,8	0,010
18	9,5	9,1	8,6	8,2	7,7	0,009
19	9,4	8,9	8,5	8,0	7,6	0,009
20	9,2	8,7	8,3	7,9	7,4	0,009
21	9,0	8,6	8,1	7,7	7,3	0,009
22	8,8	8,4	8,0	7,6	7,1	0,008
23	8,7	8,3	7,9	7,4	7,0	0,008
24	8,5	8,1	7,7	7,3	6,9	0,008
25	8,4	8,0	7,6	7,2	6,7	0,008

Table 2.4 Coefficients of Diffusion of Gases in Water

Gas	Coefficient of Diffusion D (10^{-9} m^2/s) at a Temperature of		
	10°C	20°C	30°C
N_2	1,27	1,64	2,20
O_2	1,39	1,80	2,42
CH_4	1,16	1,50	2,02
CO_2	1,30	1,68	2,26
H_2S	1,09	1,41	1,90
H_2	3,98	5,13	6,90

Table 2.5 Correction Factor $\sqrt{D_{10}/D_T}$

T (°C)	0,0	0,1	0,2	0,3	0,4	0,5	0,6	0,7	0,8	0,9
5	1,0977	1,0957	1,0936	1,0916	1,0896	1,0875	1,0855	1,0835	1,0815	1,0795
6	1,0774	1,0754	1,0734	1,0714	1,0694	1,0674	1,0655	1,0635	1,0615	1,0595
7	1,0575	1,0556	1,0536	1,0516	1,0497	1,0477	1,0458	1,0438	1,0419	1,0399
8	1,0380	1,0361	1,0341	1,0322	1,0303	1,0284	1,0265	1,0245	1,0226	1,0207
9	1,0188	1,0169	1,0150	1,0131	1,0113	1,0094	1,0075	1,0056	1,0037	1,0019
10	1,0000	0,9981	0,9963	0,9944	0,9926	0,9907	0,9889	0,9870	0,9852	0,9834
11	0,9815	0,9797	0,9779	0,9760	0,9742	0,9724	0,9706	0,9688	0,9670	0,9652
12	0,9634	0,9616	0,9598	0,9580	0,9562	0,9545	0,9527	0,9509	0,9491	0,9474
13	0,9456	0,9438	0,9421	0,9403	0,9386	0,9368	0,9351	0,9333	0,9316	0,9299
14	0,9281	0,9264	0,9247	0,9229	0,9212	0,9195	0,9178	0,9161	0,9144	0,9127
15	0,9110	0,9093	0,9076	0,9059	0,9042	0,9025	0,9008	0,8992	0,8975	0,8958
16	0,8941	0,8925	0,8908	0,8892	0,8875	0,8858	0,8842	0,8825	0,8809	0,8793
17	0,8776	0,8760	0,8744	0,8727	0,8711	0,8695	0,8679	0,8662	0,8646	0,8630
18	0,8614	0,8598	0,8582	0,8566	0,8550	0,8534	0,8518	0,8502	0,8487	0,8471
19	0,8455	0,8439	0,8423	0,8408	0,8392	0,8376	0,8361	0,8345	0,8330	0,8314
20	0,8299	0,8283	0,8268	0,8252	0,8237	0,8222	0,8206	0,8191	0,8176	0,8161
21	0,8145	0,8130	0,8115	0,8100	0,8085	0,8070	0,8055	0,8040	0,8025	0,8010
22	0,7995	0,7980	0,7965	0,7950	0,7936	0,7921	0,7906	0,7891	0,7877	0,7862
23	0,7847	0,7833	0,7818	0,7803	0,7789	0,7774	0,7760	0,7745	0,7731	0,7717
24	0,7702	0,7688	0,7674	0,7659	0,7645	0,7631	0,7617	0,7602	0,7588	0,7574

Table 3.1 Oxygenation Capacity of Simcar-Cones (data from manufacturer)

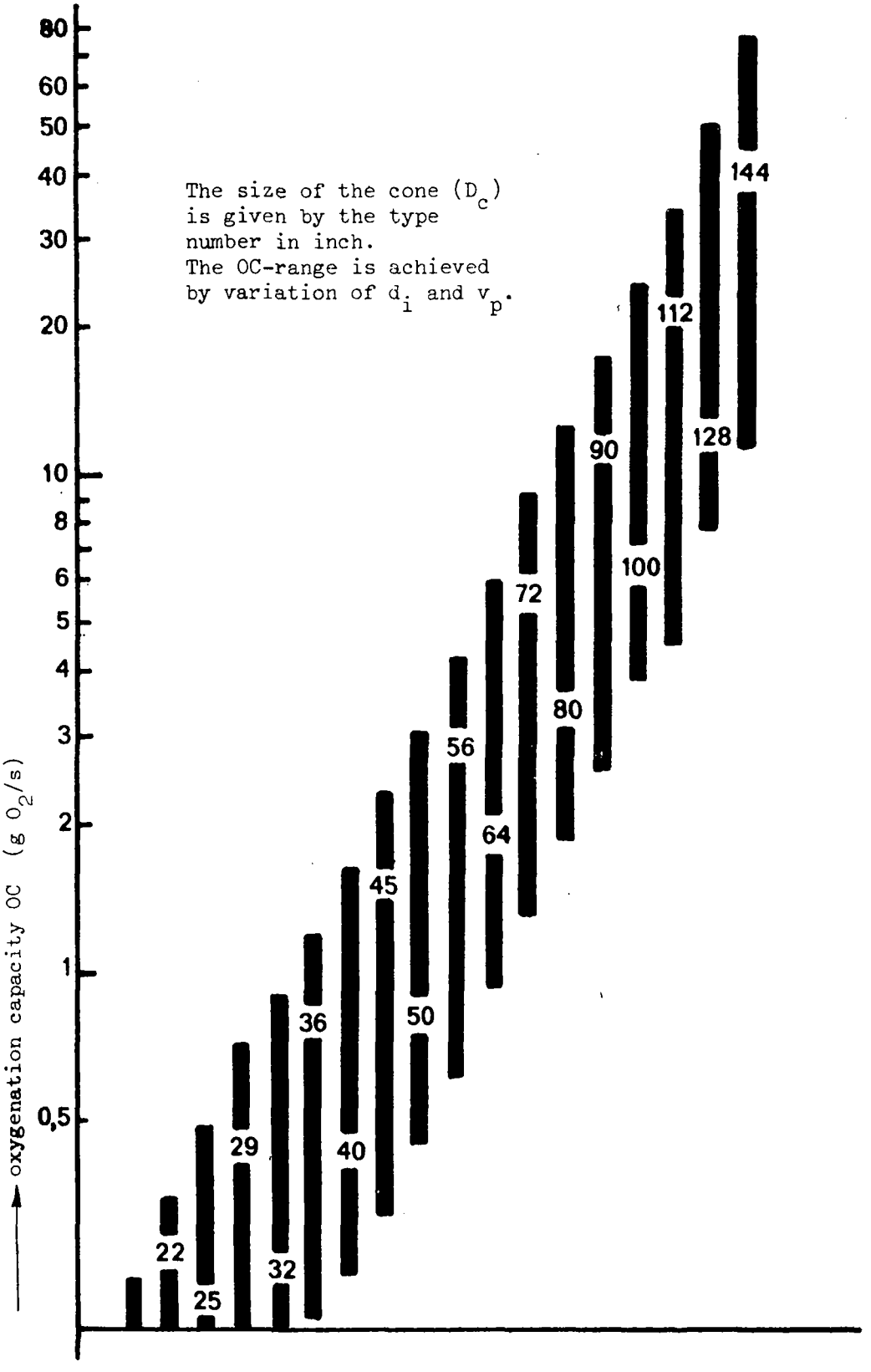

Table 3.2 Oxygenation Capacity and Tank Dimensions for Gyrox-Cones (as given by manufacturer)

Type		OC	Tank Dimensions (m)	
closed (S)	open (SE)	g O_2/s	from	to
71 S		1,1	5 x 5 x 1,2	6 x 6 x 1,5
	70 SE	1,4	5 x 5 x 1,2	7 x 7 x 1,5
81 S		2,5	5 x 5 x 1,2	7 x 7 x 1,8
	80 SE	2,8	5 x 5 x 1,2	10 x 10 x 1,8
93 S		2,9	5 x 5 x 1,2	12 x 12 x 2
	90 SE	4,7	6 x 6 x 1,2	13 x 13 x 2
107 S	100 SE	6,1	6 x 6 x 1,5	14 x 14 x 2,2
124 S	120 SE	7,5	6 x 6 x 1,5	15 x 15 x 2,7
144 S	130 SE	10,5	7 x 7 x 2	19 x 19 x 3
160 S	140 SE	13	9 x 9 x 2,5	21 x 21 x 3,5
206 S	170 SE	17	9 x 9 x 2,5	24 x 24 x 3,7
230 S	180 SE	20	10 x 10 x 2,5	26 x 26 x 3,7
254 S	200 SE	25	10 x 10 x 2,8	29 x 29 x 4
288 S	220 SE	30	10 x 10 x 3	31 x 31 x 4,5
318 S	250 SE	40	10 x 10 x 3	33 x 33 x 4,7
348 S	280 SE	42	10 x 10 x 3,3	36 x 36 x 5
390 S		49	10 x 10 x 3,3	38 x 38 x 5,5

The type number indicates the cone size (D_c) in cm.

Table 3.3 Oxygenation Capacity of Simplex-Cones, Type E
(as given by the manufacturer)

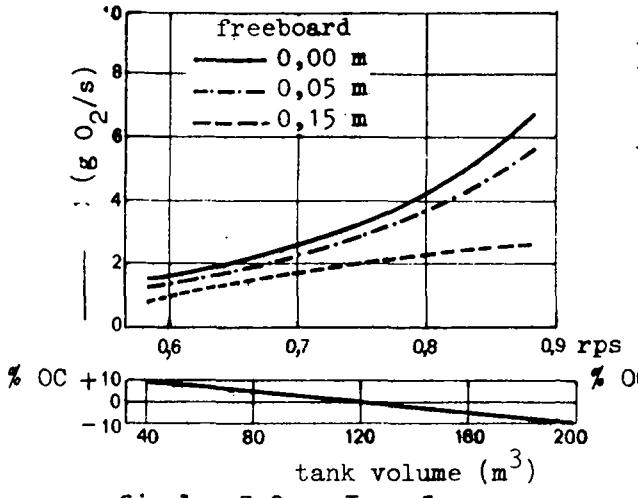

Simplex-E-Cone Type 5

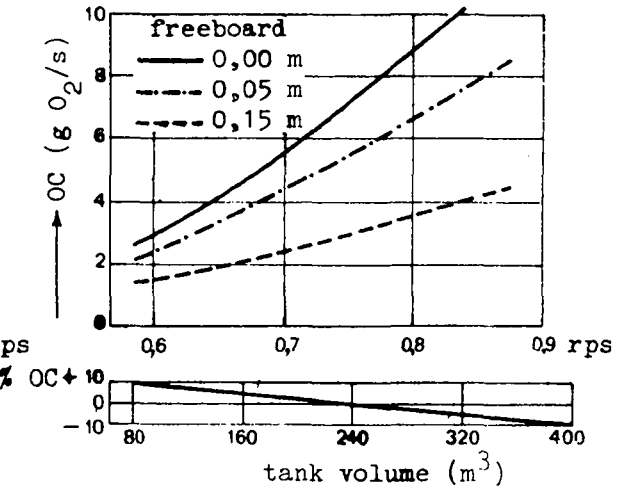

Simplex-E-Cone Type 6

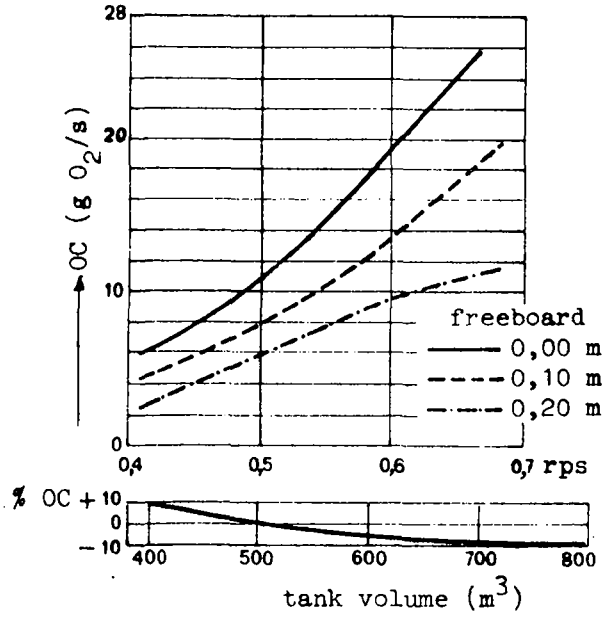

Simplex-E-Cone Type 8

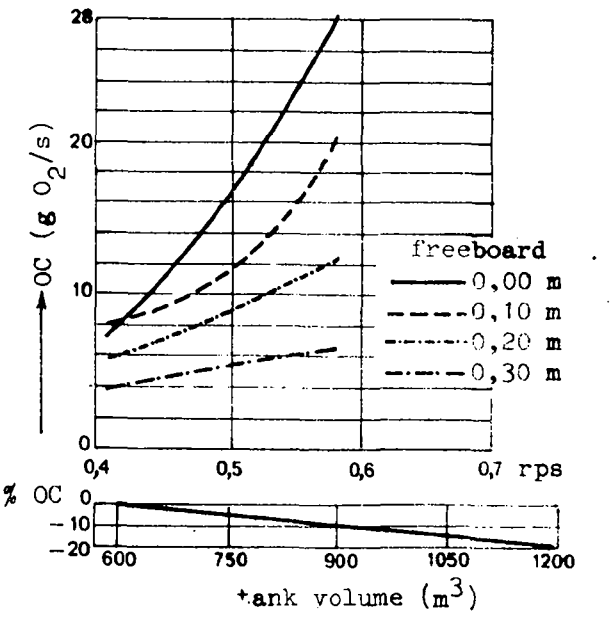

Simplex-E-Cone Type 10

Table 3.4 Oxygenation Capacity and Optimum Tank Volume for BSK-Turbines (Closed Type Favorit)

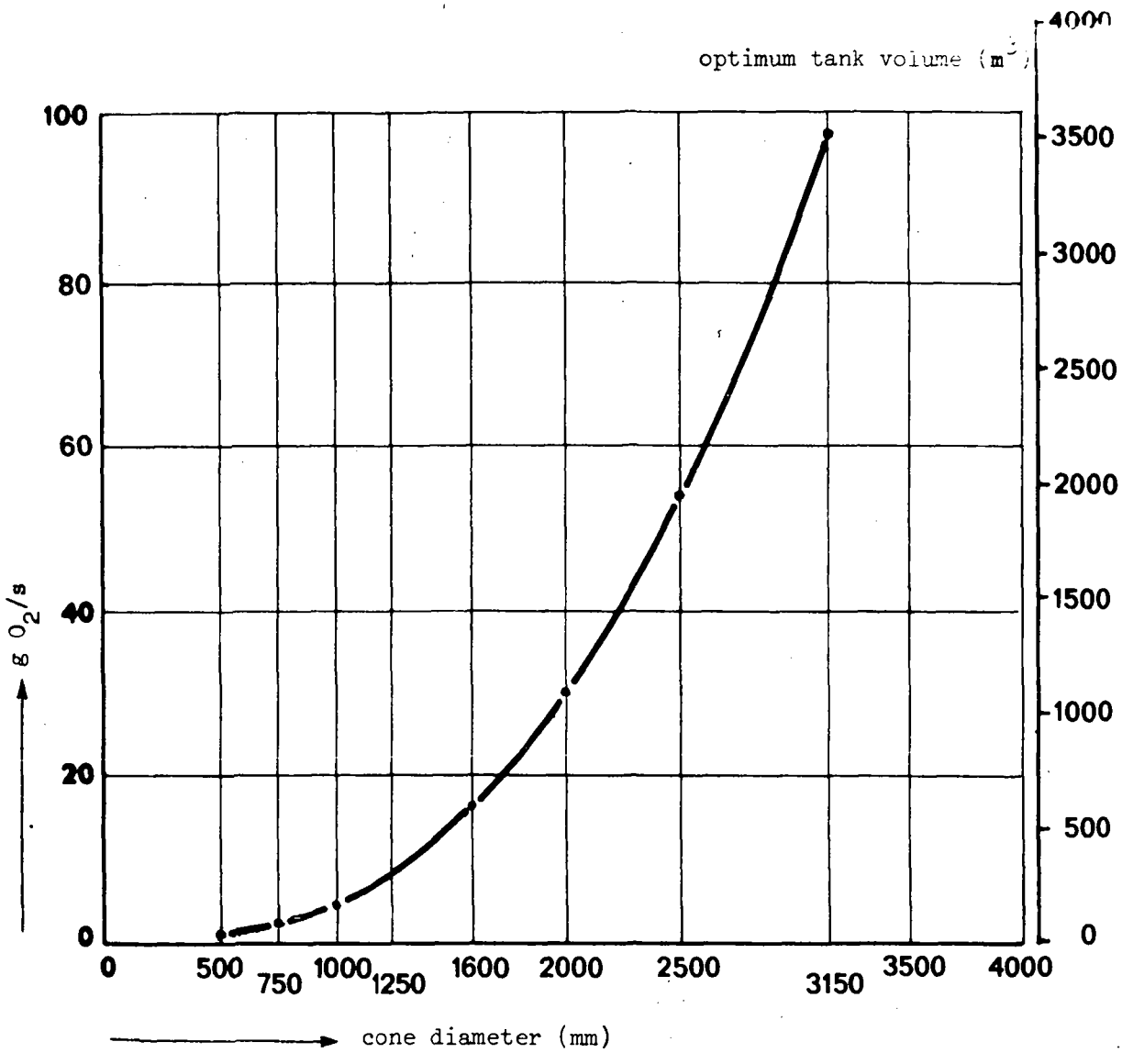

Table 3.5 Oxygenation Capacity and Tank Dimensions for Hamburg Rotors (as given by manufacturer)

Rotor dimensions in mm (comp. fig. 3.50)					OC	tank dimensions		
			jet tubes					
D_c	d	h	number	a	g O_2/s	width (m)	depth (m)	volume (m^3)
1000	350	500	6	133,0	1,9	5,00 - 6,20	1,50 - 2,00	37,5 - 76,5
1150	400	550	6	139,7	2,6	5,80 - 7,10	1,50 - 2,20	50,0 - 110,0
1350	470	650	6	159,0	4,9	6,80 - 8,40	1,60 - 2,60	73,0 - 185,0
1600	500	800	8	139,7	7,2	8,00 - 10,00	1,90 - 3,00	122,0 - 300,0
1900	620	950	8	159,0	12,0	9,50 - 11,80	2,20 - 3,60	198,0 - 500,0
2250	770	1100	8	193,7	19,4	11,30 - 14,00	2,50 - 4,20	320,0 - 825,0
2650	900	1300	8	216,0	35	13,30 - 16,40	3,00 - 4,80	530,0 - 1290,0
3100	1000	1500	10	216,0	49	15,50 - 19,20	3,50 - 5,00	840,0 - 1930,0
3600	1200	1800	10	219,1	70	18,00 - 22,50	4,00 - 5,20	1295,0 - 2600,0

Table 3.6 Specifications of the Aqua-Lator and Experimental Results

Specifications				Experimental results A			Experimental results B		
Power kW	rational rps	speed rpm	Diameter of float m	gross power input kW	OC g O_2/s	OE mg O_2/J	gross power input kW	OC g O_2/s	OE mg O_2/J
3,7	29	1750		4,45	2,0	0,45	4,45	1,9	0,44
7,5	20	1200	1,68						
11,2	20	1200							
14,9	20	1200	1,98	17,0	7,4	0,43	17,0	7,2	0,42
37,3	15	900	3,32	40,0	21,2	0,53	40,0	17.2	0,43
44,7	15	900	3,32						

Experimental Conditions

A: tank volume : 379 m^3
shape : circular
Diameter: 12,20 m
depth : 3,20 m

B: tank volume : 2430 m^3
shape : square
width : 30,0 m
depth : 3,66 m
slope of side walls: 1 : 1,4